Alma Mater Studiorum – Università di Bologna

DOTTORATO DI RICERCA IN

Ingegneria Civile, Chimica, Ambientale e dei Materiali

Ciclo XXIX

Settore Concorsuale di afferenza: 08/B1

Settore Scientifico disciplinare: ICAR/07 – Geotecnica

NUMERICAL AND EXPERIMENTAL INVESTIGATION INTO THE EFFECT OF RETENTION PROPERTIES OF PARTIALLY SATURATED SOILS FOR THE STABILITY ANALYSIS OF RIVER EMBANKMENTS

Presentata da: Carmine Gerardo Gragnano

Coordinatore Dottorato	**Relatore**
Chiar.mo Prof. Luca Vittuari	**Chiar.mo Prof. Guido Gottardi**

Esame finale anno 2017

Abstract

Stability assessment of existing earthen water retaining structure, as the case of river embankment, represents a partially unsolved problem in geotechnical engineering. This is not mainly dependent on particular lack of knowledge on saturated and unsaturated soil behaviour, for which hydraulic and mechanic soil properties and their dependence on soil state parameters and flow paths have been intensely studied and have gained a good level of confidence in the last three decades. Nonetheless, difficulties to extend recent and past theoretical acquirement to medium and large scale problems (10^2m to 10^5m), which belong to standard practice are still predominant. The periodic occurrence of critical events, like flood and high water, in combination with the urbanization expansion also in the neighbourhood of the stream system, implicates the need of a continuous and increasing attention to risk assessment related to riverbank failure occurrence. To this end, the evaluation of seepage and stability characteristics of the embankments is a fundamental problem in civil engineering, involving several geotechnical issues, and requiring probabilistic analysis to obtain reliable results. Otherwise, the strong uncertainties related to initial and boundary conditions definition and spatial variability of soil hydraulic and mechanical properties, typical for embankment structures, lead to an extensive use of simplified assumptions for both design and assessment of probability of failure in the engineering practice. Among these, can be found steady state seepage conditions in equilibrium with characteristic hydrometric level, fully saturated soil conditions, implicating highly conservative results in terms of global probability of failure and so inaccurate risk evaluation.

In order to assess the stability conditions of existing water retaining structure, a specific research has been performed, using evidence, observations, and data collected on a particular flooding case study, referring to bank's total sudden collapse occurred on January, 19th 2014, on river Secchia, north of the town of Modena (Italy). The effect of retention properties of partially saturated soils on the hydraulic and stability conditions have been investigated, accounting for hydrometric water-level time-variability; numerical studies have been performed with increasing level of sophistication, using different mathematical methodologies for probabilistic numerical analysis. Various experimental studies and site monitoring data are presented, sharing the purpose of investigating retention properties for partially saturated soils. In its entirety, the final purpose of this study is to analyse the assessment process of riverbanks stability towards global instability mechanism triggered by variable hydraulic boundary conditions. Indications and suggestions, which can eventually be referenced for similar problems or implemented in the standard engineering practice, are provided; the use of site monitoring is justified to improve present flood early-warning system able to define in continuous progressive alert level combining measured and forecasted data with numerical probabilistic analysis results.

Structure of the thesis

The thesis consists of 8 chapter. Following this introductory section, the socio-economic impact of floods are briefly described (Chapter 1), mentioning recent researches spacing from global to regional scale.

In Chapter 2 are presented theoretical backgrounds, methodological approaches, procedural tools, systems of analysis and testing, which have been, entirely or partially, used for the purpose of this research; this part, which is not structured to be fully comprehensive of the problems discussed in this work, aims to provide a general overview of the geotechnical issues involved, for a sufficient understanding of results achieved and to promote discussion.

Chapter 3 is dedicated to the description of the study case, in terms of theoretical and practical context, the introduction of information and data which represent the starting point of this thesis, and the description of preliminary analysis which aim to underline the topics which need special attention.

In the following sections, increasing attention will be then demanded on the definition of information to be used for a more reliable stability assessment of river embankments in unsaturated soil conditions, as initial and boundary conditions (Chapter 4), on the effect of time-dependent boundary conditions and soil hydraulic and retention parameters variability (Chapter 5 and 6), and on the possibility to use a fully comprehensive uncertainty propagation analysis by means of direct or indirect procedures (Chapter 7).

In Chapter 8, some applications related to the use of experimental investigation for the estimation of soil hydraulic and retention behaviour are presented. Special notes and mentions to the possibility to reduce uncertainties related to river embankments safety assessment are then provided; this final part represents both the conclusion for the present thesis and the starting point for specific experimental studies on the determination for hydraulic and retention behaviour in an instrumented riverbank, which is still in progress.

Finally, the last section gives a summary of the conclusion obtained in the research and remarks for further works.

Table of Contents

List of Figures

1 Socio-economic impacts of floods

1.1 The concept of risk: hazard, exposure and vulnerability

In the course of this thesis, problems and terms related to risk assessment are frequently debated. It could be, so, useful to provide some preliminary definition about the basic concept to this issue related. Firstly, risk is usually conceptualised to consist of three components: hazard, exposure and vulnerability.

The hazard is a term usually referred to the possible, future occurrence of natural or human-induced events that may have harmful or potentially destructive effects on vulnerable and exposed elements (White, 1973; UNDRO, 1980; Birkmann, 2006, Cardona, 2012). Although, at times hazard has been ascribed the same meaning as risk, it's currently widely accepted that it only represents a factor of the overall risk, and not a risk itself. Landslides or flooding occurrences associated with human-induced environmental alteration and climate change-related hazards are examples of such socio-natural hazards. (Lavell, 1999). The intensity of recurrence of hazard events, rather than their level of periodicity, can be estimated by use of predictive model for extreme and lower impactive phenomenon, environmental degradation forecasting analysis, investigation of human inference in natural ecosystem equilibrium.

The second term is related to the exposure and refers to the inventories of elements of a specified region in which impacting or hazardous events may occur. Hereafter, if human population, economic or environmental resources, and sites were not exposed to potentially dangerous settings, or neither located in their influence area, there would be no evidence for an estimated loss and, so, the risk would not exist. While the common usage, more than literature, often and mistakenly conflate exposure and vulnerability, they represent two distinct components of the global risk. Exposure is a necessary, but not sufficient, factor for an element at risk. It is, however, possible to be exposed but not particularly, or not at all, vulnerable, e.g. by living in a floodplain but having sufficient means to modify the water retaining structure, adapting the services exposed and mitigating potential loss. Otherwise, to be vulnerable to a potentially impacting event it is necessary also to be exposed.

Vulnerability refers to the tendency of exposed elements to suffer adverse effects when affected by the occurrence of hazard events. The vulnerability is, so, related to predisposition, susceptibilities, fragilities, weaknesses, or lack of capacities determining and guiding damaging events on the exposed elements. An early view of vulnerability in the context of disaster risk management was univocally related to the physical resistance of engineering structures and structures (UNDHA, 1992). More recent views relate vulnerability to characteristics of social and environmental processes, integrated into the context of climate change, to the susceptibility, sensitivity and lack of resilience or capacities of the exposed system to preserve and adapt to extremes and non-extremes events (Brklacich and Bohle, 2006; IPCC, 2007). The vulnerability is so defined

as a term which is mainly dependent on the occurrence of a particular hazard. However, several other factors are determinant for the risk assessment process and related to the mid-long terms effect consequent to the hazardous event occurrence, such as socio-economic diseases, lack of social networks and social mechanisms, that will aggravate or affect vulnerability levels independently of the type of hazard, excepting for their quantification. A significant part of vulnerability, which is gaining, even more, attention in recent studies (Frank et al., 2011), is also linked to deficits in risk communication. This fact would move the problems the more on the speaker side rather than on the listener side. In cases of lack of appropriate information, false risk perceptions could be the consequence, heavily impacting on the attitude and capacity of adaptation to rapid environmental changes, incipient threats or social sources of stress.

In the context of risk management, vulnerability is the most tangible manifestation of the social construction of risk (Aysan, 1993). Where exposure to events is impossible to avoid, land use planning and location decisions can be accompanied by other structural or non-structural method for preventing or mitigating risk. River floods are natural phenomena which cannot be entirely prevented and have the potential to cause fatalities, displacement of people and damage to the environment, to severely compromise economic development and undermine the economic activities of various part of the world. Flood, as defined by the Directive 2007/60/EC of the European Parliament (EU, 2007), are intended as the temporary covering by water of land not normally covered by water. In the framework of this thesis, this includes floods from rivers and torrents, for whom embankments stability evaluation has been studied in different scenarios. Flood risk means the combination of the probability of a flood event and of the potential adverse consequences for human health, the environment, cultural heritage and economic activity associated with a flood event, which can be indeed expressed as the combination of hazard, exposure, and vulnerability. The present dissertation mainly focuses on the definition of probability of failure for riverbanks, which represent a fundamental source of flood hazard in flood risk management, with specific attention to different geotechnical issues related to this topic.

1.2 Global to national scale

River flooding is a worldwide natural phenomenon, which has main incidence in flat areas. Over the last few decades, the world has experienced a rising number of devastating events (Figure 1.1). Different studies on the socio-economic impact of floods have indicated an increase of exposure of people and assets to this problem, as a general consequence of population and economic growth, in the framework of a global increment of damage due to weather-related natural disaster (Mills, 2005; IPCC, 2007). Besides, climate change may increase the frequency or magnitude of flooding (Hirabay et al., 2013).

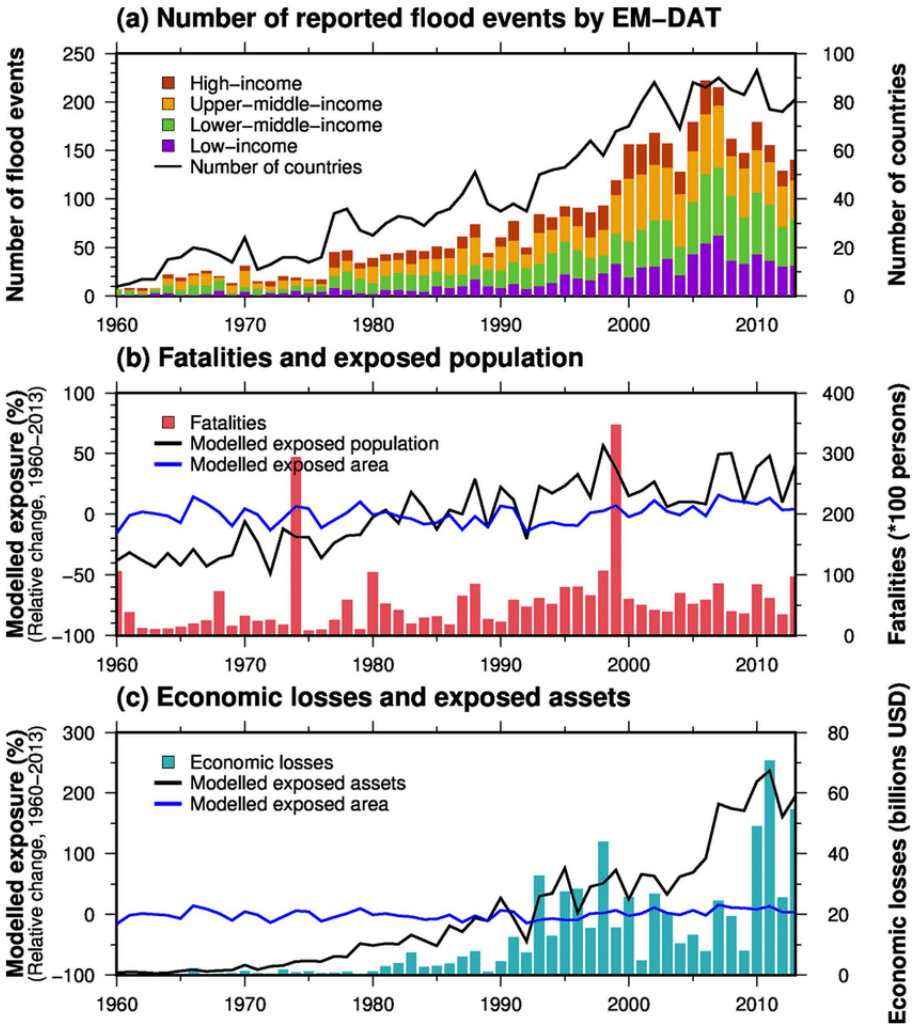

Figure 1.1. The impact of flooding is especially harmful in developing countries due to low levels of flood protection (Doocy et al., 2013). However, flood loss and damage, especially concerning numbers of fatalities, are less severe in developed versus developing countries due to past efforts to mitigate flood impacts. The estimation of flood risk level could be intended as the weighted balance between the magnitude of the flood (hazard), the number of people or the value of assets potentially affected by flooding (exposure), and the susceptibility to flood eventuality (vulnerability) (Adger, 2006; IPCC, 2012).

Flood vulnerability has changed over time and space depending on local socioeconomic development conditions, including flood protection measures (e.g., levees, dams, river management, dredging, flood warning systems and land use management), topography and hydro-climatic conditions. At the same time, flood vulnerability is greatly affected by spatiotemporal changes in populations and assets. For example, several studies indicate that unplanned urbanisation and human settlements in flood-prone regions have increased flood risk in Africa and low coastal regions (McGranahan et al., 2007), whereas displacement of people to safer areas from flood-prone regions is expected to reduce flood risk (Baldassarre et al., 2013). The number of reported flood events by the Emergency Events Database (EMDAT, 2016) from 1960 to 2013

evidence a significant increase both in the occurrence of flood and on the number of countries affected by these events, giving an idea of the global magnitude of this problem and on the growing level of care that need to be taken for reducing the vulnerability and exposure. Global mortality rates and global loss rates showed a decreasing trend, and inverse relationships were found between flood vulnerability and GDP per capita (Fig. 2), indicating, however, an improvement in flood vulnerability at the global scale since 1960 associated with economic growth (Tanoue et al. 2016). However, although a significant negative trend in global mortality rate was seen across the whole analysis period (1960–2013), the rate for the most recent period (1990–2010) did not show a statistically significant trend. This result highlights the importance of the analysis period, as well as uncertainties, when calculating flood vulnerability. The long-term trend in loss rate varies between different income levels, due to the balance between improvements in flood mitigation measures and increases in assets in flood-prone regions associated with economic growth (in particular in developing countries).

In general, flood events are strongly impacting for European embankment system, causing significant distresses and damages whether they occur. The combination of flooding from rivers, estuaries and the sea, in fact, is a significant source of hazard for large part of Europe, and the balance in terms of safety for population reveal more than 1100 fatalities and half million-people evacuation from 1998 to 2009 (Feyen and Watkissy, 2011). Critical numbers could be found also in relation to flood losses and its trend in last decades: for the period 1980 – 2011, the estimated annual damage (EAD) have increased from an average of €6 billion per year to around €20 billion per year (Kundzewicz et al., 2013). Simultaneously, insurance losses from flooding have still increased significantly, being around the 9% of the total losses (data from Münich Re., 2012). For a reliable assessment of the future impact of river floods accounting for climate change, assumptions have to be made on future socio-economic conditions that require scenarios. With the purpose to provide general outlook on the socio-economic impact of flood in Europe, emission scenarios described by the Intergovernmental Panel on Climate Change (IPCC) Special Report on Emission Scenarios (SRES) are considered; in particular, SRES A1B scenario is selected as the most representative, which is theoretically based on the consequences of a future world of rapid economic growth, new and more efficient technologies, and convergence between regions (Nakicenovic et al. 2000). The A1B scenario adopts a balance across all sources (fossil and renewable) for the technological change in the energy system. This scenario has been extensively used in recent European regional climate modelling studies, and reflects a medium–high emission trajectory, leading to central estimates of global average surface temperatures of around 3°C to 4°C relative to pre-industrial levels, through individual models show a wide range. Considering this scenario, advance prospective on the knowledge on the impacts and economic costs of river floods in the European Union and the costs and benefits of adaptation are provided in the Technical Policy Briefing Note of the Climate Cost project (Feyen and Watkiss, 2011). The projected provides estimation on the effect of river flooding events in terms of Expected Annual People (EAP) and Expected Annual Damage (EAD) for the European Union (27

countries considered at the time of the Technical Note); the complete set of results is published in the Technical Policy Briefing Note of the Climate Cost project (Feyen and Watkiss, 2011), while in this section remarkable outcomes are reported. As first, in Figure 1.2 are reported the estimated EU27 EAP affected by river floods for the considered baseline period (1961-1990), the recent past 2000s (1981-2010), the immediate future (2011-2040), the far future (2041-2070) and the remote future (2071-2100) considering the A1B scenario based on simulations driven by 12 regional climate models, assuming no adaptation to climate change. Showed results report an EAP of about 300,000 by the period 2041-2070, rising to 360,000 by the period 2071-2100, including his included the combined effects of socio-economic and climate changes; for the considered baseline climate period (1961-1990) EAP was estimated at around 167,000. It's worth to notice that socio-economic change is forecasted to provide lower estimation in terms of EAP respect to the baseline, while climate change would significantly increase the flood risk. High range in results (Figure 1.2), across the 12 regional climate models 12, evidence even significantly worst scenarios.

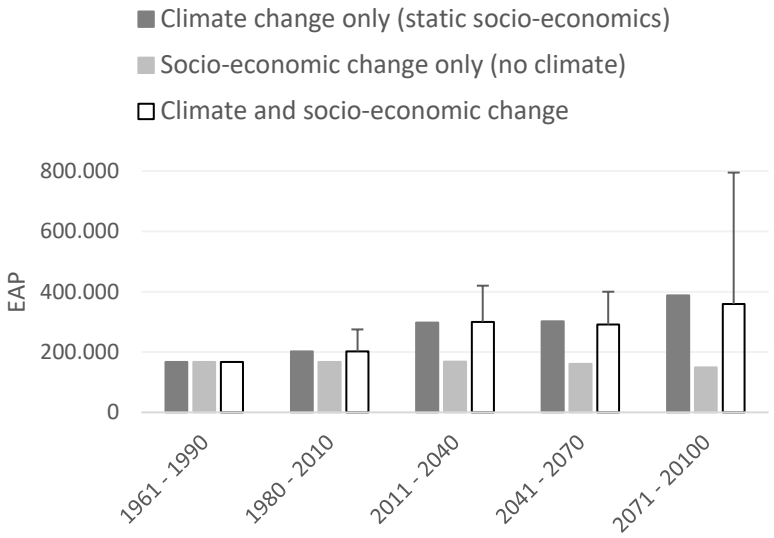

Figure 1.2. Expected Annual People (EAP) affected by river flood event in EU27 for various time period, considering the A1B emission scenario, based on simulations driven by 12 regional climate models, assuming no adaptation to climate change.

In Figure 1.3 are plotted the Expected Annual Damage (EAD) in Billions of Euros per year estimated assuming the same time period, emission scenario and type of adaptation to climate change defined for Figure 1.2. The EAD for EU27 is so estimated to be €20 Billion per year for the recent future (2011-2040) and increasingly rising up to €98 Billion per year by the period 2071-2100. In economic terms, both socio-economic and climate changes are strongly impacting on forecasted values for EAD. The distribution of flood losses (Figure 1.3) evidence that about 82% of the total losses is relate to residential areas, 7% to industry, 5% to commerce, just under 5% to agriculture and 1% to transport. As static land use and economic structure is assumed in the

analysis, the distribution of losses over the sectors remains fairly constant over time in the analysis (Feyen and Watkiss, 2011). The global flood losses are, finally, reported in terms of Cumulative Annual Damages (CAD), in Billions of Euros per year, estimated for each EU27 countries and results showed in Figure 1.4; relevant climate-related costs are expected for UK, Hungary, France and Italy.

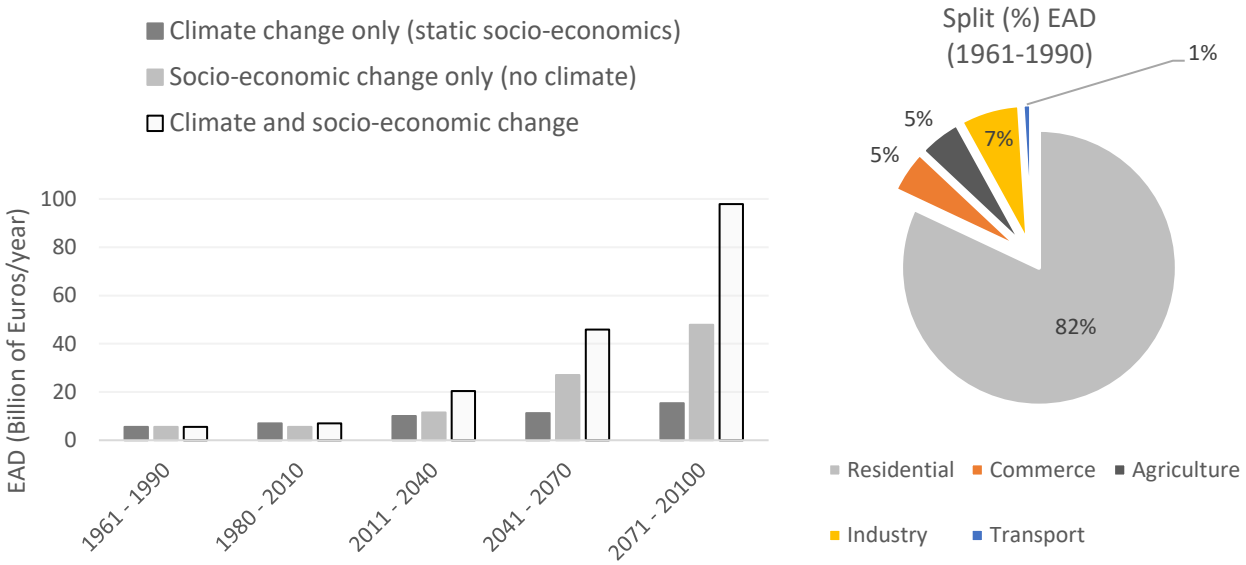

Figure 1.3. Expected Annual Damage (EAD) in Billions of Euros per year caused by river flood event in EU27 for various time period, considering the A1B emission scenario, assuming no adaptation to climate change (left); split (%) of the global EU27 EAD from floods for the baseline period (1961-1990) (right).

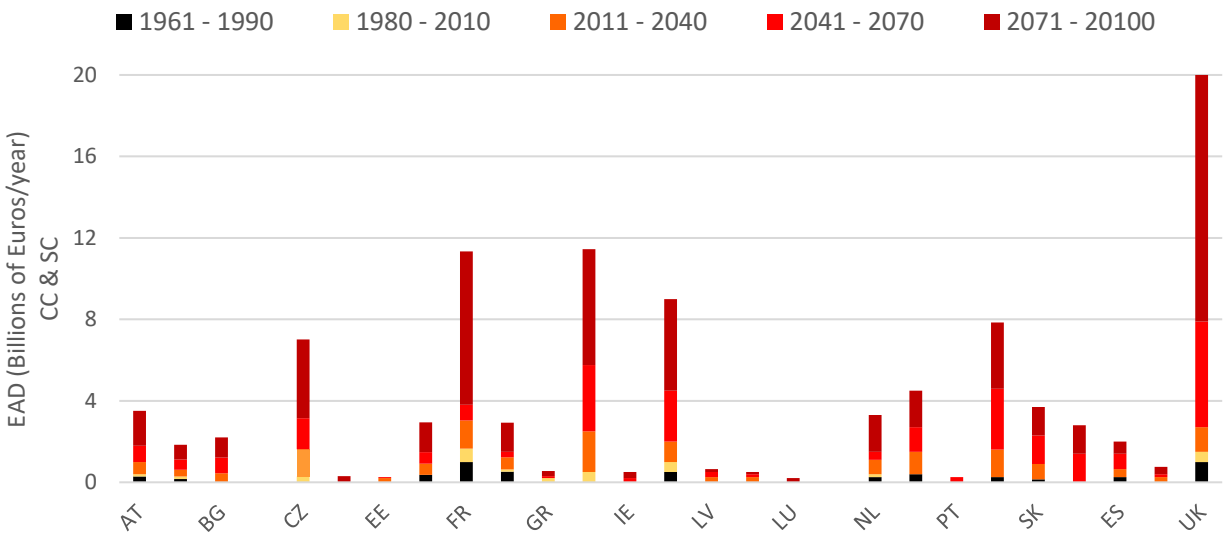

Figure 1.4. Cumulative Annual Damage (EAD) in Billions of Euros per year caused by river flood event for various time period, considering the A1B emission scenario, assuming no adaptation to climate change (CC) and socio-economic change (SC).

In the framework of the Climate Cost project, benefits of adaptation are also estimated; the hypothesis of a minimum protection level for events characterized by return period of 100 year across EU27 is assumed. Results evidence a reduction in the Estimated Annual Damage, accounting for adaptation cost, highly increasing with time, with stronger relevance for UK, France and Italy on long-term estimations, showing as adaptation could lead to significant economic benefits and can potentially reduce direct effects and cost of river floods. Significant results are plotted in Figure 1.5.

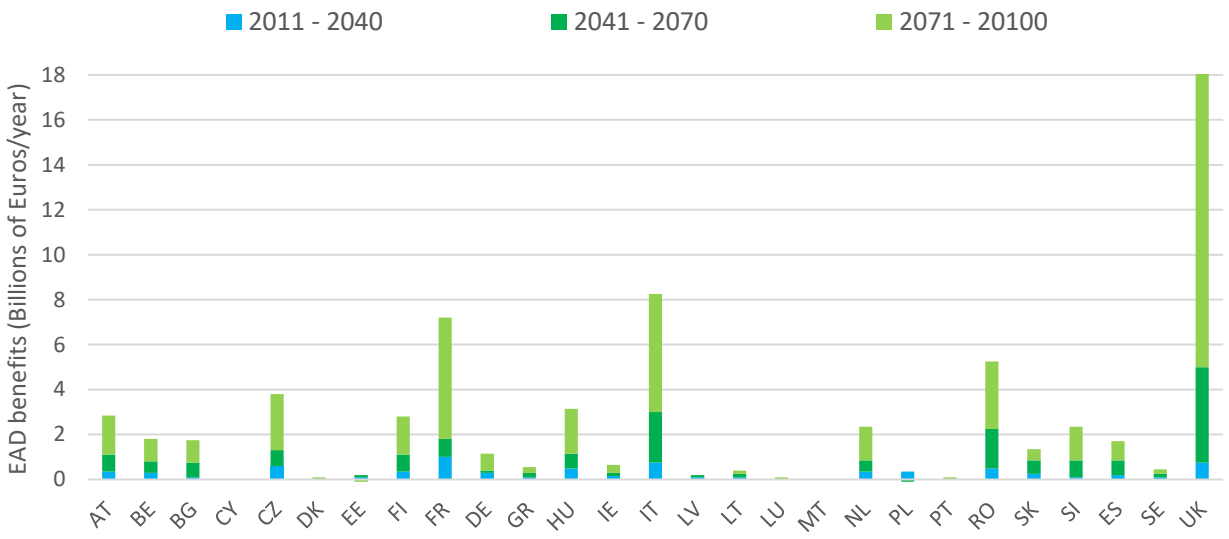

Figure 1.5. Benefits – reduction in EAD (in Billions of Euros per year) for each EU27 country, for the periods 2011-2040, 2041-2070 and 2071-2100.

In Italy, flood events belong to the context of hydrogeological instability, also concerning landslides and coastal erosion. Increasing attention has been given to these problems, as it should to be, and every year updated and comprehensive work are published by governmental and private institute on this topic. Since 2008, the Italian National Institute for Environmental Protection and Research, ISPRA (Istituto Superiore per la Protezione e la Ricerca Ambientale), has been established under the vigilance and policy guidance of the Italian Ministry for the Environment and the Protection of Land and Sea (Ministero dell'Ambiente e della Tutela del Territorio e del Mare), and is part of the network of the National System for Environmental Protection, which is made up of 21 Territorial Environmental Protection Agencies (ARPA), established by Regional Laws. It's an example of consolidated federal system, which combines the direct knowledge of the territory and its issues with the national policies for environmental protection, so as to become an institutional and technical-scientific reference point for the whole country. A technical Report by the Ministry of the Environment and Land Protection (Ministry of the Environment and Land Protection, 2008) quantifies the areas with high risk of flooding, covering area of more than 7500 km^2, corresponding to approximately

3% of the national territory; the most dramatic floods in Italy are occurred in the Po river basin. The river morphology has evolved from a geometry with irregular meandering channels controlled by discontinuous embankments to a geometry with artificial meandering or straight channels that are controlled by flood corridors and continuous riverbank protection. The major outcomes of progressive expansion of existing levees system are a decreasing flood proneness of the Upper Po sub-basin (e.g. Sesia, Tanaro, Ticino rivers) and an increasing vulnerability of the Po Plan areas (Lower Po, Po Delta) to hydrological hazards. the development of structures along the fluvial network to protect urbanized and farming areas in alluvial plains has increased average river discharge and flood peaks (Zanchettin et al., 2008). In particular, until the late 1950s, the defence system was made of discontinuous levee stretches (mostly erected since the late 19th century) that allowed a natural damping of the peak-flow discharge of the Upper Po tributaries. In the 2015, ISPRA presented an updated Report on the hydrogeological instability in Italy, including the comprehensive national maps of landslide hazard and hydraulic hazard (Legislative Decree no. 49/2010, Floods Directive 2007/60 / EC), for the harmonization and mosaicking of areas defined by the Basin Authority, Regions and Autonomous Provinces on their area of jurisdiction; in this document are described and delimited the effect of hydrogeological instability on the Italian National territories. In Figure 1.6 are plotted the percentage of territory exposed to floods characterized with different return period, ranging from 20 to more than 200 years, for each Italian region. As can be immediately seen, the graph evidence how the medium term related risk is generally diffused in large part of the Italian northern region, with a particular high incidence in correspondence of the Emilia Romagna region.

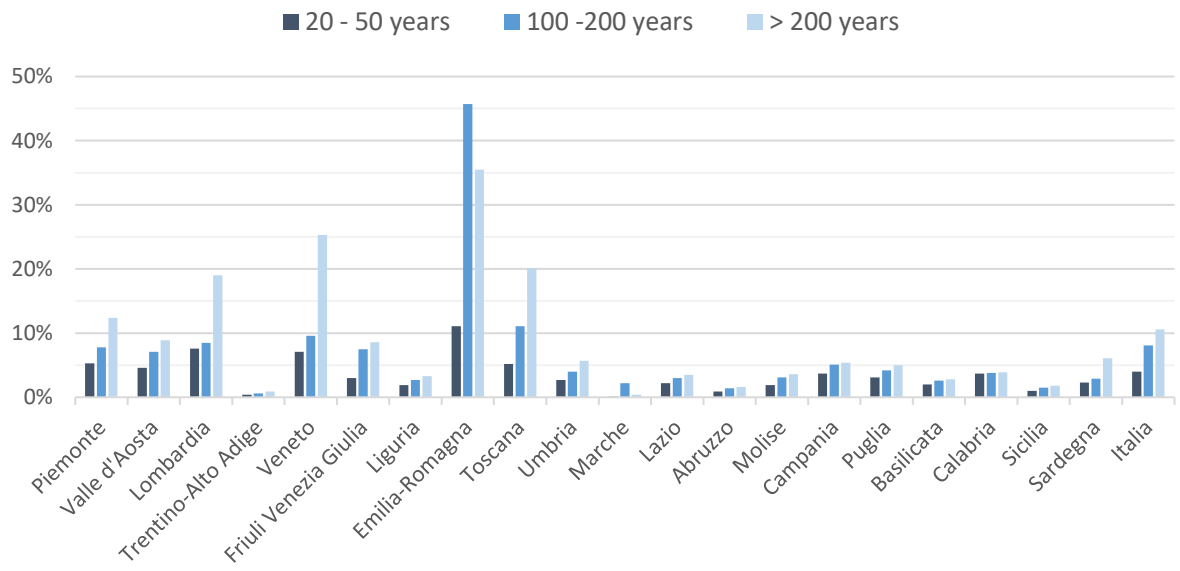

Figure 1.6. Area, express as percentage of the total, vulnerable to flood event characterized by different return period, for regional scale (source: ISPRA, 2015).

In this framework, the critical territories represent the 15.8% of the national area and cover 88.3% of the municipalities (Figure 1.7), on which stand 6,250 schools and 550 hospitals. For the 2014, 40 billion of Euros is the estimated demand for the safety measures that the Italian territory needs; however, the Italian government allocated only 180 million for the 2014-2016 triennium. Since 1956 the consumption of soil has increased by 156%, compared to a population increase of 24%; this means that every five months an area comparable to the city of Naples is overbuilded. Furthermore, global warming is leading to an inevitable worsening of these extreme phenomena. These facts highlight the man's responsibility for disasters, which caused in Italy the death of 4 thousand of people during the last fifty years. The total cost of reducing the risks of floods and landslides in Italy is, however, estimated at € 42 billion, but this estimate does not take into account the higher risks from climate change scenarios. In regard to the above discussion, a proper way of assessing flood damage amount for each hazard event on a local to a global scale for the present and the future is a demanding task for scientific communities.

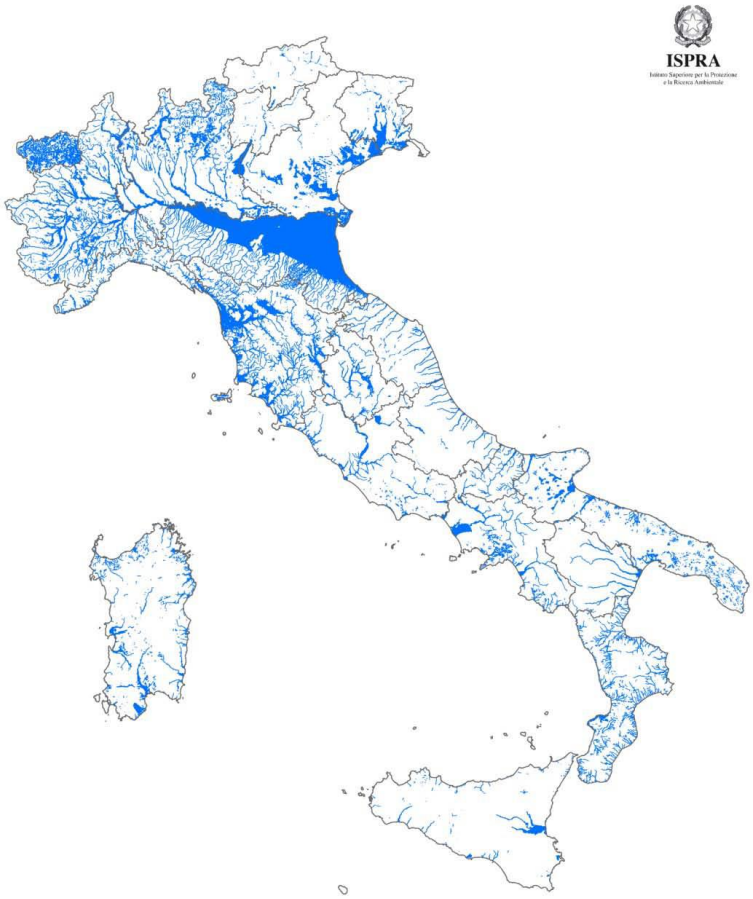

Figure 1.7. Italian mosaicking of exposure to flood events characterized by a return period ranging from 100 to 200 years (source: ISPRA, 2015).

1.3 Performance estimators for river embankments

Considering the magnitude of the problem, flood management in Europe is so requiring rapid changes, moving to a combined improvement in protection, defence and safety assessment techniques and methods which could lead to a more comprehensive flood risk management. Historically, physical and direct protection barrier against flooding has been a costly, but straightforward way to overcome many of the adverse impacts. Several potential adaptation options to address these risks have evolved in recent years. These adaptation strategies have historically used protection or accommodation to reduce risks. Protection involves the control of risks with defences (e.g. physical barriers to flooding), whereas accommodation involves adjusting human use of the flood zones (e.g. through forecasting and early warning systems, insurance, increased flood resilience). These measures include a mixture of so called 'hard' (engineering) and 'soft' (nontechnical) measures. Increasingly, such options are being seen as part of integrated portfolios. However, a residual risk always remains and complete protection cannot be achieved. Thus, managing floods involves an element of strategy. In recent years, the focus of flood management policy has shifted from technical measures (especially protection with defences) to spatial solutions that aim to create 'room for the river', as with recent examples in the Netherlands. The new policy approach tries to take account of long-term developments and risks, such as those presented by climate change. Actual requirements for design and assessment of various typology of water retaining structures are, at present, diffused on a large series of directive, statements and handbook (ILE, USACE, EU2007, for which details will be provided in the following of the present work). Even considering the various amount of issues involved in flood safety assessment, each of these texts represents an important reference for the studied problem.

With regarding to the above presented discussion, it could be proper now to introduce some mentions to a possible definition of the acceptable risk level in relation to a flooding event. Limiting this part to the specific role of vulnerability assessment, thoughtful guidelines and procedures are generally not exhaustive for the estimation of specific values of Probability of failure (P_f). Some indication on performance descriptors, referenced to water retaining structures, in comparison with Probability of failure (intended as critical loss of the designed level of serviceability) are found in USACE (1999), and showed in Figure 1.8.

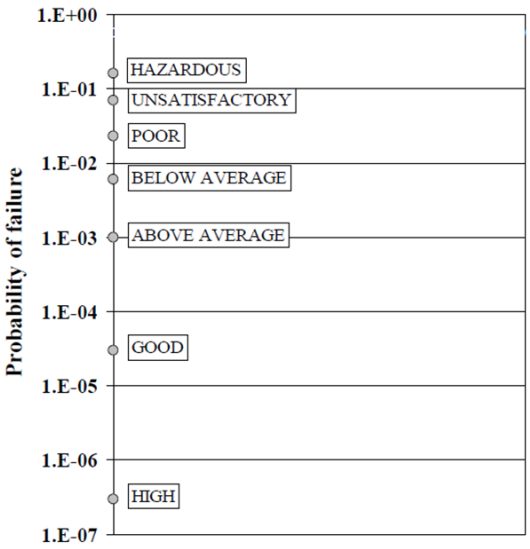

Figure 1.8. Performance descriptors compared to Pf for water retaining structures (USACE, 1999).

Taking in mind the important distinction between catastrophic event and unsatisfactory performance, which could both referred as failure occurrence even for significant differences in outcomes from exposure and hazard analysis, decisions or modifications of the acceptable values for Probability of failure should require that the following relationship has to be satisfied (Duncan, 1999):

$$\begin{pmatrix} Reduction\ in\ P_f\ associated \\ with\ more\ reliable\ design \end{pmatrix} \times (Cost\ of\ failure) < \begin{pmatrix} Added\ cost\ of \\ more\ reliable\ design \end{pmatrix}$$

Two aspects should be here focused; firstly, in view of the extremely high cost of river flood subsequent to embankment failure, it is hard to consider and recommend design procedure for river embankments which do not account for significant and conservative margin of safety; nevertheless, should be considered the possibly limited enhancement in terms of cost reduction deriving from a more reliable design for a local scale. Actual standards, handbooks and guidelines (EU, 2007; ILH, 2013; USACE, 2015) requires to assume simplified but over-conservative assumptions on hydraulic and mechanical behaviour of river embankments. However, even being topic of discussion, this approach should not be generally considered out of the design scenario, where more reliable estimation of the safety margins in operating conditions should always be considered. The exact purpose should so be to obtain a reliable risk assessment for riverbank failure occurrence, taking in mind that overrating the actual level of risk is considered as socio-economic damage as well as a possible underestimation, even if characterized by different impact in terms of consequences.

2 Theoretical background, methods and applications for riverbank stability analysis

The primary function of a river embankment is the hydraulic protection of environment when variations in retained water level occurs; design, modification and monitoring of riverbank sector are mainly conducted to improve safety towards the possible collapse mechanisms and to enhance land use planning. A basilar requirement for an earther structure is to limit seepage process through it, which could be guaranteed by sufficient low permeability for construction soils during the whole operative lifetime. This need, however, could be frequently unsatisfied; in fact, due to the large amounts of soil required for their construction, and contrary to other standard application in earthen retaining structures, the possible choice for adequate material is limited by the soil availability on-site. For such cases, it should be suggested the use of coating or intermediate elements, even if their extended use is frequently constrained to the limited economic availability to this type of structures. In fact, due to their significant extension even for minor rivers or tributary, the cost for intervention for soil embankments is generally reduced as much as possible. However, this condition is generally not associated to the application of accurate assessment procedure, which would eventually have the benefit of more reliable safety estimations and optimized design criteria; on the contrary, indeed, heavy assumptions on the hydraulic and water retention behaviour of embankments are typical in engineering practice. This could be immediately stated considering that 1) design process is generally performed in the simplified hypothesis of steady-state seepage conditions; 2) partially saturated soil conditions are seldom applied to both design and control for river embankments. Thus, traditional methodologies are standards in many applications, which are mainly determined on the base of local practices and experiences, leading to the common consideration to be sufficient for both reliable safety assessment and appropriate design criteria. The need for an accurate research study on the stability assessment of river embankments is so generally conceived to evidence the possibilities for adopting more advanced, and even commonly acknowledged, methodologies and procedures of analysis; for research purpose, in particular, this study is focused on the use of experimental and numerical investigation into the effect of retention properties of partially saturated soils on riverbanks stability. For the construction of this earthen structures, in fact, and on the base of the soil available *in situ*, fine grained soils (silty-clayey) with possibly limited percentage of coarse grained soils (sand), are generally used; compaction, largely adopted in construction phase, tends to reduce the soil hydraulic permeability and to improve mechanical properties; a significant feature of this types of soils, however, is to remain unsaturated for all the working life of the riverbank, so that the topic of this study is both critical and suitable for a consistent approach to the problem.

Discussion of methodologies of analysis, applications and results, requires introduction and references to the various topic involved. The theoretical and practical backgrounds which need special, and preliminary,

mentions involve different topic in geotechnical engineering, dealing with simplified to advanced issues. As already recalled, partially saturated soil conditions are required for a realistic safety assessment of river embankments. Possible failure mechanism of river embankment is generally intended as modification or alteration of the initial structure which lead to significant loss of serviceability and limitation to the embankment roles. Some of the most frequent, and impacting, collapse mechanism can be found in Figure 2.1. Overtopping occurs in case river water level exceed the maximum height of the embankment, and could mainly defined as a hydrologic failure. Under-seepage phenomena conventionally refers to the progression and increase of water flow and gradients at the base of the riverbank structure, generally on the transition zone between layers characterized by strong difference in hydraulic permeability; this failure mechanism typically involve saturated soil conditions, and could lead to the formation of pipes in cases significant erosion results. Excessive deformation, as well as slope instability mechanism are typical for geotechnical problems and, for riverbank applications, involves issues related to unsaturated soil mechanics, soil-atmosphere interaction and transient seepage conditions. In the following of this thesis, the main collapse mechanism which is studied is outer slope instability, which turns to be critical for the considered study case; however, the probability of failure for this mechanism constitute only one source of risk, among the various possible.

The determination of seepage and stability characteristics for a riverbank under variable hydrometric and climatic conditions generally requires the use of numerical analysis, which are in most cases performed using Finite Element Method to model the effect of time-dependent boundary conditions for determining solutions in terms of pore water pressure and suction distribution, soil water content and gradient for each nodes of a specific domain; the safety assessment towards various collapse mechanism is generally performed by means of Limit Equilibrium Analysis, Finite or Discrete Element Methods. Results accuracy is, indeed, strongly dependent on the consistency of the soil properties assigned to each node/element and mesh/discretization of the model, on the proper definition of the initial conditions and the representativeness of the boundary conditions assumed for calculation, on the proper application of probabilistic mathematical and uncertainty propagation methods. The direct and indirect measurements for unsaturated soil state variables (e.g. soil suction and water content), both at laboratory and field scale, could be of great benefits for the reliability of analysis, but still represent a demanding task in geotechnical engineering, needing general outlines and specific mentions to probes and operating system. In this section, a review of the standard methods of analysis and testing are presented and briefly discussed. Furthermore, in the forward of this thesis, the basic knowledge related to specific concepts will be progressively introduced and referenced.

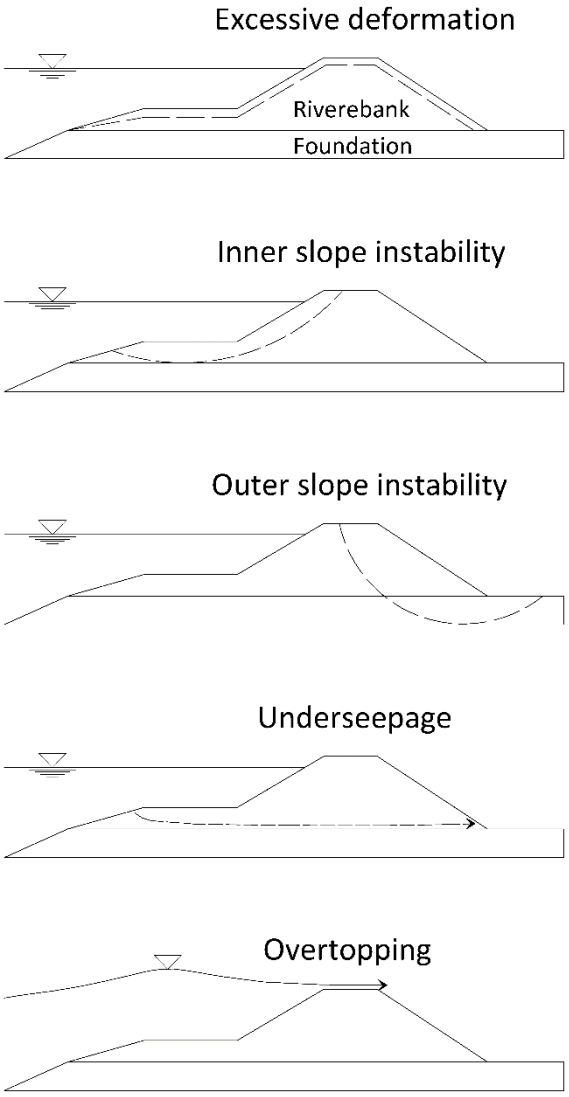

Figure 2.1. Main failure mechanism of a river embankment.

2.1 **Basic concepts for mechanic hydraulic behaviour of unsaturated soils**

Classic geotechnical problems, as well as fundaments and element of soil mechanics, are generally referred to the fully saturated or dry soil conditions; the first case assumes that void among solid particles are fulfilled by only liquid phase, gaseous phase the second. For a large amount of significant applications, as well as in various and rather simplified interpretation, these two conditions could be used for a realistic understanding of the soil behaviour. However, both fully saturated and dry conditions result as limit conditions in regard to the presence of both liquid and gaseous phases in pore space, while a wide and variable range of states are referred to partially saturated soil conditions. In this latter case, solid, liquid and gaseous phase are simultaneously present in a finite soil volume. Generally, as for the case examined in the present study, the liquid phase is referred as *water*, whereas the gaseous phase is a mixture of air and water vapour, usually

referred as *air*, and their mutual interaction, and their mutual interaction with solid phase is strongly impacting on global behaviour of the system. A large amount of geotechnical researches were involved, with various purpose, in the study of unsaturated soil mechanics, and related literature productions is generally extensive and exhaustive. In this section, brief outlines and remarks on the effect of partially saturated conditions on hydraulic and mechanical soil behaviour are provided, from capillary to actions to theoretical modelling. Principal references for mechanics of unsaturated geomaterials are here provided, which could be considered for basic to advanced concepts (Laloui, 2010; Fredlund et al., 2012); specific references are provided in the following of the present study.

2.1.1 Surface tension in air-water interface

In general, the shape of the air-water interface area is characterized by the presence of the surface tension. This phenomenon is the results from imbalanced intermolecular forces at the interface. In the interior of water phase, a liquid particle is effectively affected by a system of forces equal in all directions (Figure 2.2) and so experiences no net forces. As the liquid particle move to the air-water interface, a system of unbalanced forces is progressively experienced from the loss of an equivalent isotropic system of forces, producing a net force resulting towards the liquid phase. In order to reach equilibrium on the surface region, it is so necessaire for the liquid particle to gain an excess energy over those fully incorporated in the liquid phase; along the entire air-water interface area, a tensile pull is so generated. This tensile pull is defined as Surface Tension, T_S, producing a contractile skin for the liquid surface that acts as an elastic membrane. When the surface is in mutual contact with a solid phase, the membrane assumes a concave curvature, forming a meniscus. The balance between adhesive forces, acting between solid and liquid phase, and cohesive forces in liquid phase define the shape of the curvature; in cases the first prevail on the latter, the contact angle between solid and liquid phase will be lower than 90°, producing a concave shape for the membrane curvature towards the liquid phase; this is the typical case for soil-water contact in partially saturated conditions. For simplified geometry, the tension in the surface membrane can be easily related to the differences of pressure (Δu) evidenced at the air-water interface; for the mechanical equilibrium of vertical forces in Figure 2.2 is found that:

$$\Delta u = -4\frac{T_S}{R_S} = -2\frac{T_S}{R_S} \tag{2.1}$$

In cases the contact angle (β) is lower than 90°, the air pressure is partly sustained by the meniscus, water pressure is lower than air pressure and, thus, Δu is a negative value. Referring this phenomenon to a capillary

tube with constant diameter (d) inserted into water under atmospheric conditions, the surface tension exerted at the solid-liquid contact is able to produce an increase in height to the water column, which could be calculated with the vertical force equilibrium as:

$$h_c = 2\frac{T_S}{\gamma_w R_S} \tag{2.2}$$

Where γ_w is the water specific unit weight.

Figure 2.2. Intermolecular forces on liquid particles (left); Surface Tension phenomenon at gas-liquid interface (right).

2.1.2 Liquid retention in capillary system

These simplifications could be a preliminary, but useful, guide for introduce the effect of surface tension in partially saturated soils. The diameter of the capillary (defined on the knowledge of R_S and β) tubes can be intended as the intergranular channels, which size is defined by the size of pores; by this, h_c in soils could be considered as the height above water table for which saturated conditions (only liquid phase filling intergranular pores), which is generally referred to the capillary fringe. Considering the soil structure as a system of capillary tubes with different diameters, the effect of reduction in saturation degree (S) could be analysed considering the simplified progressive scheme of Figure 2.3. The model could be referenced as a bundle of cylindrical capillaries, which represent an early conceptual model to express the liquid retention properties of partially saturated porous media (Millington and Quirk, 1961; Mualem, 1976). This convenient idealization of soil structure enable to link the capillary height to the water content in the system; it can be, so, also considered the drying process progression dependent on the diameter distribution of the system.

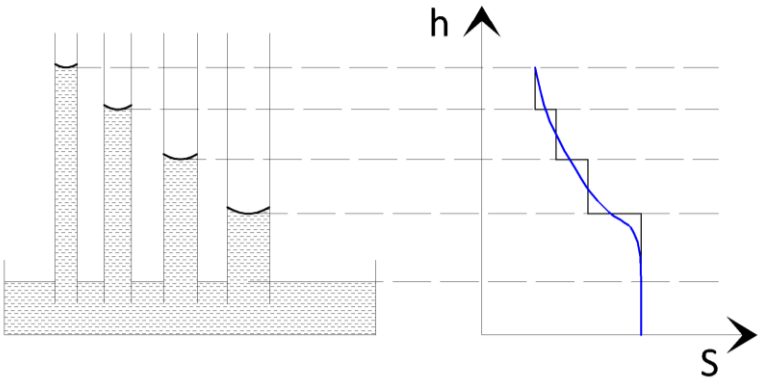

Figure 2.3. Increasing water tensions during evaporation in system of bundle capillary tubes.

Starting from a fully saturated condition, the first tubes found to desaturate are those characterized with low capillary height, higher diameter; initially, water pressure decreases with small variation in water volume. Variations in water content in the capillaries are, then, consistent with their diameters; with the evolution of the dying process, low variations of water content are associated to progressively higher variation in T_S values. The showed scheme could be intended as an elementary retention model for soils, for which the pores distribution have been idealized by a series of interconnected capillaries.

Still considering the scheme of Figure 2.2, surface tension associated to the membrane interface, places a reaction force on the wall of the capillary tube (intergranular pores, for soils), which vertical component results in a compression stress for the tube; the pressure differences between air and liquid phase (Δu), acting at their contact interface, so produces compression on the soil structure in the capillary zone, resulting in a reduction in volume and an increase in shear soil strength. This difference, acting at their contact interface, is generally referred to as soil matric suction, and represents a fundamental state variable for unsaturated soil both influencing hydraulic and mechanical properties of unsaturated porous media, as also has been schematically seen from the capillary models.

2.2 Water Retention Models for Unsaturated Soils

The determination of function expressing the relation between liquid volume and height in capillary system constitutes an essentially basic interpretation of the experimental hydraulic behaviour for partially saturated soils, for which an analogous corresponding model is represented by the water retention curves (SWRCs). These curves are the basic relations between matric potential and water content; their knowledge is fundamental in unsaturated soil physics studies with implications in a large number of applications, ranging from agronomy to geotechnical engineering, influencing plant water uptake and seepage, stress-strain, hydraulic and strength characteristics. The analysis of these curves reveals different states of saturation in a

soil, ranging from saturated to residual states, as showed in Figure 2.3. From 1 to 4, the soil experience the sequent states:

1) Saturated states, in cases negative pressure is generated in soil pores with degree of saturation equal to 1 (e.g. pores full of water);
2) Quasi-saturated soil states, as the soil desaturates from state 1), the negative pore pressure will cause the expansion of air cavities in larger pores; air phase is, therefore, still discontinuous in intergranular structure;
3) Partially saturated soil state, evidencing increasingly high (absolute) values with progression of drying process, characterized by continuous simultaneous presence of liquid and gaseous phase in pores;
4) Residual state, when liquid phase in pores is no longer continuous in pores; in this conditions, small variations in water content correspond to significant variations in negative pore pressure.

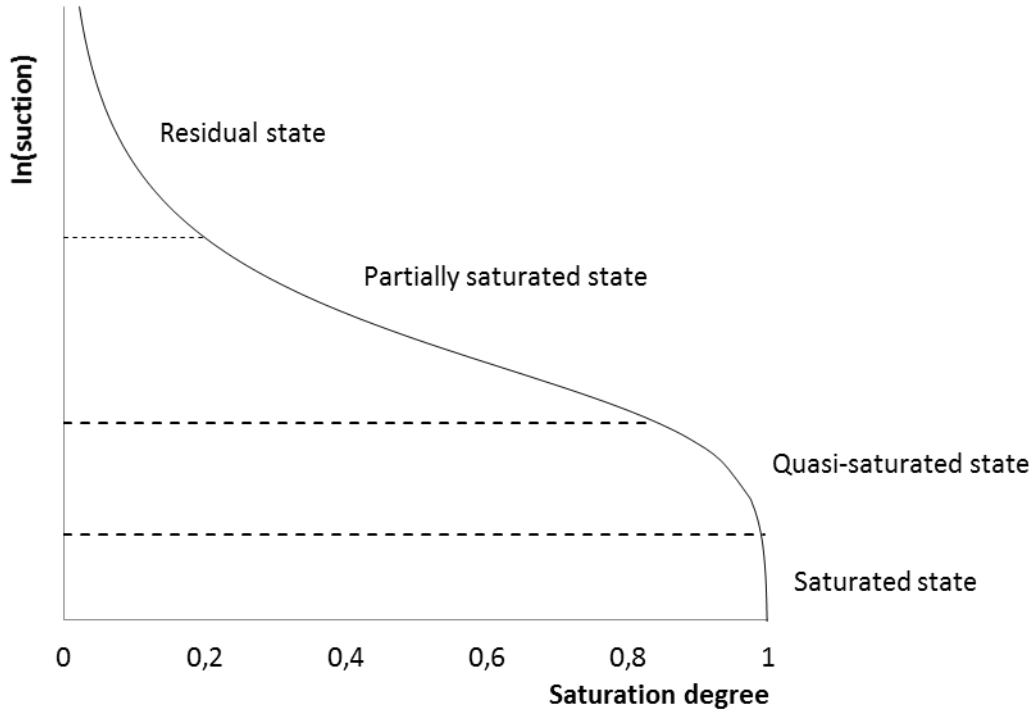

Figure 2.3. States of saturation for porous media.

The experimental soil water retention data are generally analysed by fitting numerical model able to relate soil water content to suction. In general, main requirements for widely-used model are the need of as few parameters as possible, conceivably with effective physical meaning in relation to main soil properties. In this sense, an effective and commonly mathematical model for describe soil water retention curves is represented by the van Genuchten-Mualem model (van Genuchten, 1980), often denoted as VG. The original

van Genuchten-Mualem model, widely diffused in engineering practice, provides effective saturation degree, S_e, starting from soil suction, s, and through the following equation:

$$S_e(h) = \frac{\theta - \theta_r}{\theta_s - \theta_r} = \left[\frac{1}{1 + \left(s / \alpha_{VG} \right)^{n_{VG}}} \right]^{m_{VG}} \quad (2.1)$$

Where θ, θ_s θ_r are the current, maximum and residual values of soil water content respectively, α_{VG} and n_{VG} are model parameter dictating the inflection point and the shape of the retention curve respectively. Note that some authors (Olivella et al., 2000) refer to the parameters αVG as the inverse of suction value at which the soil starts to desaturate (s_{AE}). The van Genuchten-Mualem model (VGM) here introduced, although his implementation in many geotechnical codes, has been demonstrated to being problematic when water retention data are used to predict the hydraulic conductivities (Vogel et al., 2001). Ippisch et al. (2006), in particular, evidenced that if n<2 or $\boldsymbol{\alpha}_{VG}$·se> 1, where s_e is the air-entry suction value of the soil corresponding to the largest pore radius, the van Genuchten-Mualem model leads to erroneous prediction on hydraulic conductivities. To avoid these errors, a specific air-entry value se should be included in a modified version of van Genuchten-Mualem model proposed by Ippisch (2006), defining S_c, as the saturation degree at the air-entry potential s_e, leading to:

$$S_e(h) = \begin{cases} 1 & s < s_e \\ \frac{1}{S_C} \cdot \left[\frac{1}{1 + \left(s / \alpha_{VG} \right)^{n_{VG}}} \right]^{m_{VG}} & s > s_e \end{cases} \quad (2.2)$$

Where S_c is the saturation degree at the air-entry potential s_e.

In general, the relationship between Saturation degree and soil suction is not univocal (Jaynes, 1984; Pham et al., 2005), but depends on the types of hydraulic process, distinguishing basically between drying and wetting paths; this reveal the hysteretic behaviour of soil when variation in water content is experienced with reduction (drying) or increase (wetting) in water content in the pore space (θ). A “main drying” and “main wetting” curves mark a region in the retention domain of possible states for soils, e.g. attainable pairs for soil suction – water content. Among this domain, a wide range of scanning paths define the hysteretic

region. Soil retention hysteretic behaviour is represented in Figure 2.4, where main drying, main wetting and scanning paths are together plotted. The main effect of soil hydraulic hysteresis is the so-called ink-bottle effect, and can be even equivalently considered in capillary system in case variable diameter along height is considered for each, or part, of the tubes. Due to the existence of hysteresis, unsaturated seepage and strength soil properties could be significantly affected. However, this soil issue is commonly ignored in cases of insufficient soil characterization on hysteretic behaviour and to simplify seepage analyses; however, considering that hysteresis in retention curve may generate inaccurate predictions of the distribution of pore pressure and saturation degree, even in advanced applications (Tsaparas et al., 2002; Le et al., 2012) is generally assumed main drying curve to represent the soil retention behaviour.

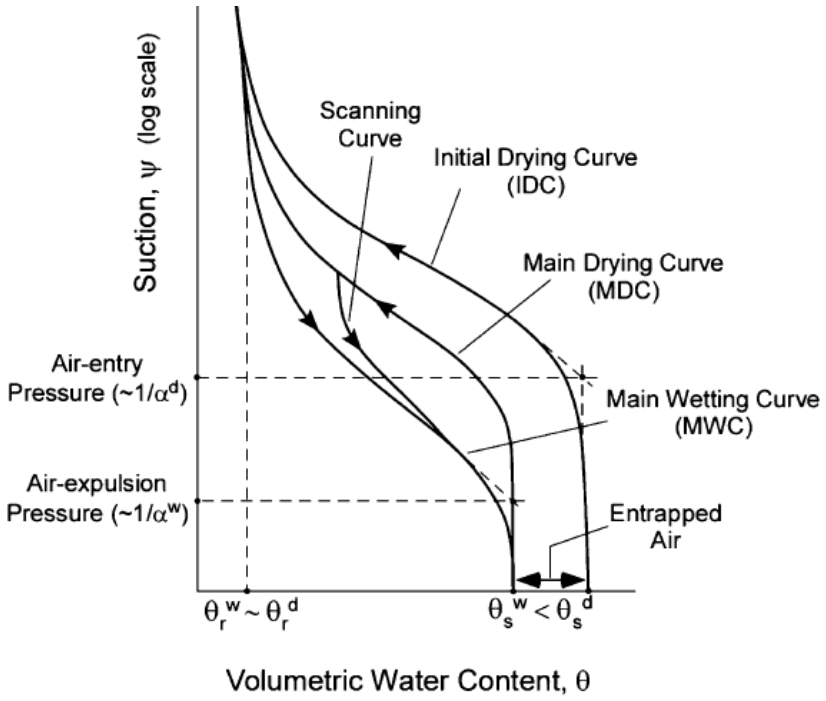

Figure 2.4. Soil water retention hysteretic behaviour.

2.3 Numerical modelling of the hydraulic and stability characteristic for river embankment

2.3.1 Seepage analysis for river embankment

A fundamental step for a reliable assessment of an embankment stability conditions is a proper definition of the pore water pressure and suction distribution, which represent an integral component of the stress state within the soil, consequently influencing the mechanical behaviour of the soil other than its hydraulic response. In general, water flow in soils is driven by energy gradients associated with the total head,

represented by the components of pressure head and elevation of the particle of fluid. Variation in values of pore-water pressure, whether positive or negative, can be induced by different stress of environmental or anthropic origin, e.g. river flood, high-water event sequences, rainfall and evapotranspiration, fluctuation of the water table height, realization of water reservoir. All these situations can be properly implemented and accounted in numerical calculation by the definition of appropriate hydraulic and climatic boundary and initial conditions for the model. The governing equation to express 2D flow for unsaturated and saturated soil considered in the present study is based on mass conservation assumption, considering rigid soil skeleton and no volume change during the seepage, and is expressed in its incremental form in the following expression:

$$\frac{\partial}{\partial x}\left(k_x \frac{\partial h}{\partial x}\right) + \frac{\partial}{\partial z}\left(k_z \frac{\partial h}{\partial z} + k_z\right) = C(h)\frac{\partial h}{\partial t} \tag{2.8}$$

Where k_x and k_z represent the soil hydraulic permeability in x and z directions, respectively, h is the total hydraulic head, t is the time and C(h) is the specific water capacity (i.e. the slope of soil-water retention curve) and is represented as the partial derivate of soil water content respect to total head (∂θ/∂h); this last term varies between -∞ and 0, and can reach significantly high negative values for soil characterized by uniform pore size distribution, and is highly non-linear with h, complicating the solution of the problem (Benson, 2007). The unsaturated flow equation is expressed as in the “h-based” formulation, which is a common choice in practical and advanced numerical calculation, which solutions are applied to the spatial domain using Finite Difference and Finite Element methods; however, have been observed that this approach provides large mass balance errors for many example calculations and different iteration method if considering simple one-step Euler time-marching algorithm, although FE errors are generally inferior to DE (Celia et al. 1990). A modified numerical approach for time-stepping, aiming to reduce significant implications, have been adopted for the analysis presented in the next chapter, for which the change in total heads in each node is used to determine a variation in time-step amplitude among a specified range, in order to reduce the convergences problems related with the mass balance solutions (Geo-Slope International Ltd 2008). The same description of mass conservation can be used for heterogeneous soil with an appropriate selection of hydraulic conductivities at each location (Gui et al. 2000). Results of the numerical calculations are expressed as the groundwater flow process, and could be described using different kind of terms adequate to describe the characteristics of the problem; e.g. piezometric head, liquid velocity, cumulative water flux, flow gradient, all computed in the nodes where the solution to the problem has been found. Historically, analyses of groundwater seepage have focused on saturated soils conditions, generally assuming a specific hypothesis on the confinement of the flow, specifying the transition surface from positive to

negative pore water pressure as an upper boundary and ignoring any flow above the phreatic line. These operative conditions have been gradually overcome for the resolution several problems in geotechnical engineering where the definition of unsaturated unconfined flow properties is strongly impacting on the final results. One of the overcited problems is certainly represented by the water seepage through a soil water retaining structure, hereafter discussed with specific reference to river embankments; however, even being the operating conditions of large part of the riverbank influenced by unsaturated soil conditions and being the flow properties strongly time-dependent even during the same high-water event, the evaluation process for the definition of pore water pressure and suction to be used in design pass through the simplified hypothesis of saturated soil conditions and steady-state seepage in equilibrium with a prescribed river level. In order to overcome these assumptions, however, a significant number of information are required, concerning the unsaturated soil hydraulic and retention parameters, the definition of the initial conditions to be used for numerical calculation and the specific knowledge on the boundary conditions to be assigned to the problem, that are not frequently available not only in common practice but also in detailed design stage. Purposes for the present thesis is to define a methodology to restrict the data required for a reliable definition of the hydraulic response of a riverbank exposed to potential flood event, induced by a series of high water event, and underline the importance of a proper monitoring river embankment evidencing the effect of different initial conditions on the stability assessment. The procedures developed to achieve these target, from one side, required the definition of several stage of analysis characterized by a different degree of sophistication, that aim to deal with the various problem discussed in this study in order to get a series of solution that should be preferred respect to the hypothesis of work actually defined, and the description of soil suction and water content probes implemented in field for different applications, from the other side. In the context of the present thesis, a series of transient unsaturated seepage analysis have been performed for a 2D numerical model for a real river embankment by means of the software SEEP/W (Geo-Slope International Ltd, 2008), aiming to set the preliminary framework for the stability assessment of river embankment under variable hydrometric conditions, presented and discussed in Chapter 3.

2.3.2 Atmospheric coupling

Soil-atmosphere interaction processes are fundamental for a proper determination of the prediction of the suction and water content condition in the vadose zone, which width depends on the incidence of the climatic boundary condition on heat and water flux in soil surface. The accuracy of this evaluation process has frequently a significant implication in the determination of seepage and stability for geotechnical problem extended to larger scale than the active zone; this is certainly the case of water retaining structures, where the variable persistence of high water level affect the progression of the phreatic line in the riverbank is however influenced by the soil suction (and water content) distribution near the ground surface, influencing

soil hydraulic and mechanical response to external stress. In order to properly take into account the surface boundary conditions under variable climatic conditions, a series of two-dimensional finite element analysis was performed coupling ground heat, liquid and vapour flow with the numerical code VADOSE/W (Geo-Slope International Ltd, 2008), focusing on the determination of the magnitude of surface infiltration and actual evaporation as surface unit flux. It is well known that the rate of actual evaporation (AE) is only equal to the potential evaporation (PE) rate when the soil is saturated, while the AE rate starts to decrease as the soil desaturates at its surface. Atmospheric coupling is achieved by calculating the soil evaporative flux as follows:

$$\text{AE} = \frac{\Gamma Q + \upsilon E_a}{\upsilon A + \Gamma} \tag{2.9}$$

where AE = actual evaporative flux, Γ = slope of the saturation vapour pressure versus temperature curve at the mean temperature of the air, Q = net radiant energy available at the surface, E_a = evaporative parameter dependent on wind speed, surface roughness, and eddy diffusion, υ = psychrometric constant, and A = inverse of the relative humidity at the soil surface. This formulation (Wilson, 1990) extend the unsaturated conditions the conventional Penman method (Penman, 1948) while calculating the evaporation from soil surface, accounting for net radiation, wind speed, and the relative humidity as boundary condition for the model. The relative humidity of the soil surface is evaluated by simultaneously solving the rigorously coupled moisture and heat flow equations also considering the vapor flow component, ensuring that all moisture flow is not overthrown when the soil hydraulic permeability decreases due to drying. The governing differential equation for the 2D hydro-thermal seepage can be expressed as:

$$\frac{1}{\rho}\frac{\partial}{\partial x}\left(D_v \frac{\partial P_v}{\partial x}\right) + \frac{1}{\rho}\frac{\partial}{\partial z}\left(D_v \frac{\partial P_v}{\partial z}\right) + \frac{\partial}{\partial x}\left(k_x \frac{\partial\left(\frac{P}{\rho g}+z\right)}{\partial x}\right) + \frac{\partial}{\partial z}\left(k_z \frac{\partial\left(\frac{P}{\rho g}+z\right)}{\partial z}\right) + Q = \lambda \frac{\partial P}{\partial t} \tag{2.10}$$

Where P = soil water pressure, P_v = soil moisture vapor pressure, k_x and k_z represent the soil hydraulic permeability in x and z directions, Q is the applied boundary flux, Dv is the vapor diffusion coefficient described by Wilson (1990), z is the position head, ρ is the water density, g is the gravity acceleration and t is the time. For heat transfer, the 2D governing equation can be expressed in differential form as:

$$L_v \frac{\partial}{\partial x}\left(D_v \frac{\partial P_v}{\partial x}\right) + L_v \frac{\partial}{\partial z}\left(D_v \frac{\partial P_v}{\partial z}\right) + \frac{\partial}{\partial x}\left(k_{tx} \frac{\partial T}{\partial x}\right) + \frac{\partial}{\partial z}\left(k_{tz} \frac{\partial T}{\partial z}\right) + Q_t + \rho c V_x \frac{\partial T}{\partial x} + \rho c V_z \frac{\partial T}{\partial z} = \lambda_t \frac{\partial T}{\partial t} \tag{2.11}$$

Where ρc is the volumetric specific heat value, k_{tx} and k_{tz} represent the soil thermal conductivity in x and z directions, V_x and V_z represent the pore water velocity in x and z directions, Q_t is the thermal boundary flux and L_v is the latent heat vaporization. The equations state that the global rates of change of flows with time is equal to the rate of change of the volumetric water or heat contents, net of the external applied flux. The mass transfer equation can be derived directly from the Richards equation for transient flow in unsaturated soils with adaptations for vapor flow added by Wilson (1990) with a modification proposed by Milly (1982). The seepage flow law is expressed as functions of pore water pressure for a direct coupling of the heat and mass conservation equations. The heat transfer law is a standard Fourier equation for conductive heat transfer with modifications for the inclusion of vapor transfer and convective heat transfer due to flowing water. VADOSE/W does include the vapor flux component in its steady-state formulation, which is only used for the determination of the initial conditions for the subsequent transient climate coupled analysis. If net infiltration rate is such that pore water pressure at the surface layer turns to be positive, then the runoff is activated by the solver and its quantity is estimated to compute zero values for pore water pressure at the ground face due to infiltration; the volume of water that seeps out or do not infiltrate is generally ignored in the subsequent calculation, in order to avoid ponded zone. Examination of the governing heat and mass transfer equations reveals that there are three unknown parameters, pore water pressure (P), temperature (T), and vapor pressure (Pv). In order to solve the equations, a third relationship between these parameter is necessary, which is expressed in the sequent form:

$$\nabla P_v = d_1 \nabla(-P) + d_2 \nabla T \tag{2.12}$$

Where d_1 and d_2 are model parameters depending on the saturated vapor pressure of free water, molecular mass of water vapor and relative humidity of air. The use of atmospheric coupling in seepage analysis here constitutes the main theoretical and numerical tool for the determination of pore water pressure and suction distributions for river embankments; presentation and discussion on results constitute a significant part of Chapter 4 to 7, which are then primarily devoted to safety assessment for river embankment procedures.

2.3.3 Slope stability assessment

The definition of stress-state in soils, its mechanical behaviour by means of constitutive modelling in association with proper failure criteria, allows to perform analytical and numerical calculations for the evaluation of safety conditions towards various collapse mechanisms. These procedures also need the definition for the triggering and, in some case, propagation of failure, that could be defined in terms of stress, deformation or their proper combination. Various failure mechanisms, including erosion, piping, overtopping

and overall stability, can arise simultaneously leading to collapse. The research activity here discussed and presented is focused on the stability conditions evaluation of partially-saturated riverbanks. Generally, for slope stability analysis the tools to be used are dependent on the type of available information on input parameters and initial and boundary conditions for the model. When Finite Element method is used to define pore water pressure, suction and stress distribution in soils, among the most suitable and common choices for safety analysis are Limit Equilibrium Methods (LEMs) and Strength Reduction Method (SRM); both procedures are implemented in different numerical codes, evidencing significant differences on their effective operation. Among the first uses of SRM are related to the definition of collapse loads for associated and non-associated plasticity law, applied to different case studies dealing with axisymmetric compression between rough plates (Davis, 1968), idealized homogeneous and composite embankment or excavation (Zienkiewicz et al., 1975), and then found large application and optimization for several geotechnical applications, as the case of slope stability analysis (Dawson et al., 1999; Pham et al., 2003; Zheng et al., 2009). Basically, the SRMs are based on the progressive reduction of soil strength properties until failure occurs; the ratio between initially available strength and strength at failure is generally defined as a Safety Factor for the found collapse mechanism and, unlike limit equilibrium methods, no restrictive assumptions need to be made on the shape or location of the failure surface or direction and module for lateral inter-forces, while the collapse mechanism may assume any profile. Nonetheless, this feature could also restrict the possibility to explore different, complex and user-defined, collapse mechanisms for the same problem, limiting the operational activities for extended and differentiated hazard and risk assessments and providing most time-consuming solutions. LEMs, otherwise, are based on the idea of discretizing a potential, and preliminary defined, instable mass into various elements, or slices, and use the theory of limit equilibrium of forces and moments to evaluate a factor by which the soil resistance should be reduced in order to lead the mass to a prescribed limit equilibrium along a selected location, defining the safety factor for incipient collapse conditions. A first complete model for the Limit Equilibrium Analysis for slopes, with particular reference to earth dams, was introduced by Fellenius (Fellenius, 1936) as the Ordinary or Swedish method of slices, even if in 1916 Patterson (1955) presented an application for the stability assessment of the Stigberg Quay in Gothenberg, Sweden, where the slip surface was taken to be circular and the sliding mass was divided into slices. Several comparisons have been proposed and discussed for results obtained using LE and SR methods, generally leading to good agreement in terms of critical slip surfaces location, but often revealing slight differences on the Safety Factor determined which are usually lower for LEM (Duncan, 1996; Griffiths et al., 1999; Liu et al., 2015). Although there seems to be some consensus that not all LE method provides reliable results, textbooks continue to describe all them in some details, and the wide selection of available methods is at best confusing to the potential user, enhancing an undeservedly their bad reputation (Lambe & Silva, 1995). In this study, Limit Equilibrium Analysis for the stability assessment of river embankment under variable external hydraulic and climatic conditions, will be performed by means of Morgenstern and Price

Method (Morgenstern and Price, 1965) using the numerical code SLOPE/W (Geo-Slope International Ltd, 2008). Newton-Raphson numerical technique is used to solve the moment and force equilibrium equations for the Safety Factors determination, basing the solution on the sum of tangential and normal forces to each slice, assuming a user defined mathematical function to describe the direction of interslice forces both for circular and composite shapes for slip surfaces. The general Limit Equilibrium solution scheme, with reference to Figure 2.5, define two factor of safety, obtained from moment and forces equilibrium equation, which could be respectively expressed as:

$$F_m = \frac{\Sigma\left[c'\beta R+(N-u\beta)Rtan\varphi'\right]}{\Sigma W_x-\Sigma Nf+\Sigma kW_e\pm\Sigma D_d\pm\Sigma A_a} \quad (2.13)$$

$$F_f = \frac{\Sigma\left[c'\beta cos\alpha+(N-u\beta)tan\varphi' cos\alpha\right]}{\Sigma N sin\alpha+\Sigma kW-\Sigma D cos\omega\pm\Sigma A} \quad (2.14)$$

Which are nonlinear equation since the normal force at the base of each slice, N, is in turn a function of the factor of safety and could be derived from the sum of forces in vertical direction on each slice, obtaining the nonlinear equation:

$$N = \frac{W+(X_R-X_L)-\left[\frac{c'\beta sin\alpha-u\beta tan\varphi' sin\alpha}{F}\right]}{cos\alpha+\frac{sin\alpha tan\varphi'}{F}} \quad (2.15)$$

Where F is equal to F_m, when solving moment equilibrium and equal to F_f when solving force equilibrium. The base normal equation cannot be solved directly, since the general factor of safety and the interslice shear forces are unknown; consequently, N needs to be determined using interactive scheme aiming to converge to a unique value for factor of safety.

Once the interslice normal force is known, the interslice shear force is computed as a percentage of the interslice normal force according to the empirical equation proposed by Morgenstern and Price (1965):

$$X = E\lambda f(x) \quad (2.16)$$

Where f(x) is a the interslice forces functions functional relationship, which describes the manner in which the magnitude of X/E varies across the slip surface and λ is a scaling constant which represents the percentage of the function, f(x) used for solving the factor of safety equations. Typical functions for f(x) are half-sine, clipped-sine, trapezoid or fully specified; when the interslice forces function turn to be constant, the Morgenstern and Price Method is referred as the Spencer Method. In Figure 2.6 is, then, showed how the half sine function and λ are used to designate the direction of the interslice forces. For a more detailed description of all stability assessment methods above introduced, and their comparisons, a large number of references can be found in literature (Fredlund, 1974; Fredlund and Krahn, 1976; Abramson, 2001), which may overlook the main targets of the present thesis.

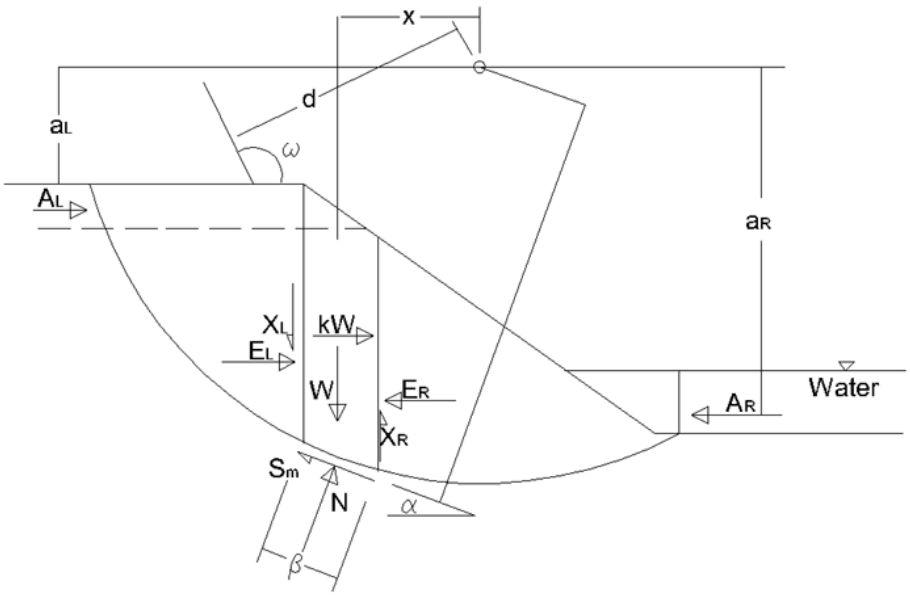

Figure 2.5. Forces acting on a slice through a sliding mass with a circular slip surface

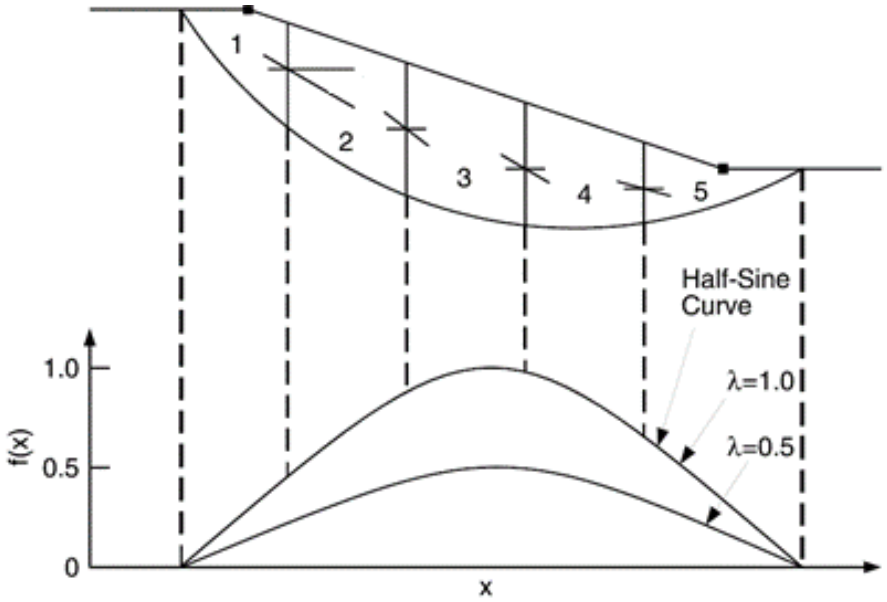

Figure 2.6. Side force designation for the Morgenstern and Price Method.

It's, however, here worth to notice that the relation between the various LE methods remain similar whether the failure surface is circular or composite, and that both Spencer (Spencer, 1967) and Morgenstern and Price Method (Morgenstern and Price, 1965) are often referred as the most reliable and widely used in geotechnical engineering practice (Griffiths et al., 1999; altre reference). However, in the following of the present work, minor importance will be devoted to the comparison between results obtained for different Limit Equilibrium or Strength Reduction methods, instead aiming to study in specific the effect of retention soil properties of partially saturated soils for the stability analysis of river embankments with reference to different hydraulic conditions and considering LEM as the basic procedure for stability assessment of river embankments.

2.4 Applied mathematical tools for probabilistic analysis

One of the main issue when using mathematical procedure for safety assessment in engineering problems is generally to deal with small probabilities of failure with the need to simulate rare events. The diffused use of numerical simulation establishes the possibilities to obtain a large number of solutions for different types of outcomes; with the specific reference of riverbank and water retaining structures, the most useful outcomes are relative to seepage and stability analysis, generally referring to hydraulic gradient, pore water pressure, suction and soil water content in various control nodes of the model domain, and to safety factors for different shapes of the critical slip surfaces. This opportunity lead to the large use of probabilistic tools for the study and description of results, even considering that soil heterogeneity and uncertainties related to

parameters estimation are significant and intrinsic for the studied problem, as for several geotechnical applications. For this reason, the practice and adaptation of various mathematical methods for describing the input data variability and the outcomes interpretation need a specific note in the theoretical background of this work. Among the various approaches and procedures discussed in literature (Baecher and Christian, 2003; Congdon, 2007; Griffiths and Fenton, 2007; Phoon, 2008), for the probabilistic study of seepage and stability analysis discussed in the following section, the Monte Carlo Method and Point Estimate Method (Rosenblueth, 1975) have been used. Substantial differences characterize these methods, on the side of computational efforts, implementation in numerical codes, significance and interpretation of outcomes. The MC method is, generally, based on a large number of deterministic analyses, and remarkable accuracy in outcomes is only achieved if the number of trials is of sufficient magnitude; thus, when the model computation is time-consuming (as for long-lasting seepage or hydro-thermal flow analysis), the Monte Carlo Simulation would not be practical for various uncertainty propagation studies (Park et al., 2012). Furthermore, the MCM requires the specification of the marginal distributions of the random variables which represent the model input parameters. Under such circumstances, PEM often constitutes a more practical alternative requiring only statistical moments of probability distribution for the input random variables to be applied, and significantly lower computational efforts (Ahmadabadi and Poisel, 2015), giving a statistical procedure applicable when low number of observation are required. In the following, brief notes on features and requirement for the two methods are presented and discussed.

2.4.1 Monte Carlo Method

The Monte Carlo method is a simple, but versatile computational procedure that is suitable when computational efforts in analysis can fit with time requirements for the considered application. It is generally considered as the most robust method used for the probabilistic analysis of geotechnical structures for the safety assessment; however, care should be always taken on the implementation procedure and on the actual efficiency in estimating small probabilities in relation to the amount of calculation required (Hurtado and Barbat, 1998; Müller, 2013; Benjamin and Cornell, 2014). Taking the name from the famed randomness of the gambling houses of Monte Carlo, the method proceeds in the hypothesis that by taking as many observations from the input data, the stochastic characteristic of the outcomes can be estimated. Once defined the probabilistic characteristics of the raw data, in terms of statistical estimators, the solution of a generic problem to the random input produced by numerical or random field generators is evaluated; this procedure is executed and repeated for as many times as are feasible, recording the response and counting the number of occurrences for a particular response observed. Monte Carlo simulations essentially replicate an experimental or numerical process, and are representative for computed results, whose accuracy is dependent on the representativeness of the set of trials to the real conditions. In theory, the method is a

reasonable procedure to be used in large and complex systems, often able to remove schematic and preventive conceptualizations typical for analytical solutions. However, in practice, Monte Carlo Method, other than being limited by constrains of computational and times efforts, cannot provide results accountable for generalization or extrapolation, and should be used in cases analytical solutions are not available, or ineffective, or approximate and require verification or validation (Fenton, 2014). In the framework of this thesis, Monte Carlo procedure have been used in combination with Limit Equilibrium analysis for the numerical determination of the low-order statistical moments of the safety factor distributions; the method, as implemented in SLOPE/W, account for a wide range of parameters to be considered as random variables, including soil strength and physical parameters and pore-water pressure distributions. As in the basic of the method, the statistical dispersion defined for each random variable parameter is used for the sampling procedure at each trial. If a large number of statistical variable is considered simultaneously in the analysis, the reliability of the safety factors distribution computed is consequently reduced if considering the same amounts of calculations, with the effect to smooth out the range of variability and with a general decrease in the probability of failure. In SLOPE/W, one or more most critical slip surfaces are first determined based on deterministic analysis performed using the mean value of the input parameters. Probabilistic analysis is then performed on these critical slip surfaces, taking into consideration the variability of the input parameters, thus leading to the evaluation of a reliability index β and the probability of failure Pf of the slope, given by:

$$\beta = \frac{\mu_{SF}-1}{\sigma_{SF}} \tag{2.17}$$

$$P_f = \frac{N_f}{N_{tot}} \tag{2.18}$$

where μ_{SF} is the mean value of the safety factor, σ_{SF} is the standard deviation of the safety factor, N_f is the number of failures (how many times SF < 1), N_{tot} is the total number of simulations, all referred to each critical surface individuated by deterministic analysis. This procedure, however, suffer for two significant issues which do not theoretically guarantee a proper the estimation of the safety assessment in cases critical slip surfaces are not predetermined and various shape for similar collapse mechanism should be investigated. Firstly, it should be considered that, once defined the geometric constrains and locations for slip surfaces to be tested, probabilistic seepage analysis should be performed for all possible mechanism or, at least, for a large number of cases; in fact, especially when stratigraphy is characterized by several layer sequences and soils parameters variability could suffer significant differences in variance, the most critical slip surfaces when considering deterministic and probabilistic analysis could not be in correspondence, leading to a possible unsafe estimation of the probability of failure when computational efforts is limited. Furthermore, at each

considered trials, the critical slip surfaces are probably to be considered variable in dependence of the sampled variables, and not supposed fixed; the analytical calculations would produce, then, safety factors distributions characterized by higher values for both μ_{SF} and σ_{SF}, producing results in terms of β and P_f which effective trustworthiness can be matter of discussion and debate. Indeed, for problems where a single calculation of Safety Factor is time consuming, e.g. in case the determination pore water pressure, suction and stress distributions in soil requires detailed Finite Element Analysis, Monte Carlo Method may be infeasible. As also mentioned before, for problems with small failure probability, MCM requires a noteworthy number of sampling in order to obtain a reliable estimation for N_f compared to N_{tot}; fundamental is, so, the importance of randomly generated input parameters used for each trial.

2.4.2 Point Estimate Method

The original formulation for Point Estiamate Method was presented by Rosenblueth (Rosenblueth, 1975) as a procedure for numerical approximation of the statistical moments of functions of random variables; even being classified among the simplified uncertainty propagation methods, the Point Estimate Method represent a powerful tool for many geotechnical application, significantly rigorously based, requiring limited computational efforts and characterized by relatively high accuracy (He and Sällfors, 1994; Baecher and Christian, 2003). In general, the applicability of the method is based on the existence of one, or more, random variables $X_{1...i}$, for which the probability distribution function, PDF, is assigned and on the dependence of a second class of variables, $Y_{1...j}$, which could be expressed by a deterministic relation $Y_{1...j} = f(X_{1...i})$. For geotechnical application, $X_{1...i}$ could be referred as a physical, mechanical or hydraulic soil properties, an external load or a geometry factor, while $Y_{1...j}$ could be the generic outcome for stress-strain, seepage or stability analysis as settlement, quantity of flow or safety factor. Working with the hypothesis that $f(X_{1...i})$ is fully defined and that the probability distributions for $X_{1...i}$ are assigned and their statistical moments exist up to the n^{th} order, the method aim to define by analytical approximation the low order moments of PDF for $Y_{1...j}$ basing on the knowledge on the low order moments of the PDF of $X_{1...I}$ and on the functions $f(X_{1...i})$. Practically, the method consists in replacing the continuous random variables $X_{1...i}$ with discrete random variables, which estimation and relative weights can be evaluated on the basis of statistical moments of continuous random variable such as mean, variance and skewness factor. Considering these discrete values for calculation, a series of $Y_{1...j}$ values are determined, through the $f(X_{1...i})$ function, and then used to define the statistical moments of the PDF for the various $Y_{1...j}$. The original PEM allowed the equivalency of the first three statistical moments (mean, variance and skewness coefficient) only for the case of a function of one random variable, which consisted for a great limitation together with the requirement of 2^N calculations for multiple variables problems; still Rosenblueth (1975) proposed a technique for reducing the number of calculation points to 2N+1 when the random variables are uncorrelated and skewness is ignored. More recently, developments of

the method lead to procedures requiring number of points estimation to 2N (Harr, 1989) or 2N+1 (Hong, 1998) even for general cases in which multiple, correlated variables are considered even accounting for skew parameter, representing significant improvement in the sampling techniques which refined, in turns, considerably the accuracy for the high-order moments of the analysis outcomes (Napa-García et al., 2017). Consequently, the accuracy of reliability estimation based on discrete sampling is comparable with that of the analytical methods for simple performance functions (Franceschini et al., 2012), founding wide application in the field of geotechnical engineering and in the computation of reliability statistics (Phoon, 2008). A brief description of the method and discrete sampling procedures, with specific reference to the procedure then implemented for the numerical analysis discussed in Chapter 7, is given below.

Let $f(X)=f(X_1, \ldots, X_N)$ be a function of N correlated and skewed random variables. The first three statistical moments (mean, standard deviation and skewness coefficient) and the correlation structure of random variables are known. The method firstly defines the point estimate locations through the statistical moments of the random variables. For each random variable two-point estimate locations are evaluated (Figure z), according to following relations:

$$X_+ = \mu_X + \left[\frac{\nu_X}{2} + \sqrt{1 + \left(\frac{\nu_X}{2}\right)^2}\right]\sigma_X \tag{2.19}$$

$$X_- = \mu_X + \left[\frac{\nu_X}{2} - \sqrt{1 + \left(\frac{\nu_X}{2}\right)^2}\right]\sigma_X \tag{2.20}$$

where μ = mean, σ = standard deviation, ν = skewness coefficient. At the next step, the method associates the following weights to point estimate locations previously defined:

$$P_+ = \frac{1}{2}\left[1 - \frac{\nu_X}{2}\frac{1}{\sqrt{1+(\nu_X/2)^2}}\right] \tag{2.21}$$

$$P_- = 1 - P_+ \tag{2.22}$$

For a function of N random variables, the method provides 2N point estimate locations, resulting from all possible combinations of point estimate locations of the random variables. The weight associated to general combination ($X_{1\pm}$, $X_{2\pm}$, …, $X_{N\pm}$) is defined as:

$$P_{\pm\pm\cdots\pm} = P_{1\pm}P_{2\pm}\dots P_{N\pm} + \sum_{i=1}^{N-1}\sum_{j=i+1}^{N}(\pm)_i(\pm)_j a_{ij}P_{ij} \quad (2.23)$$

where $a_{ij} = \rho_{ij}\,(P_i+P_i-P_j+P_j-)0.5$, ρ_{ij} = correlation coefficient between the random variables X_i and X_j, $P_{ij} = P_{1\pm}P_{2\pm}\dots P_{k\pm}\dots P_{N\pm}$ ($k \neq i$ and $k \neq i$). The statistical moments of the function f(X) can be estimated as follows:

$$E[f(x)^m] \approx \sum_{j=1}^{k} P_j f\left(X_j\right)^m \quad (2.24)$$

where k is the number of point estimate locations, P_j is the weight associated to combination j, $f(X_j)$ is the function evaluated at point estimate location j. The mean and the variance of the function f(X) can be then estimated according to the following relationships:

$$\mu_{f(X)} = E[f(x)] \quad (2.25)$$

$$\sigma^2_{f(X)} = E[f(X)^2] - (E[f(x)])^2 \quad (2.26)$$

Therefore, the reliability index β and the probability of failure P_f can be evaluated as follows:

$$\beta = \frac{\mu_{SF}-1}{\sigma_{SF}} \quad (2.27)$$

$$P_f = 1 - \Phi(\beta) \quad (2.28)$$

where Φ denotes the cumulative distribution of standard normal random variable. A Normal probability distribution of the safety factor is then assumed in order to obtain the probability of failure. A simplified graphical representation of the PEM as described above is reported in Figure 2.7.

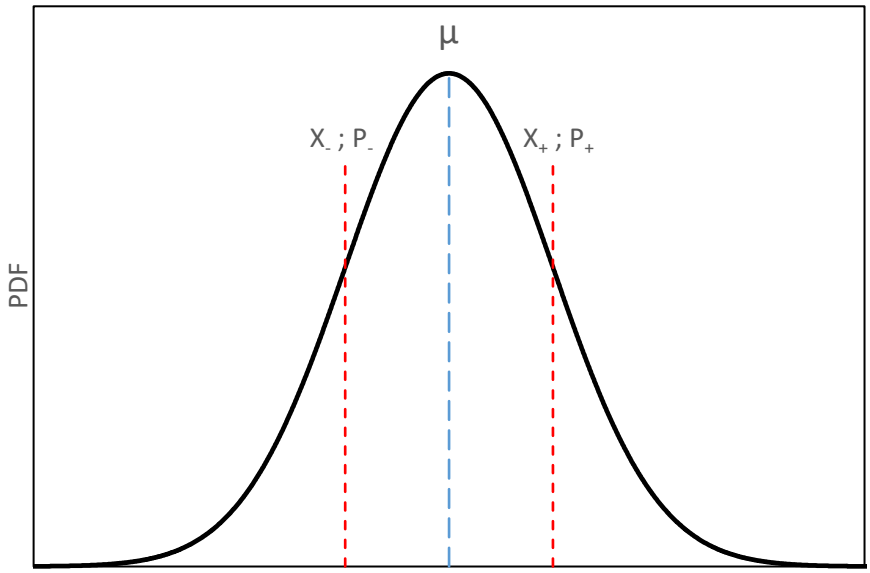

Figure 2.7. Simplified graphical representation of the PEM with the assumption of normal probability distribution function.

2.5 Laboratory measurement of soil water retention curve

Hydraulic models used for numerical calculation should be adequate to represent the specific behaviour of soil in the considered conditions (in terms of soil water content, pore water pressure and suction values and their range of variability in the problem), but even on the possibility to properly define all parameters required. The use of advanced models, in fact, often require advanced laboratory test to be completely defined, in addition to the need to be implemented in standard numerical codes for standard and advanced practice. In example, the use hysteretic retention model for transient seepage analysis is certainly more representative than the case in which only drying or wetting or scanning curves are used to represent the relation between soil suction and water content; however, rather than not being available for different numerical software, a fully comprehensive hysteretic model actually evidence limitation related to the difficulties to define all the required parameters required and their variability for significant soil volumes. In this paragraph, mention to the determination of soil water retention curve using laboratory test are briefly presented and discussed; additional details on results interpretation are given in Chapter 3 (Geotechnical characterization). Usually, soil water retention curves parameters can be estimated directly, by laboratory or in situ measurements, or indirectly, by means of pedotransfer functions. The latter, known as indirect

methods, are regression equations developed by employing large soil retention measurement databases (Twarakavi et al., 2009), allow estimating the retention parameters using knowledge on soil texture, bulk density, organic matter (Vereecken et al., 2010) and are gathering large diffusion, especially in absence of direct measurements and for increasing demand for soil unsaturated characterization at large scale, such as catchment and regional-scale. Obviously, their reliability depends largely on the quality of the SWRCs input databases, many of which were measured using pressure plate apparatus. The reference methods for water retention curves determination are, however, mainly based on laboratory tests results, while in situ measurements are typically used in conjunction with above quoted methods.

The idea of using evaporation data to determine unsaturated soil hydraulic properties was introduced by Wind (1964) and then slightly modified by several authors (Tamari et al., 1993; Wenderoth et al., 1993; Peters et al., 2008). The experiment is run by drying the soil sample, initially at saturation, measuring the evaporative water loss from the top by weighing the sample; matric suction is simultaneously monitored at various soil depths with tensiometers (Figure 2.8). On conclusion for the evaporation experiment the soil sample is dried at 105°C and weighted to calculate oven-dry bulk density. The strength of the evaporation experiment is that soil hydraulic properties are assessed from data gathered during a transient flow, which is very close to natural process occurring in subsurface soils, thereby estimating highly representative hydraulic properties of the porous medium under study (Romano and Santini, 1999).

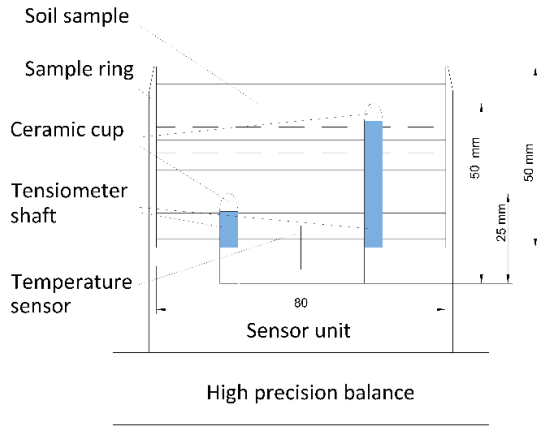

Figure 2.8. Sketch for laboratory equipment used to perform evaporation test.

The value of initial, constant evaporation rate does not depend primarily upon the hydraulic properties of the soil sample. As the local values of water content near the soil surface reduce, the duration of this initial stage is controlled by the possibility that the corresponding decrease in hydraulic conductivity is offset by increases in the gradients of pressure head. As the soil near the upper surface becomes drier, water can no

longer be delivered at the rate demanded by the external environmental conditions, and therefore the condition of a constant evaporation rate cannot be maintained any longer. Past researches (Toker et al., 2004; Delage et al., 2006) has shown that during evaporation, a very dry layer of low hydraulic conductivity would develop quickly near the soil surface, making the further increase in suction below this surface much harder, introducing inaccuracies due to lack of equalization through the sample. This would hence create a highly nonlinear suction profile along the soil column. The stage drying procedure is, so, expected to yield the most accurate results as the suction is measured after the sample has achieved equalization. On the other hand, continuous drying tends to be faster and simpler but it is likely to introduce inaccuracies due to the lack of equalization through the sample. These inaccuracies depend on factors such as sample size, shape, extent of surface exposed to drying and tensiometer position relative to the sample. Clearly, if the suction is measured on the surface of relatively large samples, the continuous drying procedure is expected to yield an incorrect water retention curve (Lourenço et al., 2007). Considering all limitations of this procedure but even practice to reduce their effect, information collected during this test are used as input data for estimating soil water retention and hydraulic conductivity functions by a parameter estimation approach. One of the main practical limitation of evaporation experiment is, then, related to the maximum amplitude in suction the instrumentation can accurately measures, usually limited to 80-90 kPa, beyond which cavitation can arises in tensiometers; for this reason, information related to soil retention properties at higher suction values should be determined using high capacities tensiometers (Lourenço et al., 2011; Toll et al., 2013; Toll et al., 2015), or coupling the evaporation test to different laboratory methodologies, e.g. the Dew Point Method.

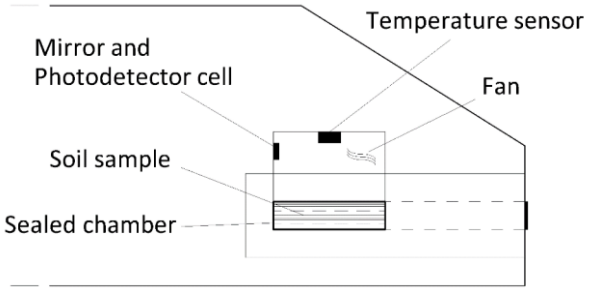

Figure 2.9. Sketch of laboratory equipment used to perform Dewpoint potential measurements.

This method is based on measurement of the relative humidity in a closed chamber above a soil sample; when equilibrium is reached between vapor and liquid phase Kelvin's equation is used to derive the water potential from relative humidity (Figure 2.9). This kind of methods have been often considered as a reference for determination of the soil potential (Gee and Or, 2002), having as strong advantage the reduced equilibration time needed and providing reliable results at very negative water potential in comparison with other methods (Gee et al., 2002; Solone et al., 2012). However, for high values of water potential and soil

close to saturation, the measures become less reliable; this is due to the logarithmic form of Kelvin's equation, with which accuracy in relative humidity measurement to at least three decimals place is necessary to catch decametric variations in water potential; the magnitude of this lack of reliability is related to the equipment accuracy in relative humidity measurements. This problem generally overcomes for very low water potential, leading to acceptable errors for measurements exceeding 1 MPa in absolute values.

The evaporation tests of this study were performed according to the procedure proposed by Romano and Santini (1999) for evaluating a parameter optimization method to determine the unsaturated hydraulic properties of different soil types. Comparison between results obtained from evaporation with conventional methods (sandbox, sand-kaolinbox, pressure plate apparatus, multi-step outflow method) lead to a good agreement in terms of water balance, soil retention (Schelle et al., 2013; Schindler et al., 2012) and hydraulic conductivity (Schelle et al., 2010). Recent developments in the method procedures allows to extend the measurement range of evaporation method acting on the air-entry pressure of the ceramic as extended tensiometeric measurement (Schindler et al., 2010a; Schindler et al., 2010b) and to account for drying and rewetting cycles (Schindler et al., 2015).

2.6 In situ measurement of water content in partially saturated soils

Soil mechanical behaviour is strictly dependent on its natural water content and its variation; this parameter is strictly related to soil suction and to soil hydraulic, and its change can provoke not negligible volumetric changes in the subsoil. Monitoring and measurement of water content represent fundamental issues in several geotechnical applications: variations in water content in riverbanks cause loss of strength that can induce, or trigger, their instability. Riverbank stability assessment is strongly dependent on the initial and boundary conditions assumed in the analysis; for this reason, a strong research improvement can be provided through the field data collection on water content and suction. Another key issue and source of uncertainties in stability evaluation is the heterogeneity of hydraulic soil properties, whose study requires adequate probabilistic approach. Therefore, it appears clear the need to measure soil water content and its variability for many geotechnical applications, so that the improvement in soil moisture measurement probes represents a topical research field for companies and research institute. In the present document, the main literature references useful to my research activities and concerning water content measurement in partially saturated soils are briefly reported and reviewed, in order to define the theoretical and practical fundaments acknowledged during this study. As could be referred to all kind of monitoring system, soil water content measurement problems can find different solutions depending on the spatial scale of measurements we have to deal with. Generally, four main scales of measurements can be defined, characterized by increasing observation area:

- local scale;
- field scale;
- catchment scale;
- regional and global scale.

Clearly, the transitions from one scale to another are not abrupt, and intermediate scale measurements could be added to this simplified classification, as also similar probes can be used at two consecutive scales; however, this spatial classification could be useful to better describe and summarize the available techniques and their applications. In particular, special references will be provided for local and field scales, representing the spatial dimensions typical for the research activities hereafter described. Actually, among the most diffused method for the site evaluation for soil water content are certainly the electro-magnetic indirect methods, which application and behaviour depends on the monitoring variable to be related to the unknown term of the problem (soil water content) by means of physical or empirical relations, defined as calibration equation. In fact, although the gravimetric method represent the reference for the direct measure of the soil water content, and generally used for the calibration of indirect methods, the most of the commercial probes are based on indirect methods (Bittelli, 2011), which evidence the considerable advantages of providing site-measurement continuous with time for each installation point, aiming to detect the time and spatial variability of the soil water content. Limiting to the only application of geotechnical interest, and to those for which direct knowledge has been achieved in the framework of the present study, among the probes using indirect methods, and having large diffusion, there are:

- Time Domain Reflectometry (in the following TDR);
- Frequency Domain Reflectometry (in the following FDR);
- Amplitude Domain Reflectometry (in the following ADR).

The TDR probes (Figure 2.10) is generally composed by a step pulse generator, which produce waves travelling on the metallic rods placed directly in the ground, and from an electronic system which measures, at regular and limited time interval, the property of the reflexed waves. The TDR probes use the measure of the dielectric constant of the soil in which are installed, which is obtained through the processing of the time required to an electromagnetic wave to cover the distance, doubled for circled path, of the part placed in soil; this quantity is then used in calibration equation, largely studied in literature (Topp et al., 1980; Robinson et al., 1990; Robinson et al., 2003) for an indirect estimation of average water content of volume of soil influenced by the measurement. This type of probe takes advantages on the differences in relative dielectric permittivity (ε_r) values characteristic for the solid, liquid and gaseous; this quantity, in heterogeneous media, depends on the dielectric permittivity of the singular constituent elements and on their volumetric component. A common approach for the estimation of the ε_r relative equivalent for soil media (ε^*_m), based

on the equation of Litchteneker (1926) which could be extended for a four phases media through the expression proposed by Heimovaara (Heimovaara et al., 1994):

$$\sqrt{\varepsilon^*_m} = \frac{\rho_d}{\rho_s}\sqrt{\varepsilon_s} + (\theta - \delta\rho_d A_s)\sqrt{\varepsilon^*_{fw}} + (\delta\rho_d A_s)\sqrt{\varepsilon^*_{bw}} + \left(1 - \frac{\rho_d}{\rho_d} - \theta\right)\sqrt{\varepsilon_a} \tag{2.3}$$

Where ε_s, ε_a, ε^*_{fw}, and ε^*_{bw}, are respectively the electric permittivity for the solid, air free and adsorbed water phases, ρ_d is the dry soil density and ρ_s is the solid bulk density, θ is the volumetric water content and the terms $\delta\rho_d A_s$ represent the fraction of the adsorbed water, being A_s and δ are the specific surface and thickness of the adsorbed water phase. The relative dielectric permittivity for soils has a real and an imaginary component, resulting generally complex the values for dielectric permittivity for singular components. In most of cases, however, it could be useful to express the dielectric permittivity through a real variable, the apparent permittivity Ka, defined by (Von Hippel, 1954):

$$K_a = \frac{\mathrm{Re}[\varepsilon^*_m]}{2}\left[\sqrt{1 + \left(\frac{\mathrm{Im}[\varepsilon^*_m]}{\mathrm{Re}[\varepsilon^*_m]}\right)^2} + 1\right] = \frac{\varepsilon'_m}{2}\left[\sqrt{1 + \left(\frac{\varepsilon''_m + \sigma/2\pi f\varepsilon_0}{\varepsilon'_m}\right)^2} + 1\right] \tag{2.4}$$

Where ε'_m, and ε''_m are, respectively, the real and imaginary components of the dielectric permittivity of soil, σ is the electric conductivity of soil and f is the wave frequency. The evaluation of K_a allows to determine the propagation velocity of a signal into a media with complex permittivity similarly to the case of media with real dielectric permittivity. The technique, then, consist measuring the signal propagation velocity through the metallic rods, through which is estimated the value of K_a using the theory of the transmission lines (Kraus and Fleisch, 1999), and the equation:

$$K_a = \left(\frac{c}{V_p}\right)^2 \tag{2.5}$$

Where c represents the values of speed light in vacuum. The values of Ka are, then, correlated to the volumetric soil water content by means of empirical correlation. At the typical operative frequencies for TDR probes, in fact, water evidence values for ε_r, even depending on the specific temperature and electrolyte in solution, of around 80, which is equal to 1 for air phase and varying in the range 4 to 16 for most solid ground particles (Wraith and Or, 1999). This significant difference make, in turn, the global values of ε_r, and particularly their variations, strongly susceptible to water content variation in soil, giving the possibility to correlate the measurement to the desired variable. These significant differences in values give to the

dielectric permittivity the strength to be highly sensitive to soil water content variation. One of the main assumption which is frequently adopted in standard practice for the interpretation of TDR data is to neglect the effect of the imaginary part of the solution given by the dielectric loss, principally due to the soil electric resistivity and dipole dielectric relaxation. This consideration, however, cannot be considered generally valid and adoptable, especially for highly conductive soils (generally clayey soils) or in presence of strong concentration of electrolytes in solution, for which cases the measured values of volumetric water content could be significantly overrated (BIttelli et al., 2008). In order to reduce the amount of the loss quantity, it has been suggested solutions regarding the use of jacket TDR (Becker et al., 2006), even though different authors (Ferré et al., 1996; Knight et al., 1997) evidenced how the use of this resolution evidenced a lower soil volume interested by the measuring field of the probes, other a potential loss of reliability.

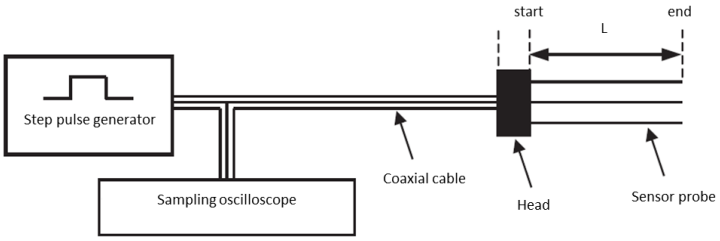

Figure 2.10. Equipment for water content using Time Domain Reflectometry (TDR).

The amplitude domain reflectometry (ADR) are categorized as indirect method for measuring water content in soils. The probe is generally constituted by a sinusoidal oscillator (100MHz), a coaxial cable with defined impedance and a multi-rod element, which represent an additional free segment of the transmission line, which impedance depends on the dielectric permittivity of the surrounding media, e.g. the soil where the probe is installed (Figure 2.11). Generally, for this kind of sensor is provided by the manufacturer a specific calibration equation (quadratic function, frequently) for each probe, or for definite categories, that converts the electric signal in apparent permittivity K_a. In several cases, as for soil characterized low and medium specific grain surface, it could be advantageous to adopt user-defined calibration equation; furthermore, it is important to notice that the apparent permittivity for low frequencies range (100 MHz) is strongly dependent on the temperature (Munoz-Carpena, 2004), and could be useful to estimate this effect through a specific laboratory calibration. It's notable here to underline that the effect of temperature on acquired data is less appreciable for TDR probes, operating in high frequency range (0.7 – 1 GHz), which provide, in general, a more reliable estimation for water content for soils in which the clayey fraction is characterized by low to medium specific surface.

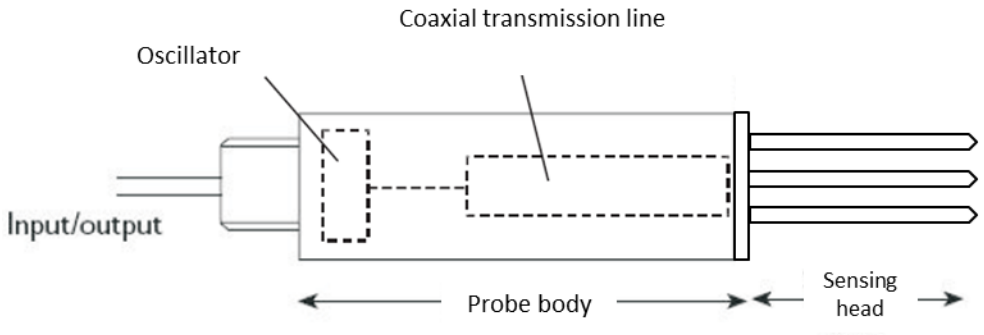

Figure 2.11. Equipment for water content using Amplitude Domain Reflectometry (ADR).

However, both ADR and TDR probes do not allow their applicability in many practical cases, due to the difficulty in the installation and maintenance phases especially for significant depth. In order to overcome to this problem have been so developed capacitive sensors for soil testing using access tube for placing sensors in site. In particular, the measurement point is moulded as one or more pair of coaxial electrodes with hollow cylindrical shape, spaced by few millimetres of insulating plastic material, and by an electric signal oscillator producing a sinusoidal wave and measuring the resonant frequency (Figure 2.12); this quantity depends on the capacity of the soil-access tube system, through the relation (Dean et al., 1987):

$$F_{res} = \frac{1}{2\pi\sqrt{L}}\left(\frac{1}{C} + \frac{1}{C_b} + \frac{1}{C_C}\right)^{0.5} \tag{2.6}$$

Where L and C are the circuit inductance and capacity, respectively, and C_b and C_c are the capacity of the base and collector of the system. The capacity (C) is itself function of the apparent dielectric permittivity of soil, following the simple relation:

$$C = gK_a \tag{2.7}$$

Where, however, *g* is a geometric parameter not easily to evaluate for non-elementary geometry. The indirect measure of the soil water content can be performed, so, using a direct correlation with the F_{res} (Paltineau and Starr, 1997), or calibrating the parameters of the equations 6 and 7 (or similar equations) to derive the values of K_a, which is in turn correlated to soil water content through the empirical relations used for TDR measurement (Kelleners et al., 2004). Similarly to ADR, the capacitive probes operate in a low range of frequency (around 100MHz); in case of measurement in clayey soils, the same consideration are, so, valuable on the need to perform a single calibration for each probes including the effect of temperature,

depending on the soil mineralogical and physical properties (Evett et al., 2006; Gabriel et al., 2010; Guber et al., 2010; Paraskevas et al., 2012). Some researchers (Dean et al. 1987) evidenced that the soil volume investigated is limited to a portion closer to the access tube, and the collected data are significantly influenced by the presence of cushion of air among the electrodes, access tube and surrounding soil, and so particular care must be taken in the installation process in order to avoid unexpected inaccuracy (Bell et al., 1987).

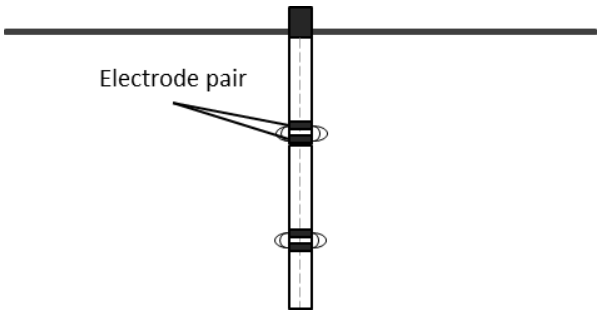

Figure 2.12. Multi-capacitive probes and relative electric fields

A proper interpretation of the site collected data cannot, however, overlook the comparison with direct laboratory measurement on soil water content and hydraulic potential (or suction), performed on undisturbed soil samples. These measures are generally coupled and, then, expressed using the soil water retention curves (SWRCs), which are the basic relations between matric potential and water content; their knowledge is fundamental in unsaturated soil physics studies with implications in a large number of applications, ranging from agronomy to geotechnical engineering, influencing plant water uptake and seepage, stress-strain and strength characteristics of soils. The main issues related to a univocal and accurate interpretation of retention data interpretation are related to the identification of the proper wetting and drying paths and, so, to proper correlate the pairs of values soil water content-suction, due to hysteresis in soil water retention curves (Parlange, 1976; Jaynes, 1984) and to uncertainties and heterogeneity related to soil properties definition (Rahardjo, 2013; Likos, 2014), representing some of the aspects that may be considered hereinafter.

3 On the role of partially saturated soil strength in the stability analysis of a river embankment: preliminary analysis under steady-state and transient seepage conditions

The study of the mechanical, hydraulic and retention behaviour of river embankment represents a key problem in civil engineering, involving topical issues for geotechnical researches. Results and advanced in this framework are generally lead to the definition of reliable design approach criteria, on the estimation of riverbank assessment towards various mechanisms of failure (included overtopping, erosion, local and global instability mechanisms), and are basically focused on the clarification of the role of unsaturated soil state, uncertainty and heterogeneity (different topics, that could be treated by means of similar mathematical tools), time dependent variability for external and actual conditions, atmospheric coupling and vegetation effects among the most. Both assessment and design aspects require to properly taking into account, even by means of progressively accurate models, these aspects and are included in global risk evaluation problems. However, there are substantial differences in the procedures, requirements and practical suggestions, in relation to the main assumptions on which they are based. Overall, with specific reference when dealing with stability problems, design approaches are completed using simplified assumptions on the seepage regime in the riverbank and initial conditions for the determination of flow characteristics; in details, steady-state conditions are assumed to model seepage through the riverbanks, while issues related to unsaturated soil state are usually neglected. This procedure generally leads to deliberately highly overconservative conclusions for probability of failure or reliability index when expressed in terms of probabilistic results. Even being arguable these main hypotheses for design approach, is however required that hazard and risk analysis should be performed in more reliable and realistic conditions; it should be, so, accounted for the transient conditions for seepage process, induced by time-dependent external conditions, considering appropriate initial conditions and realistic unsaturated soil state for the riverbank soil. A proper combination of these aspect is, so, necessaire for a consistent stability assessment process of existing river embankment, and will be considered and studied with increasing level of sophistication in part of this thesis. In the present section, a series of preliminary analysis have been performed, focusing on the role of partially saturated soil strength and initial conditions in the stability assessment of a river embankment under steady-state and transient seepage conditions, which results are hereafter presented. In specific, the influence of the initial conditions to be used in numerical analysis, and the incidence of unsaturated soil strength on the assessment of probability of bank instability under steady-state and transient seepage conditions will be quantified, and their relevant influence on risk assessment and design approach will be discussed. Starting from the database collected from a major river bank failure occurred in January 2014 (along river Secchia, near Modena, in Italy) the study case is so introduced and referenced. For the considered riverbank, decrease in soil suction values

due to a series of high water events in combination with the effect of widespread presence of animal burrows are supposed to have triggered a global instability mechanism (D'Aplos et al., 2014); consequently, overtopping and erosion rapidly contributed to create a large breach in the earthen water retaining structure system (Figure 3.1). Therefore, it is not here meant to debate further herein of the actual mechanisms that led the specific riverbank to sudden failure, but the aim of this section is to point out the attention on the main issues related to stability assessment of existing riverbank, individuating the most impactive source of uncertainties related to this problem, which are often neglected, and underlining their main effects.

Figure 3.1. Pictures of the breach area during river Secchia flooding in January 2014.

3.1 Case study: general information, river basin and geotechnical characterization

The case study considered in the present work, as introduced above, refers to a section of the river Secchia embankment structure, which was subjected to global instability phenomenon on 19/11/2014 around 06:00 am; during this event, the widespread presence of animal burrows, clearly detected near the failed section and possibly existing in it before collapse, is supposed to have triggered an overall instability mechanism (D'Aplos et al., 2014); consequently, overtopping and erosion rapidly contributed to create a large breach in the river bank (Figure 5.2). Despite the crucial weakness of the section, decrease in soil suction values due to persistent high water levels along the river was found to be a crucial issue for the riverbank failure. The specific failed bank cross section had a 7m high crown, referred to the ground level, an average 33° slope towards the river and 30° towards the land; the river longitudinal profile is locally made of a straight line, with a distance between opposite river banks rather constant and a morphologically quite flat ground surface around, at an altitude of 30-31 m above mean sea level. River Secchia flooding event, consequent to the total collapse of a 20 m-long embankment sector, involved approximately 38 million cubic meters of water, causing one casualty and long-lasting damages to a vast area around. In total, € 221 million have been allocated to restore public structures, private properties and river banks (Figure 3.2). The flooding area is

located in the southern part of the Po valley (Italy), resting on a deep alluvial Pleistocene formation, locally at least 400 m thick. The morphology is resulted from the depositional and erosional activity of the Secchia and Panaro rivers, both Po's tributaries, which drain large areas of the Emilian Apennines.

Figure 3.2. (left) Riverbank breach progression (19/01/2014 09:00); (right) riverbank sector restore operations.

Considering a 15-years observation period, the lowest water height measured in the neighbourhood of the studied section, and assumed representative for this study, is around 26.5 m a.s.l. while the maximum water height is 36.6 m a.s.l., observed on December, 26th 2009. The historical flood event registered in the last decades are relative to 1940, 1960, 1966 and 1972 for the considered embankment sector; furthermore, the last two cited event involved failure for different riverbank section and, more in specific, the 1972 failure occurred at relative small distance from January, 19th 2014 failure, which impacted the municipality of Bastiglia, Bomporto, Modena and Campogalliano (around 15 km from the recent breach). In the subsequent years, significant modifications were realized to the embankment geometry and functions, in order to improve the river discharge, by the creation of an expansion area to be used in case of flood event, and the stability conditions of part of the riverbank system. However, as demonstrated by the instability mechanism recently occurred, is not clear that safety conditions for the studied riverbank sector are guaranteed; even considering the probable weakness of the failed section, a specific and extended analysis of the embankment is required to assess its safety margins, accurately accounting for specific geotechnical related issues (as transient seepage, partially saturated soil conditions and heterogeneity) which could represent important sources of uncertainties which are frequently neglected in practical applications up to the present.

3.1.1 River Secchia basin

Referring to the "General guidelines for hydrogeological framework and intervention plan", published by the Authority for the Po River Basin in 1999 (AdbPo, last update on December, 09th 2014), River Secchia basin

cover a global surface of 2090km^2, up to the confluence whit Po River which is reached after a 172km length, and its 57% is in mountain environment, and represents the 3% of the entire Po basin. The entire catchment basin evidence a low level of hierarchization, denoting a rapidly evolving state, attested by the high number of torrential hydrodynamic process ongoing. In its plain sector, the main watercourse is confined by continuous soil water retaining structure, subjected to a progressive unicursal path characterized by a deepening level for riverbed and low hydrometric height. Its constitutive typology is influenced by the riverbank system, but even by the mountain basin characterized by loose clayey soil deposit, likely erodible. The entire hydrological system is characterized by a significant soil transport, which in turns tends to produce significant modification to the morphological profile. The basin catchment is strongly dependent from the drainage of large part of the mountain sector, and is characterized by a rapid response to precipitation event. As stated by the Regional Agency for prevention and environment of Emilia Romagna region (Arpae – Agenzia regionale prevenzione e ambiente, Emilia Romagna, Italy), the global rainfall estimated for the period 2021-2050 will be comparable, for the trimester February to March, to those occurred in historical series, but characterized by higher period of absence of precipitation, producing as effect the presence of impulsive phenomenon difficult to forecast and manage; in general, variation in the annual cumulative precipitation are expected for the Autumn season (+19%), while reduction are probable for the Winter and Spring period (-2% and -11%, respectively) (Arpae Emilia Romagna, 2017), with predictable a general amplification of the seasonal cycle (Pavan et al., 2008). An average, locally significant, decrease in annual precipitation is also detectable mostly on the western mountains of the region (-100mm decade^{-1}), but significant increases are identified in some areas close to the Po River Delta (North Eastern part of the region); local spatial patterns may, however, be susceptible to large errors (Antolini et al., 2015). These considerations aim to point out the importance of the development of tools and methodologies not only useful to represent the hydrological response of the watercourse to environmental (or anthropic) stress, but also to quantify the effect of significant hydrological event on water retaining systems and related structures, as could the cases of river flood subsequent to intensive, and/or impulsive, rainfall.

3.1.2 Geotechnical characterization

The geotechnical properties of the river bank's soil and subsoil were estimated by carrying out extensive site and laboratory investigations. Site investigation involved the execution of cone penetration tests including pore-pressure measurements (CPTUs) running up to a 14-26 m depth, distributed on three different cross sections considered representative of the collapsed bank and located near the breach: section 1 was located on the right river side, 900 m upstream the breach area, section 2 was selected on the left river side, in front of the breach area and section 3 was taken again on the right river side, but immediately downstream the

breach area (Figure 3.3). For each cross section, three CPTU tests were executed: on the river side, on the river bank top and on the landward side.

Figure 3.3. Location of the failure area and studied section.

Various dissipation west were performed at different depths from the ground surface. The series of CPTUs performed from the crest of the riverbank account for the shear wave velocity propagation measurement, by means of seismic module (SCPTU). Robertson (2009) classification, which account for semi-empirical correlations between data measured from and soil mechanical properties, were used for lithography characterization; in specific, soil types were defined on the base of an iterative procedure using the estimation for the Soil Behaviour Type Index (I_{cn}) obtained from the normalized cone resistance (Qt) and friction ratio (F_r). Interpretation of results, plotted and summarized in Figure 3.4, evidenced thath th embankment stratigraphy is moulded in three main layers:

- the riverbank soil, constituting the embankment structure and consisting in a complex alternation of silt with sand and sandy silt, hereafter named as Unit A;
- the embankment foundation, consisting in as sub-horizontal layers of sandy silty layers with local presence of clay, of 6.5m thickness on average, hereafter named as Unit B;
- the subsoil, consisting in a primarily clayey layer with local sandy-silt horizons, evidenced up to the maximum investigated depth, hereafter named as Unit C.

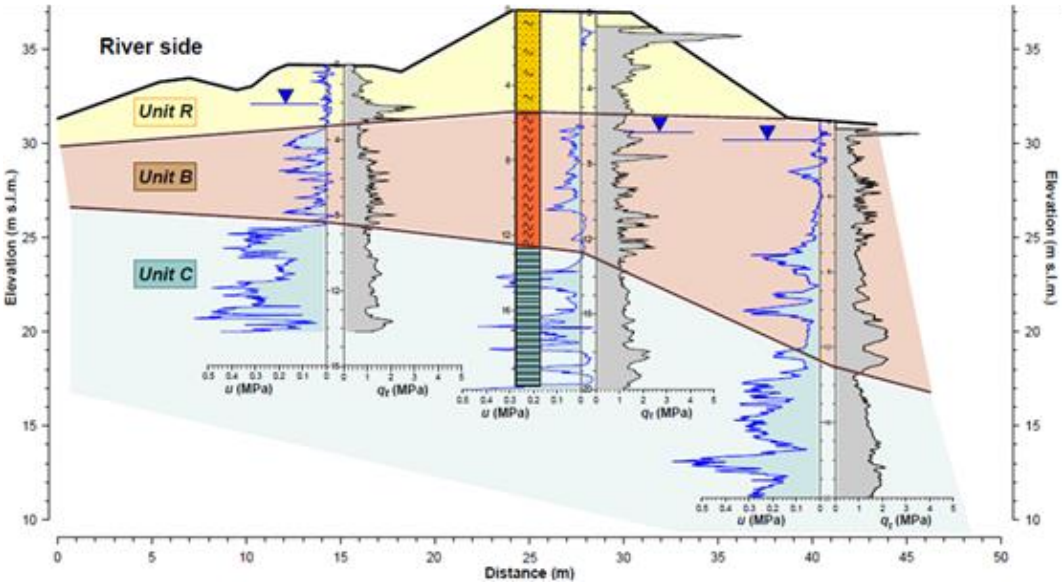

Figure 3.4. Stratigraphic profile and CPTUs results, Section 3.

Both remoulded and undisturbed samples were taken from each investigated soil section, aiming to determine the main soil geotechnical properties by means of various and comprehensive laboratory test. From standard physical investigation performed up to 5m depth from the riverbank crest, Unit A has found to be characterized by fine-grained soil percentage around 6% - 11%, characterized by a PI generally lower than 10% and natural content lower than the PL. Similar conclusions have been obtained from test performed on soil sampled from Unit B, characterized by low plasticity but, indeed, natural water content significantly generally higher, generally above the LL. Concerning Unit C, the fine-grained fraction is there characterized by high values for PI. In addition, significant local carbonate concretions were found at all depths, in percentage ranging from 7%, for subsoil, to 21% for riverbank soil, and organic matter ranging from 0.8% to 4%. Main soil physical properties, obtained from disturbed and undisturbed samples are plotted in Figure 3.5, and listed in Table 3.1, with reference to Section 1.

Soil unit	Depth	γ_n	PL	LL	IP	G_S	S	M	C	w_n
	(m)	(kN/m³)	(%)	(%)	(%)	(-)	(%)	(%)	(%)	(%)
Unit A	1.95	16.28	23	30	7	-	29.63	64.35	6.02	17.7
	3.25	16.02	16	22	6	2.707	44.57	-	-	7.4
	5.25	16.06	14	25	11	2.695	30.97	-	-	10.3

Unit B	6.25	18.71	16	26	9	-	27.05	-	-	18
	12.25	18.82	22	38	16	2.625	23.65	70.97	5.38	29.7
Unit C	15.25	18.25	31	81	50	-	1.15	-	-	38.7

Table 3.1. Soil physical properties from laboratory test investigations.

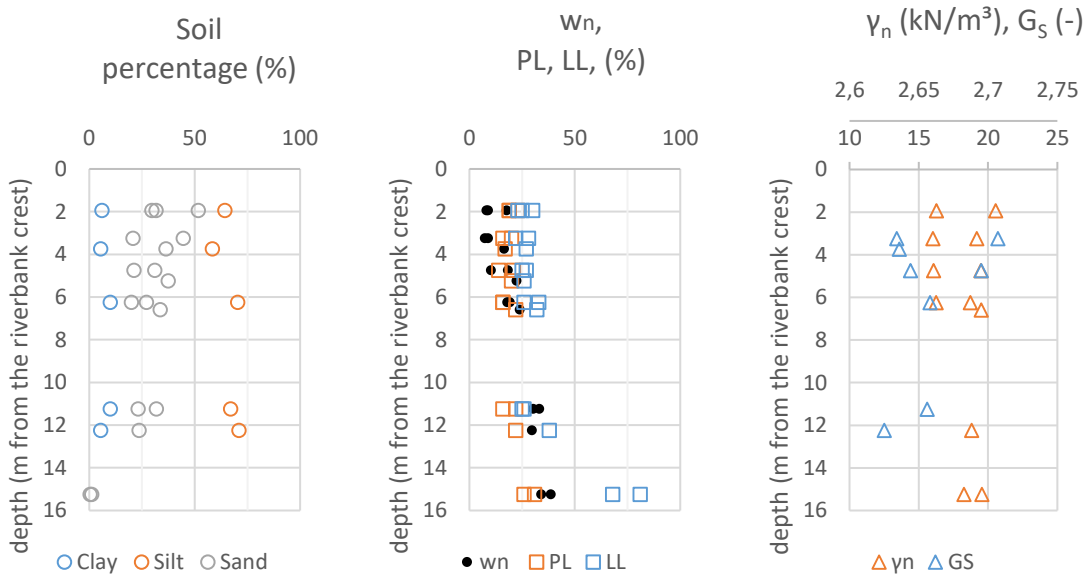

Figure 3.5. Main physical and index soil properties derived from laboratory test for all investigated sections.

Soil strength parameters for Unit A and B were determined from CPTU and SPCTU data interpretation and laboratory test (TxCID, TXCIU; DS), investigating both critical and peak conditions. Concerning Unit C soil strength parameters estimation has been only based on correlation from in situ test. Soil strength parameters to be used in this work are listed in Table 3.2, both in terms of mean value and standard deviation.

Soil Type	ϕ' (°)		c' (kPa)
	Mean value	Standard deviation	Estimated value
Unit A	32.0	1.94	0.0
Unit B	28.8	3.20	0.0
Unit C	24.9	2.40	0.0

Table 3.2. Estimated strength soil properties.

Basing on results obtained from CPTUs and from field data collected by the Casagrande piezometer installed in Section 3, the water table has been estimated at approximately 6.0m from the riverbank crest, close to the transition zone between Unit A and B. Furthermore, such groundwater table has found to be slightly sloping on the land side, characterized by a hydraulic gradient equal to 4%. Similar features have been individuated for Section 1 and 2. Soil hydraulic and retention properties, to be considered representative for Unit A, have been studied through a series of nine evaporation tests, conducted on undisturbed samples taken at depth ranging from 0.65m to 1.7m at a section located 600m downstream the collapsed area. Results elaboration in terms of main drying retention curve for each soil sample are plotted in Figure 3.6, associated to particle size distribution performed using USDA classification system. For the considered case, the widely used van Genuchten – Mualem model (van Genuchten, 1980), previously discussed in Chapter 2, has been assumed for describing the non-hysteretic relationship between soil suction and water content on drying paths, for the estimation of the effective degree of saturation and hydraulic relative permeability as function of suction, according to the following relations:

$$k_r(h) = S_e^{0.5}\left[1-\left(1-S_e^{1/m_{VG}}\right)^{m_{VG}}\right]^2 \tag{3.1}$$

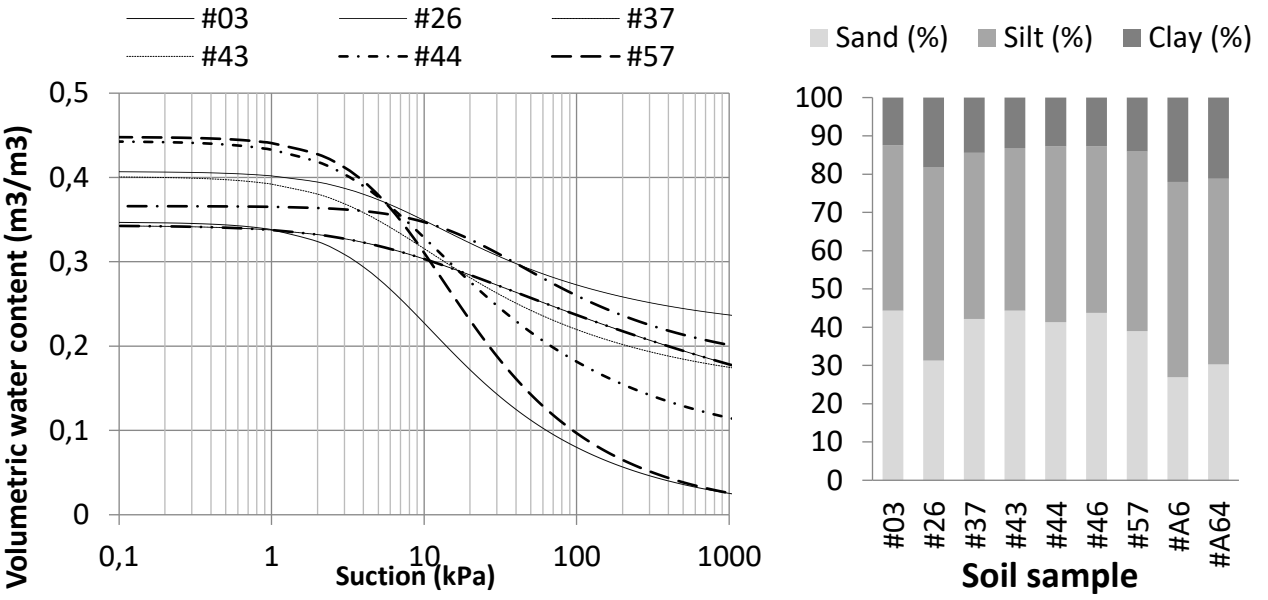

Figure 3.6. Main drying retention curves and soil particle size distribution for undisturbed samples collected from the river embankment.

The hydraulic permeability, $k(S_e)$, is so expressed as the product of the saturated permeability, k_0, estimated from in situ and laboratory test results, and relative permeability, k_r. By adopting such constitutive model and parameters, nine soil-water retention curves (SWRC) and hydraulic conductivity functions (HCF) were thus obtained. For Unit A a statistical characterization of hydraulic and retention properties was carried out on the basis of van Genuchten – Mualem parameters estimated from laboratory tests results, in terms of mean values, standard deviation, skewness and correlation structure. On the statistical significance of the considered number of set of parameters, although this number can be considered close to a lower boundary for probabilistic study, it should be considered that for this research purpose, and even more for engineering practice, the available laboratory data, obtained from undisturbed sample collected from the same soil layer, could represent a significantly sufficient source of information for the soil water retention statistical characterization; furthermore, it has also to be underlined that that every evaporation test consisted in three independent measurements; moreover, the statistical moments estimated for the unsaturated parameters are consistent with those reported in literature and different database of soil hydraulic properties, as UNSODA (Nemes et al., 2000) and HYPRES (Wösten et al., 1999). In details, results from the literature, considering both direct and indirect methods for hydraulic and retention parameters assessment (Schaap et al., 1998; Baroni et al., 2010; Phoon et al., 2010; Liao et al., 2014; Likos et al., 2014), show the following ranges for the coefficient of variation (mean value in brackets) of the Van Genuchten – Mualem model parameters: C.o.V.(θr)=10-110% (42%), C.o.V.(θsat)=5-25% (17%), C.o.V.(αvg)=20-100% (60%), C.o.V.(nvg)=3-20% (10%), C.o.V.(k0)=100-300%, which turn out to be fully consistent with the values taken into account in the present study. For Unit B and Unit C, an estimation of hydraulic conductivity at saturation was made. Mean values of all soil hydraulic properties mentioned above are listed in Table 3.3.

	θ_r	θ_s	α_{VG}	n_{VG}	k_0
	(m^3/m^3)	(m^3/m^3)	(kPa)	(-)	(log(m/s))
Riverbank	0.079	0.395	0.164	1.328	-5.804
Foundation	-	-	-	-	-5.725
Subsoil	-	-	-	-	-8.886

Table 3.3. Average values of estimated hydraulic soil properties.

In relation to the soil water content, the unit weight in unsaturated conditions has been expressed as:

$$\gamma_{unsat} = [(1 - \theta_s)\gamma_w G_S + \gamma_w \theta] \quad (3.3)$$

Being γ_w the unit weight of water, g the gravitational load, and G_S the soil particles specific gravity, for which the average values listed in Table 3.1 have been assumed.

The hydraulic conductivity function is used to estimate the unsaturated soil permeability, is dependent on the assumed retention model and has been here estimated as (van Genichten, 1980):

$$k(\theta) = k_0 S_e^{0.5} \left[1 - \left(1 - S_e^{1/m}\right)^m\right]^2 \tag{3.4}$$

3.2 Numerical analysis

Seepage characteristics and stability conditions of the collapsed Secchia's river bank have been evaluated using a two-dimensional numerical model based on actual geometrical, stratigraphic, geotechnical and hydrological data summarised in the previous section and discussed in the Technical report on the causes leading the collapse of Secchia riverbank section on January, 19th 2014, discussed in D'Alpaos et al. (2014); different study have been performed using data and information collected after the failure, aiming to investigate different aspects of the hydraulic and stability behaviour of the riverbank in unsaturated conditions (Gottardi et al., 2016; Gottardi and Gragnano, 2016; Gragnano et al., 2016). Considering time variable as part of the problem, important sources of uncertainties are related to the definition of initial conditions and the time dependency of boundary conditions, in addition to those related to soil parameters definition in relation to intrinsic heterogeneity and lack of complete information on spatial variability. However, even in view of these issues, transient modelling is unavoidable for a proper definition of seepage characteristic of existing riverbank during high-water event. In order to gradually deal with this topic, different stages for numerical analysis will be discussed and results presented in this work. In specific, in this preliminary stage (Chapter 3), remarks and observation will be provided on the importance of accountancies of unsaturated soil and transient conditions for the riverbank seepage and stability analysis, using simplified hypothesis on initial and boundary conditions, assuming soil strength properties as variable for the safety assessment, but disregarding the effect of hydraulic and retention soil properties related uncertainties. For this purpose, three cases have been considered for analysis, varying the seepage conditions and initial conditions to be adopted in the analysis; in particular:

- Case 1: seepage characteristics determined in transient flow condition induced by retained water and rainfall infiltration, starting from realistic initial condition;
- Case 2: seepage characteristics determined in transient flow condition induced by retained water and rainfall infiltration, starting from simplified initial conditions;

- Case 3: seepage characteristics determined in steady-state flow conditions in equilibrium with the maximum water level recorded during the specific flooding event.

3.2.1 Modelling the hydraulic response of the riverbank

Saturated and unsaturated flow has been modelled using the Finite Element software SEEP/W (Geo-Slope International Ltd 2008), which is formulated in terms of total hydraulic head. The code can perform a two-dimensional, finite element seepage analysis using the equations of motion and mass conservation. Partial differential equations governing steady-state free surface flow in saturated soil conditions is given by:

$$-k_0 \nabla \left(\frac{u_w}{\gamma_w} + z\right) = \mathbf{0} \tag{3.5}$$

where k_0 is the soil hydraulic permeability at saturation, u_w is the pore water pressure and z is the vertical elevation coordinate. In the case of unsaturated soils, the hydraulic conductivity is a function of water content and pore water pressure. Relationships between volumetric water content and pore water pressure and between hydraulic conductivity and pore water pressure are defined by soil-water retention curves (SWRC) and hydraulic conductivity functions (HCF), respectively. In transient seepage analysis, the water flow per unit area, q, is calculated using generalized Darcy's law:

$$-k_r k_0 \nabla \left(\frac{u_w}{\gamma_w} + z\right) = \boldsymbol{q} \tag{3.6}$$

Notice that only flow of water in the liquid phase has been considered in this part of the study. Pore water pressure distributions were computed using boundary conditions adequate for this phase, described below, and assuming, for the present stage of analysis, hydraulic parameters as deterministic variables, equal to their average values.

3.2.1.1 Initial and boundary conditions

Various hydraulic conditions have been considered for each seepage analysis, differing on the assumptions on pore water pressure and suction distribution to be used at the beginning of the transient flow considering, at the first step of the seepage analysis, the soil in the embankment has been assumed as unsaturated. In a

first hypothesis, relative to Case 1, the initial pore water pressure distribution has been directly assigned to the model; the hypothesis considered for the initial conditions are the water level at 30 m, suction linearly decreasing since -39kPa value in correspondence of the centre of bank, located 4 meter above water table, then increasing up to zero value at the surface level. The purpose in considering this assumption is to simulate a suction distribution which could be considered typical for a bank in a wet period, individuating a central bank core with lower suction values (depending on the former external hydraulic conditions), approaching zero values at surface correspondence (possible in wet seasons due to atmospheric interaction, disregarded at this phase of analysis). This hypothesis has been considered as acceptable by several authors (e.g. Casagli et al., 1999; Rinaldi et al., 2004; Calabresi et al., 2013, Sleep et al., 2013); furthermore, in absence of specific site measurements, this simplified assumption has been considered as adequate also for the purposes of this part of the study. Retained water level has been introduced as time-dependent boundary conditions in transient seepage analysis, assigning linearly variable total hydraulic head values on the river side nodes. In addition, rainfall infiltration has been modeled as water flow to boundary surface. Hydrometric values and precipitation data have been recorded during flooding in the neighbourhood of the considered event and rainfall event starting from 25 December 2014, in the neighbourhood of the studied section. Potential seepage faces have been defined during the no rainfall periods along the boundary surfaces, which limit the infiltration in soil when zero pressure is reached in the boundary nodes (Geo-Slope International Ltd 2008). The maximum water level at bank failure moment has been assumed equal to 35.9 m (D'Alpaos et al., 2014). Differently, for Case 2, two different hypotheses have been used for the initial distribution of suction above the phreatic line, considering a hydrostatic increment (in absolute value) above the phreatic line up to a maximum of -10kPa (Case 2') and without considering a limitation for suction values (Case 2'). For all considered Cases, hydrostatic pore water pressure regime has been adopted beneath the water level for initial conditions; in Figure 3.7 recorded water level and precipitation have been plotted, together with linear function used in the numerical model as total hydraulic head boundary condition.

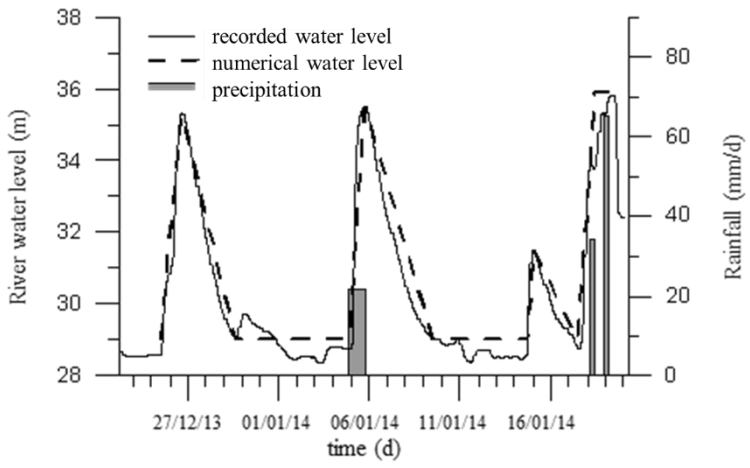

Figure 3.7. Flood hydrograph, rainfall hyetograph and numerical total hydraulic head boundary condition recorded and modelled from 25 December 2013 to 19 January 2014.

In Case 3, lastly, steady state seepage analysis has been conducted assuming a 35.9 m retained water level on riverside, which is the maximum water level recorded during the specific flooding event (January, 19th 2014), the water table at ground level on landward and soils hydraulic conductivities constants and equal to saturated values, and hydrostatic distribution has been assumed for suction values above the phreatic line.

3.2.2 Probabilistic limit equilibrium analysis

Pore water pressure distribution resulting from seepage analysis have been used as input for limit equilibrium analyses. In order to account for the uncertainty related to the variability of soil shear strength parameters, stability analyses have been conducted assuming the soil dam and foundation ϕ' as random variable with normal distribution, using mean values and standard deviations listed in Table 3.3. Limit equilibrium analyses were performed using Morgenstern and Price Method (1965), both in steady state and transient flow conditions. Suitable geometrical constraints were defined in order to identify the slip surfaces which better represent a significant collapse mechanism with respect to overall stability. Geometrical constraints typically consist of two boundary ranges, at the top and toe of the slope, for entry and exit points for slip surface generation and a minimum depth condition. The number of entries and exits can be specified as the number of increments along these two lines. In this study, the minimum slip surface depths were assumed to be 4m for the outer instability mechanisms. The geometrical constrains and the typical critical slip surfaces are shown Figure 3.8. In particular, with red-line are evidenced the slip surfaces consistent with key-in constrains; in grey-line are evidenced the error surfaces, which do not fully satisfy the geometrical requirements (e.g. slip surfaces enters or exit points beyond specified limits, slip surface shallower than defined minimum depth). In practice, the software connects a point along the entry area with a point along the exit area to form a line. At the mid-point of this connecting line, SLOPE/W creates a perpendicular line. Radius points along the perpendicular line are created to form the required third point of a circle. This radius point together with the entry and exit points are used to form the equation of a circle. SLOPE/W controls the locations of these radius points so that the circle will not be a straight line (infinite radius), and the entry angle of the slip circle on the crest will not be larger than 90 degrees (undercutting slip circle).

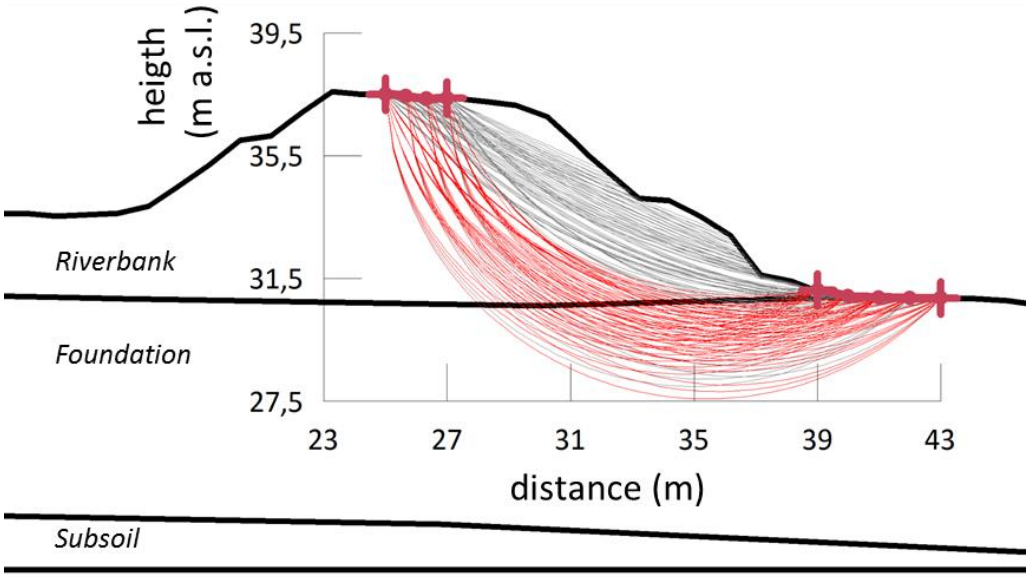

Figure 3.8. Typical slip surfaces considered in stability analysis for global safety assessment.

In addition to the circle slip surfaces defined by the user, the software allows the possibility of incrementally altering only portion of the slip surface (Greco, 1996), through an optimization process which is dependent on the pore water pressure and suction distribution used for limit equilibrium analysis; this means that the optimized slip surface is not fully specified by the user, but defined by the software starting from the geometry of the most critical (in terms of safety factor) among the user-defined slip surfaces, through an iterative procedure which allows some control parameters, as the tolerance in comparing safety factor, the maximum number of optimization trials and the number of line segments (Geo-Slope International Ltd, 2008). In locations above the groundwater table, the Vanapalli et al. (1996) failure criterion has been eventually adopted to define the soil strength to be used in the limit equilibrium analysis, given by:

$$\tau = c' + \sigma_n tan\varphi' + (u_a - u_w)S_e tan\varphi' \qquad (3.7)$$

where S_e is the effective degree of saturation. The first part of the equation describes the saturated shear strength when the pore-air pressure, u_a, is equal to the pore water pressure, u_w, in fully saturated or dry soil condition. This part of the equation is a function of normal stress since the shear strength parameters c' and ϕ' are constant for a saturated soil. The second part of the equation provides the shear strength contribution due to suction, which can be predicted using the soil water retention curve (Fredlund and Vanapalli, 2002). This equation implies that the unsaturated soil strength contribution varies with the degree of saturation and suction. The shear strength contribution due to the matric suction ($u_a - u_w$) is equal to tanϕ' up to the air-

entry value (AEV) of the soil, so that the conventional equation for estimating the shear strength of saturated soils can be used up to the AEV for unsaturated soils: as soil desaturases, the unsaturated soil strength contribution varies due to higher suction values acting over a smaller area. The above described formulation is implemented in the software adopted for limit equilibrium analysis, SLOPE/W (Geo-Slope International Ltd, 2008). It is worth observing that the use of data from the only evaporation test lead the Authors to disregard issues related to soil hysteresis. Even considering that the modelled process is typical for wetting paths, the suction and soil water content values for the considered case and riverbank soil are typical for scanning paths, for which characterization specific laboratory tests are required; however, preliminary analysis performed using literary suggestion for wetting retention curves and related parameters estimation (Likos et al., 2014) evidenced that the use of data from a drying branch generally do not provide results on the unsafe side for the riverbank stability assessment, aim of this work. Indeed, although the assumption of non-hysteretic hydraulic behavior might tend to overestimate the suction values for an effective degree of saturation, the relative permeability will be then underrated by the van Genuchten - Mualem model (van Genuchten, 1980), with evident consequences on the flow regime and leading, at the end of high water events, to a minor progress of the phreatic line, even when initial conditions are defined in terms of suction. The above described considerations produce opposite effects on numerical stability evaluation, and one prevalence on the others should require to be stated for each analysis. The probabilistic analysis has been performed using the Monte Carlo method, according to the procedure implemented in the software SLOPE/W, allowing to consider the mechanical soil parameters as variable for Monte Carlo method. In details, one or more most critical slip surfaces (as defined by the user) are first determined based on the mean value of the safety factor. Probabilistic analysis is then performed on these critical slip surfaces, taking into consideration the variability of the input parameters. The number of Monte Carlo trials in an analysis is dependent on the number of variable input parameters and the expected probability of failure and, in theory, increase as the expected number of critical slip surface characterized by a safety factor minor is significantly low. Fundamental to the Monte Carlo method are the randomly generated input parameters that are processed into the deterministic model. In SLOPE/W, this is done using a random number generation function, using a uniform function distributed with values between 0 and 1.0. The generated random number is then used to get a new parameter value for the sampling function. As suggested in the software Theory Manual, the number of Monte Carlo trials to be conducted can be generally in the order of thousands. This may not be sufficient for a high level of confidence with multiple variables; for the purpose of this study, a number of 100.000 trials has been considered sufficient to define the probability of failure and reliability index related to stability assessment of the riverbank. Using a normal distribution as probability density functions for the soil strength parameters, the sampling function (Figure 3.9), defined as the inverse of cumulative distribution function, has a relatively straight segment in the middle. The implication of this is that parameters around the mean will be sampled more often than values at the extremities of the sampling function.

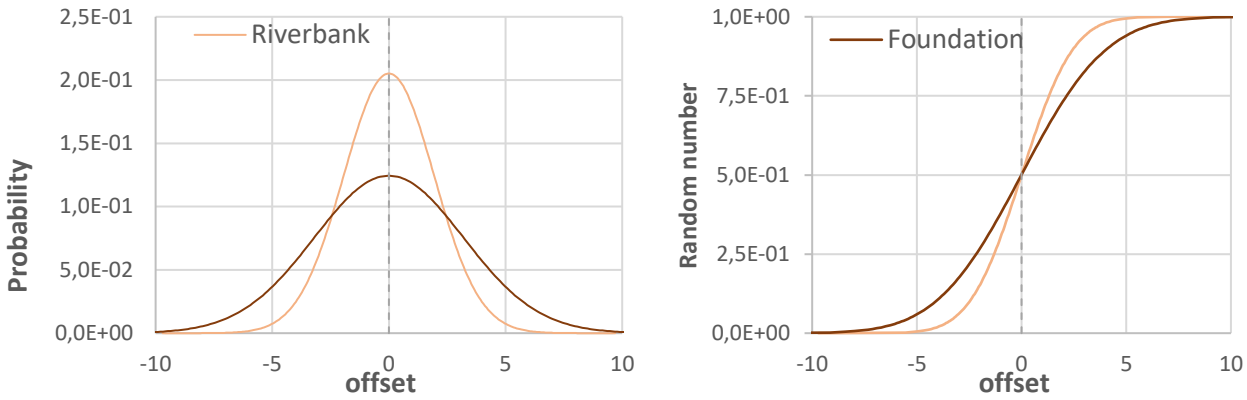

Figure 3.9. Probability density function and cumulative distribution function of the offset considered for riverbank and foundation soils in Monte Carlo simulations.

3.3 Results and discussion

In this section are summarized and discussed the principal results obtained from seepage and probabilistic limit equilibrium analysis performed for Cases 1, 2', 2'' and 3. Figure 3.10 shows the computed pore water pressure distributions at the initial stage, obtained from the transient seepage analysis by applying the boundary conditions mentioned above and assuming the hydraulic parameters as deterministic variables and equal to their average values, while in Figure 3.11 are plotted the pore water pressure and suction distribution computed at the end of the transient seepage analysis.

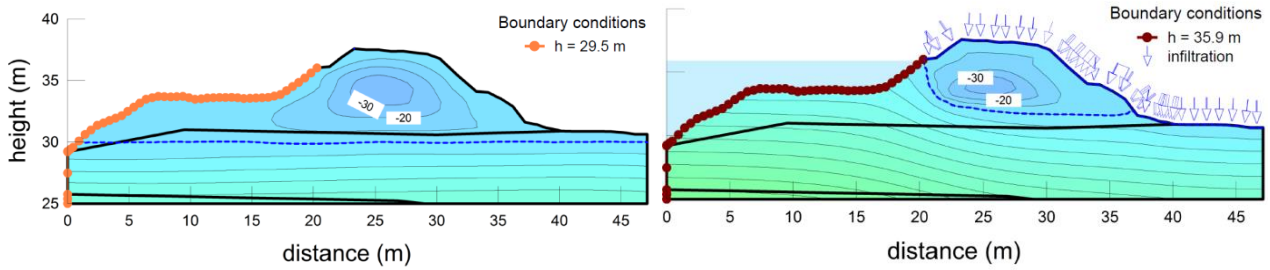

Figure 3.10. PWP distribution in the initial (left) and final (right) stage of transient seepage analysis: increment between two adjacent isolines is 10 kPa.

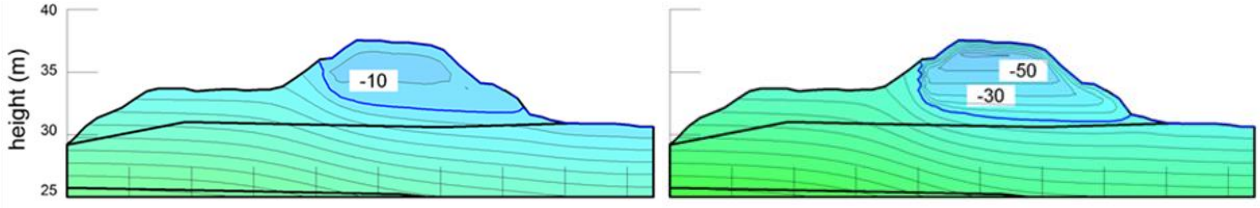

Figure 3.11. PWP distribution in the final stage of transient seepage analysis for Cases 2' (left) and 2'' (right); increment between two adjacent isolines is 10 kPa.

Significant differences can be evidenced between the showed results, obtained using the same boundary conditions but different assumptions on initial conditions. The higher progression of the phreatic line is determined in correspondence of the Case 2'; this is mainly dependent on the higher initial soil saturation degree, depending on the lower (absolute) values for soil suction, which in turns influence the soil permeability, higher for the considered Case. Differently, from the same basis, the higher suction values and lower progression of the phreatic line is obtained for Case 2'', while Case 1 can be considered as a possible state among the two other extreme cases.

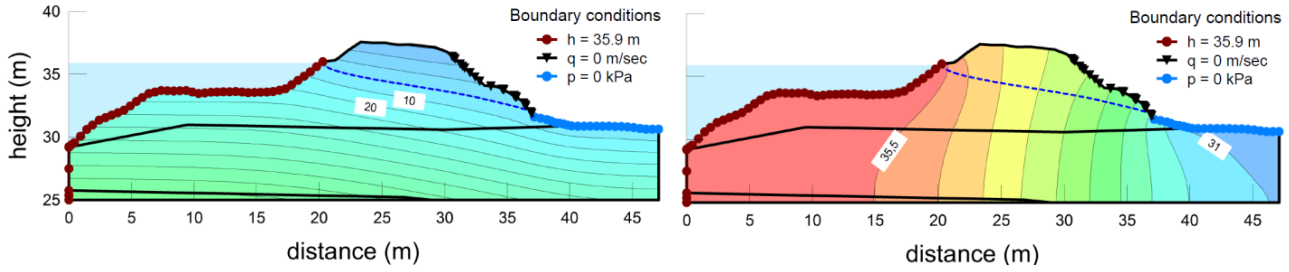

Figure 3.12. Results of steady state seepage analysis: increment between two adjacent isolines is 10 kPa for pore water pressure (left) and 0.5 m for total head distribution (right).

However, important differences can be observed comparing results obtained transient with steady-state analysis (Figure 3.12). In this last condition (Case 3), in fact, the progression of the phreatic line is significantly higher, and so the corresponding saturated zone for the soil riverbanks. Even if not representative for the specific flooding event, Case 3 could be, however, meaningful to stress the limited riverbank safety state in case of persistent high water.

Analysis results, summarized in Table 3.4 for the third hydrometric peak and showed in Figure 3.13 for all elapsed time step, are presented in terms of mean values and standard deviations of Factor of Safety (FS), together with the reliability index and the probability of failure, and plotted as probability density function and cumulative distribution function of safety factor for global instability mechanisms. Confirming what was considered from seepage analysis, probabilistic stability analyses in transient seepage conditions provide very low probabilities of failure for both inner and outer slope, not showing real chances of a riverbank instability. This result would suggest that the considered conditions are not able alone to account for the collapse occurred; in fact, other issues, as hydraulic parameter variability and possible presence of animal burrows have been called upon to have triggered the instability mechanism leading to final collapse. Furthermore, the probability of failure is strongly dependent on suction distribution, induced by the different initial conditions affecting the riverbank, meaning that the effect of initial conditions in terms of suction has a strong influence on seepage and stability analysis results.

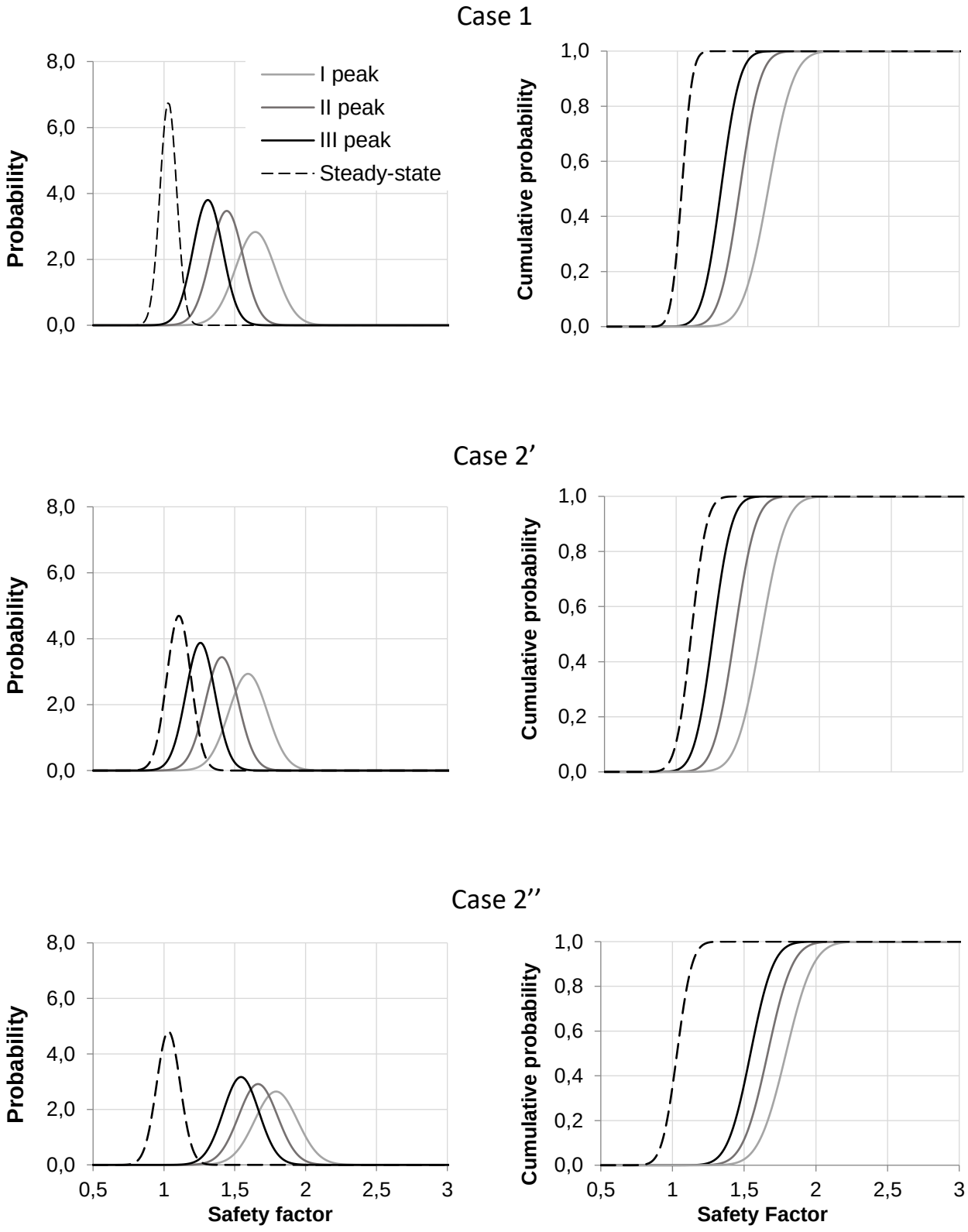

Figure 3.13. Comparison between Case 1…3 in terms of probability density function and cumulative distribution function of safety factor.

However, hydrostatic suction profile above phreatic line does not represent a realistic hypothesis and lead to results on the unsafe side for mobilized shear strength, while the use of simplified assumption could lead to more reliable results in terms of probability of failure respect to steady-state conditions.

	Case 1	Case 2'	Case 2''	Case 3
μ_{SF}	1.310	1.258	1.544	1.032
σ_{SF}	0.105	0.103	0.126	0.083
β	2.950	2.498	4.307	0.381
P_f (%)	$1.83 \cdot 10^{-1}$	$4.75 \cdot 10^{-1}$	$1.00 \cdot 10^{-2}$	$35.6 \cdot 10^{0}$

Table 3.4. Results of probabilistic analysis for Cases 1…3 for the third considered hydrometric peak.

This part of the study aims to underline the importance of an accurate geotechnical characterization based on extensive site and laboratory test campaign for mechanical (physical and strength parameters) and hydraulic (saturated and unsaturated soil properties) soil characterization. Steady state seepage coupled with fully saturated soil conditions has been showed to represent excessively prudential assumptions for a proper risk assessment, meaning that transient seepage analysis are an essential and unavoidable tool for assessing the probability of river bank failure. The probability of failure is, however, strongly dependent on suction distribution, induced by the different initial conditions affecting the riverbank, and so the definition of initial conditions represents a crucial point for transient seepage analyses and is a fundamental issue in safety assessment, which influence should be deeply studied by means of numerical analysis in absence of direct measurement.

4 On the effect of hydrometric water-level time-variability on riverbank stability evolution

In the framework of environmental and socio-economic protection from natural hazard, the design and assessment of water retaining structures plays a key role, as well as the procedures and methods for the evaluation of stability and safety conditions. A possible underestimate of the probability of collapse can produce unexpected and critical losses, while unreliability is mainly cause for erroneous choice for mitigation measures; both these aspects necessarily need to be avoided for a proper riverbank stability evaluation. In general, water pressure is the main source of load in reducing the stability of a flood embankment. Its effect both includes increase in pore water pressure in soils, due to seepage process through the riverbank and foundation materials, and the external forces acting on the embankment. Both are dependent on the river water level during flood event, but the latter are mainly dependent on the water flow characteristics in terms of velocity and volume rate, while the firsts are primarily influenced by the duration of the high-water event sequences and on soil-atmosphere interaction phenomenon. At the present, in European Practice, the estimation of water levels and pressure is guided by the requirements of Eurocode 7 – Geotechnical Design (2004), which provide characteristic and design values for water levels to be used in the seepage and analysis; these values are derived on the base of the hydro-geological data for the considered river basin, and are suggested to be considered in probabilistic analysis, in case sufficient amount of data are available. Following these requirements, current suggestion from the EG9, the Evolution Group 9 of the Eurocode Committee, is to assume a water level characterized by a 1% probability of being exceeded in the design life of the structure; this information have been provided considering generally a return period at least equal to the duration of the design situation as a characteristic level and in consideration to the expected working life of the embankment structure. Then, design water level for Ultimate Limit States requires a margin of safety over the characteristic level derived by either direct assessment or by adding a margin of safety. Hoever, no specific recommendations are given on the margin that should be applied to achieve the required probability of occurrence. (Pickles and Sandham, 2014). However, EN 1997-1 (2.4.4(1)) states that water levels should be treated as geometrical data, and factorising characteristic levels to obtain design water levels do not seem to be the most appropriate choice. Moreover, EN 1997 is primarily concerned with the design of new structures; a number of publications provide detailed examination of Eurocode 7 together with general overview on the assessment of existing embankments, including Bond and Harris (2008) and the International Levee Handbook (Ciria, 2013). Water retaining embankments are usually assessed under the simplifying assumption of steady state conditions in equilibrium with the design values. Indeed, for riverbank seepage assessment, this assumption is likely to be necessary only in the design of persistent situations and, frequently, it provides highly conservative results in terms of global safety. In the assessment of existing embankments, transient conditions can be accounted for, by adopting the characteristic hydrograph for a

specific flood defence sector, whose maximum water level is defined by the characteristic value for a specific design situation. The distribution of pore water pressure could be determined based on site specific monitoring or calculation, by means of analytical formulations or numerical analyses, and a proper combined use of these different tools could certainly reduce uncertainties regarding the boundary and the conditions at the beginning of a high-water event, besides the uncertainties on the soil hydraulic and mechanical properties. Although there are obvious advantages in making codes of practice as prescriptive as possible, the need for careful evaluation of the full range of representative scenarios cannot be underrated, particularly for situations in which water pressure has the dominant role (Simpson, 2011).

In an attempt to improve the present models for their vulnerability evaluation, a novel methodology have been conceived to account for the time dependent response of dykes and levees in partially saturated conditions, through the use of simplified assumption on boundary and initial conditions. In specific, a basic spectral analysis has been conducted on the hydrometric data recorded from stream gauges on the Secchia river, north of the city of Modena (Italy), in order to define the principal characteristics of the time-dependent hydraulic boundary condition acting on the embankment. Water flow through the riverbank has been determined by the use of transient seepage analyses for which a series of synthetic hydraulic boundary conditions have been defined basing on spectral analysis main results. The method has been presented in Gragnano et al., 2016); in this section, an overall insight to the proposed approach for riverbanks stability evaluation is given, focusing on the methodological issues in the discussion of preliminary results.

4.1 Methodology and application

4.1.1 Synthetic hydrograph

Potential flooding is a critical factor in the safe design of structure and risk management. The magnitudes of floods are described by flood discharge, flood elevation, and flood volume, which variation with time represent hydrographs. In one of its simplest form, a hydrograph is a graphical representation of run-off rate against time, which reflect and synthetize the complex characteristics of hydrological process. One of these characteristics, the duration or persistence of the water level above a specific level, can generally vary in a limited range for a particular watershed, regardless of the value of the peak flow from a specific storm, assuming a constant storm duration and intensity. There are different types of hydrographs which include natural hydrograph, where the studied variable is directly recorded at a stream gaging site, and artificial hydrograph, that define variability of a prescribed hydraulic properties with time basing on data processing and theoretical approaches, to be used for design of water-related structures. Being not possible and suitable the direct measurement of the flow properties for all the section of general interest, several methodologies have been developed to define the characteristic and the propagation of the water flow in a prescribed basin

area, referring to the case of river and stream, and could be here useful to give some notes and references regarding some of the most used tools in flood protection and risk management. Generally, these methods can be grouped into different categories, depending on the types of approach used, where can be found statistical analysis of gage data, used for streams which have a large number of years of recorded flood data. This method involves fitting a probability distribution to the data, and using the parameters of the distribution to estimate floods. Others approaches require the use of regression analysis to correlate watershed characteristics to streamflow using recorded data to define some predicting equation. A largely diffused method for the estimation of hydrograph is represented by the Unit Hydrograph (UH) theory. This theory, firstly introduced by Sherman (1932) and originally conceived for gauged watersheds only and successively extended to various cases (Rosso, 1984; Bhunya et al., 2009), could be intended as the analogous to the unit-impulse response (UIR) function, proper of telecommunication or electrical field studies (Singh et al., 2014), and assumes as basic hypothesis a linear hydrologic system, and time invariant (Dooge, 1973); the hydrograph is, then, represent one inch of runoff, uniformly distributed from the watershed during a specified time. While failing to describe the runoff distribution precisely, because of its limiting assumptions, the theory is recognized as being a good predictive tool as it reflects the characteristics of the basin it represents, and became the basis of many synthetic unit hydrograph (Hoffmeister and Weisman, 1977) methods. More in general, it has been used the diction of synthetic hydrograph representing a formulation based on watershed properties, as land use, vegetation cover, geometry of the riverbank, storm characteristics, and generally conceived to synthetically simulate the effect of natural hydrographs for ungagged watersheds.

4.1.2 Frequency domain analysis

The starting point of the proposed approach is the frequency-domain analysis on the hydrometric measurement of water levels. Frequency-domain analysis is a tool of utmost importance in signal processing applications and is widely used in such areas as communications, geology, remote sensing and image processing. Its principal feature is to evidence how the energy of a signal is distributed over a range of frequencies; moreover, a frequency-domain representation could also include information on the phase shift that must be applied to each frequency component in order to recover the original time signal with a combination of all the individual frequency components. A signal can be easily converted between the time and frequency domains with some mathematical operators, denoted as transforms. A common example is the Fourier Transform, which decomposes a function into a sum of sine wave components. For time-discrete signal, represented by a vector h of dimension n, which data are assumed to be separated by a constant interval in time:

$$dt = 1/f_s \quad (4.1)$$

where f_s is the sampling frequency, the computational basis of spectral analysis is the Discrete Fourier Transform (Stoica and Moses, 2005). The vector h can be represented through its Discrete Fourier Transform (DFT) which gives in turns a vector y of length n, expressed using the same unit of the input signal, which terms are defined as:

$$y_{k+1} = \sum_{j=0}^{n-1} \left(e^{-2\pi ijk/n} \cdot h_{j+1} \right) \quad (4.2)$$

where the notation i is used for the imaginary unit, and k and j for indices that run from 0 to n-1, corresponding to vector range. The DFT is, so, expressed by complex values; the absolute value of y at index k+1 measures the amount of the frequency present in the data. DFT with large number of points are common in many applications; direct application of the definition of the DFT to a data vector of dimension n requires n multiplications and n additions, for a total of $2n^2$ floating-point operation; this does not include the generation of the powers of the complex part of the solution. To compute million-point DFT, the computational complexity could be inappropriate for many practical uses; it has so been introduced the Fast Fourier Transform, a DFT algorithm which reduces the number of computations needed for n points from $2n^2$ to $2 \cdot \lg n$, where lg is a base-2 logarithm. FFTs were first discussed by Cooley and Tukey (1965), although Gauss had actually described the critical factorization step as early as 1805; further and more detailed references could be found in literature (e.g. Bergland, 1969; Strang, 1993). When using FFT algorithms, a distinction is made between the window length, l_w, and the transform length, l_t; the window length is the length of the input data vector, while the transform length is the length of the output, the computed DFT. Generally, it is useful to study the frequency response referring to the power of the signal, defined as the absolute squares of each y_{k+1} divided by the transform length. The power spectrum is then referred as the representation of the frequency content of the signal, and shows the strength of the variations as a function of frequency.

As most of signal studied using spectral analysis, recorded hydrograph represents a deterministic discrete-time data sequence, obtained by sampling a continuous-time signal at fixed time rate (e.g. water level). This could allow estimating efficiently its principal component frequencies using the discrete Fourier transform (DFT) and Fast Fourier Transform (FFT) algorithms, and studying the signal in the frequency-domain space, evidencing how the signal energy is distributed. Hydrometric data presented in this study were collected from river Secchia streamgauge in Ponte Bacchello (Lat. 44.747546, Lon. 10.98734) north of the city of

Modena, with an hourly sampling frequency, so that f_s = 1/3600 sec. However, a direct spectral analysis of hydrograph signal could lead to unrealistic results, as large amplification at low frequency, mainly ascribable to its shape and high dissymmetry respect to a zero (or a mean) value. In order to overcome these issues, it could be useful derive the signal to be studied from the difference between the recorded hydrograph and (one of) its moving average; through this operation it could be successfully possible to process data for obtaining a time-series with peaks and valley oscillating around zero, representing the river flood wave succession. Generally, moving averages are used, in processing historical data series, to provide a reliable trend-following indicator; the strength of a moving average is its ability to filter out data noise from random values fluctuation. The only significant difference between the various types of moving averages is the weight assigned to the most recent data: simple moving average (SMA) apply equal weight to all values; exponential and weighted averages apply more weight to recent values. The critical element in a moving average is the duration of the observation periods used in calculating average, here named as width. The triangular moving average (TMA) is in effect a double-smoothed SMA, in which the weights are assigned in a triangular pattern centered on the middle part of the data interval, in order to smooth out short-term fluctuation and highlight long-term trends or cycles. The TMA calculates a first simple moving average for all values included in the observation period, then calculates a second simple moving average on the first moving average with the same width, and expressed by:

$$TMA = \sum_{p=0}^{w}\left(SMA_p\right)/w \tag{4.3}$$

where w is the width of the observation period. In this study, a triangular moving average (TMA) has been used to properly representing the water level trend variation over time, assuming w = 241 (i.e. observation time equal to 10 days + 1 hour). Then, the hydrometric data have been post-processed, obtaining a proper signal trough the difference between the observed data series and its TMA, as:

$$dh(t) = h(t) - TMA[h(t)] \tag{4.4}$$

where d(h) is a time-discrete function having the same length of h(t) and TMA[h(t)] vectors. In Figure 4.1 an example of the results is reported, showing h(t), TMA[h(t)] and dh(t) for the period July, 15th 2013 – July, 15th 2015.

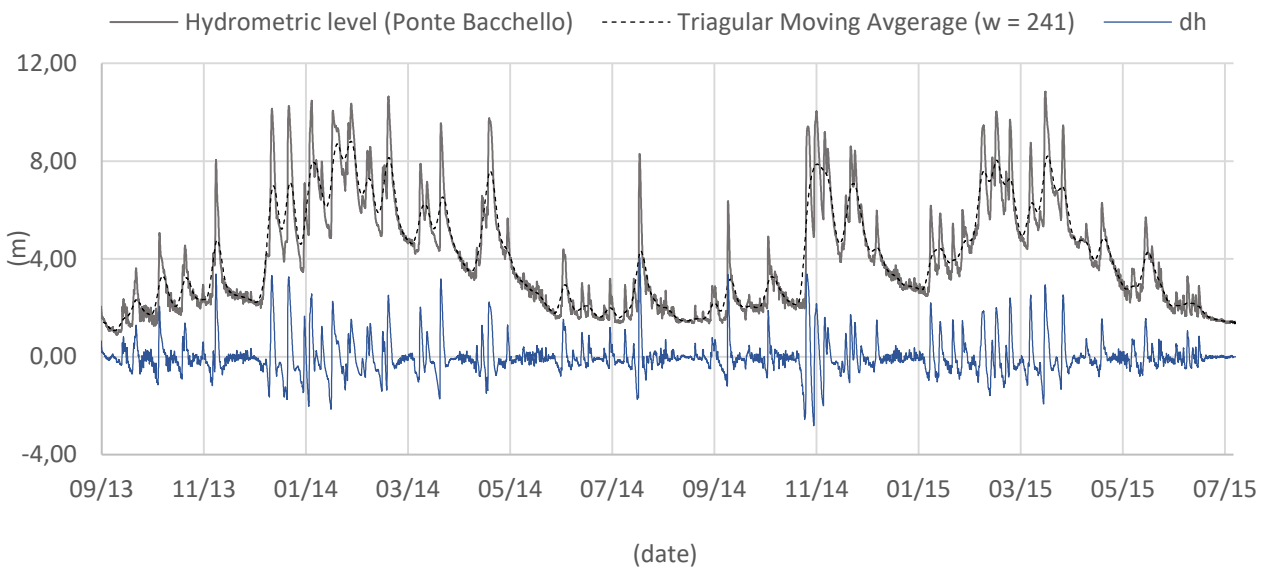

Figure 4.1. Registered data h(t), in grey-solid line, triangular moving average TMA[h(t)], in black-dashed line, and their difference dh(t), in blue-solid line, for relative hydrometric water level of the river Secchia, Ponte Bacchello remote station, for the period July 2013 – July 2015.

The approach has been applied to the hydrometric water level values collected on the Secchia river from the stream gauge in Ponte Bacchello (Ponte Bacchello remote station) during the period July 2000 – July 2015, obtaining the time-discrete function dh(t) for 15 years. These data have been, then, processed through spectral analysis, using the FFT algorithm with a lt = 2000000, aiming to identify the principal component frequencies, and to create a hydrometric power spectrum for the considered site; the results are showed in Figure 4.2, where the power of the dh(t) signal is plotted in the frequency-domain space. As can be seen, the critical incidence in terms of signal power corresponds to a frequency value equal to 1.5·10-6 s^{-1} and time period 7.6 days. This value is, so, interpreted as as the most representative condition in terms of wave length for the considered riverbank section. It has to be noticed that no scaling factor was applied to the DFTs output in this study, as the main aim is just to point out the overall shape of the spectrum. Eventually, the moving average is used as baseline for the hydraulic response of the river bank, and the spectral analysis on the deviation from the baseline is performed to characterize the faster waves, which characterize high water events. It is worthwhile noting that such a choice would be rigorous only for a linear system, while its validity for a non-linear system could be a matter of debate. Nonetheless, the numerical results obtained by superposing the baseline with relevant high water scenarios are compared to the results obtained by performing continuous analysis in the time domain, to verify the feasibility and the limitations of the approach.

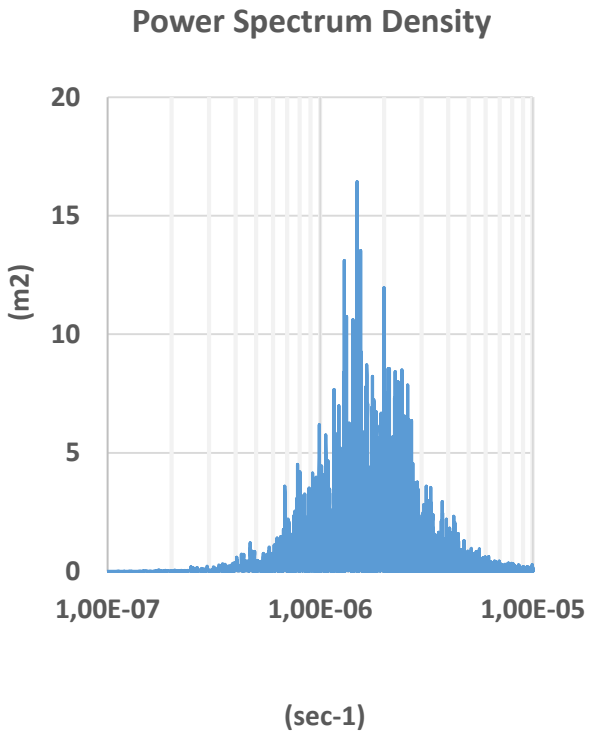

Figure 4.2. Power spectrum density of the dh(t) discrete-function for 15-years observation period, in the frequency-domain space

4.2 Numerical modelling of the hydraulic response

For the determination of the pore-water pressure and suction distribution, to be used in the riverbank stability evaluation, a two-dimensional numerical model of the riverbank section was considered, using the data and the information discussed in the previous section. The quantification of soil evaporation and of soil water content dynamics near the soil surface are critical in the physics of land-surface processes on regional and global scales, in particular in relation to mass and energy fluxes between the ground and the atmosphere. Although it is widely recognized that both liquid and gaseous water movement are fundamental factors in the quantification of soil heat flux and surface evaporation, their computation is still rarely considered in most models or practical applications. Moreover, questions remain about the correct computation of key factors such as the soil surface suction values distribution, having strong influence on the initiation process of underground hydraulic seepage and sensible effect on soil resistance (Bittelli et al. 2008). In order to properly consider all the climatic and hydraulic conditions, which directly influence the seepage response of the riverbank, a two-dimensional finite element analysis was performed coupling ground heat, liquid and vapour flow with the commercial code VADOSE/W (Geo-Slope International Ltd, 2008), for which both saturated and unsaturated conditions are accounted for. The code includes the use of climatic boundaries to

simulate the effect of soil-atmosphere interaction and root-water uptake relation to solve Richard's flow equation; however, vegetation effect was disregarded in this study. Penman-Wilson (Wilson, 1990) method is implemented to compute the actual evaporation as a function of the estimated potential evaporation. This formulation is able to account for net radiation, wind speed, and the relative humidity of both the air and the soil surface while calculating the evaporation from the soil surface. The relative humidity of the soil surface was evaluated by simultaneously solving the coupled moisture and heat flow equations, while in this model the effect of wind and vegetation was disregarded. The theoretical formulation and the correspondent governing differential equations for two-dimensional seepage are summarized in the reference manual (Geo-Slope International Ltd, 2008). Verification and validation for the specific code have been widely discussed in literature, founding good agreement with experimental cases and numerical predictions comparing different codes (Scanlon, 2002; Benson, 2007). For the present case, thermal conductivity and volumetric heat capacity has been assumed equal to 0.88J/s/m/°C and 2510kJ/m^3/°C, constant for the analysis; these values have been considered typical for soil type on the base of typical values for the specific and volumetric heat capacity of various materials (Harlan and Nixon, 1978). Numerical parametric study on the effect of soil thermal properties have been, thus, performed, finding limited variations in significant results in terms of overall slope stability, in the range typical for soil minerals. Adaptive time stepping, determined by software routine on the base of maximum change in total head per step, have been considered for the transient thermos-coupled analysis; convergence problems are, in fact, a significant matter for the performed analysis, particularly in case rainfall event are modelled when in surface nodes are experiences extremely high (absolute) values of soil suction. For the set of analyses presented in this Thesis, allowable time step range have been defined with minimum and maximum values equal to 600 and 3600 seconds, respectively. Minimum pressure head and temperature difference in the comparison iteration criteria has been assumed 0.005m and 0.1 °C, respectively.

4.2.1 Initial and boundary condition

Frequent fluctuations in negative pore water pressure are produced by rainfall, variations in the river level, evapotranspiration and variations in the capillary fringe of the groundwater. As a consequence, the suction pattern recorded on site is in general quite different from the hydrostatic linear profile (Rinaldi and Casagli, 1999; Calabresi et al., 2013), generally assumed in preliminary stability analyses. The assumption on the initial condition, in terms of suction and pore water pressure (PWP) distributions and in absence of direct in situ measurement, represents a crucial point in riverbanks seepage and stability evaluation, both for its significant uncertainty and the strong influence on the final results. In this study, a transient coupled hydro-thermal analysis was performed using the climatic and hydrometric data measured from July, 15th 2013 to July, 14th

2014 for the model spin-up. This period was considered sufficiently long to erase the effect of the initial hypothesis on the calculated pore pressure, basing on various references (Rinaldi et al., 2004; Calabresi et al., 2013). This way, a suction and PWP distribution representing a realistic initial condition was determined, for the subsequent numerical simulation. Similar procedure has been adopted for numerical analysis in Gottardi et al. (2016). Results given in Figure 4.3, in terms of PWP, refer to a time step analysis representing July, 15th 2014, 00:00; the increment between two adjacent isolines is 10 kPa and the blue bold line indicates the phreatic line. However, in situ measurements such as those proposed could avoid the need for model spin-up and would corroborate the results obtained by this numerical expedient, which relies on several assumptions.

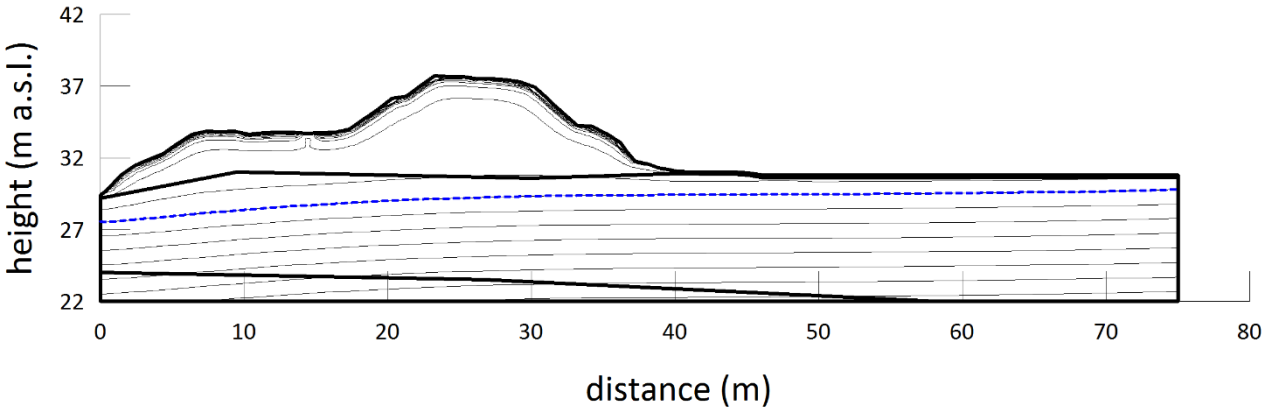

Figure 4.3. Initial pore water pressure distribution for the riverbank numerical model; analysis time-step refers to July, 15th 2014, 00:00.

Assuming the PWP distribution showed in Figure 4.3 as the initial condition, two different set of transient coupled hydro-thermal analysis have been performed using both hydrometric data measured during the period July, 15th 2014 – July, 15th 2015, and its TMA 241-width, showed in Figure 4.4, in addition to the climatic data registered in the neighbourhood of the studied section. Infiltration in soil occurs during precipitation at a rate governed by the hydraulic properties of the profile, while precipitation exceeding the infiltration capacity is assumed to be run-off. Evaporation is assumed to occur from the soil surface and is bounded by the potential evaporation rate (PE). During rainfall event, the code compute a net flux through the boundary surface that is equal to the difference between the precipitation and the potential evaporation rates.

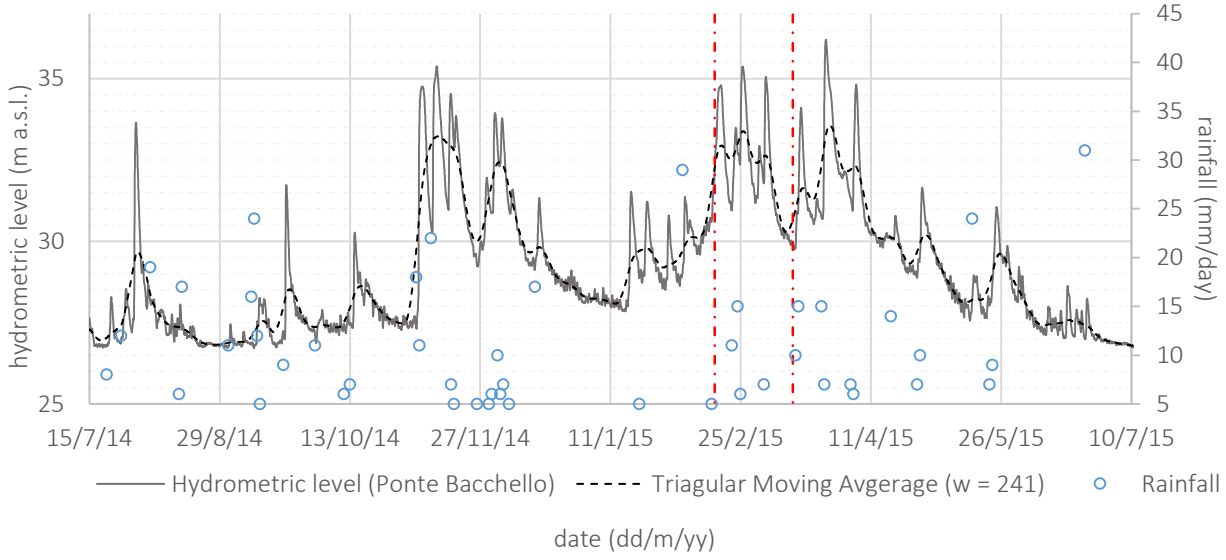

Figure 4.4. Registered data h(t), in grey-solid line and triangular moving average TMA[h(t)], in black-dashed line, for hydrometric water level a.s.l. for the river Secchia, Ponte Bacchello remote station, for the period July, 15th 2014 – July, 14th 2015. The specific studied event is evidenced in red dash-dot line (February, 16th 2015 – March, 09th 2015).

To simulate the effect of a high water sequence event, using the results obtained from spectral analysis, a sinusoidal wave has been superposed to the hydrometric baseline represented by the TMA 241-width. The representative event considered in this study refers to the period February, 16th 2015 – March, 15th 2015, evidenced by the dashed-dot red lines in Figure 4.4. The sinusoidal wave has a period equal to 7.6 days, which corresponds to the frequency with the maximum power in the spectrum analysis (Figure 4.2), and an amplitude of 3.0 m, equal to the difference between the maximum hydrometric recorded value for the considered event and the TMA estimate on February, 16th 2015. The hydrometric level obtained adding the sinusoidal wave to TMA value at February, 16th 2015 at 05:00 has been used as boundary condition for the numerical analysis. The time history of the boundary conditions used in the two analyses are plotted in Figure 4.5, together with the time-steps at which the results of the numerical analyses and the following stability analysis are compared and discussed. The use of sinusoidal wave to represent the hydrometric level time-variability have been used in literature to study the effect of soil hydraulic hysteresis and heterogeneity on the stability of embankment under transient seepage (Liu et al., 2015; Liu et al., 2016), but for study case that was not referenced to a real water retaining structure, without accounting for soil-atmosphere interaction and disregarding topics related to a proper initial conditions determination. However, it is necessaire here to notice that, in general, the hydrometric peak does not represent the critical step for riverbank assessment; in fact, the maximum progression of the phreatic line and the minimum stability conditions are estimated with some delay to the maximum water level (Ridley et al., 2004; USACE, 2006). Indeed, the choice to refers hydrometric peak as time-step for riverbank assessment is derived to the possibility to refers to a comparable external load conditions among the various considered cases. Riverbank seepage and stability characteristics

in correspondence of the maximum water height, even not being the most hazardous for safety assessment, are however a significant index for the hydraulic and mechanical behaviour of the system; this is particularly true in cases complex hydrographs are considered, so that the sequences of hydrometric peaks may have a significant interplay effect on results. Further discussion on the critical step for transient seepage analysis in different hypothesis on initial conditions, considering different mathematical approaches for probabilistic studies are discussed in Chapter 7.

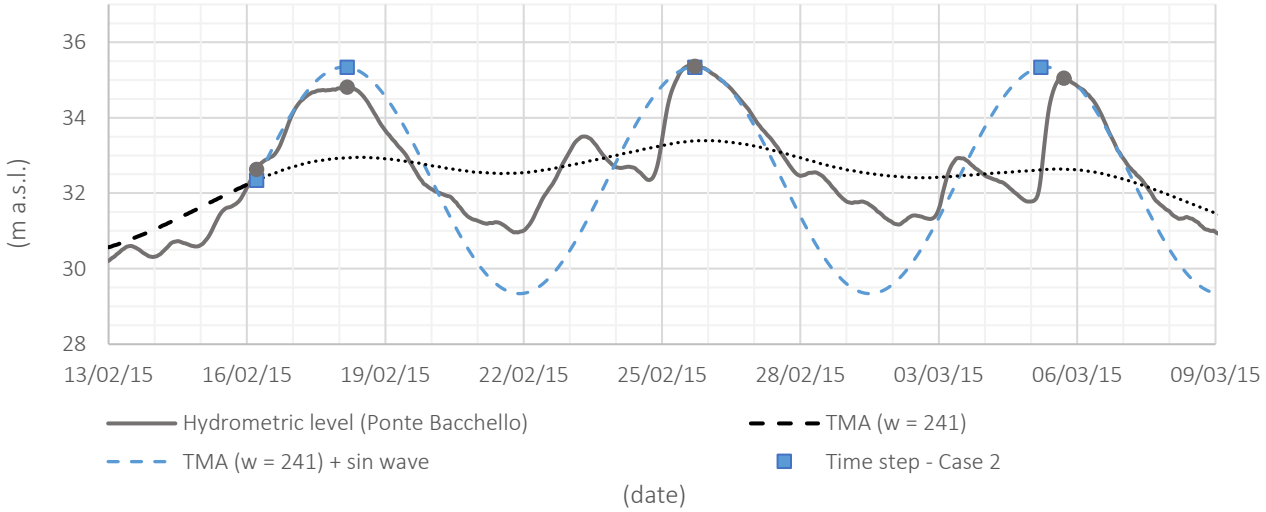

Figure 4.5. Registered data, h(t) in grey-solid line, triangular moving average, TMA[h(t)] in black-dashed line, and sine-wave overlapped to the value TMA[h(16th February 2015 00:00)] = 32.34 m a.s.l. for hydrometric water level a.s.l. for the river Secchia, Ponte Bacchello remote station, for the period February, 16th 2015 – March, 09th 2015. Grey circled and blue squared markers indicate the time steps at which results are shown.

Using the PWP distribution showed in Figure 4.3 as initial condition, two different scenarios has been investigated, differing on the hydraulic boundary conditions. In particular, it has been considered for the first scenario (named as "Case 1") river water levels measured during the period July, 15th 2014 – July, 14th 2015, and for the second scenario (named as "Case 2") its TMA 241-width to which has been overlapped a sinusoidal wave from February, 16th 2015 – March, 09th 2015. Concerning the second case, one of the possibilities to represent a simplified hydraulic boundary conditions was thought to be a sinusoidal wave superposed to the hydrometric baseline represented by the TMA 241-width estimated for the whole high-water event (Figure 4.6). The advantages in using this hypothesis could certainly be to reproduce more realistically the registered water level; in fact, using a time-variable baseline could be possible to describe more consistently the rise and the reduction of the river level. However, two important issues should be, then, considered: firstly, using a sinusoidal wave with constant amplitude could not be possible to predict precisely all the peak water level, especially for long-lasting event. Secondly, the use of a time-variable base line requires the knowledge on the hydrometric water level measurement for all the considered event; this

could be possible for assessing the stability conditions of existing water retaining structures in relation to past events, but could not be relevant for a predictive model. in this study, Case 2 stands for a practical and simplified application for the proposed approach.

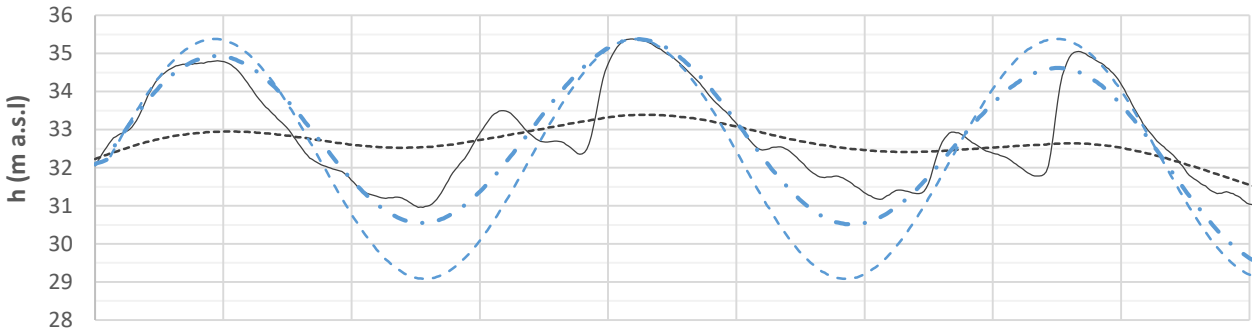

Figure 4.6. Registered data h(t), in blue-solid line, triangular moving average TMA[h(t)], in blue-dashed line, and sinusoidal waves superposed to constant, in orange solid line, and variable baseline represented by the TMA relative to hydrometric water level of the river Secchia, Ponte Bacchello remote station, for the period Febraury – March2015.

4.3 RESULTS AND DISCUSSION

Four time-steps (Figure 4.5) have been selected, corresponding to the initial condition of the high water event sequence and the subsequent three peaks of the hydrometric level for the two cases. In Figure 4.7. Pore water pressure distribution at different stages during the period February, 16th 2015 – March, 09th 2015, using the registered hydrometric water level (left) and a sinusoidal wave with characteristic frequency for the specific site (right) the PWP distributions estimated by the unsaturated seepage analysis are shown. Soil-atmosphere interaction was accounted for, in both Case 1 and 2.

The largest differences in the pore-water pressure distribution between the two cases are mainly evidenced on the riverside slope, where the influence of the high-water event before February, 16th 2015, considered in Case 1, reduces the absolute values of suction, compared to Case 2. On the inland, the PWP distribution, at the beginning of the considered time period, mainly depends on the climatic boundary conditions and on the soil-atmosphere interaction, resulting similar in both cases. For the steps from 1 to 3, which correspond to the first two peaks of the hydrometric level in both analysis, the phreatic line as well as the PWP distribution nearby the outer slope are affected locally by the hydraulic boundary conditions, but the pressures in the core of the embankment calculated in the two cases match well in the two cases. The slight differences in the results of the two cases in correspondence of the inner slope, can be ascribed mainly to

the difference between the waveforms considered in the two analysis cases; to reduce these, other waveform shapes, characterised by different rates of hydrometric level variation in the rise and drawdown phases (e.g. log-normal, Weibull distribution) could be more appropriate to accurately simulate high water events, when multiple cycles are considered.

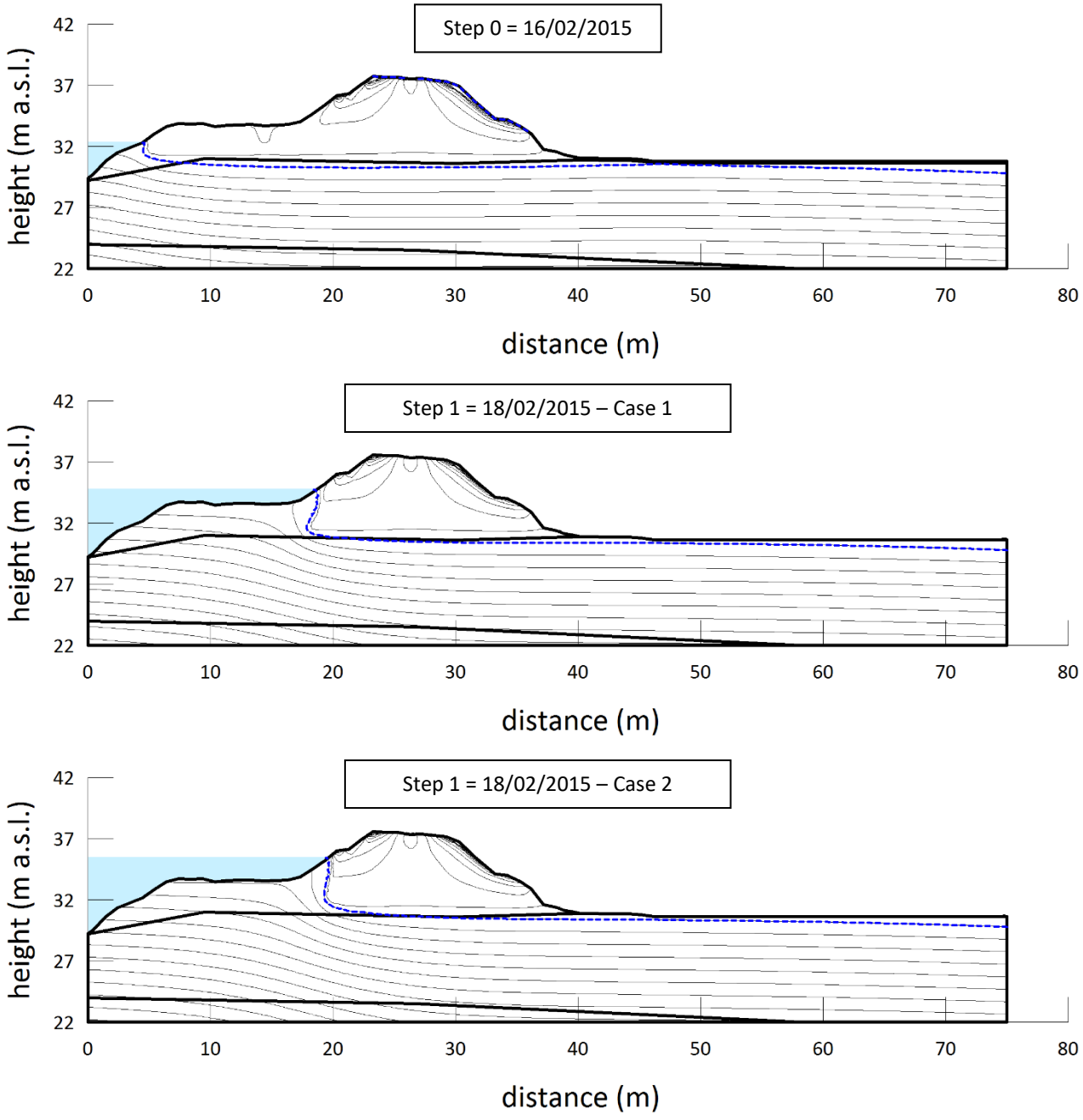

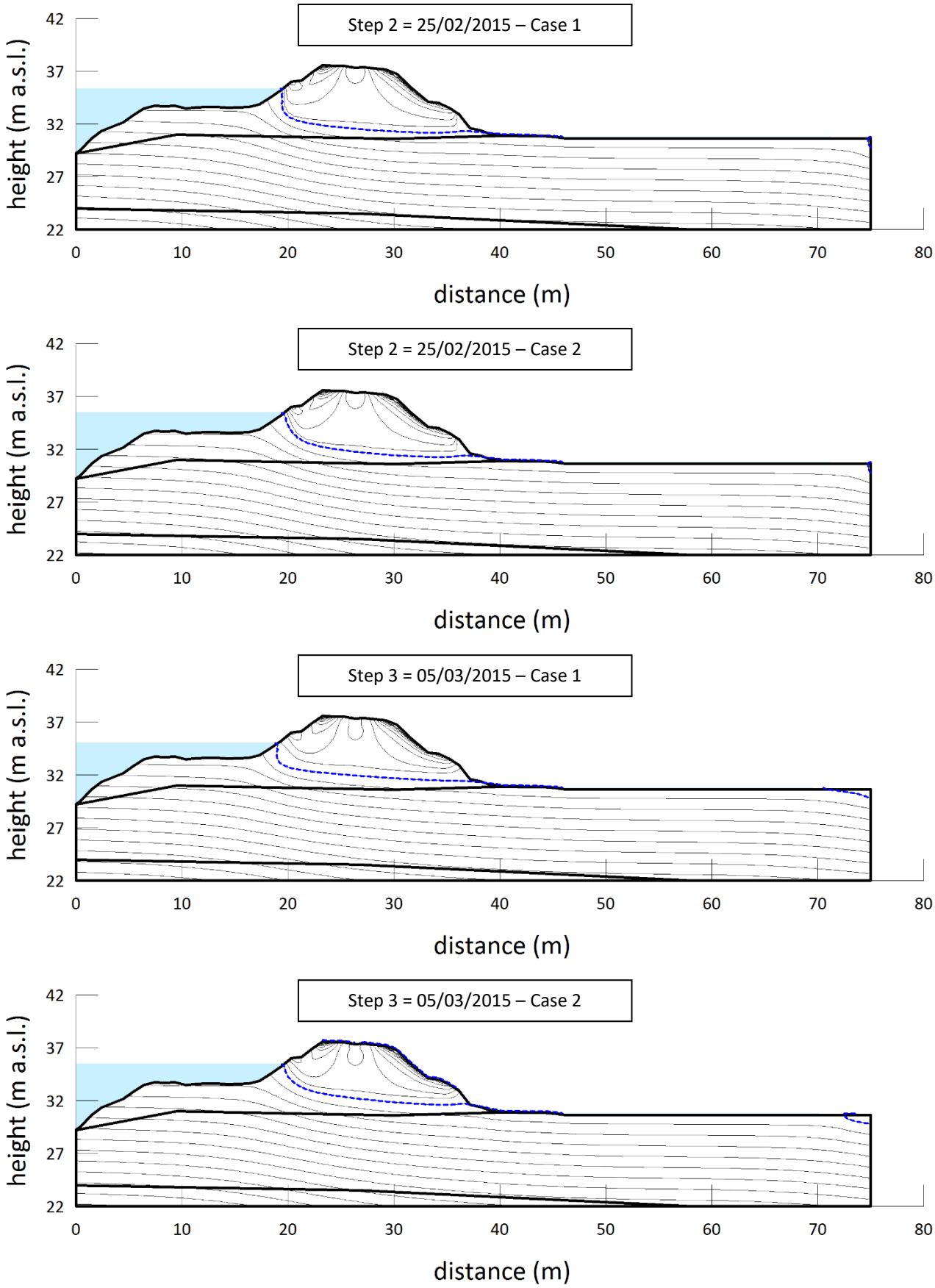

Figure 4.7. Pore water pressure distribution at different stages during the period February, 16th 2015 – March, 09th 2015, using the registered hydrometric water level (left) and a sinusoidal wave with characteristic frequency for the specific site (right)

The reduced amount of suction values on the top of the riverbank is mainly due to the influence of rainfall infiltration, and on the combined effect to allow surface water to pound on climate boundary conditions.

Using the PWP distributions obtained by the previous analysis, the outer slope stability conditions have been studied by means of limit equilibrium analysis adopting the Morgenstern and Price method (Morgenstern and Price, 1965), at each considered step for both cases. The analysis was performed through the Monte Carlo method (100 000 simulations) on critical surfaces defined by specific geometrical constraints (e.g. entry and exit point range; minimum slip surface depth), to investigate the instability mechanisms. The friction angles of the various soil layers were the only random variable introduced in the analysis. In Figure 4.8 the estimated Safety map is shown, indicating the zone where critical slip surfaces occur (in red), referring to the specific event.

The mean values of the Factor of Safety (μ_{FS}) distribution together with the reliability index (β) are shown in Table 2, for both case cases with reference to the considered calculation steps. The results shown in Table 2.2 show that the two approaches produce similar probabilities of failure for the landward potential instability mechanisms, which are directly dependent on the riverbank core hydraulic response characteristics, due to the similar PWP distribution shown in Figure 4.7. Pore water pressure distribution at different stages during the period February, 16th 2015 – March, 09th 2015, using the registered hydrometric water level (left) and a sinusoidal wave with characteristic frequency for the specific site (right). The values of μ_{FS} and β, in fact, are in good agreement in the two cases and provide similar estimations for the riverbank stability conditions. Slight difference is mainly evidenced in step 1, in which Case 2 forecasts safer conditions than Case 1, despite the higher value of the river water level, mainly due to the different initial PWP distribution adopted in the two cases at step 0.

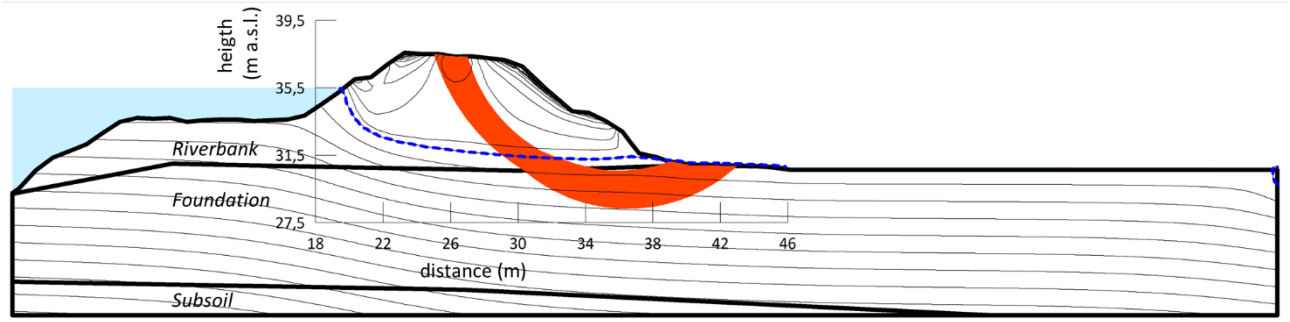

Figure 4.8. Riverbank safety map for the considered high water event. The area where slip surfaces have the lowest FS are drawn in red; the most critical surface is drawn in white; a minimum slip surface depth equal to 4 m was assumed

	μ_{FS}		β	
	Case 1	Case 2	Case 1	Case 2
Step 1	1,53	1,52	3,570	3,688
Step 2	1,36	1,34	3,187	3,124
Step 3	1,31	1,29	2,923	2,801

Table 4.2. Results of probabilistic stability analysis for Case 1 and 2; mean value of FS distribution and reliability index are shown for each considered calculation time-step.

A methodology for assessing stability conditions of existing water retaining structure has been here presented and discussed. The theoretical base of the proposed approach is constituted by a mathematical study of riverside water level measurements, which aims to individuate a hydrometric spectrum for a specific site. Through this operation, the amount of frequency present in data, and its principal characteristics, could be identified in order to obtain a characteristic range of variation for the input data respect to typical seasonal trend. Afterwards, series of transient seepage numerical analysis are needed, firstly, to define proper initial conditions in terms of pore water pressure and suction distribution for the specific problem and, then, to investigate the effect of hydrometric water level time-variability on seepage and stability evaluation.

In this section, results obtained through spectral analysis, referring to data collected from river Secchia streamgauges, have been used to identify a simplified but representative hydraulic boundary condition to be assumed in numerical models. Initial condition in terms of PWP and suction has been established performing seepage analysis, accounting soil-atmosphere interaction, for an adequate period of time. Registered (Case 1) and simplified (Case 2) hydrometric water level have been used as boundary condition to evaluate riverbank seepage and stability conditions, obtaining consistent and similar results in terms of Factor of Safety and reliability index. Although Case 2 simulations represent a basic example of the proposed approach, this methodology could be a prelaminar as useful tool to forecast and assess vulnerability conditions for existing riverbanks, achieving good predictive models using historical hydrometric data series. Further researches for a simpler definition of the initial conditions for the seepage analysis as to get a better comprehension of the influence of hydraulic, retention and mechanical soil parameters on the results, are performed and discussed.

5 Assessing the stability conditions of existing water retaining structure

In the previous Chapter (4), a novel methodology for describing hydrometric water level time-variability in the assessment of riverbank stability has been introduced and some preliminary applications described. Results presented showed a good agreement in terms of reliability index and, so, safety margins towards overall instability mechanism obtained assuming two different hypotheses (Case 1 and Case 2) on the hydraulic boundary conditions in the seepage analysis. In particular, in the first case, the hydrometric water height measured in the neighbourhood of the collapsed section was directly assigned to the nodes of the inner slope of the model (river-side) while, in the second case, a sinusoidal wave was superposed to a hydrometric baseline represented by the TMA 241-width value estimated in correspondence of the beginning of the high-water event registered in February in Ponte Bacchello. In this framework, Case 1 could be referred to a realistic back-analysis while Case 2 represents the application of a simplified method to model the problem, for which one unknown variable (the hydraulic boundary conditions in correspondence of a high-water event) has been replaced by a possibly known term depending on an available historical data series. In particular, it has been showed that the use of a synthetic hydrograph, built on the base of the frequency-domain analysis on the hydrometric measurement of water levels, could represent an appropriate tool to, eventually, forecast and assess the vulnerability conditions for existing riverbanks, for that specific example. This finding has been obtained on the basis of analysis performed on a well-studied riverbank section, and it's a direct consequence of the similarity between the boundary conditions assumed for the two studied Cases. Although this similarity can be function of the representativeness of the considered simplified hydrograph respect to the one recorded, that could be considered adequate for the type of analysis performed, it's required to the purpose of this study to extend the investigation for different hypothesis on the synthetic boundary conditions; furthermore, aiming to extend the use of this method and in order to evaluate its potential applicability, it's necessaire to study in deep the effect of soil parameters on seepage and stability results. This Chapter will be, then, demanded to the description of results from several types of analysis characterized by different level of sophistication, that could lead the assessment of the stability conditions of existing riverbanks from preliminary phase on.

5.1 On the use of synthetic hydrographs for the assessment of the hydraulic response of riverbank

In this section, the analyses performed to study the effect of different profiles of synthetic hydrographs on the hydraulic response of the considered riverbank section will be presented; then, numerical results

obtained will be discussed and will constitute a useful guide to define the critical conditions for global safety for a number of subsequent high-water peaks with various wave lengths. The methodology used for the definition of the models and the initial and boundary conditions refers to the procedure described in Chapter 4, and will be hereafter discussed and explored with specific focus on the different features respect to the application previously presented.

5.1.1 Initial and boundary conditions

Using the geometrical and geotechnical information described in Chapter 3, the riverbank seepage characteristics has been evaluated using the two-dimensional FEM code VADOSE/W, by performing transient coupled hydro-thermal flow analysis. The PWP distribution used as initial condition for the seepage numerical analyses has been obtained considering the period July, 15th 2013 to July, 14th 2014 for the model spin-up; then, analysis have been performed using the hydrometric and climatic data recorded in the period July, 15th 2014 to February, 15th 2015, as also specifically described in Chapter 4. Using the PWP distribution determined in the last step of this analysis, three boundary conditions have been considered, representing different profiles in terms of hydrometric level, one for each synthetic hydrograph. In details, starting from the results of the frequency-domain analysis on the hydrometric data recorded from the stream gauges placed in Ponte Bacchello, a possible range of variation for the most frequent and impactful length of the sine-waves has been individuated. Most of the signal energy, around the 75% of the total, is distributed in a frequency range varying from $7.7 \cdot 10^{-7}$ sec^{-1} and $3.3 \cdot 10^{-6}$ sec^{-1} (see Figure 5.1), corresponding to time periods equal to 15.0 and 3.5 days, respectively, with a dominant value in correspondence of a frequency equal to $1.5 \cdot 10^{-6}$ sec^{-1} and time period 7.6 days (see Table 5.1). These values are interpreted as the characteristics wave lengths for the considered riverbank section, which detect the critical events period, ranging from 3.5 to 15.0 days, and strong incidence at 7.6 days. Aiming to represent the effect of a high-water sequence, e.g. the event registered from February, 16th 2015 to March, 09th 2015, a series of sine-waves of constant period and amplitude was superposed to a hydrometric baseline, represented by the triangular moving average (TMA) 241-width value estimated in correspondence of the beginning of the registered high-water event. The considered baseline height is, furthermore, equal to the hydrometric record of the 15th of February, 32.1m; this particular condition could forewarn, generally, a rapid growth for the river flux. However, a time-shift has been considered for the sine-waves in order to let the hydrometric peak of synthetic and real hydrographs match in time. The periods considered in this study are intended as characteristics wave lengths for the riverbank section, $fc1^{-1}$, $fc2^{-1}$ and $fc3^{-1}$, which could be referred as the maximum, the average and the minimum time-distance between two following water peaks of a synthetic hydrograph; the amplitude of each sine-waves is 3.15 m, equal to the difference between the maximum hydrometric record for the considered event and the considered baseline.

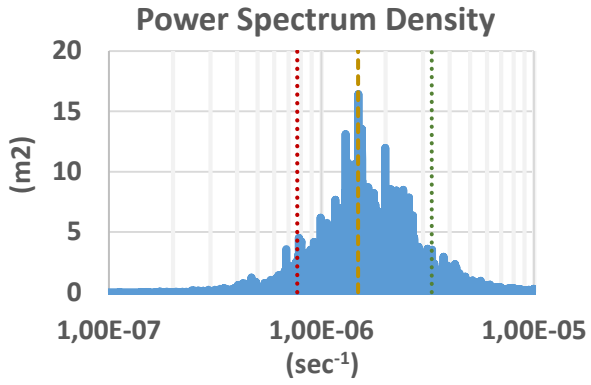

	frequency	Equivalent period
	(s^{-1})	(day)
fc1	$7.7 \cdot 10^{-7}$	15.0
fc2	$1.5 \cdot 10^{-6}$	7.6
fc3	$3.3 \cdot 10^{-6}$	3.5

Figure 5.1. Power spectrum density of the dh(t) discrete-function for 15-years observation period, in the frequency-domain space, with evidenced the characteristics wave lengths for the studied riverbank section.

Table 5.1. Values of frequency and period corresponding to the characteristics wave lengths.

In Figure 5.2 are plotted the sine-waves, oscillating around zero (which represent the baseline here considered), used to describe the synthetic hydrograph profiles in the numerical analyses; their combination with the baseline represent Case fc1, Case fc2 and Case fc3. In absence of more accurate studies, it was assumed that wind, humidity, temperature and rainfall data collected between the first and the second peak of high-water event registered from February, 16th 2015 to March, 09th 2015 have been cyclically considered as climatic boundary conditions on for each subsequent peak of the synthetic hydrographs, taking care of spreading the amount of rainfall as function of the sine-wave lengths. It worth to notice that the hypothesis on the climatic data, used for the analysis assuming the synthetic hydrographs as boundary conditions, received here less attention than other aspects of the work.

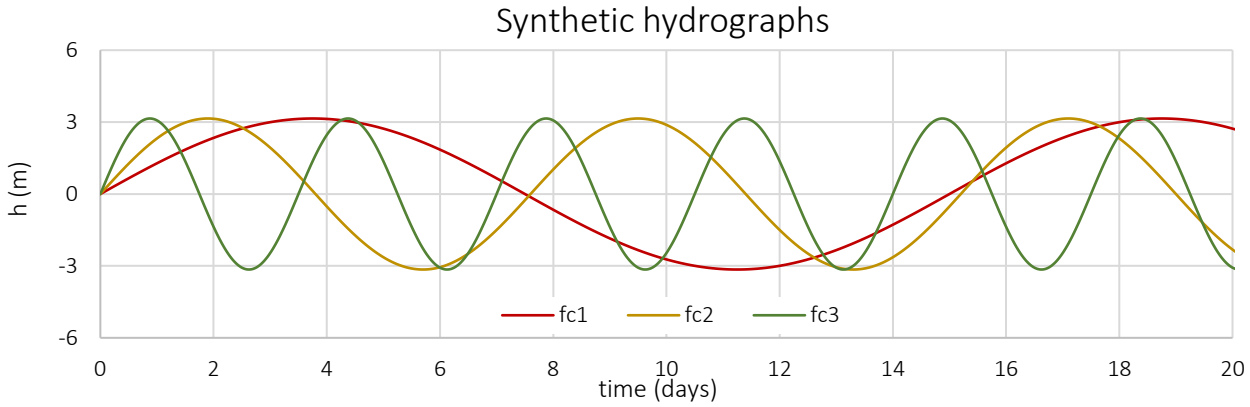

Figure 5.2. Sine-waves characterized by different periods used to define the different synthetic hydrographs used in the numerical seepage analysis.

5.1.2 Description of the output

In order to summarize the most significant results of the analysis and to propose suitable comparison between the various hypothesis on the profile of the hydrographs, it could be useful to refer one, or more, output provided by the calculation to a critical or limit condition. For the purpose of this study, a limit state for transient seepage analysis could be represented by the steady-state conditions, in which pore water pressure distributions are in equilibrium with prescribed boundary conditions for assigned soil properties, and independent by the time variable; this conditions is, besides, generally assumed for the simplified stability assessment of water retaining embankments, considering design values for water height. The numerical output considered is the total head evaluation at specific measurement points of the riverbank, representative for system; the total head, or hydraulic head, is a measure (in units of length) of the potential of the water fluid and is defined as:

$$H = h_z + h_p + v^2/2g \tag{5.1}$$

where h_z is the position head and is associated to the elevation of the point respect to a reference system, h_p is the pressure head is a measure of the pore pressure of the water in the soil, and $v^2/2g$ is the kinetic head and is associated to the equivalent velocity of the water flow in the considered soil; this last component is certainly negligible considering the values of hydraulic conductivity and gradient of this study. In Table 5.2 the coordinates of the control nodes are listed and in Figure 5.3 their labels and positions in the numerical model are showed; from left to the right they are named as left, top left, top, top right, right, bottom right. It is significant here to notice that the considered points are all part of the riverbank layer.

	left (lt)	top left (t.lt)	top (t)	top right (t.rt)	right (rt)	bottom right (b.rt)
x (m)	20,30	23,27	26,25	29,23	32,22	35,19
y (m a.s.l.)	30.73	30.73	30.73	30.73	30.73	30.73

Table 5.2. Coordinates of the control nodes considered for the output. Height is expressed in m above sea level.

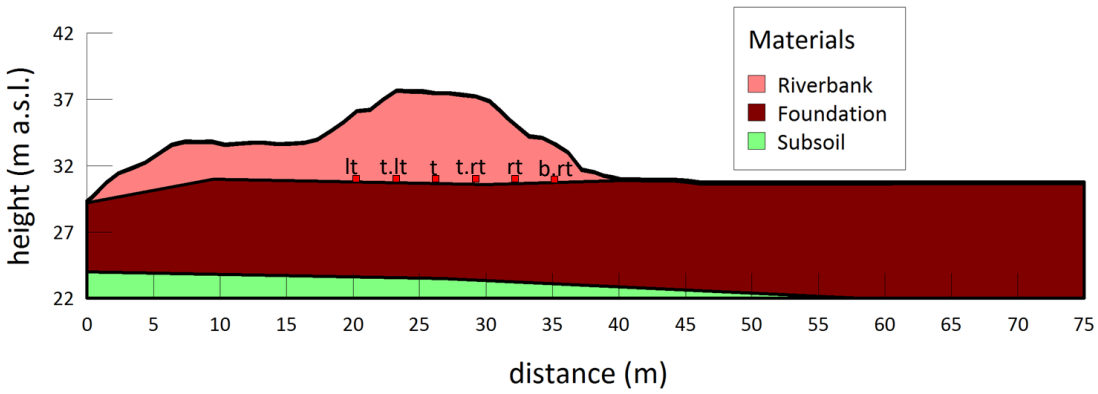

Figure 5.3. Position of the control nodes in the numerical model; from left to the right: left, top left, top, top right, right, bottom right.

The labels of the control nodes refer to their projection in correspondence of the ground level profile. The height of the reference system has been, then, assumed at 29.73 m a.s.l., corresponding to the average height of the water table derived by piezometric measurements during the dry season. Geo-Studio software calculation procedure uses the Gauss quadrature scheme (Golub and Weolsch, 1969) to compute the numerical solution at specific nodes, involving sampling the element characteristics at specific points known as Gauss points and then adding up the sampled information. The consequent values of the piezometric heads estimated at various step of the transient seepage analyses have been divided by their equivalent for steady-state conditions in equilibrium with the maximum hydrometric level reached during the considered event. This ratio, dimensionless and hereafter referred as h_d, is equal to 1 when the steady-state conditions are reached and is zero when the piezometric heads in the control nodes is equal to the height of the water table in the dry season, and is schematically reported in Figure 5.4. The values of h_d in the various control nodes represents a useful index, in this study, for the progression of the phreatic line in the riverbanks during a high-water event and their fluctuations in the range 0 to 1 could be considered to synthetically summarize the hydraulic response of the entire system at different types of hydrographs. It is, furthermore, here important to remark that direct measurement of h_d in the suggested control nodes could be possibly achieved by means of piezometric measurement, making this index suitable for comparison with monitoring data.

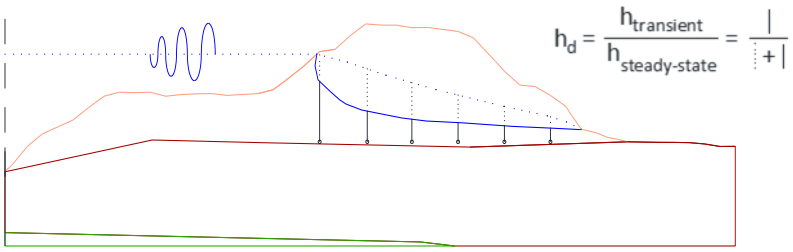

Figure 5.4. Scheme of the dimensionless head, h_d, in the control node; in straight line is represented the transient condition while in dot line are represented the steady state condition. The time step considered for the results correspond to the peak values of the various hydrographs, synthetics and real.

5.2 Seepage analysis: results and discussion

In Figure 5.5 the values of h_d evaluated by the unsaturated seepage analysis using the synthetic hydrographs are shown for all the considered control nodes; seven subsequent waves have been considered for comparison at each Cases, differing for the frequency considered for the sine-waves: *fc1*, *fc2* and *fc3*. As can be seen by the results showed, the progression of the phreatic line for any transient seepage analysis doesn't reach the position estimated in steady-state conditions (Case 3); in fact, the values of h_d are always lower than unity for all the considered Cases, even at the last of the considered time step which corresponds to the seventh consecutive wave. This first remark could be intended as a preliminary confirmation of the highly safe results that could be provided by working with the steady-state seepage flow hypothesis. Considering these output, it seems that the pressure heads in the control nodes, for the assumed reference system, state to a maximum of around the 75% - 85% of the values in limit condition. In particular, the maximum values are almost reached in correspondence of the third peak for the Case fc1, when the higher characteristic period for the sine-waves is assumed, and around the fourth peak for the Case fc2 (corresponding to Case 2, previously described, in terms of hydraulic response), when average characteristic period for the sine-wave is assumed. Differently, for the Case fc3, even in correspondence of the seventh consecutive wave defined by minimum characteristic period, the increase in height of the piezometric line is constantly appreciable, meaning that the stable conditions need more consecutive events to be reached.

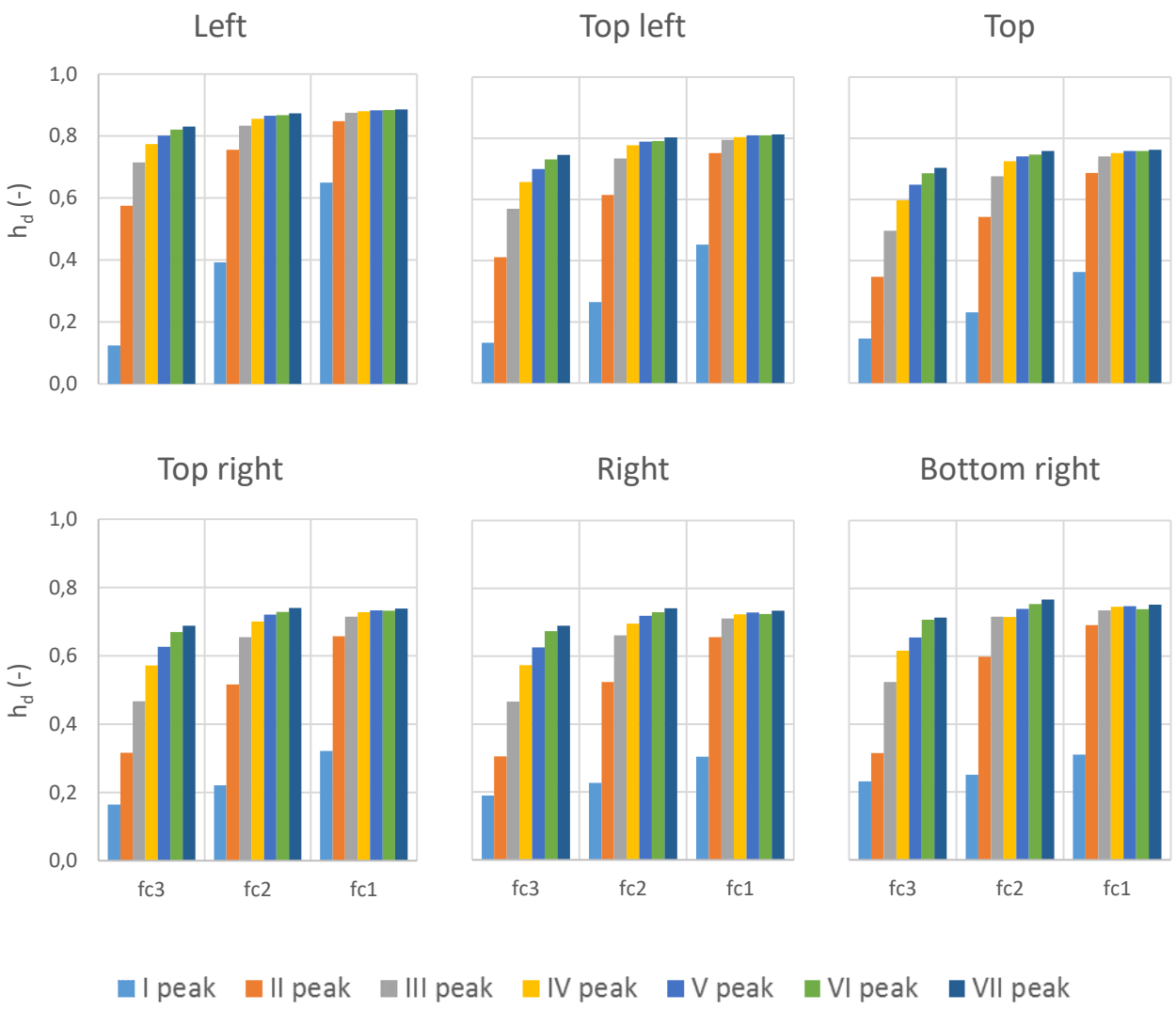

Figure 5.5. Dimensionless head of the control nodes, from the unsaturated seepage analysis using synthetic hydrographs as hydraulic boundary conditions, at various time steps corresponding to the peak value of the hydrometric heights.

In general, the growth in h_d values is more long lasting if considering the control nodes on the right side (toward landward) of the riverbank, meaning that those nodes require more, or more persistent, subsequent peaks to reach a final and stable condition with regards to the position of the phreatic line. In Figure 5.6 the values of h_d estimated at the time step considered for the various cases (real and synthetic hydrographs) are plotted as function of the elapsed time; in particular, the time is expressed in days starting from the beginning of the high-water sequences, on February, 15th 2015. This representation of the output evidence the variation of the hydrometric head with time during high-water events, by means of numerical calculations. It can be noticed that, using synthetic hydrographs and for the assumed hydraulic and retention soil parameters, result seems not to be strongly dependent on the period of the sine-waves, characteristics for the section, but principally on the duration of the event; in fact, a comparable estimate of the progression of the phreatic line into the riverbank could be provided quite irrespectively from the shape of the various hydrographs, but

mainly dependent on the elapsed time. This could mean that, in example, the hydraulic response of the riverbank in presence of 2 or 6 consecutive water peaks with period equal to 3.5 days can be equivalent to its alike in presence of 1 or 2 consecutive water peaks with period equal to 15 days with an approximation acceptable for the purpose of this study, if assuming that h_d and the control points could be representative for the hydraulic response of the riverbank and considering that the initial phase of the event is the growth of the hydrometric level from the initial baseline.

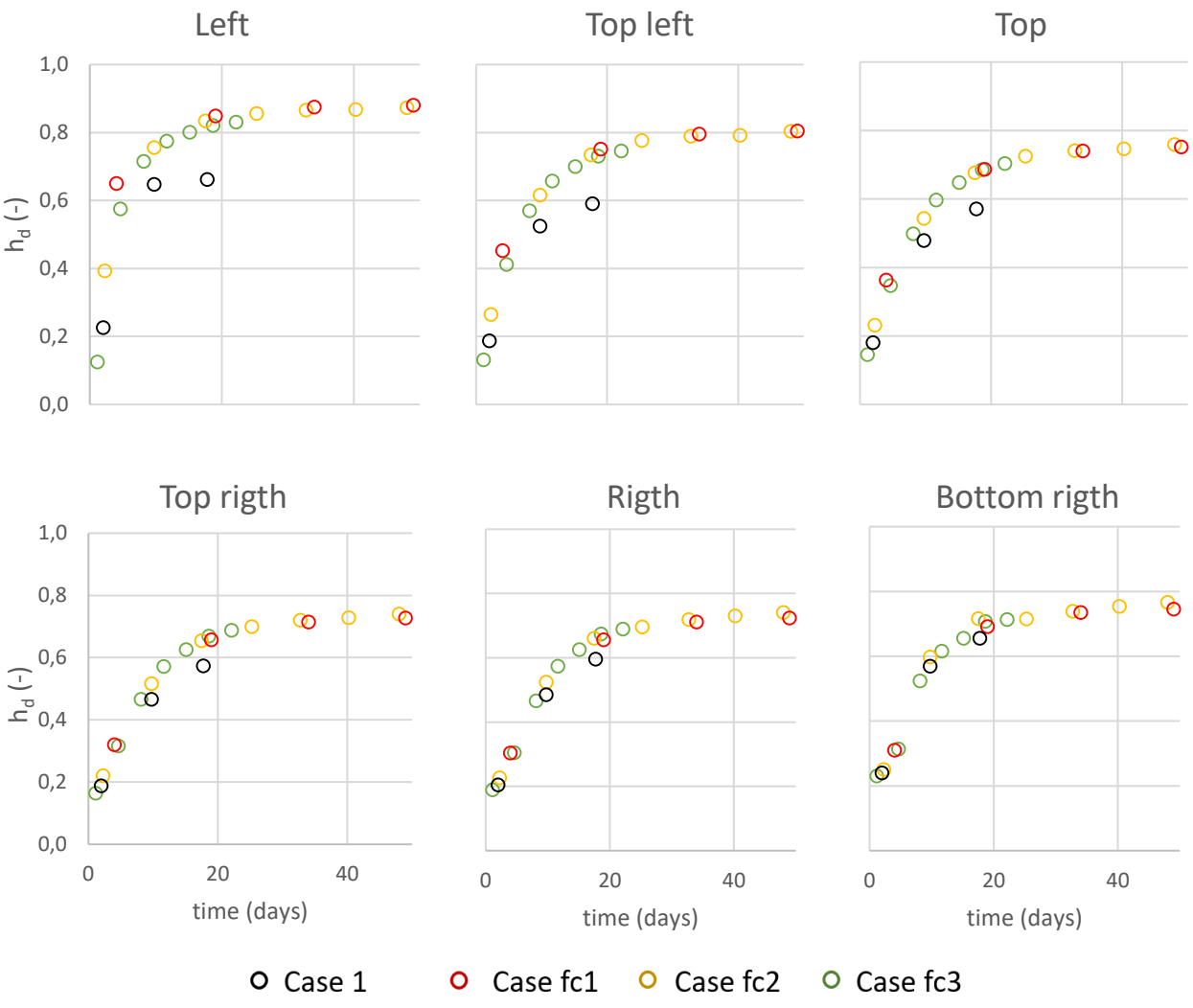

Figure 5.6. Dimensionless head of the control nodes from the unsaturated seepage analysis using real and synthetic hydrographs as hydraulic boundary conditions, plotted as function of the elapsed time (expressed in days from the beginning of the high-water sequence).

In addition, with reference to the output showed in Figure 5.6. Dimensionless head of the control nodes from the unsaturated seepage analysis using real and synthetic hydrographs as hydraulic boundary conditions, plotted as function of the elapsed time (expressed in days from the beginning of the high-water sequence).,

it can be highlighted that results obtained using the real hydrograph (Case 1) are always lower than those estimated using the synthetic hydrographs (Cases fc1, fc2 and fc3) as boundaries conditions; this finding means that, for the all duration of the considered events, the progression of the phreatic line using the proposed method is generally closer to the one estimated in limit state, represented by the steady-state conditions (Case 3). For this reason and regards to the considered cases, it could also be stated that the hydraulic performance of the riverbank, and consequently the safety assessment towards global instability mechanisms, stands on the safe side when using the synthetic hydrographs with characteristic frequencies obtained by the spectral analysis on the hydrometric measurement of water levels; this remark is, however, valuable in the hypothesis that a realistic estimation of the seepage properties of the riverbank could be referred to Case 1.

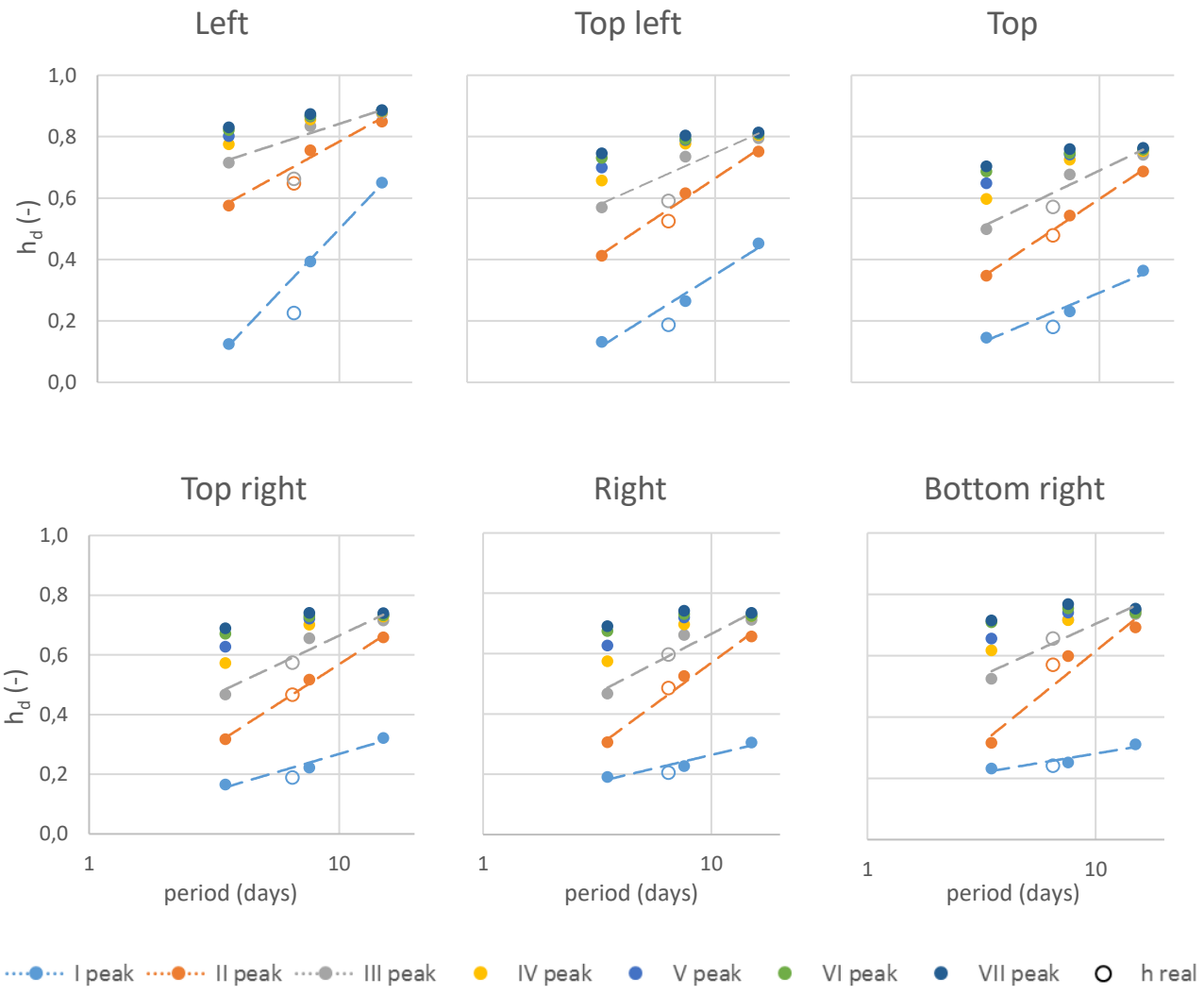

Figure 5.7. Dimensionless head of the control nodes from the unsaturated seepage analysis using the real and synthetic hydrographs as hydraulic boundary conditions, as function of the period of the sine-waves (expressed in days from the beginning of the high-water sequence).

In Figure 5.7 are, then, showed the h_d values estimated in correspondence of the various high-water peak as function of the period of the sine-waves assumed for the synthetic hydrographs (in logarithmic scale), for the various cases and control nodes.

It can be noticed that the hydraulic behaviour of the riverbank subjected to the real hydrograph could be represented with good approximation through a synthetic hydrograph with an appropriate value for the period of the sine-waves, being also possible to approximate the relation h_d – log10t to a linear function up to a number of consecutive sine-waves equal to three; e.g., in the considered case, this period has been assumed equal to 6.5 days, finding a good agreement with the theoretic lines representing the functions h_d – period for the various control nodes.

5.3 Sensitivity of hydraulic and stability results to material properties

Once defined the boundary conditions representing the high-water events for the proposed method, which are described by a series of sinusoidal waves superposed to a hydrometric baseline characteristic for the considered time period, the effect of hydraulic and retention soil parameters on results needs to be debated in specific. The PWP distribution resulting from numerical analysis mainly depends on the initial and boundary conditions, as seen in the previous section, and on the hydraulic and retention soil parameters initially assumed (in case the soil deformability during the seepage process would be disregarded). Conserving the assumption on the initial conditions as described in Chapter 4, the influence of the uncertainty and variability of the hydraulic and retention soil parameters on the results has been investigated, in this phase of the study, by simplifying the problem as possible; for this purpose, steady-state and transient seepage analysis have been performed assuming different set of initial parameters, for which the values of the soil hydraulic and retention properties have been singularly varied on the base covariance and skewness of their distribution from the mean values (referring to geotechnical characterization discussed in Chapter 3). By this, a sensitivity study has been carried out in order to assess the influence of each parameters, among their range variation, on the hydraulic and mechanic behaviour of the riverbank; comparison among the various Cases presented to individuate, in first approximation, the sets of parameters that could be referenced as the most hazardous in terms of global stability and, finally, used for evaluate the margin of safety over characteristics events. Suction and pore water pressure distribution from seepage analysis are used as input values for the limit equilibrium analysis. In order to express the safety conditions for a specific riverbank toward global and local instability mechanisms.

5.3.1 Soil hydraulic and retention parameters

Seven sets of input hydraulic and retention parameters were used for Unit A, differing for the values assumed for saturated hydraulic conductivity, and the *α* and *n* parameters of the van Genuchten soil water retention curve, considered the most influent for hydraulic and mechanical behaviour, whose values are listed in Table 1. In detail, Set 1 refer to the case in which all parameters are assumed to be equal to the mean values estimated during geotechnical characterization, while in Sets 2 to 9 each of the considered parameters is in turn modified to account for the estimated site variance considering the standard deviation and skewness of the distribution that was singularly estimated starting from the laboratory data obtained from evaporation test, which results was described in previous sections. In Figure 5.8. Soil water retention curves, on the left, and Hydraulic conductivity functions, on the right, estimated by using the hydraulic and retention parameters listed in Table 1. are showed the soil water retention curves and the hydraulic conductivity functions considered assuming for the van Genuchten – Mualem hydraulic model (van Genuchten, 1980) the values of *α*, *n*, ϑ_{sat} and *k* listed in Table 5.3. The parameter *m* is omitted since it depends on *n*. The model adopted in this work, used for fitting the experimental data, comprises a non-hysteretic relation to estimate the effective degree of saturation, S_e, and consequently the hydraulic conductivity, from soil suction, s, calculated as the difference between pore air pressure, u_a, and pore water pressure, u_w, in the porous media. Average constant values for the hydraulic conductivity were used for Units B and C, as anyway they were not principally involved in the hydraulic behaviour of the riverbank and generally in saturated conditions.

	Set 1	Set 2	Set 3	Set 4	Set 5	Set 6	Set 7	Set 8	Set 9
α (kPa)	6,11	6,11	6,11	14,01	4,91	6,11	6,11	6,11	6,11
n (-)	1,328	1,483	1,175	1,328	1,328	1,328	1,328	1,328	1,328
θ_{sat}	0.395	0.395	0.395	0.395	0.395	0.395	0.395	0.437	0.355
k (m/s)	$1.57 \cdot 10^{-6}$	$1.57 \cdot 10^{-6}$	$1.57 \cdot 10^{-6}$	$1.57 \cdot 10^{-6}$	$1.57 \cdot 10^{-6}$	$5.80 \cdot 10^{-6}$	$1.36 \cdot 10^{-7}$	$5.80 \cdot 10^{-6}$	$1.36 \cdot 10^{-7}$

Table 5.1. Set of hydraulic and retention soil parameters assumed to be variable in the first phase of analysis.

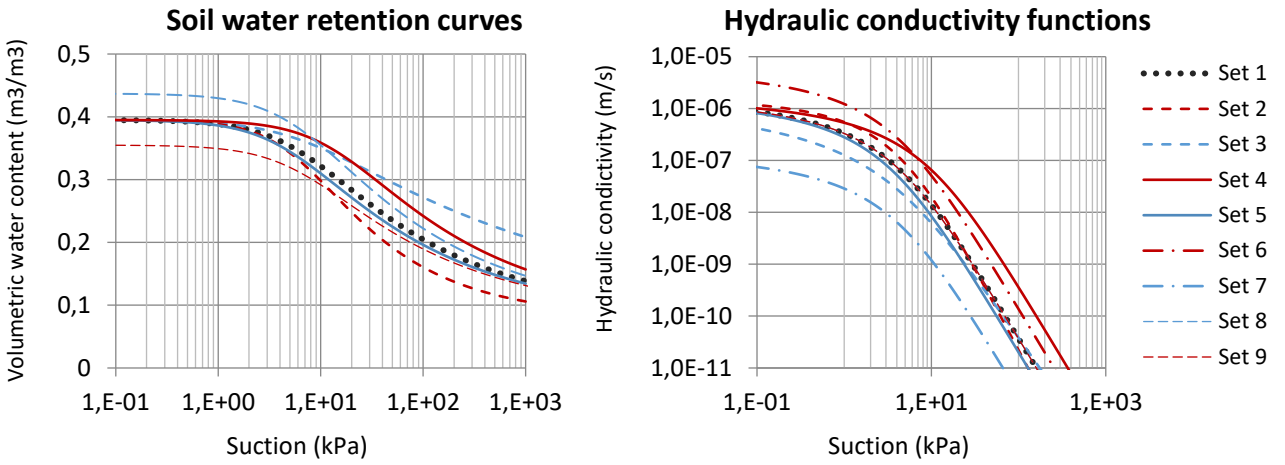

Figure 5.8. Soil water retention curves, on the left, and Hydraulic conductivity functions, on the right, estimated by using the hydraulic and retention parameters listed in Table 1.

For a general comprehension of the results, it's important to notice that in transient seepage analysis the flow in the model domain may differ from the outgoing flux, due to water storage or release. The amount of water out of balance is function, obviously, of the hydro-thermal boundary conditions and its variation with time depends on soil retention models adopted for the analyses, which both influence soil hydraulic conductivity and storage capacity determining velocity and rate for water seepage. Storage is generally defined as the amount of water retained in the pores of a soil under negative pore-water pressure; considering lower values for *n* parameter in van Genuchten equation, i.e., which defines SWRC with flatter slope and could be representative for non-uniform grained soil and larger distribution for pore sizes, the change in volumetric water content for increasingly negative pore-water pressure would be lower compared steeper function, but for equal values of C the volumetric water content turns to be generally higher; changes in α parameter, instead, mainly influence the suction range corresponding to the prime inflection of the SWRC, which define the air-entry value (AEV). An increase in AEV produces, commonly, an increase in the height of the capillary fringe, where water flow rate is equal to the saturated hydraulic conductivity.

5.3.2 Results and discussion

The control nodes selected for the output visualization are those considered for the previous section (Figure 5.3); the peaks of various hydrographs, real and synthetics, have been considered as time step. To represent the hydraulic behaviour of the riverbank in different hypothesis on the soil parameters, the dimensionless height values of the control nodes have been estimated for all the considered time step. In the next pages, predominant importance will be given to the presentation and discussion of the results of the analysis performed varying the α and *n* parameters of the van Genuchten soil water retention curves, being the most relevant for this study, while the results of the analysis performed varying the hydraulic conductivity and θ_{sat}

will mainly be reported in Appendix, being their interpretation clearer and univocal in terms of global safety for the riverbank. Moreover, the θ_{sat} parameter could be generally determined by laboratory measurement or deduced from site characterization of the soil volumetric state; for this reason, it is commonly excluded from the inverse estimation of retention parameters, even considering its significant variability and influence on soil hydraulic and mechanical behaviour (that will be even discussed in Chapter 7). In Figure 5.9 are plotted the dimensionless head computed in the control nodes in correspondence of the first six hydrometric peaks of the synthetic hydrograph when *fc2* is used as frequency for the series of sine-waves (Case fc2), assuming hydraulic and retention parameters described in Set 1, 2 and 3. For the showed cases, the maximum values for h_d and, consequently, the highest progression of the phreatic line are estimated using the lowest value for the parameter *n* (Set 3). Being the relative permeability of the porous media computed from the suction values, estimated on the base of the hypothesis on the initial and boundary conditions, a reduction of the value of the parameter *n*, consequently, decrease the hydraulic conductivity estimates for a considered suction value. However, the difference in the results tends to reduce with the increasing number of the consecutive water peaks, meaning that the influence of the retention parameters became lower when the higher is the progression of the phreatic line and when the riverbank soil is generally more saturated. This remark can be evidenced also by the average values of covariance of the h_d computed for each time step using Set 2 and 3, reducing from an initial value of 30% to around 7% after the third hydrometric peak (see Fig. 5.9). In general, it can be generally assumed that the maximum values for the pressure head estimated in the control nodes do not reach the values assumed in steady-state conditions even using Set 3; in this case, assuming the third and fourth hydrometric peak as the most representative for a realistic but critical event, it can be noticed that the maximum values of total head in the control nodes belong to the range 89% - 72% of the values assumed in steady-state conditions, differing from the values assumed for the Set 1 for less than 5% on average. Using the PWP and suction distributions obtained from seepage analyses, the stability of the embankment have been studied by means of limit equilibrium analyses adopting the Morgenstern and Price method and the Vanapalli failure criterion to account for the unsaturated soil strength contribution. The analyses were performed through Monte Carlo procedure (100,000 simulations) on critical surfaces defined by specific geometrical properties, to investigate landward instability mechanisms and using as standard variable the friction angle of the riverbank and foundation soils. The minimum slip surface depths were assumed to be 4m; general features on the stability analysis are provided in Chapter 3. The results of the stability analyses are quantified in terms of the reliability index ($\beta=(\mu_{SF}-1)/\sigma_{SF}$), where μ_{SF} is the mean value of safety factor and σ_{SF} its standard deviation computed with MC procedure, so that a higher β value represents a lower probability of failure for a given collapse mechanism. The values, obtained for each input dataset, are showed in Figure 5.10 in correspondence of the first four peaks of the synthetic hydrograph when *fc2* is used as frequency for the sine-waves; with the progression of the high-water event, the global

safety is generally reduced, with strong incidence among the second and the third hydrometric peak for all cases.

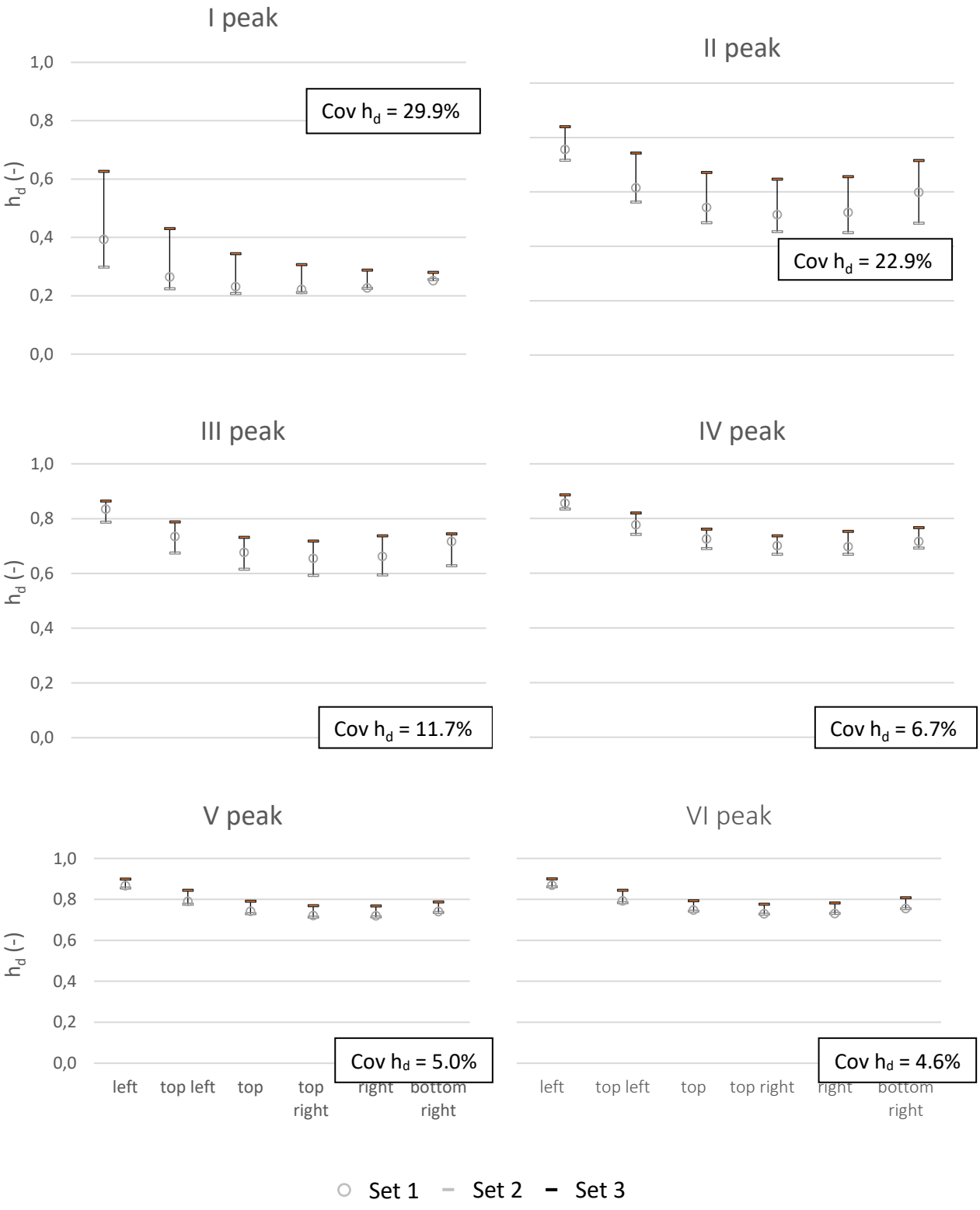

Figure 5.9. Dimensionless head of the control nodes computed using as boundary conditions the synthetic hydrograph when *fc2* is used as frequency for the sine-wave, varying the *n* parameter of the van Genuchten soil water retention curve.

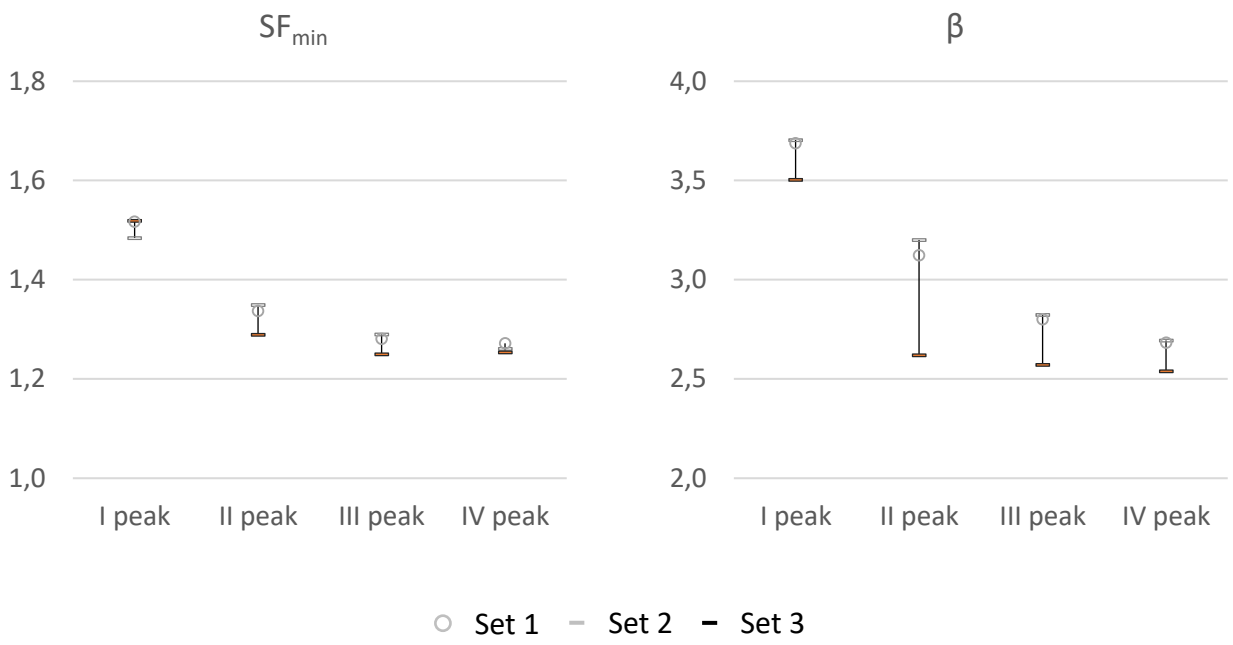

Figure 5.10. Results of the probabilistic stability analyses, by the minimum value of safety factor, SF, and reliability index, β, varying the *n* parameter of the van Genuchten SWRC, for Case fc2.

The higher relative permeability of soil achieved using Set 3 for the whole transient seepage analysis, is the most impactive factor also influencing the safety assessment towards global instability mechanisms; this leads to the lowest values for the reliability index among the considered cases. Comparable remarks can be observed when using *fc1* and *fc3* as frequency for the sine-waves of the synthetic hydrographs; results are reported in Appendix in order to avoid repetition in the comments.

Similarly, in Figure 5.11 are reported the values of h_d computed in the control nodes for the various hydrometric peak of the synthetic hydrograph when *fc2* is used as frequency for the series of sine-waves, assuming hydraulic and retention parameters described in Set 1, 4 and 5. In the showed case, the differences among the results are significant only for the first two hydrometric peaks, but in general are limited respect to cases in which the n parameter of the van Genuchten soil water retention curve was assumed as variable. The average values of covariance of the h_d computed for input datasets 4 and 5 - at each considered time step, and reported in Figure 5.2, are lower than 20% still at the first time-step and rapidly decrease since to values around 2% still at the third consequent hydrometric peaks. Being the relative permeability of the soil computed for Set 5 generally higher, the progression of the phreatic line in the riverbank is, consequently, closer to the steady-state conditions. However, the hydraulic behaviour of the riverbank in correspondence of several consecutive waves, in terms of h_d, is generally equivalent for the showed cases. In Figure 5.12 are then showed the results obtained from the stability analysis, in terms of minimum value of the mean safety

factor and reliability index, using the PWP and suction distribution obtained at each of the considered time step for limit equilibrium analysis.

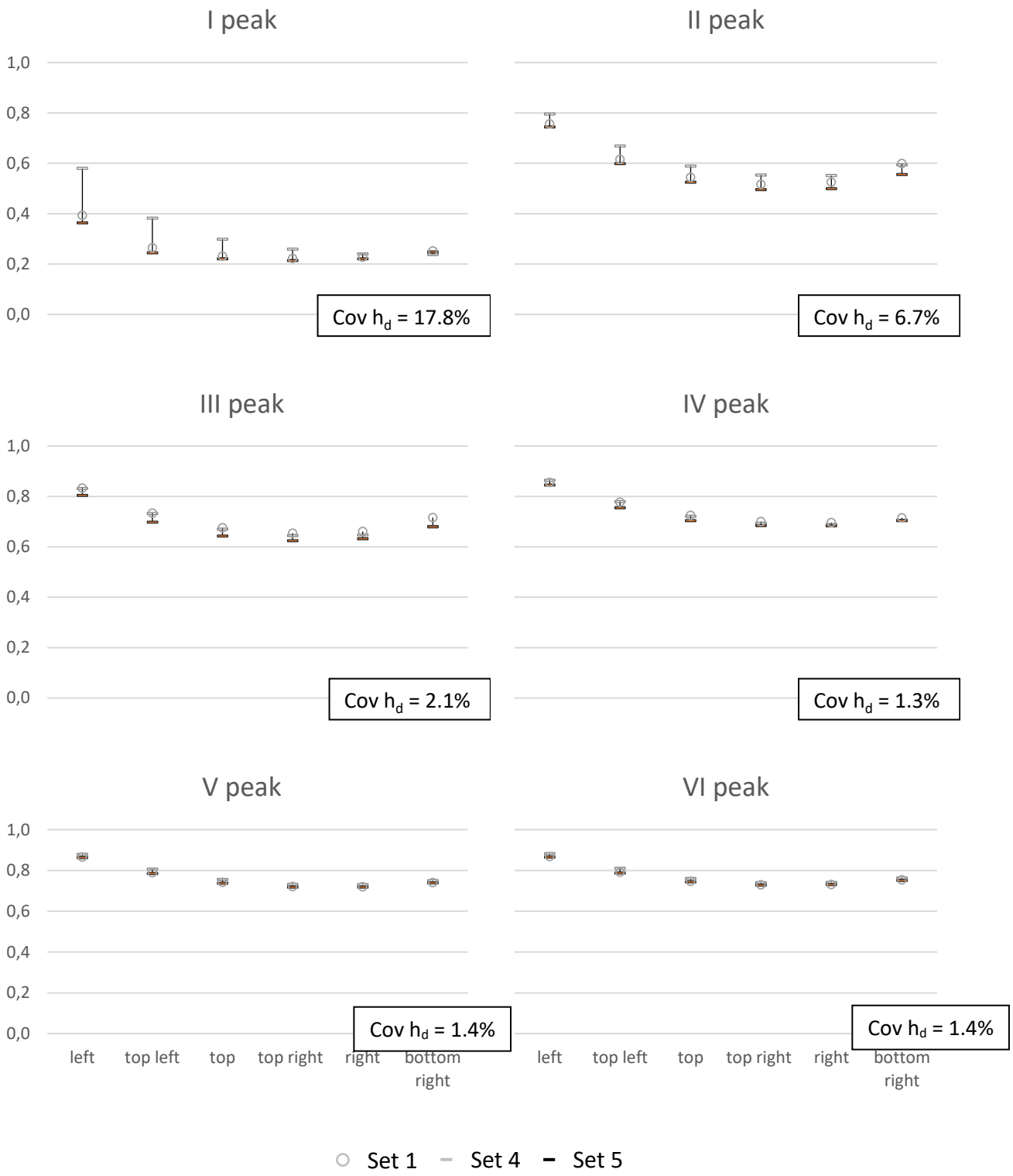

Figure 5.11. Dimensionless head of the control nodes computed using as boundary conditions the synthetic hydrograph when *fc2* is used as frequency for the sine-wave, varying the *α* parameter of the van Genuchten soil water retention curve.

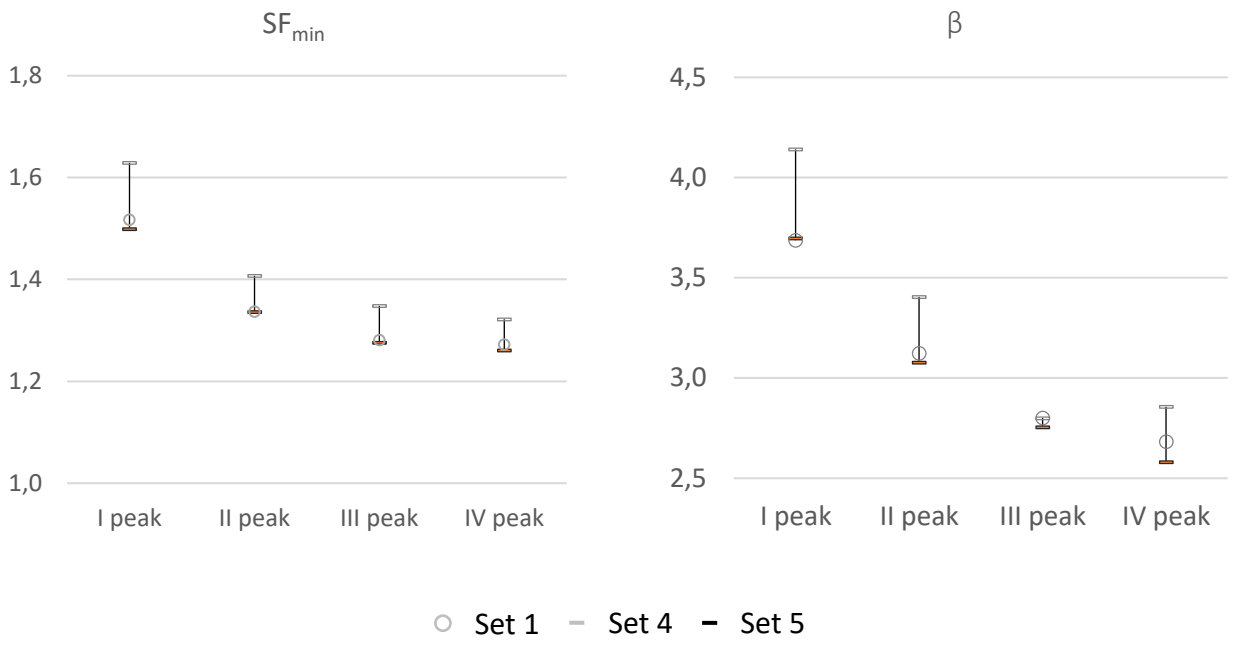

Figure 5.12. Results of the probabilistic stability analyses, by means of the minimum value of the mean of safety factor, SF, and reliability index, β, varying the α parameter of the van Genuchten SWRC, for Case fc2.

Differently from what it may seem just considering the showed results of the seepage analysis, the lowest margins on safety conditions refer to the Set 5 for all considered time steps. This finding is mainly due to the use of Vanapalli failure criterion for the unsaturated strength, which is directly dependent on the soil saturation degree that assumes higher values in the riverbank for the Set 4 compared to analysis when Set 5 and 1 are used for the considered range of suction.

A clear explanation for the correlation found between the various parameters of the soil retention model and the stability characteristics (factor of safety and reliability index) can be debated considering the volumetric water content and soil suction profiles computed for the second hydrometric peak of the real hydrograph in correspondence of the middle of the riverbank (progressive = 26.3m), plotted in Figure 5.13a and 5.13b, interpreted in combination with Soil water capacity functions plotted in Figure 5.14. Soil water capacity functions estimated by using the hydraulic and retention parameters listed in Table 1, in $\log_{10}$ scale in range 0,01 to 10 kPa (a) and natural scale from 10 to 40 kPa (b).. As can be seen, water storage, when using Set 3 for retention model, is significantly higher compared to other cases, producing higher values for water content profile; this effect is partially notable for Set 5, which also evidence higher values for soil suction above the phreatic line due to the increase in AEV, producing a linear increment up to the vadose zone influenced by climatic conditions (in presence of rainfall infiltration for the considered time step).

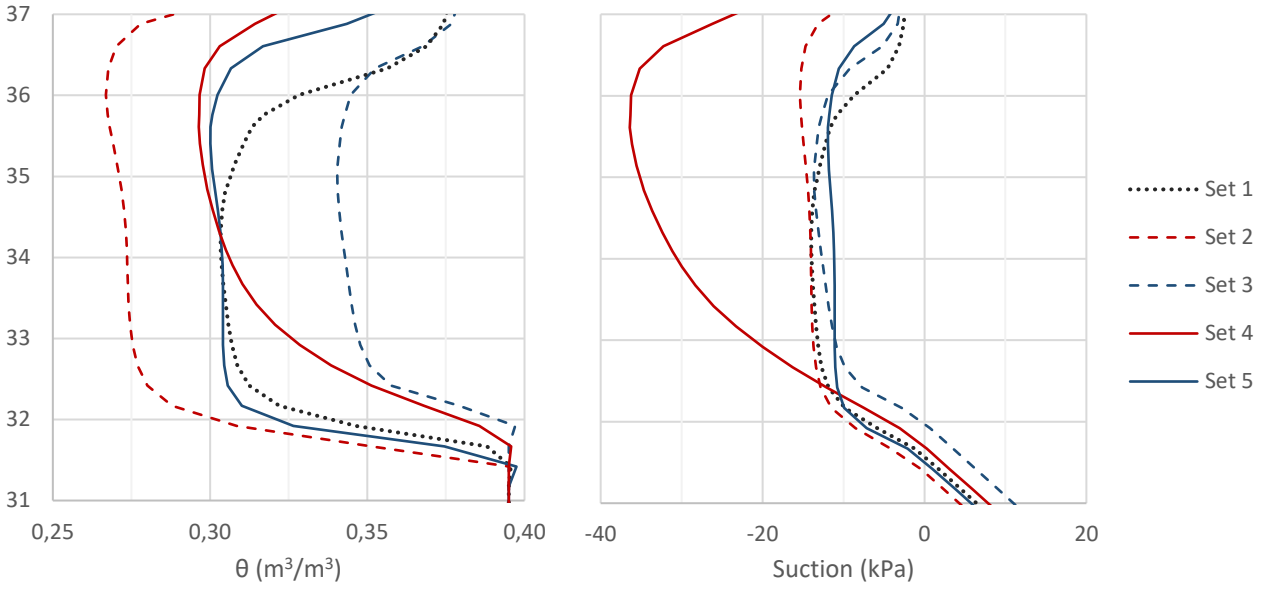

Figure 5.13. Soil water content (a) and suction (b) profiles at x = 26.3m, for seepage analysis performed varying *n* (Set 2 and 3) and *α* (Set 4 and 5) parameters for the van Genuchten retention model respect to average properties, computed in correspondence of the second hydrometric peak of the registered hydrograph.

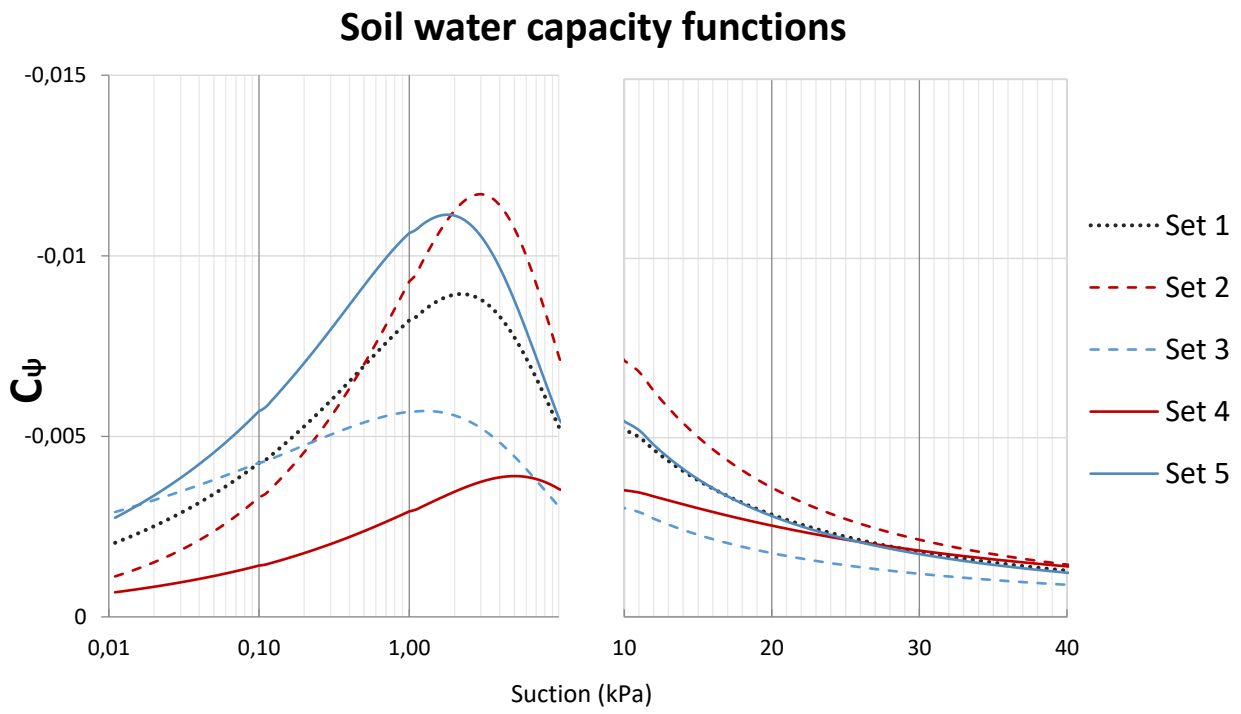

Figure 5.14. Soil water capacity functions estimated by using the hydraulic and retention parameters listed in Table 1, in $\log_{10}$ scale in range 0,01 to 10 kPa (a) and natural scale from 10 to 40 kPa (b).

In riverbank soil, the variations in soil water content are mainly due to the inclination to release (in drying) or adsorb (in wetting) water. For low suction values and saturation degree close to 100%, higher tendency in water exchange (Figure 5.14a) produce a predominant sensitivity to water flow inside the riverbank for seepage analysis performed using Set 3 rather than Set 5, evidenced by a difference in the height phreatic line of about 40cm. However, due to a lower peak value in C_ψ, the soil water retention for Set 3 is generally higher compared to those specific for Set 4 and Set 2, for which the soil tends rapidly to desaturate, producing significant differences in hydraulic conductivity and water content profile. Considering the suction range from -10kPa to -40kPa (Figure 5.14b), the higher values in C_ψ are relative to SWRC obtained assuming Set 2 as retention parameters (higher value for *n*), subsequently Set 4 and 5 SWRCs and, then, Set 3; this, even consequently to the main soil retention properties and equal value for θ_{sat}, attributes the higher values to water content profile obtained for analysis performed using Set 3, with a generally slighter variation with depth. Considering a higher value for α parameter (Set 5), the saturation zone due to capillarity is certainly extended, but the progressive reduction in soil water content above the capillary fringe are still significant, leading to higher values for soil suction in the riverbank. Similar conclusion can be stated from results obtained at different time steps. In Figure 5.15 are, then, summarized the main results obtained from the unsaturated seepage and stability analysis performed for Set 1, 3 and 5. In specific, the average of the values of h_d computed at the control nodes in correspondence of each hydrometric peaks of the various hydrographs, real and synthetics, and the reliability index estimated at the considered time step are plotted as function of the elapsed time, expressed in days from the beginning of the high-water sequence. The showed results evidence that the shape of the synthetic hydrograph assumes more importance as higher is the relative permeability of the soil for the operative suction level. In fact, the variance between the values of h_d, being equal the elapsed time step, is higher for Set 3, for which the most impactive event is the synthetic hydrograph considering *fc1* as frequency for the sine-waves. The consistent trend obtained for the values of β and average h_d at various time step, point out that the output discussed for the seepage analysis can be representative for the hydraulic behaviour of the riverbank, and used as index for global safety assessment.

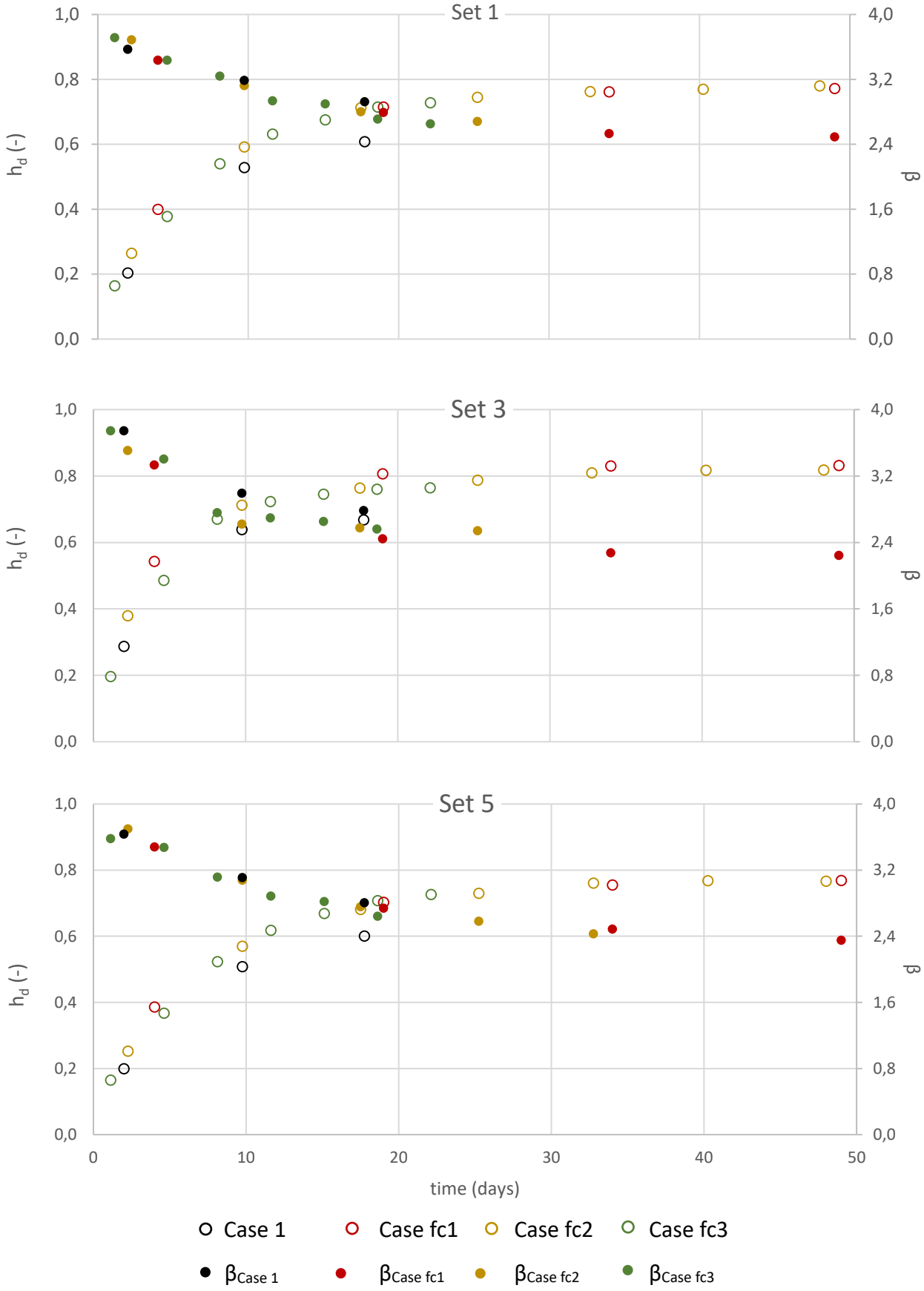

Figure 5.15. Dimensionless head of the control nodes from the unsaturated seepage analysis using real synthetic hydrographs as hydraulic boundary conditions (left axes), and reliability index (right axes) for the considered time step as function of the elapsed time (in days from the beginning of the high-water sequence).

As final remarks, it can be assumed that an average value of 0.8 for h_d (Set 3), punctually ranging from 0.72 to 0.89, represents the most critical condition in terms of progression of the phreatic line in the riverbank, and should be compared to an average value of 0.6 (Set 1), representing a realistic estimate on the base of the performed analysis.

In Liu et al. (2015) has been proposed a non-dimensional variable to explore the effect of interplay of an external cyclic water level on safety assessment of riverbank under transient seepage conditions; this parameter, named as Lk has been expressed as:

$$L_k = Tk_{sat}/H \tag{5.2}$$

and depends on the characteristic period of the water level fluctuation (T), on the saturated soil conductivity (k_{sat}) and on the height of the riverbank. Sinusoidal curves characterized by the same amplitude and trapezoidal 2D model represented the boundary conditions and geometry for the problem, respectively. For the specific case, the Authors found that when the time period is small respect to k_{sat}, the effect of pore water pressure and water content changes in transient seepage analysis produce limited variations in SF values; this finding was related to the effect of soil hydraulic hysteresis on the stability embankment under transient seepage analysis, which was the aim of the study. However, the Authors even states that the Lk variable could be a good indication for design purpose, being possible to find a critical value of Lk since the interplay role between two consecutive waves is significant. The use of this index has been adapted to the present work to evidence the effect of interplay among the various considered Cases. Three values for T have been adopted, equal to 15days, 7.6days and 3.5days (corresponding to sine-waves characterized by fc1, fc2 and fc3 as frequencies); H has been expressed as the difference between the top of the riverbank and the lower hydrometric values assumed for synthetic hydrographs. Results from probabilistic seepage analyses (Cases fc1, fc2 and fc3) have been correlated to the estimated values for Lk using Set 1, Set 6 and Set 7; in particular, are considered the variations in the minimum mean SF values computed among the first two hydrometric peaks ($\delta\mu_{SF}$) and for a prescribed elapsed time ($\Delta\mu_{SF}$). This last variation is referred to a time equal to 15days starting from the first hydrometric peak, being the minimum period required for the occurrence of two consecutive waves for all Cases; in specific, $\Delta\beta$ has been so estimated among the 1st and the 5th hydrometric peak for Case fc3, among the 1st and the 3rd for Case fc2 and among the 1st and the 2nd for Case fc1. In table 5.4 are reported the values of the variable Lk estimated for various Cases, while in Figure 5.16 are reported the values of $\delta\mu_{SF}$ and $\Delta\mu_{SF}$ with Lk.

Period		Lk (-)		Baseline
(days)	Set 1	Set 7	Set 6	(m)
15	2,42E-01	2,10E-02	8,95E-01	29,1
7,6	1,23E-01	1,06E-02	4,53E-01	29,1
3,5	5,65E-02	4,90E-03	2,09E-01	29,1

Table 5.4. Lk variable estimated for Cases fc1, fc2 and fc3 considering Set 1, 6 and 7 for hydraulic parameters.

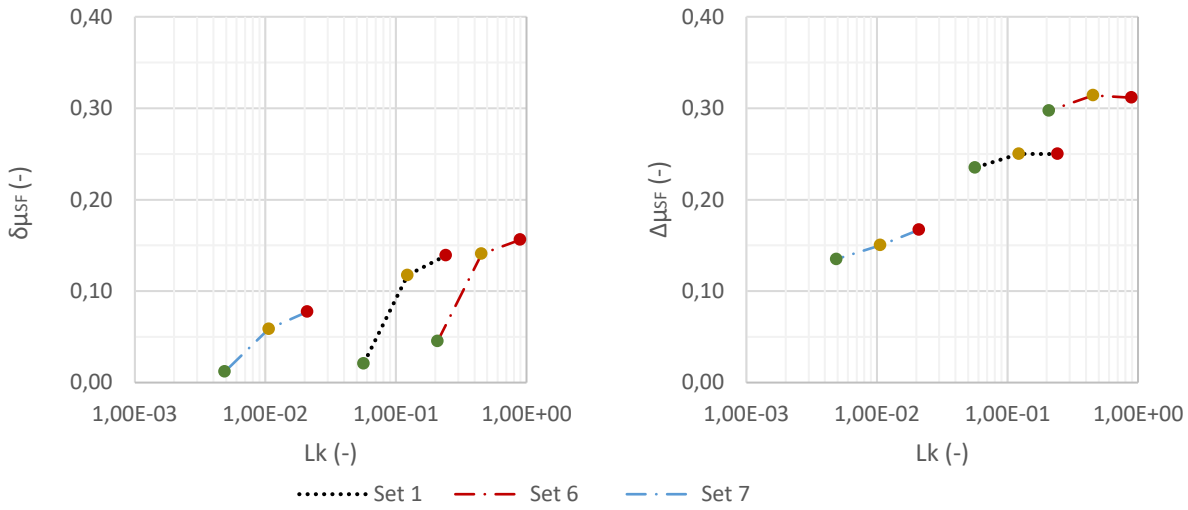

Figure 5.16. Variation of minimum μ_{SF} among the first two hydrometric peak (left) and for an elapsed time equal to 15days subsequent the first high

Results showed in Figure 5.16 evidence the strong incidence of k_{sat} in stability assessment; in fact, considering the same Cases (in terms of frequency for the synthetic hydrograph) the variation of μ_{SF} after 15 days from the first hydrometric peak (Δ) is mainly dependent on this parameter, while rather constant from among various Cases; however, when considering the differences between the first two hydrometric peaks, characteristic periods for the sine-waves have a significant influence on the values of $\delta\mu_{SF}$. This should be evidenced considering that variations in $\delta\mu_{SF}$ are more evident among the same Set of parameters (1, 6 and 7) rather than the same Case (fc1, fc2 and fc3); inversely are, however, the incidence of k_{sat} and T (or fc) for variations in $\Delta\mu_{SF}$.

It's useful here to notice that the effect of hysteresis, disregarded in the present study, would certainly provide a more reliable assessment for seepage and stability analysis, nut generally reducing the absolute differences in the hydraulic response among the various considered Cases; in fact, being the main drying curve a higher boundary for the hydraulic paths, in the s-S_e plane, the variation in soil water content during

a wetting process (e.g. by means of a rising river water level or rainfall infiltration), associated to a suction variation from a specific value on main or scanning paths, would be lower than the case of a drying process; this would means that, for the suction range and soil type typical of this problems, the relative permeability would be generally higher using a non-hysteretic model defined by the main drying curves, even if wetting process is typical during river floods. Furthermore, on the use of data from only drying branch, it is worth to notice that the use of Vanapalli (1996) failure criterion, in conjunction with the use of experimental data obtained only from drying branch, do not particularly provide estimates on the unsafe side for the stability evaluation. In fact, if it is certainly true that the assumption of non-hysteretic hydraulic behaviour will tend to overestimate the suction values for a specific degree of saturation, on the other side it has to be considered that the relative permeability will be consequently underrated using the van Genuchten - Mualem model (van Genuchten, 1980), influencing the flow regime and leading, at the end of high water events, to a minor progress of the phreatic line, even considering that initial conditions are assumed in terms of suction. The above described considerations produce opposite effects on numerical stability evaluation, and one prevalence on the others should require to be stated for each analysis and considering various hypothesis on soil parameters, initial and boundary conditions.

5.4 Methodological approaches for the definition of synthetic initial and boundary conditions in the assessment of river embankment stability

As previously mentioned, a proper description of the initial conditions to be assumed in numerical analysis is essential in order to obtain reliable and consistent results for the assessment of riverbank stability. Nevertheless, their assumption is characterized by high uncertainty, even considering the rarely available direct measurements on soil water content and suction for entire riverbank sectors. Moreover, the definition of suitable boundary conditions that could be representative and simplified for specific cases but providing realistic results in terms of stability conditions is still a demanding task for geotechnical standards in terms of riverbank stability assessment. Considering outcomes and remarks discussed in the previous sections, two simplified approaches for safety assessment of riverbank section are hereafter presented. Different applications, characterized by different level of sophistication, will be presented and their features discussed. In particular, for a first level of approximation the pore water pressure and suction distribution in correspondence of the beginning of the high-water sequence will be directly assigned, reducing the efforts needed to define the initial conditions; for a second level of approximation, instead, pore water pressure and suction distribution in the riverbank are defined to be directly used for the stability analysis, overcoming the whole phase of seepage analysis.

5.4.1 First level of approximation: Simplified Approach 1

Aiming to simplify the evaluation process of pore water pressure and suction distribution in correspondence of the most critical time step for the stability assessment of riverbank sections and to reduce the efforts required to model spin-up, the initial condition to be used in correspondence of the beginning of a high-water sequence are directly assigned in numerical analysis. In details, the pore water pressure distribution is determined assuming the hypothesis of steady-state conditions in equilibrium with a water level defined by a realistic baseline for the considered period, e.g. the TMA 241-width value considered at the beginning of a high-water event equal to 32.1m (a.s.l.). Then, suction values are here assigned assuming a hydrostatic increase from the phreatic line and from the ground level up to a maximum (absolute) value of pressure head equal to 1.5m. This hypothesis, based on the results of transient seepage analysis previously discussed, requires the knowledge on the hydrometric baseline and a maximum value for suction, which could be both derived on the base of the considered period and type of soil. Through this procedure, the definition of the pore water pressure and suction distribution to be used for limit equilibrium analysis, for assumed input datasets, only depends on the assumption of the boundary conditions representing the high-water event in transient seepage analysis. In Figure 5.17 the pressure head distribution to be used as initial conditions for transient seepage analysis, referred to Set 3, is showed; increment between two adjacent isolines is 0.5m; the phreatic level (zero pressure) is represented by the blue bold line.

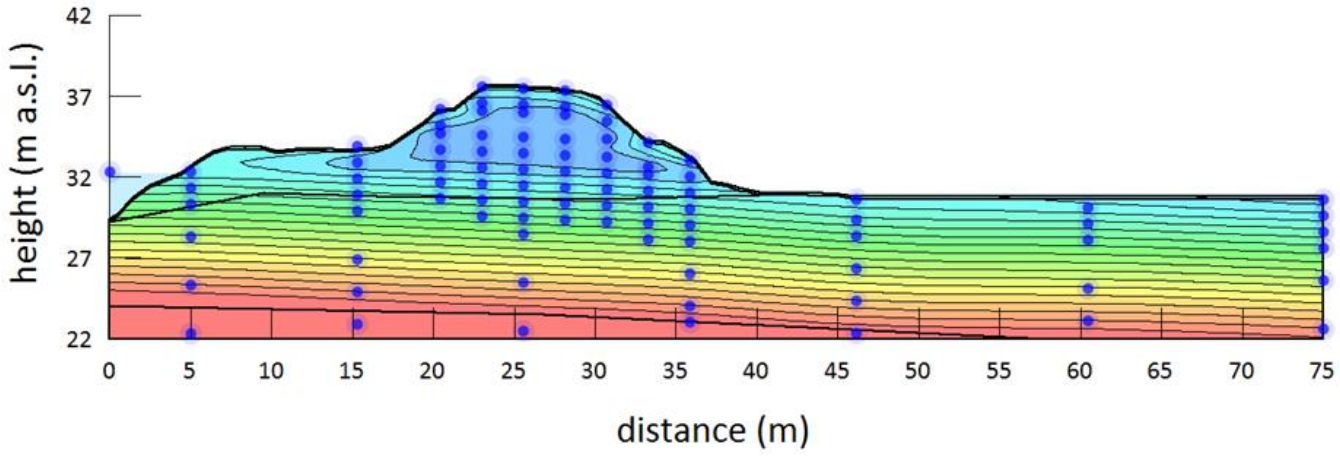

Figure 5.17. Pressure head distribution to be used as initial conditions for transient seepage analysis, referred to Set 3.

Once defined the initial h_p distribution, a series of transient seepage analysis have been performed using as boundary conditions the real and synthetic hydrographs described in previous sections; limit equilibrium analyses have been, then, performed in correspondence of the various hydrometric peak in order to assess the stability conditions of the riverbanks.

5.4.2 Second level of approximation: Simplified Approach 2

A second level of approximation has been considered for a simplified riverbank safety assessment; the pore water pressure and suction distribution to be used in limit equilibrium analysis has here been directly assigned to the model, on the base of analysis performed in transient seepage conditions and discussed in previous sections. A spatial function has been so defined, firstly assuming the phreatic line progression as a rate of the steady-state conditions; results in terms of h_d, obtained from previous analysis, have been used as input data for pressure head in the control nodes, considering values varying in the range 0.75≈0.85. Pore water pressures below the phreatic line have been assumed as in steady-state condition. The maximum absolute value of suction considered above the phreatic line is equal to 1m, expressed in terms of water potential; atmospheric pressure has been assumed in correspondence of the ground level. Using this discrete known-terms, the overall continuous pore-water pressure and suction distribution has been defined by the solver using the Kriging interpolation technique; this procedure involves the fitting of a discrete function to a series of spatially distributed points, with the possibility to include in the calculation weighting coefficients that can be then used to compute values for any other point in the domain, as could be proper in case of direct measurement of soil water content or suction. Although the solving of a large problem using this technique requires considerable computer storage, it has been found that a small number of designated points can provide reasonably accurate results (Geo-Slope International Ltd, 2008). In Figure 5.18 is showed the pressure head distribution assigned to the model using results obtained from seepage analysis on Case fc2 and Set 3. Increment between two adjacent isolines is 1m; blue circled dots represent the known-terms of the spatial function; red squared dots evidence the nodes at maximum the suction level in the numerical model.

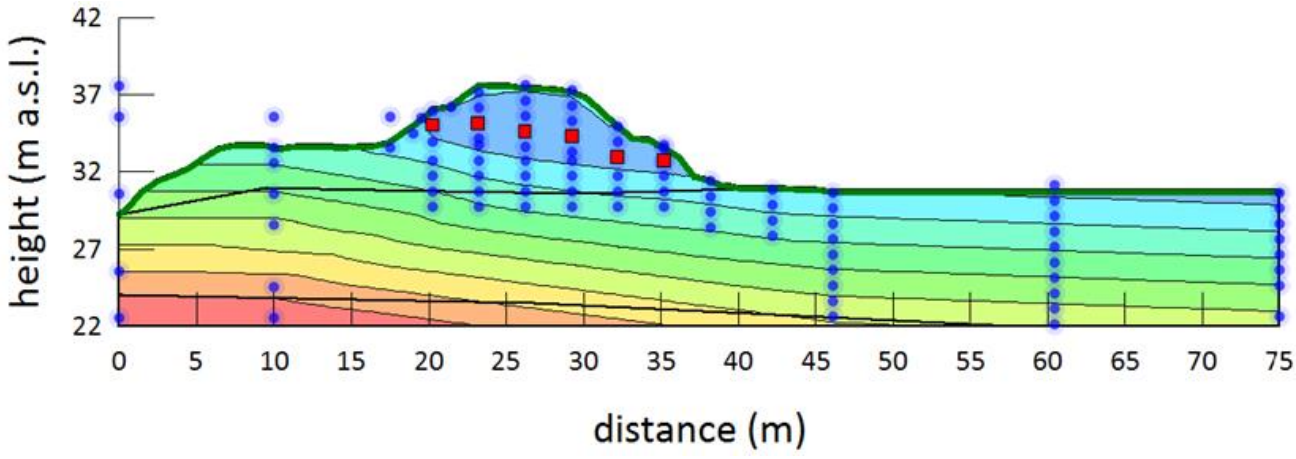

Figure 5.18. Pressure head distribution for the riverbank numerical model in second simplified approach, representing the third hydrometric peak using *fc1* as sine-wave frequency for the synthetic hydrograph and Set 3 as input dataset.

Through these assumption, it could be possible to decoupling transient to limit equilibrium analysis, highly reducing the computational efforts required for the riverbank stability assessment; all uncertainties related to initial and boundary conditions definitions, and soil parameters variability, are synthesized by mean of a precautionary pore water pressure and suction distribution. This approach has been tested for the most critical but realistic time step, corresponding to the fourth hydrometric peak using *fc1* as and the third hydrometric peak using *fc2* and *fc3* as synthetic hydrographs, for Cases 1, 3, 5.

5.4.3 Results and discussion

In this section are presented and discussed results obtained using various approaches for riverbank stability assessment. In particular, have been considered:

- Case 1: Initial conditions determined considering the period July, 15th 2013 to July, 14th 2014 for the model spin-up; real hydrograph, using hydrometric data collected in Ponte Bacchello, assumed as boundary conditions for the model. Probabilistic limit equilibrium analyses have been performed using pore water pressure and suction distribution evaluated in correspondence of the (three) hydrometric peak by means of transient coupled hydro-thermal flow analysis;
- Case fc2: Initial conditions determined similarly to Case 1. Synthetic hydrograph has been used as boundary condition, described by a series of sine-waves of constant period ($fc2^{-1}$) and amplitude (3.15m) superposed to a hydrometric baseline represented by the TMA 241-width value estimated in correspondence of the beginning of the high-water event registered from February, 16th 2015 in Ponte Bacchello. Probabilistic limit equilibrium analyses have been performed using pore water pressure and suction distribution evaluated in correspondence of four hydrometric peak by means of transient coupled hydro-thermal flow analysis;
- Simplified Approach 1: Initial conditions directly assigned to the model (see Fig. 5.17). Boundary conditions and time step considered are equivalent to Case *fc2*;
- Simplified Approach 2: Limit equilibrium analysis have been performed using pore water pressure and suction distributions directly assigned to the model, on the basis of observation and remarks from transient seepage analysis performed for Cases fc1, fc2, fc3, as described in previous sections;
- Case 3: Pore water pressure distribution to be used in limit equilibrium analysis has been determined by steady-state seepage analysis in equilibrium with the maximum hydrometric level measured for the considered hydrograph, and hydrostatic suction distribution above the phreatic line, up to a maximum (absolute) of 35kPa in correspondence of the top of the riverbank.

In Figure 5.19 are plotted the critical values for mean safety factor and reliability index obtained from limit equilibrium analysis performed using input dataset 3 and 5 at various considered hydrometric peaks. Results

evidence that, for all cases, the use of simplified and synthetic methods is always a conservative procedure. However, the differences among the various considered cases can be significant. The use of steady-state conditions in equilibrium with the maximum hydrometric level measured during high water event implicates highly conservative results and so inaccurate risk evaluation, even considering that a hydrostatic shape for suction distribution has been assumed above the phreatic line determined for the seepage; in terms of global probability of failure, the difference with Case 1 results of about two order of magnitude. Differently, simplified approaches presented in this section provide more accurate results in terms of global safety, if we refer to Case 1 as a realistic procedure for assessment of the riverbank stability. In general, the more, and most impactful, source of uncertainties we neglect for the problem, the more conservative would be the results. As consequence, the use of Simplified approach 2, defined assigning to the model pore water pressure and suction distributions to be directly adopted in limit equilibrium analysis, provides the lower values for reliability index and minimum value for the mean safety factor, though significantly higher than Case 3, finding that the hypothesis based on results from Case fc3 the less conservative among the three considered (as could be expected). Then, the use of Simplified Approach 1, based on the knowledge of the hydrometric baseline, characteristics wave lengths for the considered riverbank sector and their amplitude, which could be all derived from hydrometric data recorded from stream gauges on the Secchia river, provide good-predictive results considering the limited computational efforts and the free-access sources required.

Results from Case fc2, despite being the most reliable among the proposed methods, provide a limited, but continuous with elapsed time step, improvement in the assessment of riverbank stability for the considered events respect to Simplified Approach 1. Differences can be, however, found if compared to Case 1, that could be mainly ascribed to the shape of the synthetic hydrograph, more evident for input dataset 3. This consideration, although not being compromising for the proposed methodology, could be considered as an acceptable, conservative, errors if compared to results provided using steady-state conditions, but even considering that few simplified literature approaches could be find in present literature for the stability assessment of water retaining structure.

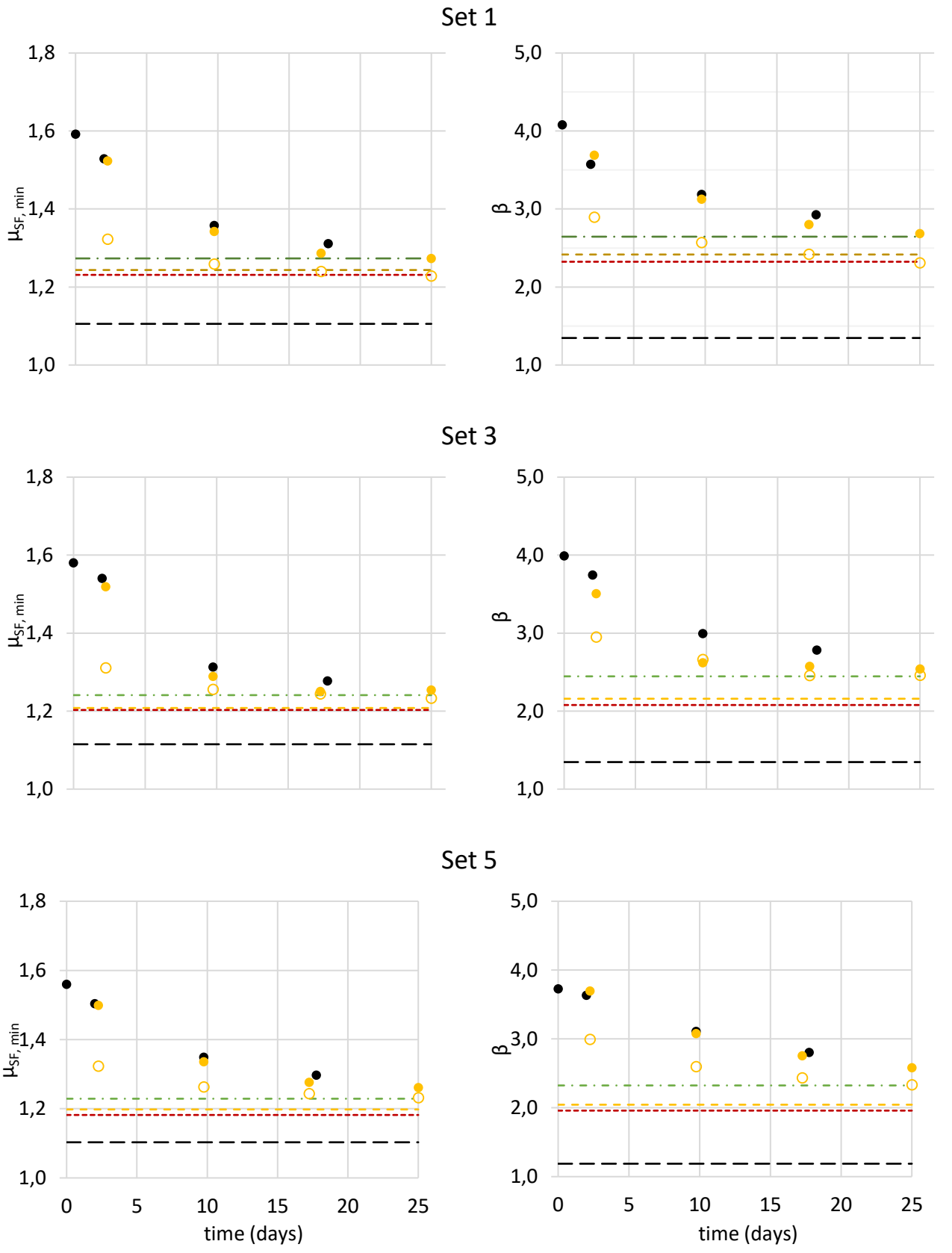

Figure 5.19. Results of the probabilistic stability analyses, by means of the minimum value for mean safety factor, SF, and reliability index, β, for dataset 1, 3 and 5.

6 Extended use of synthetic hydrographs and simplified methods for the assessment of existing riverbank

At this point of the study, an appropriate validation of the proposed synthetic and simplified approaches would require two more phases: firstly, it's necessaire to extend the applications of the methods to different events; then, it's required to compare the numerical results with monitoring and experimental data. The first step is useful to generalize the remarks and observations found during the numerical analysis discussed in the previous section, which was only referred to a specific high-water event, registered from February, 16th 2015 to March, 09th 2015. Furthermore, considering events characterized by different duration and water height, occurred in different seasonal period, is possible to underline the topical features of the proposed approaches; the purpose is, so, to cover and delimit, eventually, a specific range of application. The second step aim to improve and approve the reliability of the method, gained on the base of possible comparisons with soil suction and water content measurements in the riverbank during a series of high-water peaks. However, only the first of the proposed phases has been generally explored in the present thesis, and will be hereafter discussed; two additional events, in fact, have been considered for the numerical analysis, in order to extend the use of synthetic and simplified approaches presented in Chapter 4 and 5. Differently, the use of direct monitoring data to validate the present numerical analysis is still in progress in parallel research project, which requires specific and systematic studies, whose main features will only briefly presented in the last Chapter of this thesis.

6.1 Application of the proposed method to different high-water event

Aiming to extend and verify the possible applications of synthetic and simplified hydraulic conditions for the assessment of existing riverbank, two additional high-water events have been considered for the numerical simulations. Specifically, referring to hydrographs registered at different times during the year at the same control station (Ponte Bacchello), it could be possible to detect and overtake the possible dependence of general observations to a particular event and climatic conditions, underlining the features of the proposed method for different situations. For this purpose, considering February as the central part of the rainy season, two series of high-water peaks have been selected, in November and March/April, referring respectively to the beginning and the final part of the rainy season and, so, characterized by different assumptions on the initial and boundary conditions.

6.1.1 Realistic and synthetic hydrographs

The high-water event considered in this section refer to the time periods:

a. November, 04th 2014 to November, 19th 2014;
b. February, 16th 2015 to March, 09th 2015;
c. March, 16th 2015 to April, 08th 2015.

Hydrometric data measured in the three range of time, and the related values of Triangular Moving Average (w = 241), are evidenced in Figure 6.1. It can be observed that the considered events differ on their significant characteristics, and firstly on the shape of their hydrographs. In fact, the first event is characterized by high-water peaks closer in time (with a characteristic period of about 4 days), with the last two reaching the lower hydrometric heights; in the last event, inversely, the time-distance between two subsequent river waves is significantly higher (around 10 days), with a predominant amplitude for the second peak. Lastly, the second event (referred as Case 1 in the previous section) is characterized by an intermediate value for the time-distance of the waves length (around 7 days), and similar values for the hydrometric peaks. Hereby, referring to the approach that has been previously studied and through a simplistic but useful hypothesis, the first event could be associated to a synthetic hydrograph characterized by a waves frequency lower than *fc2*, the last event to a wave frequency higher than *fc2*, and the second event to a wave frequency of *fc2*.

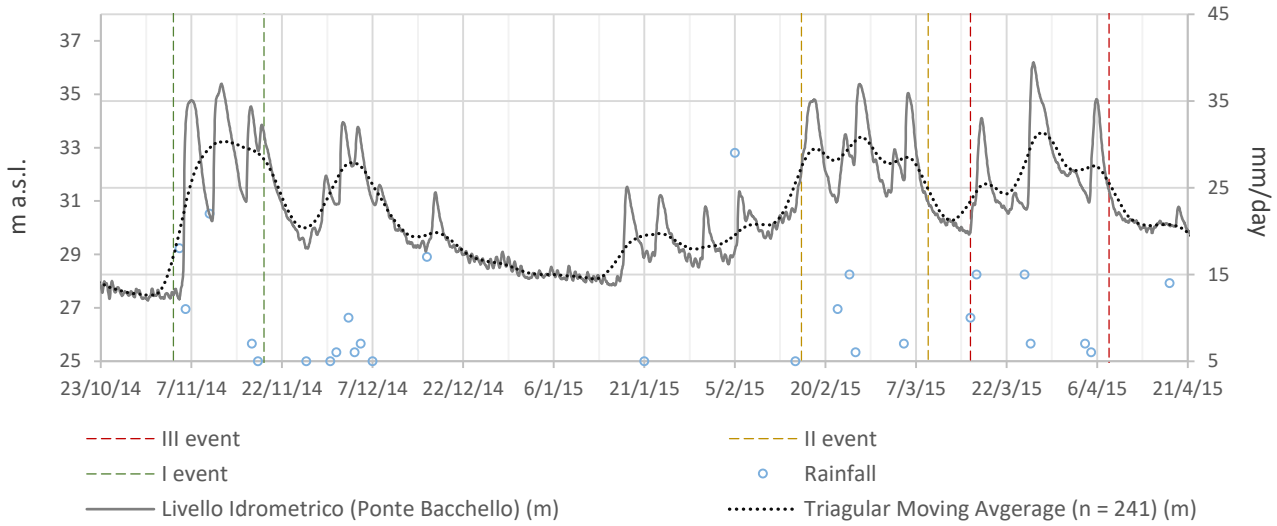

Figure 6.1. Registered data, in grey-solid line and triangular moving average, in black-dashed line, for hydrometric water level a.s.l. for the river Secchia, Ponte Bacchello remote station, during the period October, 03th 2014 – May, 31th 2015. The three studied events are evidenced in green- (November, 04th 2014 – November, 19th 2014), yellow- (February, 16th 2015 – March, 09th 2015) and red- (March, 16th 2015 - April, 08th 2015) long dash lines. Daily precipitations are plotted using unfilled blue-bordered circle.

Through these considerations, aiming to extend the number of applications for global safety assessment through the proposed methodology, and for verify its feasibility, the measured water levels have been represented by means of synthetic hydrographs using as characteristic frequencies:

- *fc2* and *fc3* for the first event;
- *fc1*, *fc2* and *fc3* for the second event;
- *fc1* and *fc2* for the third event.

Moreover, even if all the considered high-water sequences are generally part of the rainy season, they refer to different hydrometric initial conditions. In particular, the first event (November, 04th 2014 to November, 19th 2014) occurs at the beginning of the wet season, when the river level away from precipitation is around 27 m a.s.l., on average. In this period, the height of the phreatic line in the soil landward is generally higher than the river level, meaning that the river drains part of the groundwater. Furthermore, being the studied section not affected by significant rainfall, the riverbank soil is expected to have a saturation degree close to the lower values reached during the year. Otherwise, the second (Febraury, 16th 2015 to March, 09th 2015) and the third event (March, 16th 2015 to April, 08th 2015) occurs during the crucial and final part of the wet season, characterized by a generally higher river level, that on average and in absence of precipitation increase from 28m a.s.l. (January-Febraury) to 30m a.s.l. (March-April). These features can be intended as different hypothesis on the initial conditions, represented using a hydrometric baseline varying with the considered period. A crucial point for the applicability of the proposed method is, then, to univocally individuate the hydrometric baseline height, the amplitude and phases of the sine-waves for the synthetic hydrographs. In the previous section, the synthetic hydrographs were defined assuming as baseline the triangular moving average (TMA) 241-width estimated in correspondence of the beginning of the registered high-water event, when the hydrometric height was equal to the river level recorded on Febraury, 15th 2015. However, this assumption can be directly applicable only in case the TMA 241-width values are known for the considered event, as in case of a back-analysis process; otherwise, the hypothesis on the baseline, the amplitude and phases of the sine-waves could be found to be inconsistent when considering different applications. With the purpose to define, as much as possible, a reliable and relevant method for riverbank global stability evaluation accounting for transient seepage conditions, general indications need to be provided for the initial and boundary condition assumptions. In specific, as hydrometric baseline is here considered a significant value for the river water level in relation to a specific seasonal period, e.g. the monthly average value of the TMA 241-width.

Referring to the high-water events considered in this section, the hydrometric baseline considered for the first event is equal to 27.5m, while for the third event is equal to 30.0m. Through these considerations, it turns out that the hydrometric baseline for the second event was equal to 29.1m, if considering the sine-waves starting from the lowest value in oscillation (-3.15m, in Chapter 5). which represent a reasonable value

for the period mid-January to mid-February. In Figure 6.2 are finally plotted the realistic and synthetic hydrographs used in the numerical analysis discussed in this section, together with the riverbank shoulder and crest heights.

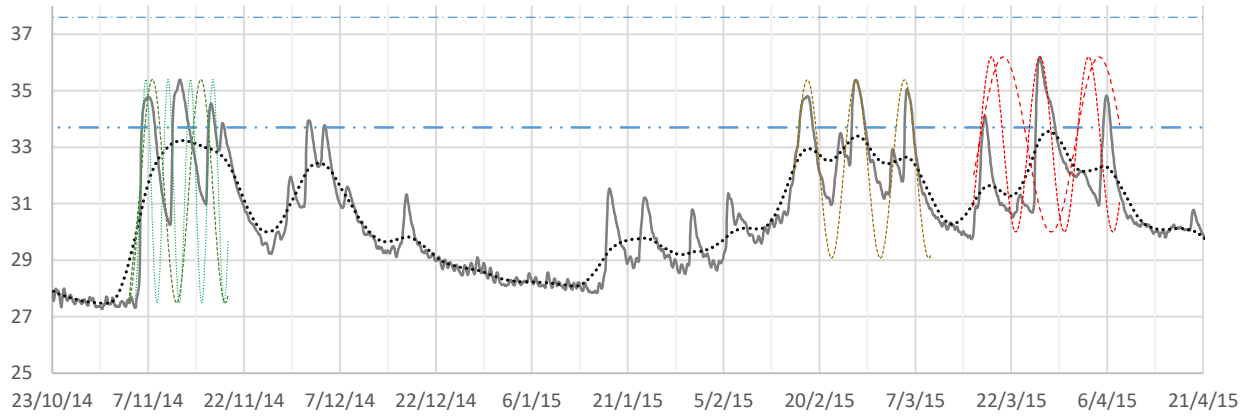

Figure 6.2. Registered data, in grey-solid line, and triangular moving average, in black-dashed line, for hydrometric water level a.s.l. for the river Secchia, Ponte Bacchello remote station, during the period October, 03th 2014 – May, 31th 2015. The synthetic hydrographs are evidenced in green- (November, 04th 2014 – November, 19th 2014), yellow- (February, 16th 2015 – March, 09th 2015) and red- (March, 16th 2015 - April, 08th 2015) dahs lines. In blue lines, dash-dot and long dash-dot, are evidenced the riverbank shoulder and crest heights.

The amplitude of the synthetic hydrographs refers to the maximum hydrometric data registered during the specific high-water event, and will be slightly different among the considered events; 3.95 and 3.1m are used for the first and third event, respectively. A shift of half period has been considered as initial phase for the sine-waves, so that the initial hydrometric value the synthetic hydrographs is equal to the baseline height. Seepage through the riverbank has been evaluated using the two-dimensional FEM code VADOSE/W, performing transient coupled hydro-thermal flow analysis. The hydraulic boundary conditions for the transient seepage analysis are, so, represented by a series of subsequent sine-waves, with specific frequency varying from 3.5 days to 15 days for different cases. In the following paragraphs, the analyses are named using Case 1 or Case $fc_{1...3}$, depending on the type of hydraulic condition (registered data or synthetic hydrograph with characteristic frequency equal to *fc1*, *fc2* and *fc3*, respectively). Subscript letters from *a* to *c* are used for specifying the high-water event; in details, subscript letter *a* will indicates the event registered in November 2014, subscript letter *b* the event registered from February to March and subscript letter *c* the event registered from March to April; e.g. Case 1_a indicates the analysis performed using as hydraulic boundary conditions the registered hydrometric data collected in Ponte Bacchello from November, 04th 2014 to November, 19th; Case $fc1_c$ indicates the analysis performed assuming as boundary conditions a synthetic hydrograph characterized by a period for the sine-waves equal to 15 days and baseline equal to 30m, representing the event registered from March, 16th 2015 to April, 08th 2015.

6.2 Numerical analysis

In the present chapter, will be presented and discussed result obtained by means of seepage and stability analysis, for which three series of transient coupled hydro-thermal analysis have been considered. Each series refers to a specific observation time-period:

a) November, 04th 2014 to November, 19th 2014;
b) Febraury, 16th 2015 to March, 09th 2015;
c) March, 16th 2015 to April, 08th 2015.

For each series, four kind of seepage analysis have been performed, varying the initial and boundary conditions, specific for the time-period, according to the approach defined in paragraph 7.2 and assuming as soil hydraulic and retention parameters the values listed in Table 5.1, defined as:

- Case 1: initial conditions are determined through the model spin-up, as discussed in Chapter 4. Registered hydrograph and climatic data are used as boundary conditions for transient seepage analysis;
- Case fc1…3: initial conditions are determined through the model spin-up, run to the beginning of the considered time-period (Chapter 4). Synthetic hydrographs defined through a series of sine-waves, with characteristic frequency ranging from *fc1* to *fc3*, superposed to a hydrometric baseline dependent on the considered seasonal period, are assumed as hydraulic boundary conditions. Climatic data are assigned in correspondence of each river level growth, taking care of spreading the amount of rainfall as function of the sine-wave lengths;
- Simplified Approach 1: initial conditions defined using as hydrometric baseline a significant value for the river water level in relation to a specific seasonal period, e.g. the monthly average value of the TMA 241-width; pore water pressure distribution is determined through the hypothesis of steady-state conditions in equilibrium with the hydrometric baseline assumed for the considered period; suction values above the phreatic line are assigned assuming a hydrostatic increase from the phreatic line and from the ground level up to a maximum (absolute) value pertinent with the considered period. Hydraulic and climatic boundary conditions are assigned as for Case fc1…3;
- Simplified Approach 2: Pore water pressure and suction distribution to be used in the stability analysis have been directly defined by means of simplified assumption, generalizing results obtained from transient seepage analysis performed in Cases 1 and fc1…3.

As also specified in Chapter 5, the various approaches above listed are distinguished by a different degree of sophistication, and are characterized by a decreasing level of computational effort and required data to achieve the desired results; however, a consequential and progressive reducing level of reliability, in terms of safety assessment, has to be considered. In example, the use of the first, realistic, approach (Case 1) could

provide a confidently representative estimation of the seepage and stability characteristic for the riverbank, assuming that all hydraulic and mechanical soil properties are adequately identified), but would also require the knowledge of all hydrometric and climatic data for the specified time period; on the other hand, the synthetic (Case fc1…3) and simplified (S.A. 1 and 2) approaches, as discussed in Chapter 4 to 6, would provide slight variations respect to the results obtained using the realistic approaches, the more tending to the safe side with the increasing in approximations and decreasing of the necessaire source of knowledge. These considerations, on the author mind, are fundamentals for the evaluation on the applicability and trustworthiness for any assessment process, and have been tested, in best wishes, at any step of the present work.

The control nodes considered for the hydraulic output refer to the points of the FE model selected at the bottom of the riverbank soil layer, firstly defined in Chapter 5, while the time step selected for the output are in correspondence of the hydrometric peak of the various hydrographs; at each selected time step, probabilistic limit equilibrium analyses have been performed using pore water pressure and suction distribution determined through seepage analysis. Specific restriction on the shape and dimensions of the critical slip surfaces (considering an overall instability mechanism occurrence, instead of referring to singular critical slip surfaces) and soil strength properties as standard variables have been used. In the next sections, hydraulic and stability results obtained using different approaches and set of parameters are compared, in relation to the various series of analysis.

6.3 The evolution of riverbank stability condition with external conditions

Aiming to estimate the influence of the occurrence period of a high-water event during the year, results obtained from seepage and stability analysis for different time-period among the wet season (from November to May, considering the site environmental characteristic), using registered hydrometric level and climatic data, are firstly showed and discussed. All results here presented are obtained using Set 1, defined assuming the average values for all hydraulic and retention parameters, focusing on the comparison between different events impact on riverbank hydraulic and mechanical response. The complete set of results will be discussed in the following sections and, however, resumed in Appendix. In Figure 6.3 are plotted, together with the soil layer profiles, the results in terms of total head, as meters above sea level, estimated in the control nodes (Chapter 5) at the beginning and end of the high-water event (Fig. 6.3a and 6.3c), in correspondence of the maximum hydrometric level for each event, both in transient (Fig. 6.3b) and steady-state (Case $3_{a...c}$, Fig. 6.3d) seepage conditions.

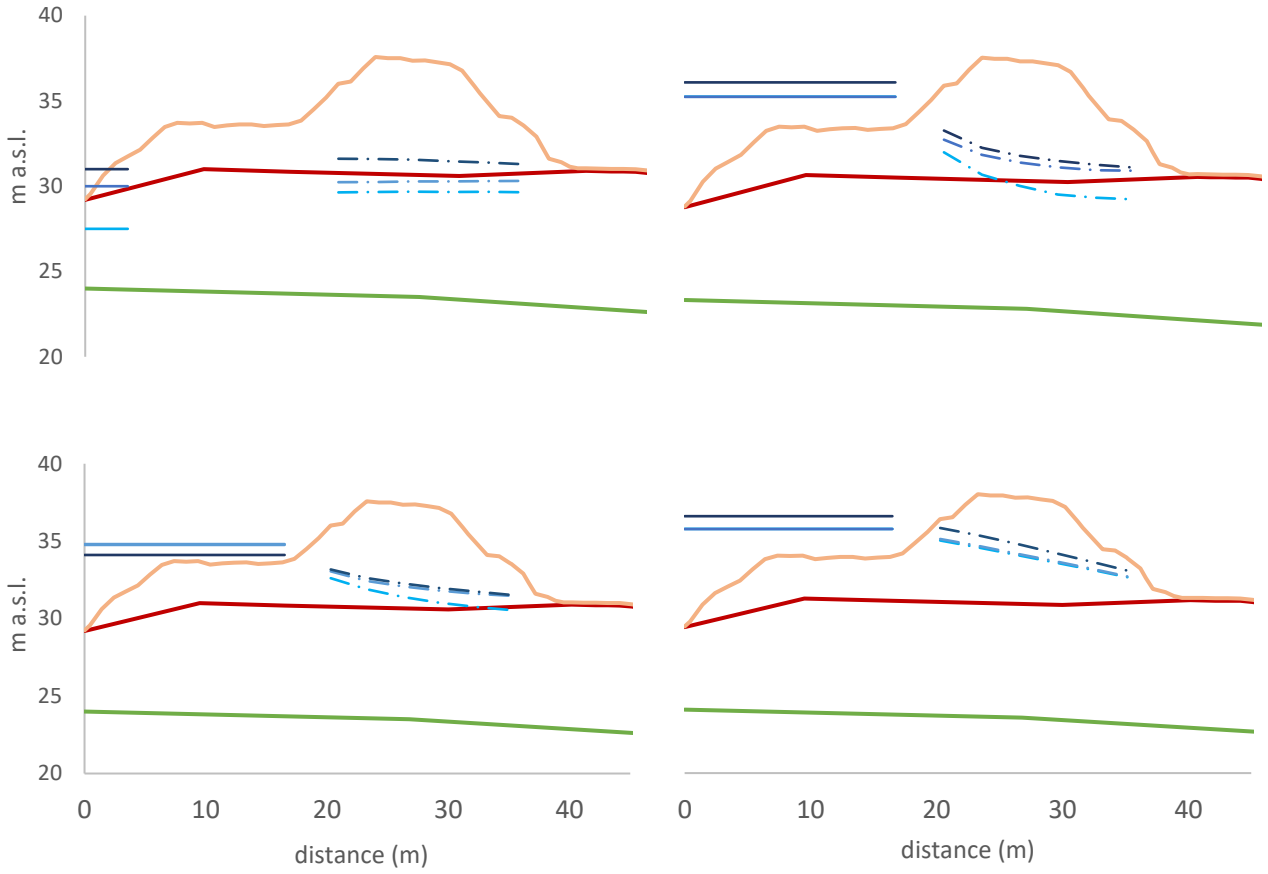

Figure 6.3. Results of transient coupled hydro-thermal seepage analysis in terms of total head estimated a) at the beginning of the high-water sequence, b) in correspondence of the maximum hydrometric value, c) at the end of the high-water event, d) in steady-state conditions (Cases $3_{a...c}$) in equilibrium with the maximum water level reached during the various considered event.

The lower values of total head are relative to Case 1_a for all considered time-step and seepage conditions; furthermore, for Case 1_a, the values of total head estimated at the final step are also significantly higher than those estimated in correspondence of the maximum hydrometric level, while generally lower differences can be appreciated for Case 1_b and 1_c. These findings are directly dependent on soil saturation and suction distribution computed at the beginning of the considered events, producing lower relative permeability and, consequently, a minor progression for the phreatic line in the riverbank for Case 1_a; this event occurs at the beginning of the wet season, meaning that climatic and initial conditions, in terms of cumulative rainfall and hydrometric baseline respectively, have a significant incidence on the hydraulic response of the riverbanks. However, for all considered time-step and Cases, transient seepage results significantly differ from those obtained in steady-state conditions, clearing that accounting for time-variability in riverbank seepage assessment process is required to obtain reliable results. In order to quantify the differences in hydraulic response between the various Cases, could be useful refer to h_d values in the control nodes, estimated through transient coupled hydro-thermal seepage analysis, plotted in Figure 6.4 for all considered time step.

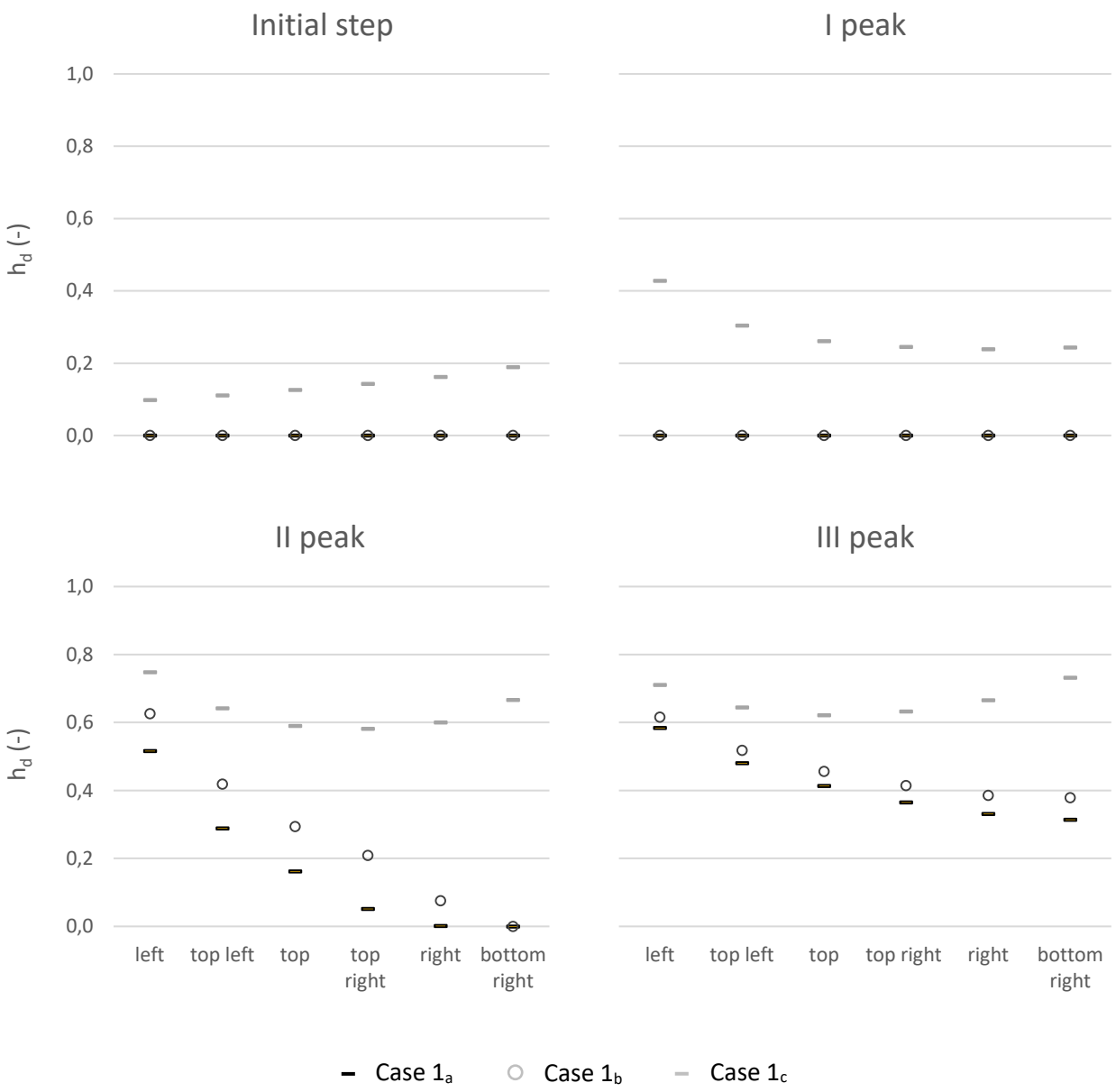

Figure 6.4. Dimensionless head, h_d, of the control nodes computed using as boundary conditions the realistic hydrographs registered for the each of the considered events, in correspondence of the beginning of the high-water sequences and the various hydrometric peaks.

Still referring to Case 1_a, it can be seen that the first hydrometric peak has a negligible effect on the phreatic progression in the riverbank, being the total head in the control nodes comparable to the height of the water table in the dry season; in some way, this situation can be found also for Case 1_b and 1_c, in which the first hydrometric peak only produce slight variations in the progression of the phreatic line in the riverbank. Furthermore, the effect of the second hydrometric peak for Case 1_a do not globally affect the hydraulic response of the riverbank, being evidenced significant variation in the values of h_d only up to the central part

of the riverbank layer. Differently, in Case 1_b and 1_c the effect of the second hydrometric peak is significantly higher for all the control nodes, meaning that this event induces strong variation in the hydraulic response of the riverbank. This occurrence can be referred to Case 1_a only in correspondence of the last hydrometric peak, where a significant increment for h_d respect to the initial conditions can be stated for all control nodes. In Cases 1_b and 1_c, differently, the third hydrometric peak tends to produce a variation of minor impact respect to the preceding, however more evident for Case 1_b where the water level is approximately constant for all the registered waves. By these observations, it can be immediately highlighted the importance of the time-occurrence of high water event sequences, which may have significant (Case 1_b and 1_c) or negligible (Case 1_a) impact on the phreatic progression in the riverbank up to the second hydrometric wave, for the considered Set of parameters. This is mainly due to the suction distribution in the riverbank at the beginning of the various events, strongly influencing the soil permeability and, consequently, the hydraulic response of the system to a rapid river level rise. In order to relate the hydraulic response of the riverbank to its stability conditions, probabilistic limit equilibrium analysis have been performed in correspondence of all the elapsed time-step.

In Figure 6.5 is plotted the evolution of the reliability index, β, with time in the wet season, over the registered hydrograph. As it can be seen, the safety conditions towards global instability suffer a strong reduction along the entire period of study, varying from an initial value of β = 4.141 in correspondence of the first elapsed time-step, in November, 04th 2014, to a final value of β = 2.818 in correspondence of the third hydrometric peak measured on April, 5th 2015, meaning that the probability of failure (P_f) is varied of more than one order of magnitude.

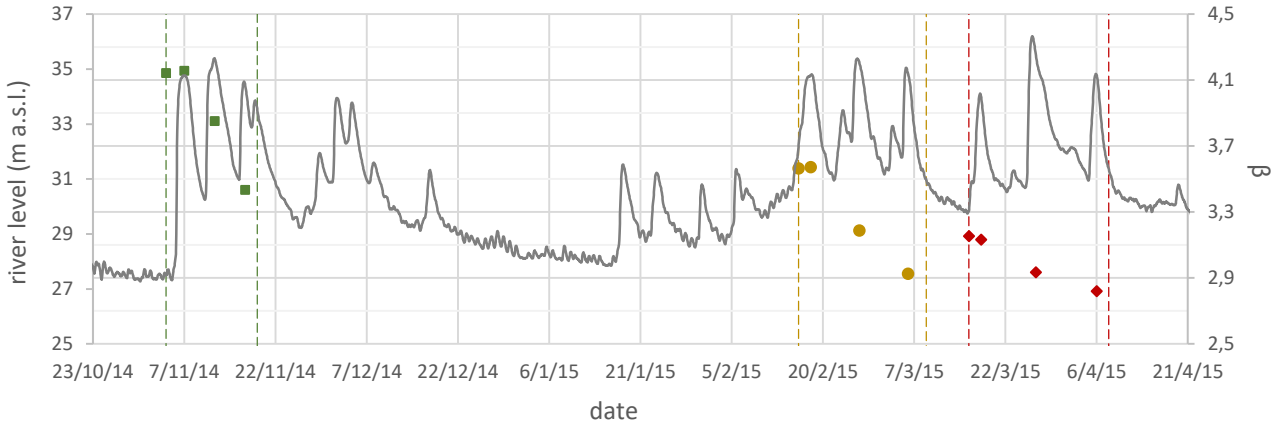

Figure 6.5. Registered data, in grey-solid line for hydrometric water level a.s.l. for the river Secchia, Ponte Bacchello remote station, during the period October, 03th 2014 – May, 31th 2015. The three studied events are evidenced in green- (November, 04th 2014 – November, 19th 2014), yellow- (February, 16th 2015 – March, 09th 2015) and red- (March, 16th 2015 - April, 08th 2015) long dash lines. Probabilistic limit equilibrium analysis results, in terms of reliability index, are plotted in correspondence of the elapsed time-step.

In addition, the margin of safety estimated at the end of a high-water event and at the beginning of the consecutive one, are comparable; this is evident for Cases 1_a and 1_b, but also remarkable for Cases 1_b and 1_c, even considering the significant time-distance between the first two events, and the reduced overall stability conditions for the last two events. These two aspects, in fact, tend to produce consistent variation in the height of the phreatic line in the riverbank when the hydrometric peak is no longer persistent, but have a limited influence on the shape of soil suction distribution above the phreatic line (Figure 6.6), in relation to the climatic conditions.

In order to clearly evidence the effect of unsaturated soil suction on the seepage and stability characteristics, in Figure 6.6 are plotted profiles for soil water content and pore water pressure and suction. The showed values are computed for the embankment at the beginning of each considered high-water event, e.g. for the time step corresponding to November, 04th 2014, Febraury, 16th 2015 and March, 16th 2015; selected progressives are 20.3m and 26.3m, equal to the x-coordinates of left and top control nodes. As can be seen, significant differences among the three cases can be mostly attributed to the height of the phreatic line, which is in correspondence of the saturation values for soil water content and zero value for pore water pressure, which maximum variation is about 2.5m. This feature could be attributed as the main impacting on seepage characteristic for the riverbank during the three event. Soil suction and water content profiles above the phreatic line evidence similar trends for all Cases, mainly depending on the retention parameters assumed for the considered analyses. Reduction in soil saturation in correspondence of soil surface is evidenced left nodes profiles, while this trend is evident only for Case 1a in correspondence of central nodes profile; this estimation is mainly due to the possibility to pound for rainfall water, which has been considered in the analyses, causing increment in water infiltration from the top of the riverbank, while on the slopes run-off is generally predominant in absence of significant precipitation events. However, noteworthy differences in suction (and water content) distributions in the central part of the riverbank, between 31m to 35m a.s.l. can be appreciated only for Cases 1_c. this means that climatic stress, by itself, do not strongly affect soil saturation values among the first two meters from the soil surface, but high-water events are required; in specific, is the effect of the series of hydrometric peaks registered from February, 16th 2015 to March, 09th 2015 determining the initial conditions for Case 1_c. For each considered event, the lower values of β are always computed at the last considered time step, meaning that the reduction of safety margins could be primarily influenced by the duration of the high-water event, starting from an initial value dependent on its occurrence through the year, rather than the maximum height of hydrometric peak. Of relevant interest, could be the comparison of the results of probabilistic limit equilibrium analysis performed for Cases $1_{a...c}$ and in steady-state seepage conditions in equilibrium with the maximum hydrometric level reached during each event (Case $3_{a...c}$); the comparison is expressed in terms probability, and cumulative probability, density function of safety factor (SF) plotted in Figure 6.7. The results are expressed for the most critical slip surface, detected among the ones considered admissible and representative for a global instability mechanism; the

lower P_f do not always correspond to the minimum among the mean values of the safety factor (μ_{SF}), taking in proper consideration the standard deviation of the and the shape of the SF distributions (σ_{SF}). As can be seen, the most critical step in terms of P_f, considering transient seepage conditions, is represented by the third hydrometric peak for Cases $1_{a...c}$, ranging from 0.03% (November, 17th 2014) to 0.24% (April, 06th 2015), that express a progression up to a significant value for riverbank vulnerability towards global failure; however, these terms are still largely lower than the values of Pf estimated for Cases $3_{a...c}$, expressing unrealistic safety margins and differing in several order of magnitude. All above discussed probabilistic results are reported in Table 6.1 for Cases $1_{a...c}$ and $3_{a...c}$.

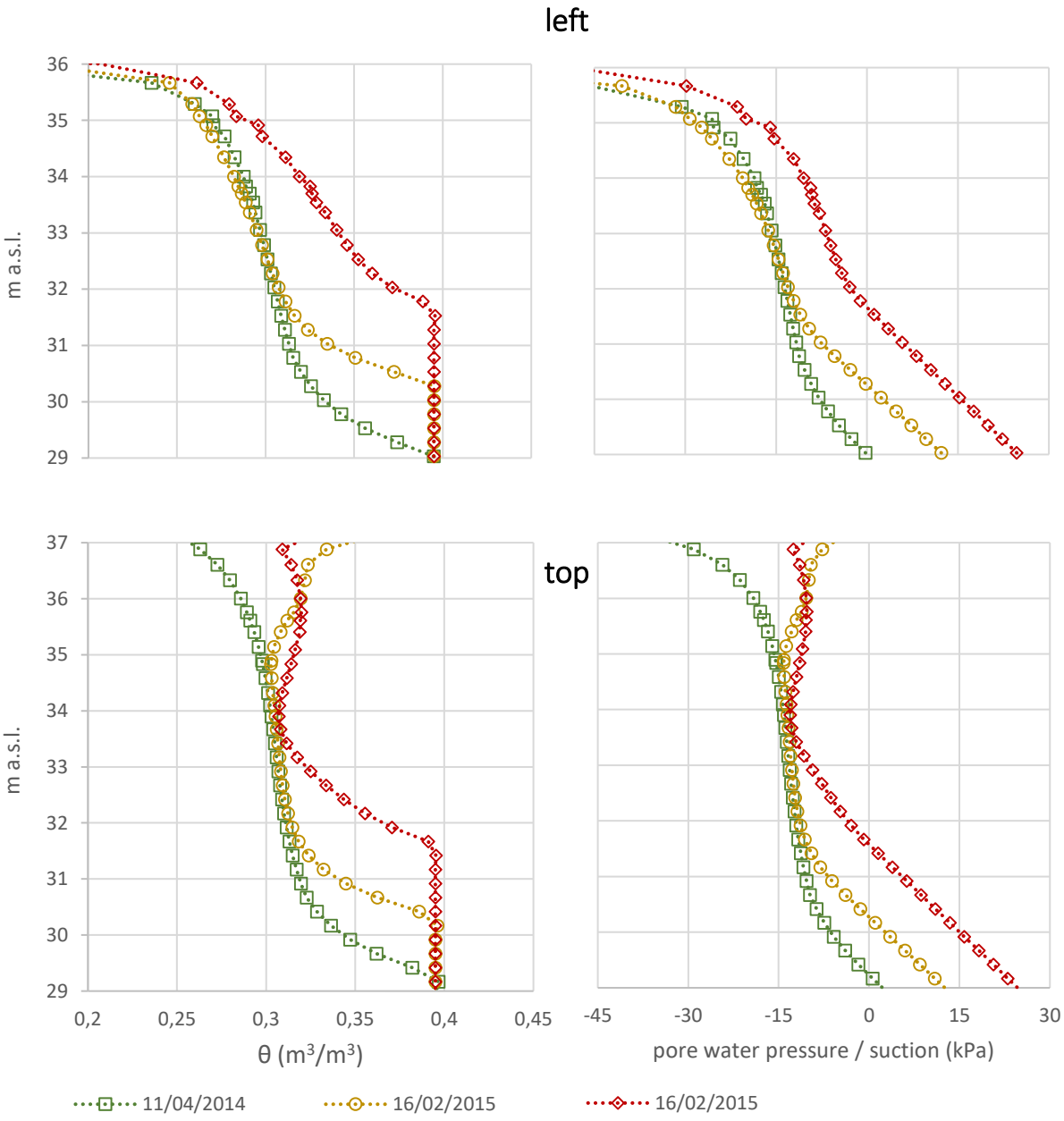

Figure 6.6. Soil water content (left) and suction (right) profiles at x = 20.3m (top) and x = 26.3m (down), computed in correspondence of the beginning of the three considered event.

Case 1a

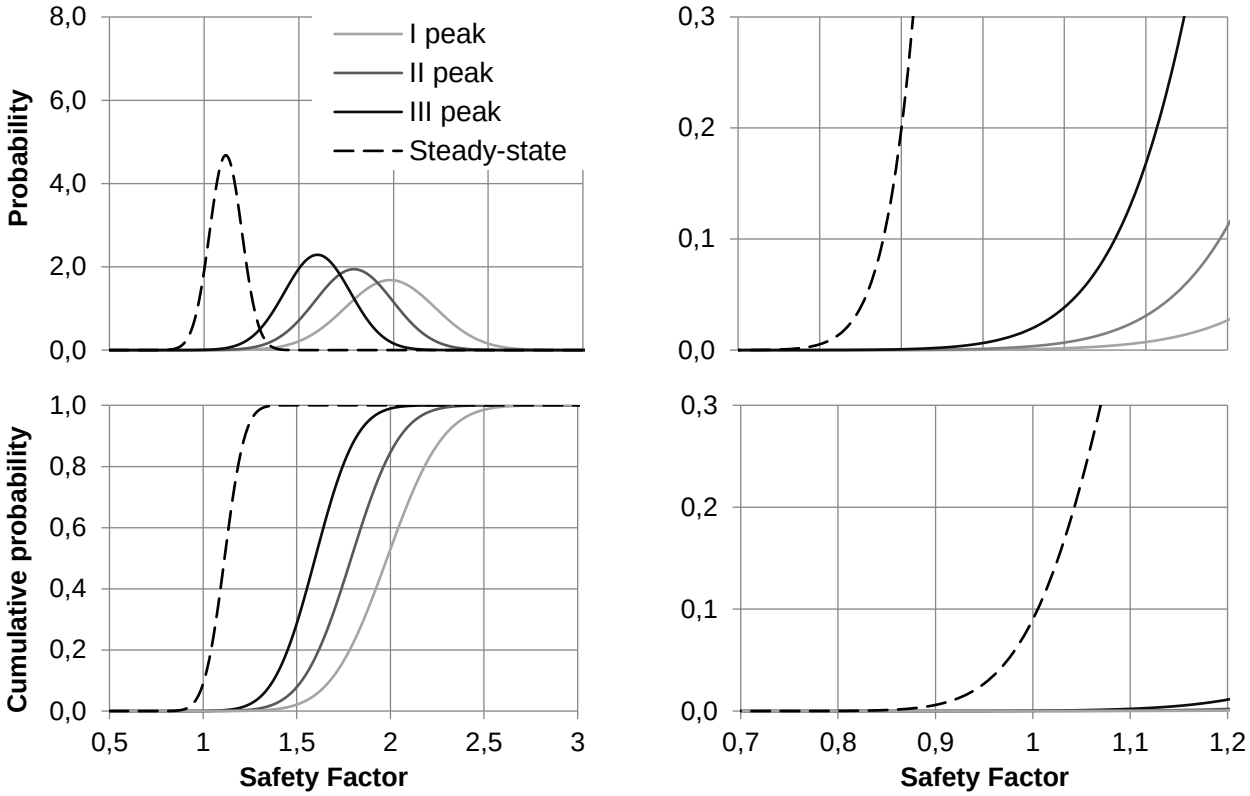

Case 1b

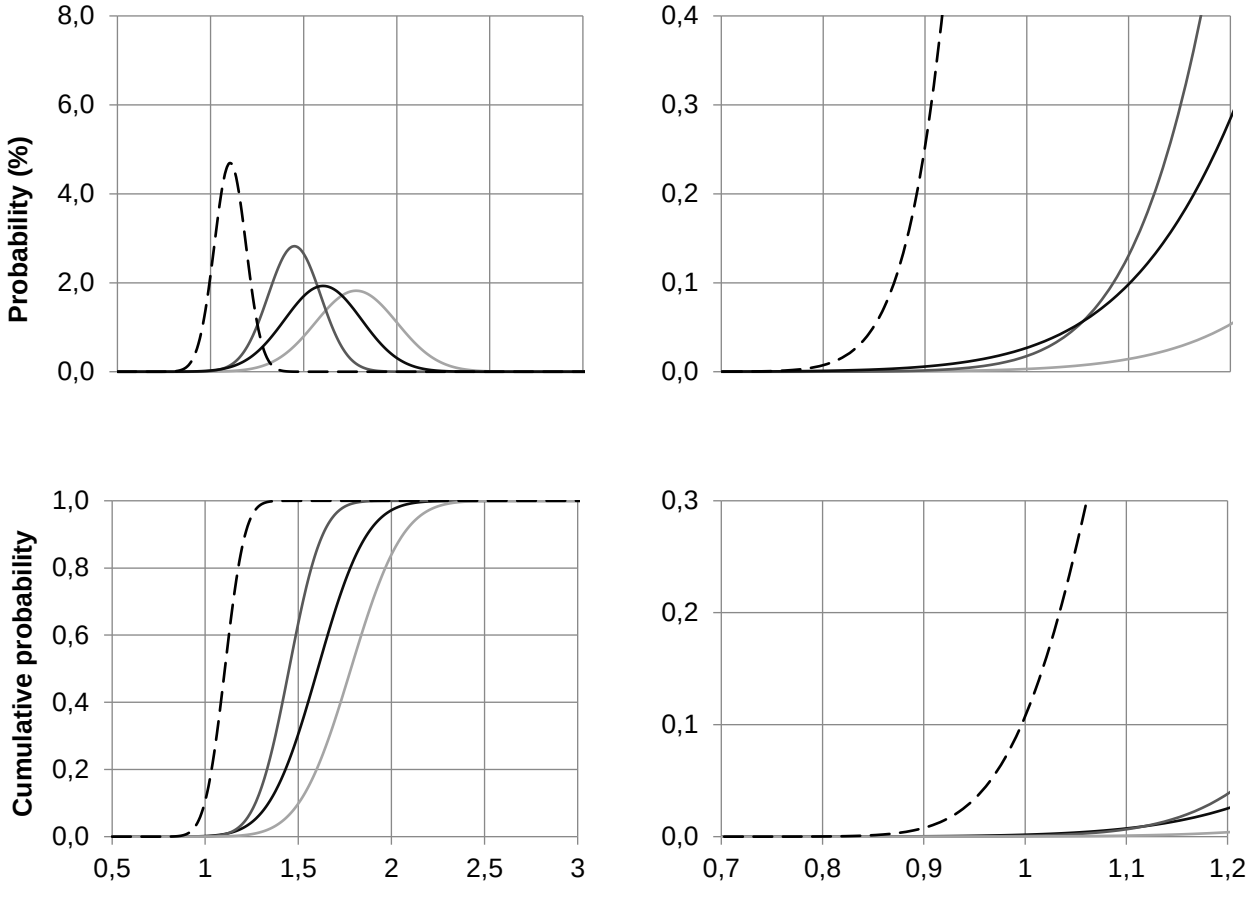

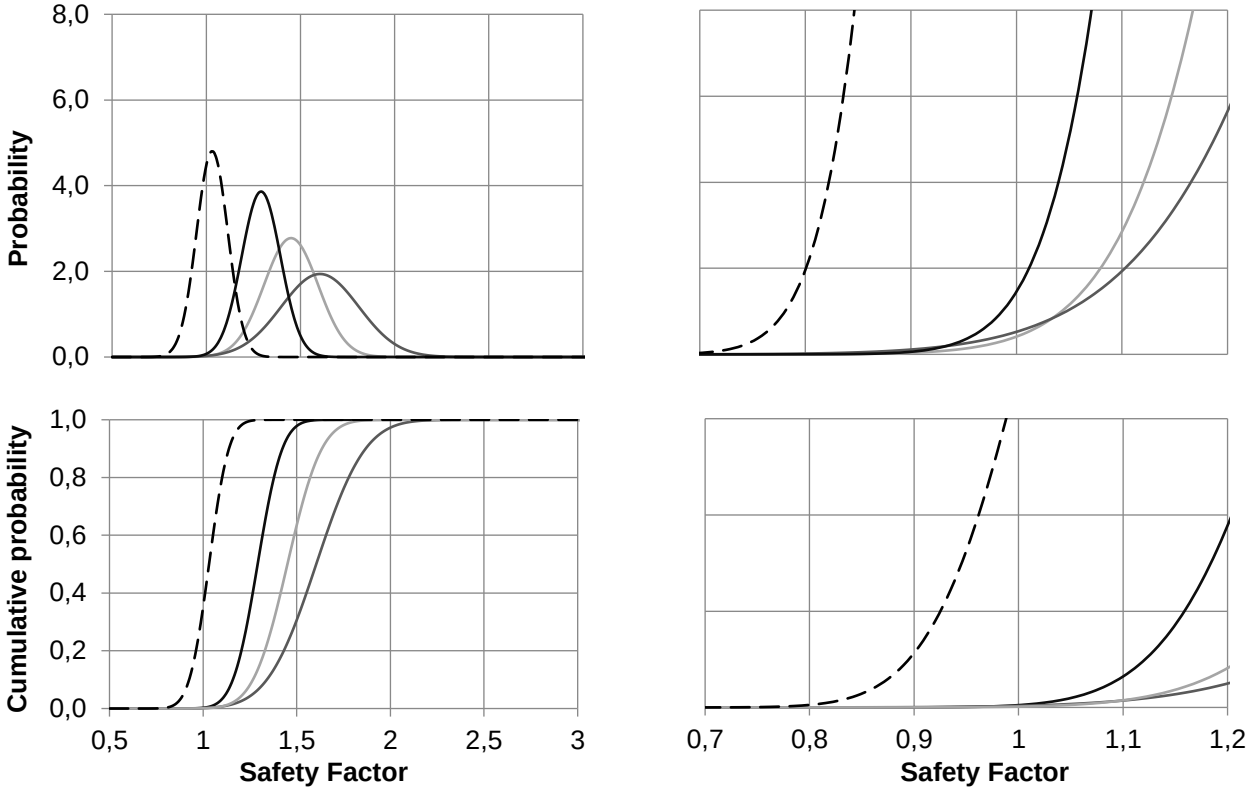

Figure 6.7. Comparison between Cases $1_{a...c}$ and steady-state conditions in terms of probability density function of safety factor, for overall instability mechanism on outer slope.

	I peak			II peak		
	Case 1a	Case 1b	Case 1c	Case 1a	Case 1b	Case 1c
μ_{SF}	1.983	1.782	1.450	1.791	1.450	1.604
σ_{SF}	0.237	0.219	0.144	0.205	0.141	0.206
β	4.141	3.570	3.132	3.851	3.186	2.934
P_f (%)	$1.46 \cdot 10^{-3}$	$8.01 \cdot 10^{-2}$	$2.31 \cdot 10^{-1}$	$6.36 \cdot 10^{-3}$	$2.22 \cdot 10^{-1}$	$6.75 \cdot 10^{-1}$
	III peak			Steady-state		
	Case 1a	Case 1b	Case 1c	Case 3a	Case 3b	Case 3c
μ_{SF}	1.598	1.605	1.291	1.114	1.105	1.032
σ_{SF}	0.174	0.207	0.103	0.085	0.085	0.083
β	3.432	2.924	2.818	1.342	1.241	0.381
P_f (%)	$1.00 \cdot 10^{-1}$	$6.52 \cdot 10^{-1}$	$8.70 \cdot 10^{-1}$	9.51	11.55	35.78

Table 6.1 - Probabilistic results of limit equilibrium analyses using MC method in transient and steady-state seepage conditions for the global instability.

In addition, it can be here noticed that the increase of P_f (in $\log_{10}$ scale) with time seems to evidence a linear trend, similarly to what was evidenced for the average values of h_d estimated in the control nodes in correspondence of the elapsed time-step; all these values are plotted in Figure 6.8. This trend seems to suggest that a limit condition for the riverbank seepage and stability behaviour has not been yet reached, meaning that the time variable is still predominant in this evaluation process, respect to the height of each hydrometric peak. These conditions on h_d and P_f are consistent with the assumptions on soil hydraulic and retention parameters (Set 1) and hydraulic boundary conditions (Case $1_{a...c}$) assumed for the seepage and limit equilibrium analysis; however, its's expected to achieve an increment lower than linear considering event more persistent in time (Case $fc_{1...3}$), or assuming lower values for unsaturated soil strength (Set 5) and higher for soil permeability (Set 3, 7).

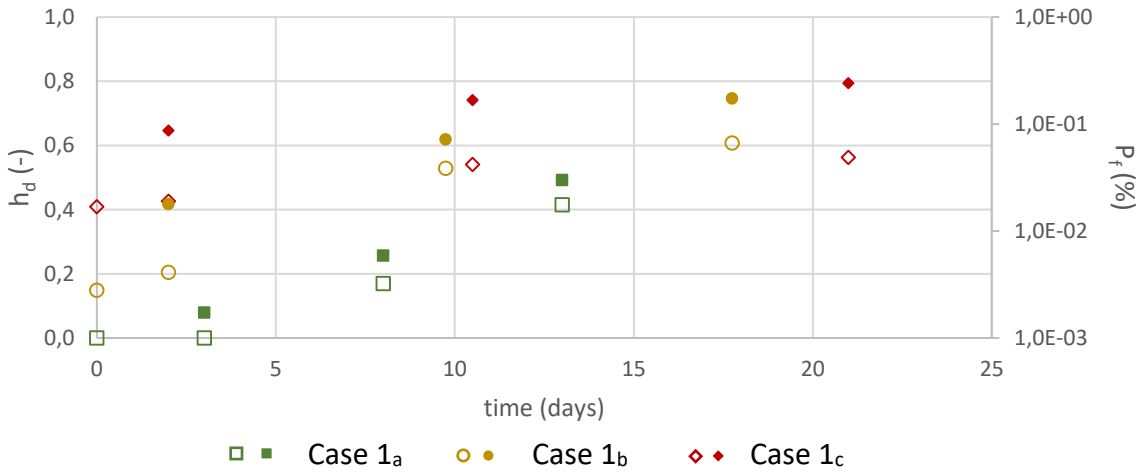

Figure 6.8. Dimensionless head of the control nodes from the unsaturated seepage for Cases $1_{a...c}$ (h_d, left axes), and probability of failure (P_f, right axes) for the considered time step as function of the elapsed time (in days from the beginning of the high-water sequence).

6.4 On the use of synthetic hydrographs to assess riverbank stability for different external conditions

In order to extend the use of synthetic hydrographs as hydraulic boundary conditions for the seepage analysis in the riverbank safety assessment process, and to define its range of applicability, three series of transient hydro-coupled analysis have been performed using sequences of sine-waves to represent a high-water event. In addition to the analysis presented in the previous chapter, the measured water levels have been represented by means of synthetic hydrographs using as characteristic frequencies:

- *fc2* and *fc3* for the first event;
- *fc1*, *fc2* and *fc3* for the second event;
- *fc1* and *fc2* for the third event.

as described in paragraph 6.1.1, with specific reference to Figure 4.2. Probabilistic limit equilibrium analyses have been performed, similarly to those described in the previous sections, by means of Monte Carlo method (100.000 trials), using Morgenstern and Price method for the determination of the safety factor for each slip surface identified by the geometric restriction described in section 2.2. As still done before, the reliability, and then the accuracy, of the results obtained using simplified approaches is determined by comparison with results obtained from analysis performed using registered hydrographs and climatic data as boundary conditions, and spin-up of the model for initial conditions; this conditions is particularly valuable in cases the shape of synthetic hydrograph has a marked similarity with the registered one, in terms of height and persistence of the various hydrometric peaks, and when the studied event can be considered independent from the previous in terms of hydraulic response. Results obtained using the steady-state hypothesis for seepage conditions in equilibrium with the maximum water level (Case 3) have been, indeed, considered as reference as outcomes of a largely over-conservative assessment process. Results and remarks hereafter presented and discussed have been obtained assuming Set 1 soil parameters, not accounting for variability of hydraulic and retention soil properties, with specific reference for the first (November, 04th 2014 to November, 19^{h} 2014) and the third (March, 16th 2015 to April, 08th 2015). In Figure 6.9 are plotted the values of h_d with time, evaluated in the control nodes of the model in correspondence of the hydrometric peaks for registered (Case 1_a) and synthetic (Case $fc2_a$ and $fc3_a$) hydrographs. The observed trend is similar to what was found in Chapter 5, for which the hydraulic response of the riverbank expressed in terms of h_d, is formerly dependent on the elapsed time, rather than the shape of the considered hydrographs. However, a perceptible variation of the phreatic line inside the riverbank can be found only after the second hydrometric peak for Cases 1_a and $fc2_a$, the third for Case $fc3_a$. Furthermore, a remarkable agreement can be found in the showed results between Case 1_a and Cases $fc2_a$ and $fc3_a$, evidencing the possibility to use the proposed synthetic approach for define the hydraulic response of the riverbank to a high-water event, as well as the direct definition of a realistic hydrograph for the hydraulic boundaries. The use of synthetic hydrograph is also convenient in order to define a state for which the progression of the phreatic line seems to reach a critical condition for the considered hydrometric baseline and peak heights; this conditions can be defined for values of h_d varying from 0.82 to 0.69, from left to right nodes, and require a time-period of approximately 35 days to be reached.

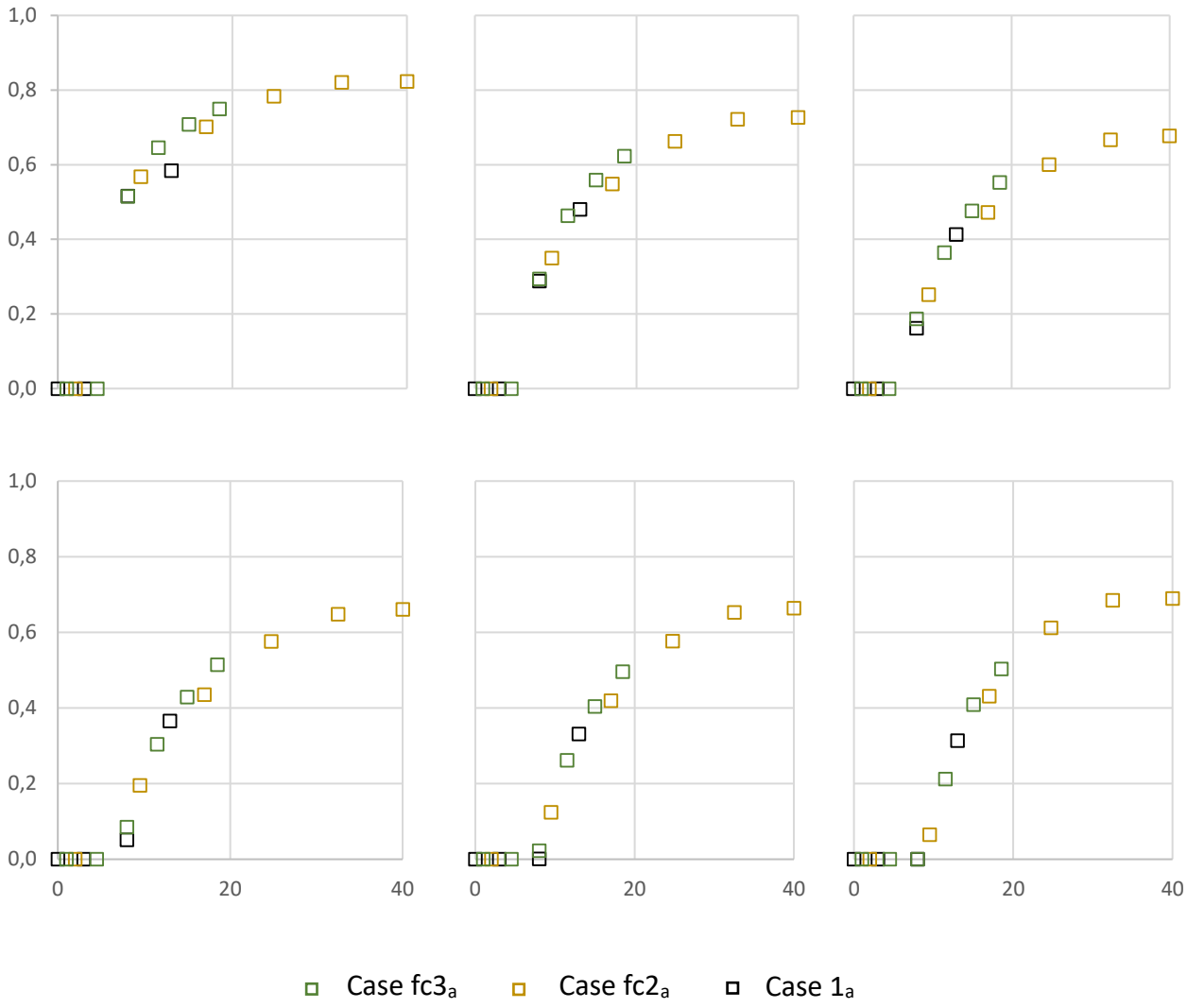

Figure 6.9. Dimensionless head of the control nodes from the unsaturated seepage analysis using real (Case 1a) and synthetic (Case fc2a and fc3a) hydrographs as hydraulic boundary conditions, plotted as function of the elapsed time (expressed in days from the beginning of the high-water sequence).

In Figure 6.10 are, then, showed the reliability index obtained from probabilistic limit equilibrium analysis performed in correspondence of the hydrometric peaks of realistic and synthetic hydrographs for which results have been showed in Figure 6.9. Showed data evidence the appreciable agreement between results obtained using realistic and synthetic hydrographs, still evident for the hydraulic response of the riverbank in terms of h_d. These considerations directly derive substantially from the shape of the registered hydrograph, characterized by a series of hydrometric peaks of comparable height and persistence, and so, theoretically synthetized by a sinusoidal wave superposed to a hydrometric baseline. In addition, is still confirmed the substantial dependence on the elapsed time for the reliability index estimated using synthetic hydrographs, while quite irrespectively from the characteristic frequencies of the sine-wave sequences. The results of probabilistic limit equilibrium analysis are listed in Table 6.2 with reference to mean value, standard

deviation, reliability index and probability of failure computed for the most critical slip surface (in terms of β) using M-C method (100.000 simulations).

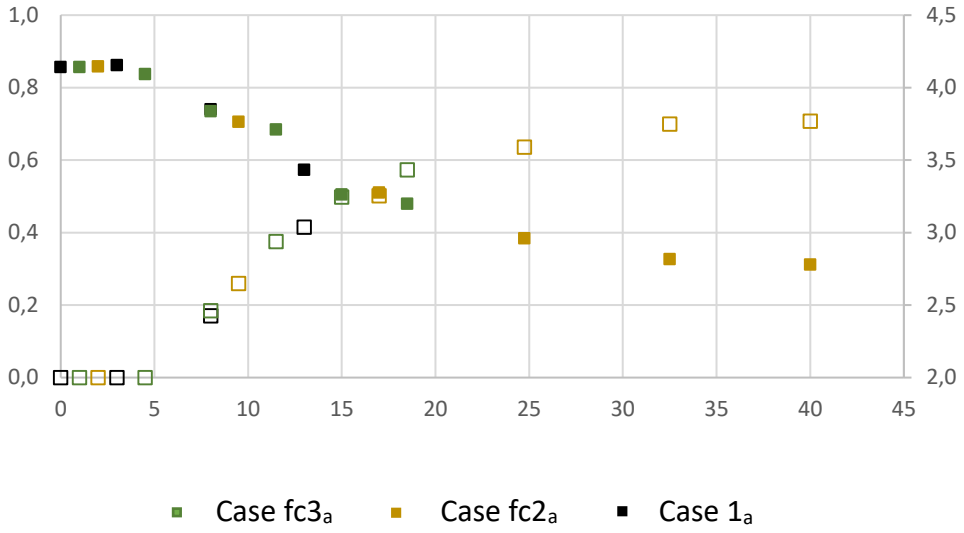

Figure 6.10. Reliability index for the considered time step as function of the elapsed time (in days from the beginning of the high-water sequence) estimated by means of probabilistic limit equilibrium analysis.

	I peak		II peak		III peak	
	Case $fc3_a$	Case $fc2_a$	Case $fc3_a$	Case $fc2_a$	Case $fc3_a$	Case $fc2_a$
μ_{SF}	1.987	1.984	1.837	1.743	1.782	1.511
σ_{SF}	0.238	0.237	0.204	0.197	0.204	0.156
β	4.142	4.146	4.093	3.764	3.836	3.275
P_f (%)	$7.21 \cdot 10^{-3}$	$7.18 \cdot 10^{-3}$	$2.86 \cdot 10^{-2}$	$7.42 \cdot 10^{-2}$	$7.00 \cdot 10^{-2}$	$1.59 \cdot 10^{-1}$

	IV peak		V peak		VI peak	
	Case $fc3_c$	Case $fc2_c$	Case $fc3_c$	Case $fc2_c$	Case $fc3_c$	Case $fc2_c$
μ_{SF}	1.696	1.636	1.574	1.291	1.466	1.286
σ_{SF}	0.187	0.215	0.198	0.103	0.146	0.103
β	3.711	2.960	3.263	2.815	3.199	2.778
P_f (%)	$1.37 \cdot 10^{-1}$	$2.42 \cdot 10^{-1}$	$1.87 \cdot 10^{-1}$	$2.70 \cdot 10^{-1}$	$2.07 \cdot 10^{-1}$	$2.85 \cdot 10^{-1}$

Table 6.2. Results of the probabilistic limit equilibrium analysis computed for the critical slip surfaces for Cases $fc2_a$ and $fc3_a$.

With regards to the third high-water event, in Figure 6.11 are plotted the values of h_d estimated in the control nodes in correspondence of the elapsed time-step, the hydrometric peaks of realistic (Case 1_c) and synthetic hydrographs (Cases $fc1_c$ and $fc2_c$). As also observed in the previous series of analysis, the results obtained using synthetic hydrographs seems to be not affected by the characteristic frequency for the sine-waves, but mainly on the elapsed-time. Furthermore, a stable condition for the progression of the phreatic line is reached still after the second hydrometric peak, for Case $fc2_c$, or even the first, for Case $fc1_c$, meaning that the hydraulic response of the riverbank has soon reached a critical condition, for the considered boundary conditions and soil parameters, for which the values of h_d in the control nodes vary in the range 0.92-0.74, from left to the right of the model. However, it can be immediately stated that this situation is far to be determined for Case 1_c, and that the use of synthetic hydrographs, regardless to the characteristic frequencies considered for the sine-waves, tends to overestimate the progression of the phreatic line in the riverbank, being the estimates of h_d always higher of about 10% to 44%, with an average of about 22% considering all control nodes and time step. This consideration can be produced by two different aspects: firstly, it has to be noticed that the realistic and synthetic hydrographs used for the third event are evidence significant differences, particularly for what concerns the first hydrometric peak; this is, in fact, characterized by a variation on the maximum reached height of about two meters in favour of the synthetic approaches (for which all the hydrometric peak are equal to the maximum value reached in the analysis). The effects of this difference tend to reduce with time, but still remaining evident both in correspondence of the maximum registered water level and at the end of the considered event (where also the registered and hydrometric hydrograph suffer a difference of about 1.3m respect to the synthetic ones). An additional aspect, however, contributing to this difference can be individuated with the limited temporal distance distinguishing the third considered event (March, 16th 2015 to April, 08th 2015) with the second considered event (February, 16th 2015 to March, 09th 2015). In this conditions, in fact, the two event are obviously not independent, as also demonstrated by the relative high values of h_d that cannot be fully attributed to the climatic conditions specific for the period (hydrometric baseline equal to 30m a.s.l. and frequent precipitation).

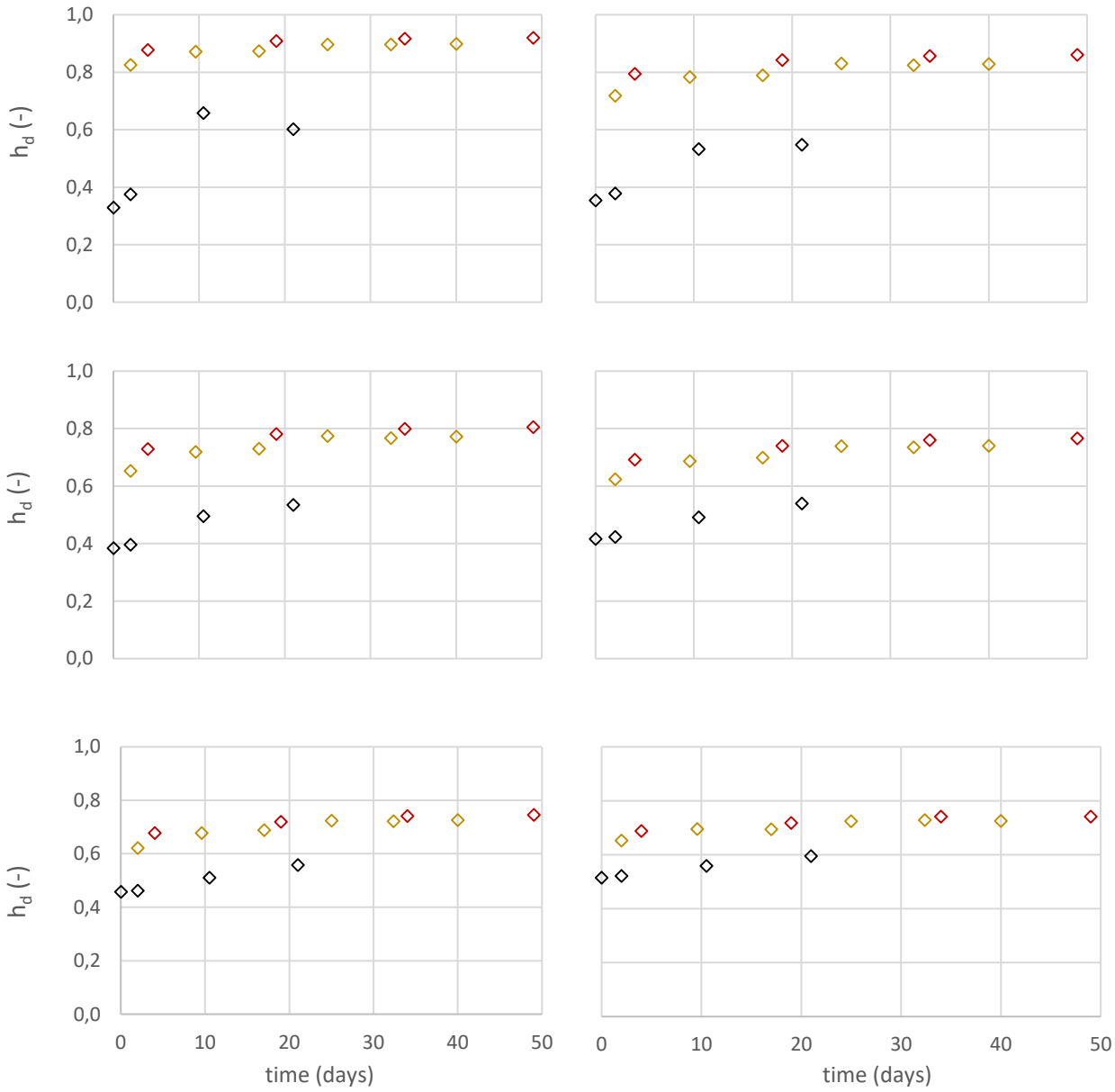

Figure 6.11. Dimensionless head of the control nodes from the unsaturated seepage analysis using realistic (Case 1_c) and synthetic (Case $fc2_c$ and $fc3_c$) hydrographs as hydraulic boundary conditions, plotted as function of the elapsed time (expressed in days from the beginning of the high-water sequence).

It follows that the synthetic hydrographs starting at the beginning of the third event could be considered as a theoretical continuation of the previous event, and through this could also be motivated the h_d values assumed in the control nodes for the subsequent hydrometric peaks, while Case 1_c hydrograph evidence a first low increment in water level which has a significantly lower effect in terms of wetting process for the riverbank and progress of the phreatic line. With these considerations, suitable comparison could be obtained from values obtained for IV hydrometric peaks on for Case $fc2_b$ (Chapter 5).

An evidence of the above described consideration can be found also in the results of probabilistic stability analysis performed in correspondence of the hydrometric peak for registered and synthetic hydrographs; in order to clarify the effect of the high-water event (Case 1_b) that anticipate the one considered here (Case 1_c), in Figure 6.12 are plotted the time-dependent values of reliability index and h_d, on average among the control nodes, with estimated for Cases 1_b, 1_c (registered event), $fc1_c$ and $fc2_c$ (synthetic event), assuming negative values in the scale of time to express occurrence of the second high-water event respect to the third one. Being, however, clear that results obtained for Cases $fc1_c$ and $fc2_c$ are significantly overconservative, respect to those obtained for Case 1_c, and considering that the stability assessment seems to reach a stable condition similarly to what may be stated from Figure 6.11, data plotted in Figure 6.12 can provide a clearer interpretation of the hydraulic response of the riverbank, and its safety characteristics, during the third event. The overall differences in terms of global safety expressed as P_f for the critical slip surfaces evidenced synthetics rather than realistic hydrographs is, here, of about one order of magnitude in correspondence of the maximum values, as showed in Table 6.3.

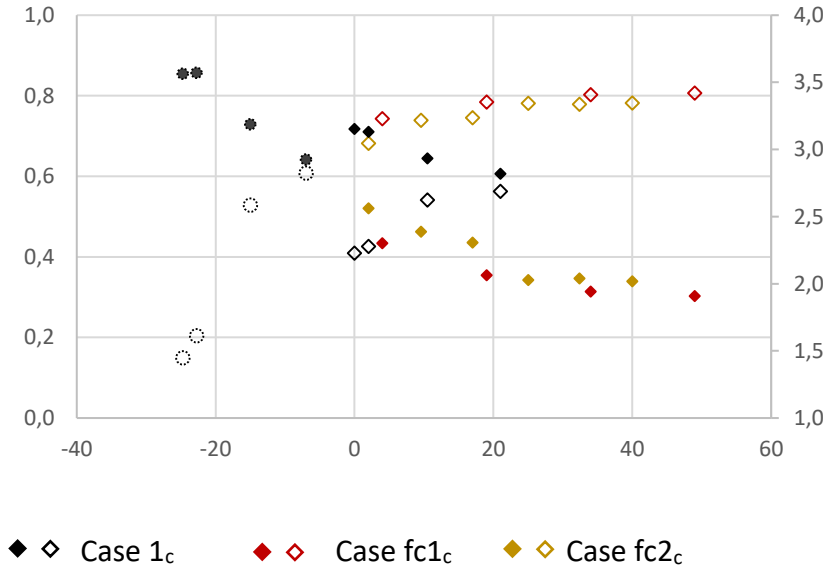

Figure 6.12. Dimensionless head of the control nodes from the unsaturated seepage analysis using realistic (Case 1_b and 1_c) and synthetic (Case $fc1_c$ and $fc2_c$) hydrographs as hydraulic boundary conditions (left axes), and reliability index (right axes) for the considered time step as function of the relative time, expressed in days from the beginning of the third high-water event.

	I peak		II peak		III peak	
	Case $fc1_c$	Case $fc2_c$	Case $fc1_c$	Case $fc2_c$	Case $fc1_c$	Case $fc2_c$
μ_{SF}	1.226	1.257	1.200	1.225	1.186	1.217
σ_{SF}	0.098	0.100	0.097	0.094	0.096	0.094
β	2.303	2.562	2.065	2.387	1.943	2.308

P_f (%)	$8.10 \cdot 10^{-1}$	$6.23 \cdot 10^{-1}$	1.620	$8.45 \cdot 10^{-1}$	2.255	1.035
	IV peak		V peak		VI peak	
	Case $fc1_c$	Case $fc2_c$	Case $fc1_c$	Case $fc2_c$	Case $fc1_c$	Case $fc2_c$
μ_{SF}	1.183	1.195	-	1.197	-	1.195
σ_{SF}	0.096	0.097	-	0.097	-	0.097
β	1.909	2.029	-	2.041	-	2.018
P_f (%)	2.440	1.780	-	1.715	-	1.825

Table 6.3. Results of the probabilistic limit equilibrium analysis computed for the critical slip surfaces for Cases $fc1_c$ and $fc2_c$.

6.5 On the influence of soil hydraulic and retention parameters on riverbank response for different flood event

In this paragraph, will be given an insight to the influence of soil hydraulic and retention parameters on seepage and safety characteristics for a riverbank under different series of high-water event, characterized by a variable time occurrence during the year. Results presented in the previous paragraph, obtained in different boundary conditions for realistic and synthetic hydrographs assuming the average values for soil hydraulic and retention parameters, are compared to those obtained using Set 2 to 5; comparison with results obtained using Set 7 can be found in Appendix. In Figure 6.13 are plotted the values of h_d computed in the control nodes for Case 1_a, using dataset 1, 2 and 3, obtained varying the *n* parameters of the van Genuchten-Mualem unsaturated model. Showed results evidence remarks and observation provided also in Chapter 5 on the influence of retention properties on riverbank hydraulic behaviour under the effect of the realistic hydrograph registered in February 2015 (Case 1_b). In fact, the phreatic progression is significantly higher for Set 3 at all considered time-step, whether values of h_d from II peak further on are comparable to those obtained in correspondence of the II peak for Case 1_b; this finding might be used to state that, being characterized by higher relative permeability, an high-water can singularly increase significantly the saturation degree of the riverbank soil, leading to a situation closer to steady-state conditions in case a second high water event would overcome, respect to scenarios estimated for Set 1 and 2. The final elapsed step could be defined as the most critical for all considered set-ups, but evidencing significant differences between them, meaning that the influence of soil retention parameters is significant for the considered Case (1_a), and this is mainly attributed to the diffused conditions of partial saturation characterizing the riverbank soil at the beginning of the considered event.

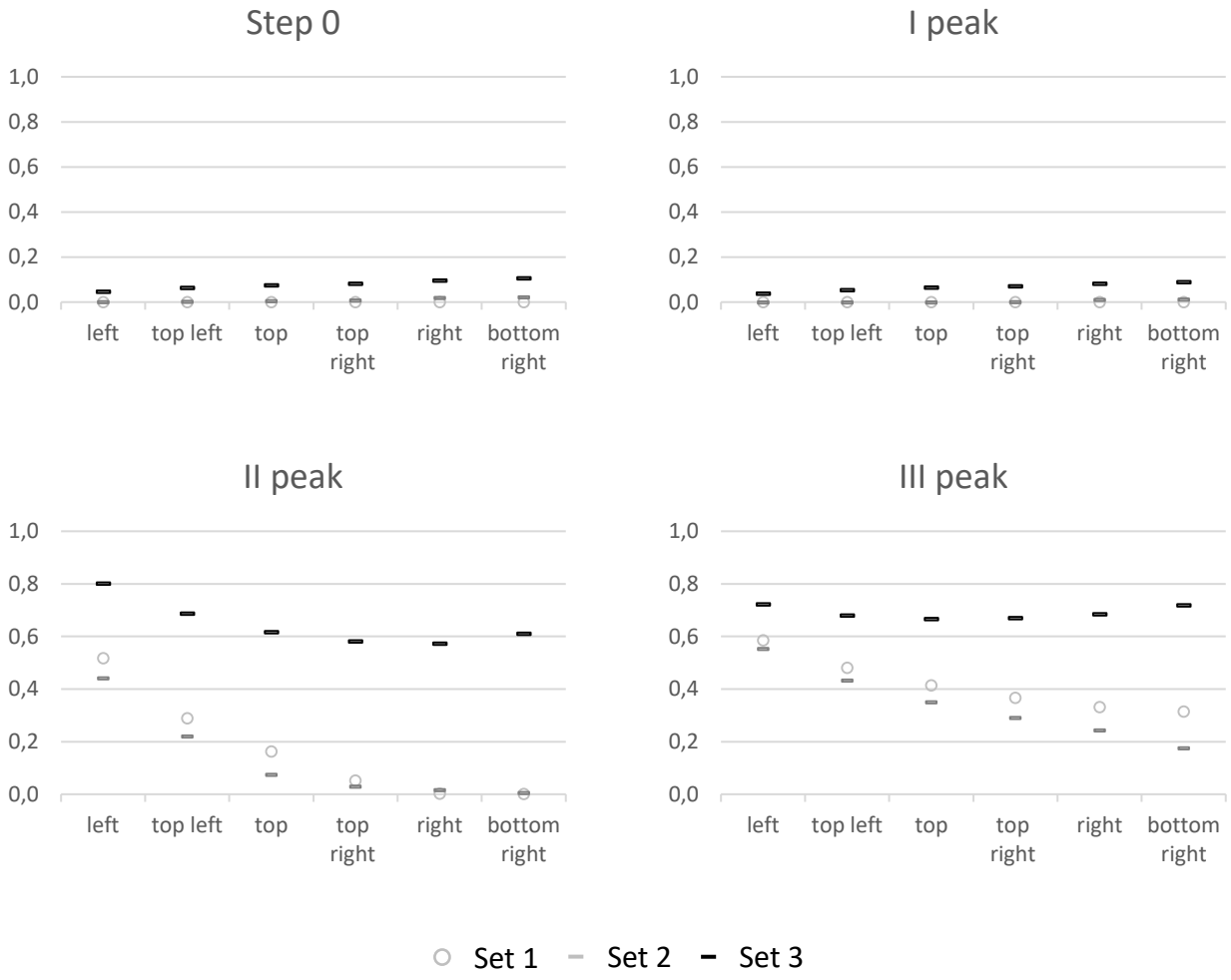

Figure 6.13. Dimensionless head of the control nodes computed using as boundary conditions the synthetic hydrograph for Case 1_a, varying the *n* parameter of the van Genuchten soil water retention curve.

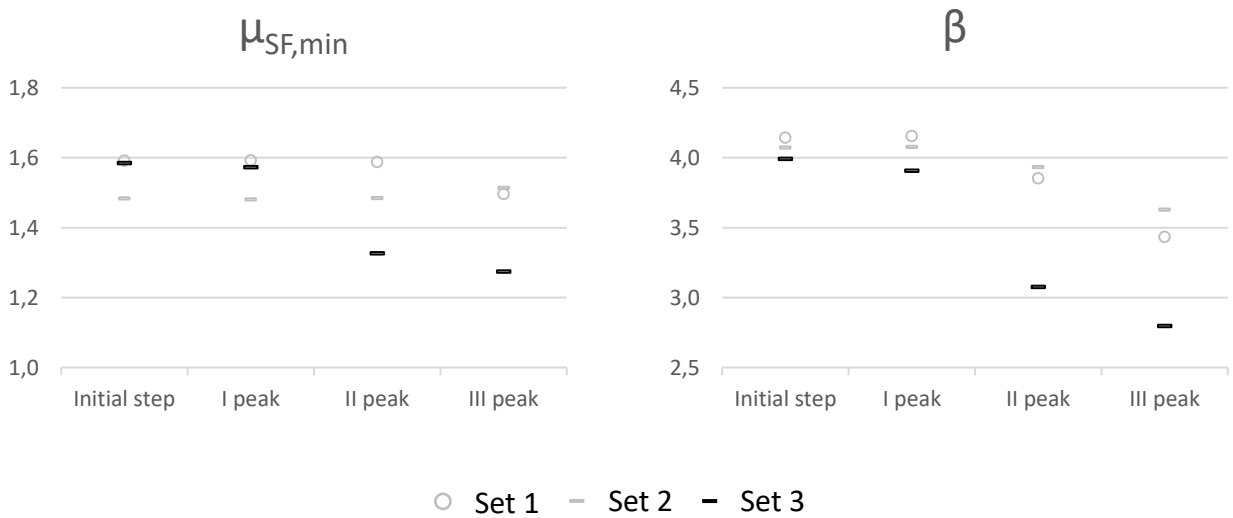

Figure 6.14. Results of the probabilistic stability analyses, by means of the minimum value of the mean of safety factor, SF, and reliability index, β, varying the *n* parameter of the van Genuchten SWRC, for Case fc2.

Probabilistic slope stability analyses have been, then, performed using pore water pressure and suction distribution computed in the elapsed time step; results obtained in terms of reliability index and minimum average value of safety factor distribution estimated using Monte Carlo method (100.000 trials) are plotted in Figure 6.14, proving that the scenario determined using Set 3 is the most critical for riverbank safety assessment, for the overall event. Showed results also evidence the lower variability in stability conditions using Set 2, mainly depending on a minor influence of the boundary conditions on the pore water pressure and suction distribution in the riverbank. Furthermore, the lower values of $\mu_{SF,min}$ resulting using Set 2, up to the second hydrometric peak, result on the minor influence of unsaturated soil strength, lower for equal suction values respect to soil dataset 1 and 3 considering the adopted strength failure criterion, which is both dependent on suction values and saturation degree. This finding cannot be extended to the values of reliability index computed in the same elapsed step, being associated to a different critical slip surfaces respect to the slip surface to whom are referred the values of μ_{SF} for the initial step and the first hydrometric peak, insisting for a significant part on the Foundation soil, which is characterized by a higher variation of the strength properties distribution. In Figure 6.15 and 6.16 are plotted the results evaluated at the various time-step from seepage and stability analysis, obtained using Set 1, 4 and 5 (meaning that the α parameter of the van Genuchten soil water retention curve has been varied). It can be seen that up to the third time-step, results do not show significant variation with time, being the influence of the first hydrometric peak negligible in terms of h_d and safety assessment. Subsequently sensible increase in the phreatic progression could be evidenced, with small differences among the various analysis; however, stability results do not tend to diverge, mainly because the difference in μ_{SF} and β values are due influence of α parameter on strength properties, rather than on the seepage process. Of relative interest are the results obtained on Case 1_c varying the soil unsaturated properties, which produces variations significantly smaller to those observed for Cases 1_a and 1_b, reported in Appendix. However, an overall remark could be to consider Set 3 and Set 5 the most critical among the ones considered for comparisons, as still demonstrated for the Case 1_a.

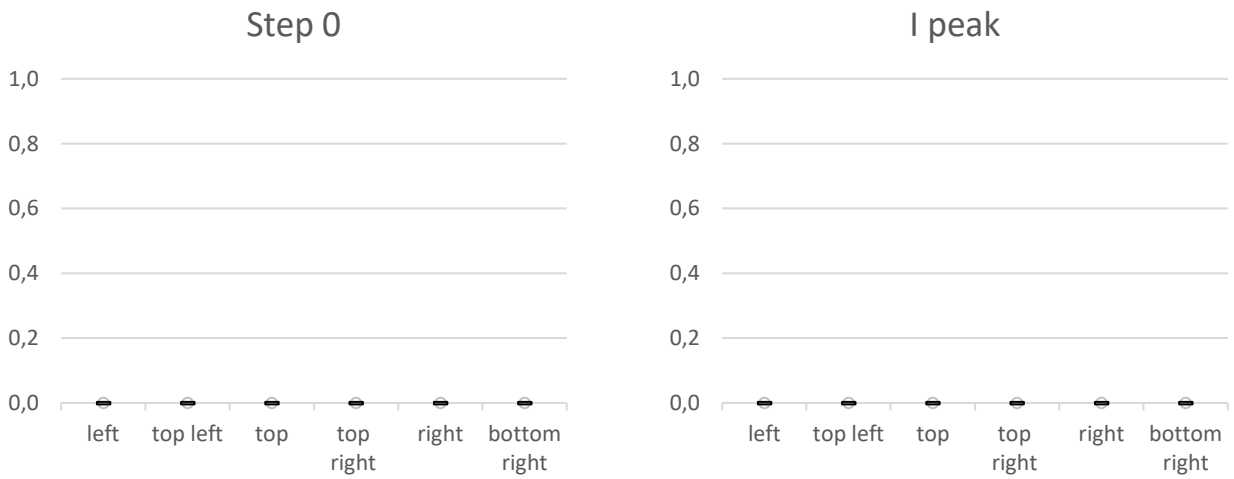

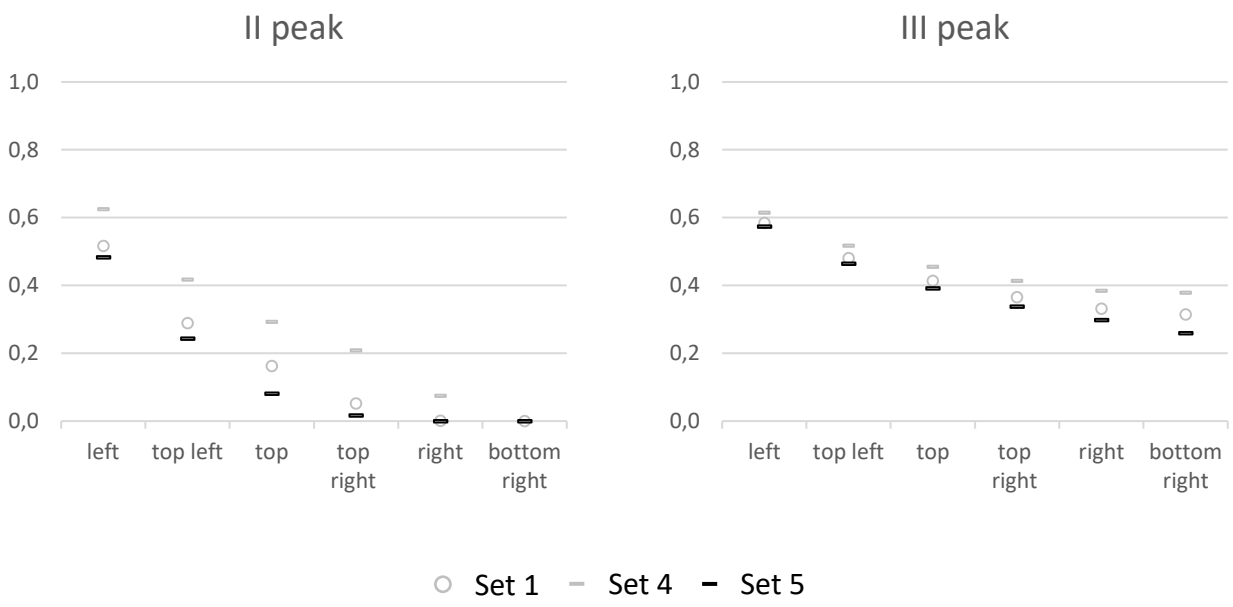

Figure 6.15. Dimensionless head of the control nodes computed using as boundary conditions the synthetic hydrograph for Case 1_a, varying the α parameter of the van Genuchten soil water retention curve.

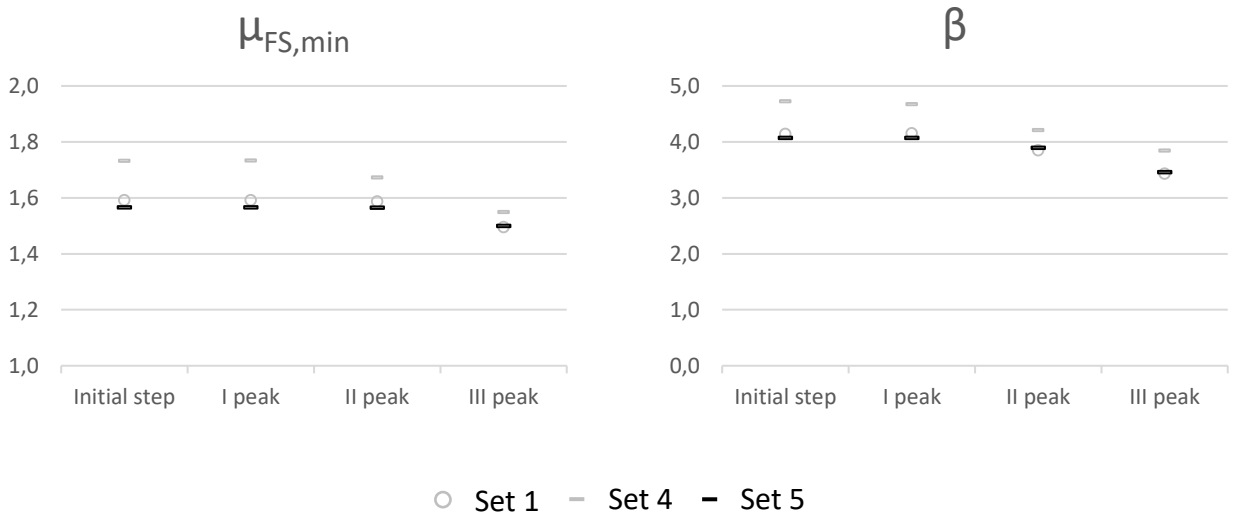

Figure 6.16. Results of the probabilistic stability analyses, by means of the minimum value of the mean of safety factor, SF, and reliability index, β, varying the α parameter of the van Genuchten SWRC, for Case fc2.

Aiming to study and, then, to compare the most critical configurations for the riverbank stability, three series of transient thermos-coupled seepage analysis have been performed using synthetic hydrographs consistent with the considered events (paragraph 6.1), assuming hydraulic and retention parameters defined dataset 1, 3 and 5. Pore water pressure and suction distribution computed in correspondence of the hydrometric peak of the various hydrographs (recorded and synthetics) have been, then used to perform probabilistic limit equilibrium analysis; results in terms of the most critical reliability index obtained from each analysis (conducted by means of 100.000 trials of the Monte Carlo method) have been plotted in Figure 6.17 in

function of the elapsed time from the beginning of the high-water event. It is relevant to notice that the riverbank safety assessment follow three different trends in case soil evidence a relative permeability consistent with Set 1 and 5, for the considered suction operative range; this behaviour tends to be less relevant in correspondence high-water events characterized by a duration higher than 30 days; after this period, the overall stability conditions seems to be leaded by the height of the hydrometric peak affecting the water retaining structure. The role of the occurrence of the high-water event during the year is, however, still relevant, being the lower values of reliability index always determined in correspondence of the analysis performed for the period March-April 2015. A significant remark is provided comparing results obtained using Set 3 for hydraulic and retention parameters. For this set of analyses, stability conditions assessment for the riverbank provide similar outcomes, for the first and the second events, in terms of reliability index values and their time variability, particularly considering high-water sequences lasting for more than 10 days (determined by different consideration on wave length and persistence). After that, reliability index tends to gradually reduces up to a critical value, which would be primary dependent on the height of the water peaks. This condition seems to be achieved still at the first hydrometric peak of the synthetic hydrographs associated with Case 1_c, which provide a strong margin of safety respect to the use of registered one. Critical conditions seem to be reached, however, for all considered set of analyses, showing the minor effect of retention parameters when the phreatic line progression reach a maximum stable height.

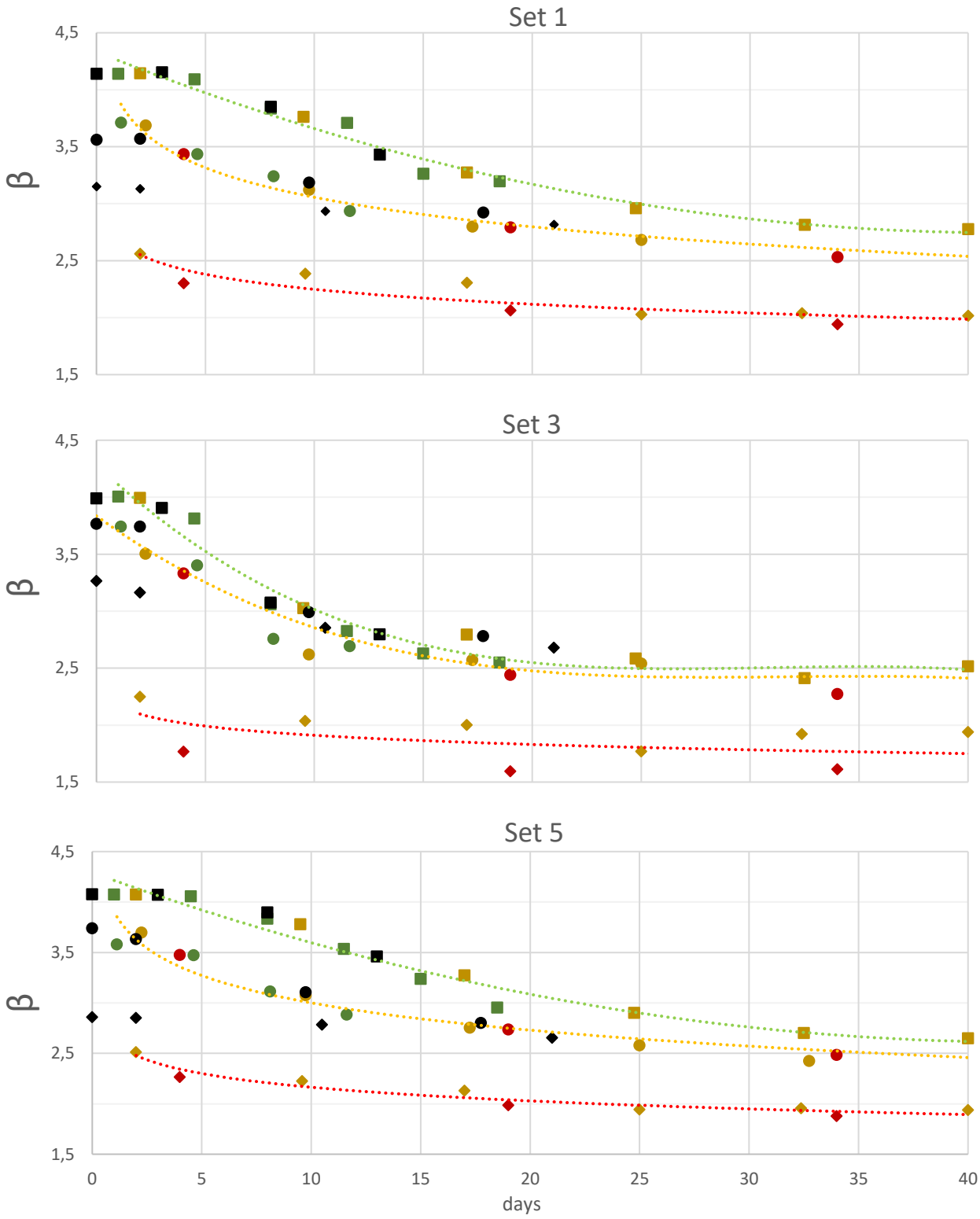

Figure 6.17. Reliability index computed in correspondence of the hydrometric peaks for the various hydrographs (registered and synthetics) plotted as function of the elapsed time expressed in days from the beginning of the high-water sequence; squared-dots and green trendline represent event *c* related analysis; circled-dots and orange trendline represent event *b* related analysis; rhombus-dots and red trendline represent event *a* related analysis.

6.6 On the extended use of simplified approaches for the definition for the assessment of river embankment stability

In this section, results and remarks obtained from the use simplified approaches for the definition of seepage and stability characteristics will be presented and discussed; the definition of initial and boundary conditions to be used in transient flow and limit equilibrium analysis refer to the methodology discussed in Chapter 5, and will be hereafter briefly described. Special attention will be, instead, given to the comparison between the application of the proposed approach to events occurred in different time along the wet season, referred as Case a, b and c in the previous sections. Two different level of approximation will be used for the riverbank stability assessment, characterized by different level of approximation, amount of information and computational efforts required for numerical calculation. In particular, the first level of approximation, referred as Simplified Approach 1, consist in the definition of the initial conditions in terms of pore water pressure and suction distribution, mainly dependent on a hydrometric baseline height and maximum suction values for the riverbank, to be used for transient thermo-coupled seepage analysis; in correspondence of specific time-step, probabilistic limit equilibrium analyses are, then, performed for the safety assessment. The second level of approximation consist in the complete definition pore water pressure and suction distribution for the riverbank to be used for stability analysis, which has been possible using observation and remarks obtained from the large amounts of results obtained from Cases 1, and $fc_{1...3}$ for different time series. Similarly to the scheme of Chapter 5, the following cases have been considered:

- Case $1_{a...c}$: Initial conditions determined considering the period July, 15th 2013 to July, 14th 2014 for the model spin-up; recorded hydrograph, using hydrometric data collected in Ponte Bacchello, assumed as boundary conditions for the model. Probabilistic limit equilibrium analyses have been performed using pore water pressure and suction distribution evaluated in correspondence of the various hydrometric peaks;
- Case $fc1...3_{a...c}$: Initial conditions determined similarly to Case 1. Synthetic hydrograph has been used as boundary condition, described by a series of sine-waves considering different period (*fc1…3*) and amplitude variable with the considered event, superposed to a hydrometric baseline represented by the monthly average value of the TMA 241-width in absence of high-water event. Probabilistic limit equilibrium analyses have been performed using pore water pressure and suction distribution evaluated in correspondence of the various hydrometric;
- Simplified Approach $1_{a...c}$: Initial conditions directly assigned to the model (Fig. 6.18). Boundary conditions and time step considered are equivalent to Case $fc2_{a...c}$;
- Simplified Approach $2_{a...c}$: Limit equilibrium analysis have been performed using pore water pressure and suction distributions directly assigned to the model (Fig. 6.18 and 6.19), on the basis of

observation and remarks from transient seepage analysis performed for Cases fc1…3$_{a…c}$, as described in previous sections;

- Case 3: Pore water pressure distribution to be used in limit equilibrium analysis has been determined by steady-state seepage analysis in equilibrium with the maximum hydrometric level measured for each Cases, and hydrostatic suction distribution above the phreatic line.

Theoretical procedures used for defining spatial pore water pressure and suction distributions for Simplified Approach 1 and 2 have been presented in Chapter 5, and will be hereafter briefly described with reference to Case a and c. Initial conditions used for S.A.1 have been obtained on the base of the height hydrometric baselines considered for the two event, equal to 27.5m in November 2014 and 30.0m in March 2015. Hydrostatic pore water pressure distribution has been assumed beneath the phreatic line; above the phreatic line suction increment have been considered with the aim to replicate results obtained from seepage analysis for Cases 1$_a$ and 1$_c$; minimum pressure head values are assumed to be equal to -2m and -1.5m for S.A.1$_a$ and S.A.1$_c$, respectively. Pore water pressure and suction distributions used as initial conditions for S.A.1$_a$ and S.A.1$_c$ analysis are plotted in Figure 6.18 and 6.19. Input points used to define the solutions to Krigged surfaces are highlighted in blue circled dots; maximum (absolute) values of soil suction points are evidenced by red square dots. Increment between two adjacent isolines is 0.5m, and colour shading starts from the minimum values of suction. Aiming to define pore water pressure and suction distribution used for S.A.2$_{fc1…3,a…c}$, results obtained from seepage analysis performed using both synthetic and real hydrographs have been considered; two main features have been taken into account, that are the height of the phreatic line in the control nodes, express as a percentage of piezometric head computed in steady-state conditions, and the maximum (absolute) values for soil suction.

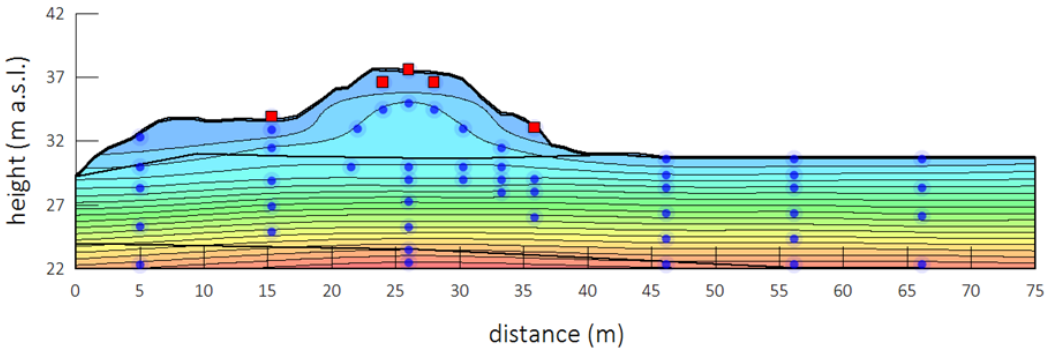

Figure 6.18. Pressure head distribution used as initial conditions for transient seepage analysis, referred to S.A.1$_a$.

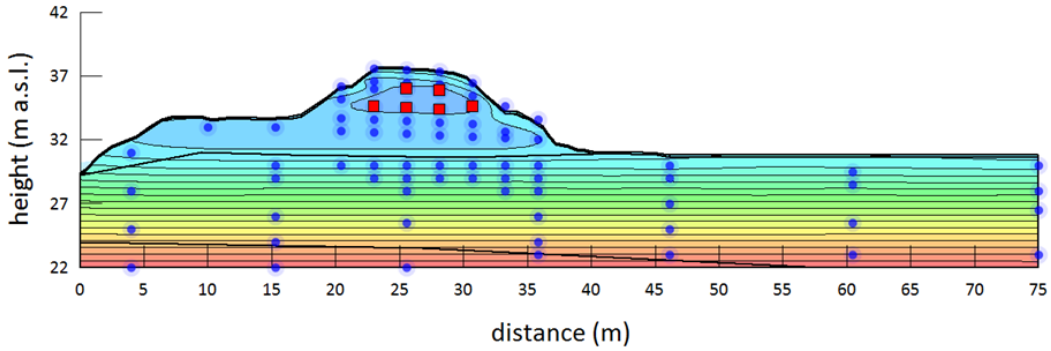

Figure 6.19. Pressure head distribution used as initial conditions for transient seepage analysis, referred to S.A.1_c.

In Figure 6.20 is showed the spatial functions used for limit equilibrium analysis for S.A.$2_{fc3,a}$, representing the fourth hydrometric peak for Case $fc3_a$, which main features are the minimum pressure head, equal to -1.5m in correspondence of the red squared dots, and piezometric head for the control nodes corresponding to 0.85-0.8 h_d; similarly, in Figure 6.21 are showed the values for pressure head defined for S.A.$2_{fc1,c}$, representing the second hydrometric peak for Case $fc1_c$, characterized by a maximum (absolute) value for soil suction equal to -1.5m (in correspondence of the red squared dots) and h_d in the control nodes equal to 0.9-0.8.

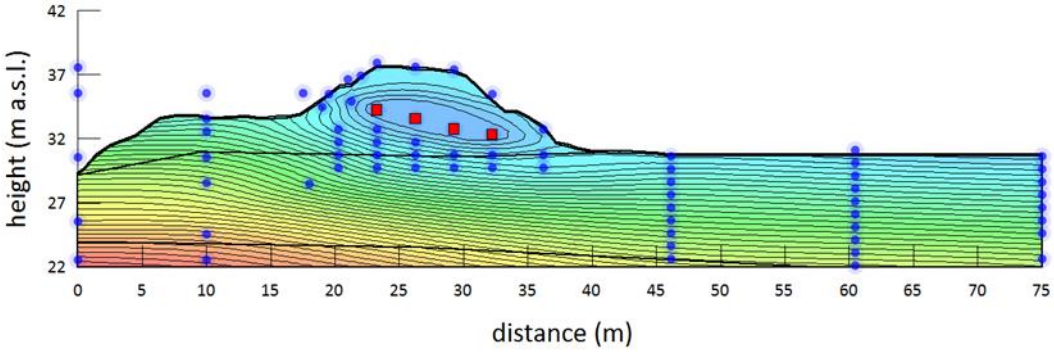

Figure 6.20. Pressure head distribution for the riverbank numerical model in S.A.$2_{fc3,a}$.

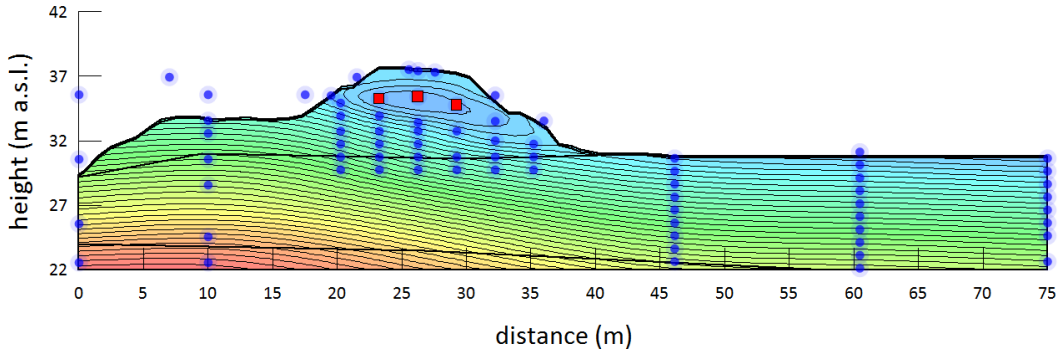

Figure 6.21. Pressure head distribution for the riverbank numerical model in S.A.$2_{fc1,c}$.

In the following, results presented obtained using Set 1 for soil parameters are present, being previously discussed the effect of hydraulic and retention properties on seepage and stability characteristic for the riverbank. In Figure 6.22 are plotted the results obtained from probabilistic limit equilibrium analysis performed for all above cited Cases, considering for the event a) sine-wave characteristic frequencies equal to *fc2* and *fc3*, and for the event c) sine-wave characteristic frequencies equal to *fc2* and *fc3*. Generally, a suitable agreement is obtained using S.A.1, whose stability assessment always stands on the safe side for all considered events; this remarks could, then, be fully extended to S.A.2, for which the margins of safety are in all cases higher even than those computed for Case 1, confirming the possibilities to properly represent the stability conditions of river embankments by simplified conditions, however without considering steady-state assumptions (Case 3), which always provide largely over-conservative margins of safety. Finally, in Figure 6.23 are provided the results of probabilistic limit equilibrium analysis obtained for all realistic and synthetic cases considered in this Chapter, plotted in order to better visualize the possibility of the proposed approach to stand on the safe side for riverbank stability assessment, getting a more reliable estimation for high reliability index (lower probability of failure), e.g. Series c (from March, 16th 2015 to April, 08th 2015) and resulting more conservative for low reliability index (higher probability of failure), e.g. Series a (from November, 04th 2014 to November, 15th 2014).

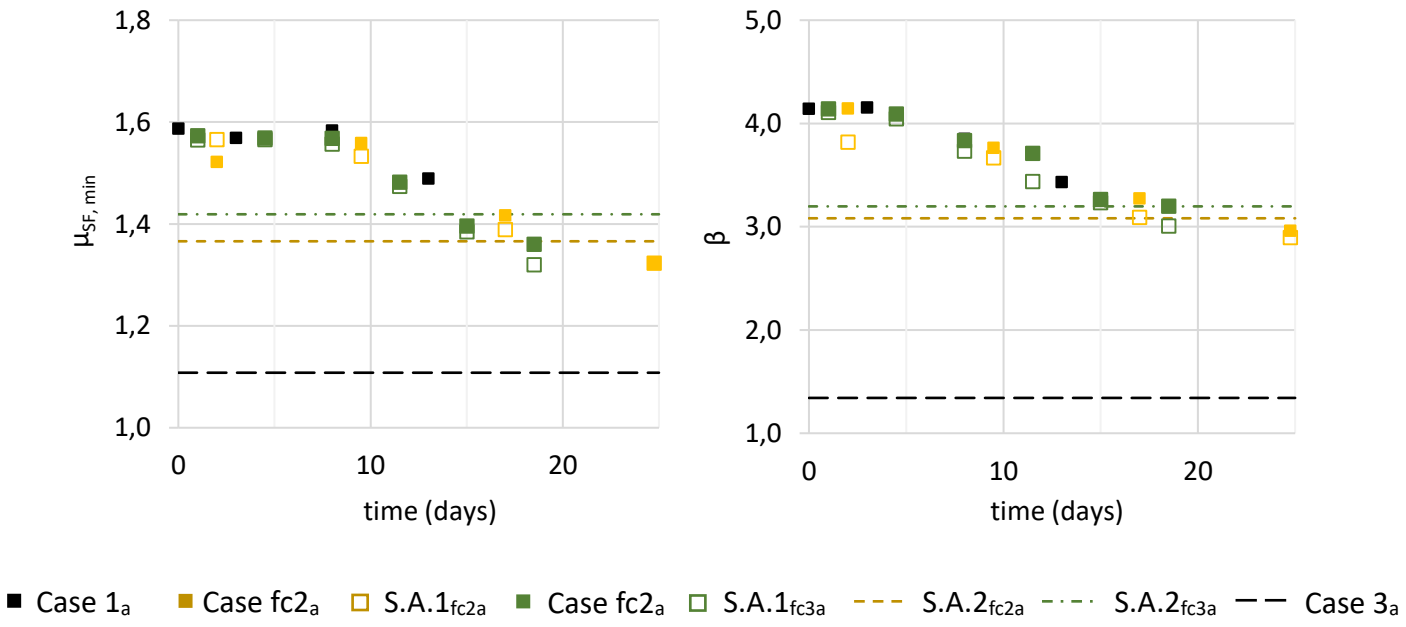

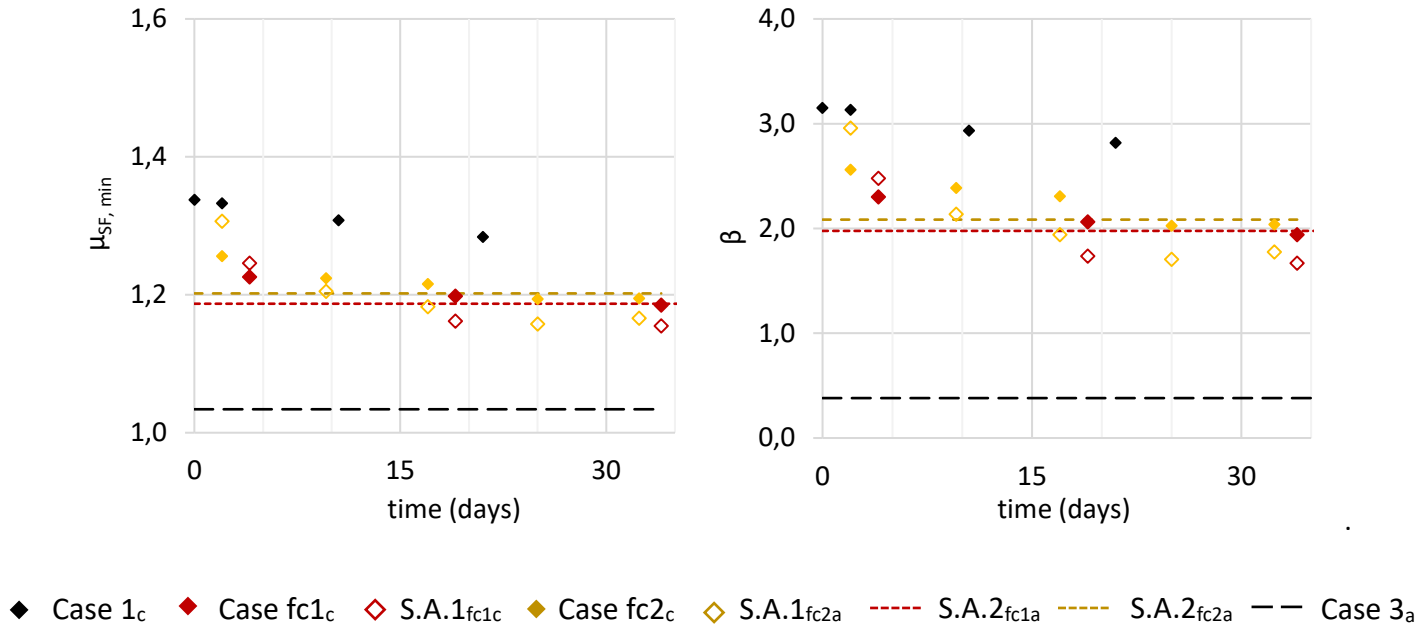

Figure 6.22. Results of the probabilistic stability analyses, by means of the minimum value for mean safety factor, SF, and reliability index, β, for dataset 1.

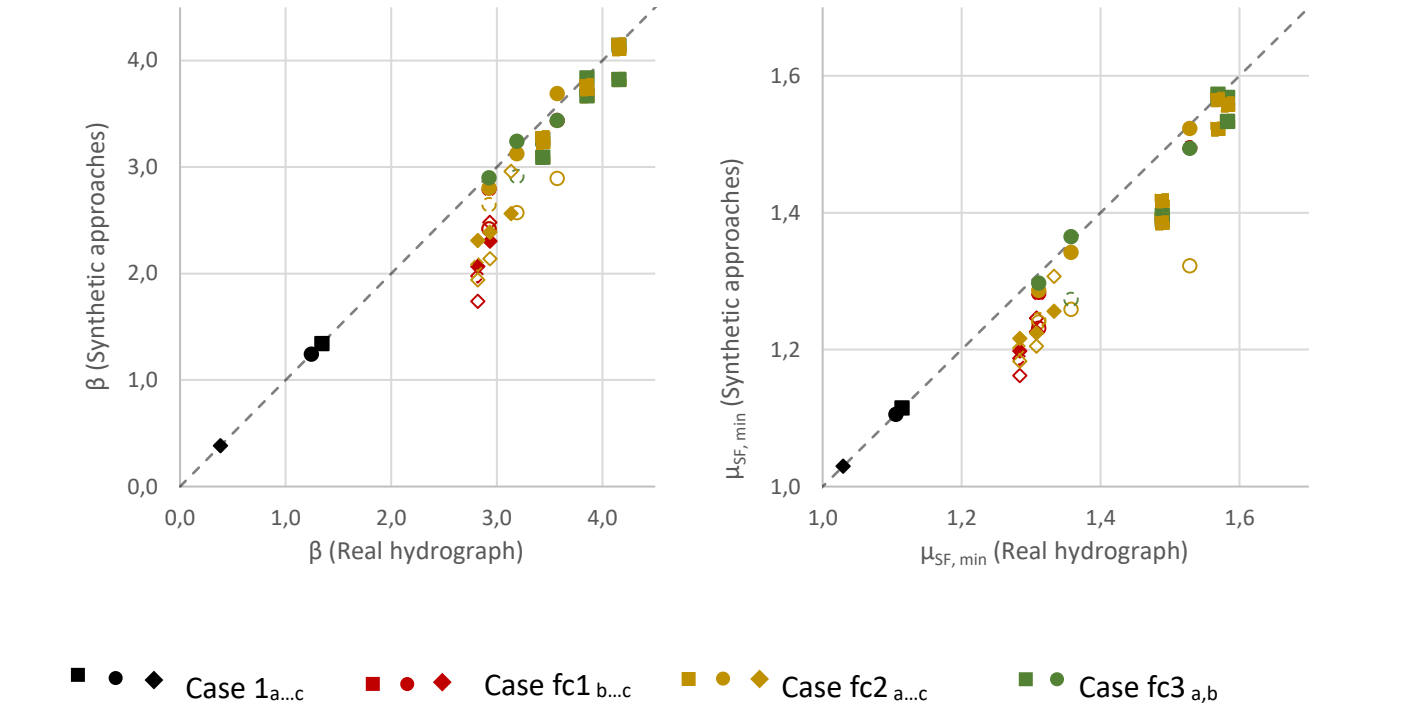

Figure 6.23. Results of the probabilistic stability analyses, by means of the minimum value for mean safety factor, SF, and reliability index, β, for dataset 1 computed using realistic and synthetic approaches.

7 On the combined effect of hydraulic, retention and strength soil parameters variability in riverbank safety assessment: from seepage to stability analysis

As all earthen structures, riverbank's material evidence heterogeneity referred to mechanical and hydraulic properties that cannot be disregarded when accurate safety assessment is required. Analysis and results presented in the previous sections evidence that hydraulic and retention soil parameters have a strong influence on the stability evaluation of riverbanks, both for their direct effect on seepage characteristics and strength properties; furthermore, estimation for this issue and methodology for simplified to more accurate safety assessment have been. However, is still required for the present study the discussion on the use of a comprehensive methodology for probabilistic seepage analysis. Although the use of probabilistic methods in combination with slope stability analysis is currently diffused both in ordinary practice and research applications, accounting for soil heterogeneity and uncertainty towards hydraulic and retention parameters in seepage analysis would generally require a large amount of numerical simulation and accurate knowledge for soil properties. In fact, properly accounting for this source of uncertainty in safety assessment is still a demanding task for standard and advanced applications in civil engineering and risk management towards embankment failure. Solution to this problem could be represented by the use of uncertainty propagation methods, which allows propagating the errors from input data to final result.

Among the various methods proposed and used for geotechnical application, the Point Estimate Method have found large application, both in combination with LEM and FEM programs, as valid and consistent alternative to more accurate methods as Monte Carlo Method, which proper and reliable practice is often time-consuming and highly-computing demanding. Specific details on features and remarks for the PEM are discussed in Chapter 2 and in the wide literature references available and suggested. In this section, a topical study on the combined effect of hydraulic, retention and strength soil parameters variability in riverbank safety assessment have been performed. For the application of PEM, a series of transient thermo-coupled seepage analysis have been performed using main hydraulic and retention parameters as standard variable; consequently, stability analyses have been performed by means of limit equilibrium method, considering riverbank and foundation soil strength parameters variable as well. In addition, probabilistic stability analysis performed on the base of deterministic seepage analysis have been performed using MC method, assuming for various cases pore-water pressure distribution as variables for the limit equilibrium analysis; comparison between results obtained with the various application of methods for safety assessment are hereafter presented and discussed.

7.1 Methodologies and applications

In Chapter 5, the effect of variability of soil hydraulic and retention properties on seepage and stability results have been investigated by means of numerical analysis using different dataset, obtained singularly varying each of the topical properties, operating suddenly a sensitivity study under different hydrometric time-dependent conditions. This procedure, however, lead only a partial examination of the problem, which have been studied performing separated deterministic seepage analysis and consistently accounting only for soils mechanical parameters variability.

To properly consider the combined effect of hydraulic and retention soil parameters variability into the safety assessment of riverbank towards collapse mechanism, it is so required to determine a pore-water pressure distribution whose variability should be significant for the problem and directly used for stability analysis. To this purpose, two probabilistic methods have been here adopted: the first consists in the Point Estimate Method, a statistical procedure applicable when low number of observation are required (see Chapter 2); this could necessarily be the case of seepage analysis for extended time-period, for which a strong limitation is given by the computational efforts required for each estimation. The method, as implemented for the purpose of the present Thesis, allows to estimate the low-order statistical moments (here focusing on mean and variance) for results defined by the unique existence of solutions to mathematical problems. This means that both hydraulic and safety outputs could be intended as probabilistic terms, obtained by series of deterministic seepage and stability analyses once the probability distribution functions for input parameters are assigned. The second method used for probabilistic analysis is the Monte Carlo Method, which basically allows for the determination of low-order statistical moments of the safety factor distribution, defined by routine analysis for which the input parameters are defined on the base of the assumed sampling functions; this method, as discussed in Chapter 2, requires a large amount of trials (50.000 to 100.000 have been considered for LE analysis in this study) to obtain reliable results in terms of probability of failure. For this reason, and considering how the method is implemented in numerical codes used in the present Thesis (see Chapter 2), Monte Carlo Simulations appears as an unfeasible procedure to directly consider for the models the variability of hydraulic and retention parameters in seepage analysis.

However, a possible application for the MCM allows to assume pore water pressure and suction values as probabilistic parameters for stability analysis. In this way, the seepage analysis results are, for each trial, adjusted by an offset value defined by a sampling and distribution functions, constant for each runout analysis; this opportunity has been explored to indirectly consider the variability of hydraulic and retention parameters on safety assessment. Comparison between results obtained from the application of the two Methods, considering various procedure, are presented in this Chapter, focusing on features and relative benefits obtained by their application to various cases.

7.2 Application of PEM for the probabilistic seepage assessment of riverbank

The event considered for the probabilistic seepage study is the high-water sequences occurred from February, 16th 2015 to March, 09th 2015; deterministic seepage analyses for this event have been previously described and results discussed in different part of Chapter 4 to 6, referred as Case $1_{(b)}$. Point Estimate Method have been here used to perform a fully comprehensive study for probabilistic behaviour of both hydraulic and stability response of the riverbank.

For probabilistic seepage analyses, two-dimensional FEM code VADOSE/W have been used, computing transient coupled hydro-thermal flow; both climatic and hydrometric data collected in the neighbourhood of the studied section have been used as boundary conditions.

A crucial point is, however, a proper definition of initial conditions to be assigned to various analyses; in fact, being each estimate of PEM specific for a univocal set of hydraulic and retention parameters, it is arguable the use of a solely pore water pressure distribution to be generally assigned as initial conditions. Nevertheless, performing an extended spin-up of the model for each combination, as done in Chapter 5 for Set 1 to 9, would reduce one of the main advantage in using PEM for Geotechnical studies, which is finally to be computationally less onerous than other probabilistic procedures. In order to overcome this issue, initial pore water pressure distribution have been assigned coherently to Simplified Approaches 1 (Chapter 5 and 6), with the aim to realistically simulate suction distribution typical for a bank in a wet period, individuating a central bank core with lower suction values, approaching zero values at surface correspondence. This hypothesis, however coherent with results obtained from various deterministic seepage analysis discussed in previous Chapter, has been considered generally acceptable by several authors (e.g. Casagli et al., 1999; Rinaldi et al., 2004; Calabresi et al., 2013, Sleep et al., 2013) and, in absence of specific site measurements, has been considered here adequate. With the aim to provide suitable resolutions for different constrains of computational and times efforts, the use of two different hypotheses for initial conditions have been tested for probabilistic seepage analysis:

- in a first application, each seepage analyses have been performed using hydrometric and climatic conditions registered from November, 04th 2014 to March, 09th 2015, considering pore water pressure and suction distribution defined for $S.A.1_a$ as initial conditions (Figure 6.18);
- in a second application, each seepage analyses have been performed using hydrometric and climatic conditions registered from February, 16th 2015 to March, 09th 2015, considering pore water pressure and suction distribution defined for $S.A.1_b$ as initial conditions (Figure 5.17).

The first application of Point Estimate Method, hereafter named as PE-I, is conceived to obtain a pertinent model spin-up for each seepage analysis, determining variable initial conditions for the high water event occurred from February, 16th 2015 to March, 09th 2015. By this, the initial conditions determined for the

probabilistic study are dependent on the set of hydraulic and retention parameters assumed; consequently, the effect of variability of unsaturated soil hydraulic parameters in assessing the riverbank seepage and stability characteristic is fully accounted. In the second application of Point Estimate Method, referred as PE-II, the initial conditions, equal for all seepage analysis, are referred to the hypothesis formerly used for $S.A.1_{fc2}$. In general, the application of PE-I should represent a more accurate and reliable approach, whilst PE-II guarantee minor computational efforts. For both procedure, implemented by using GeoCmd routine (Geo-Slope International Ltd, 2008), a series of 16 complete transient coupled hydro-thermal flow analysis have been performed, considering as standard variable the following hydraulic parameters: θ_{sat}, n, α and k_{sat}. The statistical characterization of unsaturated hydraulic parameters was carried out on the basis of laboratory tests results, in terms of mean values, standard deviation, skewness and correlation structure. For sediments of soil Foundation and Subsoil, only an estimate of hydraulic conductivity at saturation was provided. Mean values of the hydraulic properties mentioned above are listed in Table 5.1, whilst Table 7.1 shows the additional statistical moments obtained for soil Unit A. The parameter m_{VG} is omitted since it depends on n_{VG}. The correlation matrix of hydraulic parameters of Unit A is presented in Table 7.2. For comparison, deterministic seepage analyses assuming average values for hydraulic and retention parameters are then presented and discussed. Showed values are derived from statistical study performed in Gottardi et al. (2016), in which a topical research have been performed for accounting for the intrinsic variability of unsaturated soil hydraulic parameters in assessing the probability of river bank failure.

	$1/\alpha$	n	θ_{sat}	$Log_{10}k$ (m/s)
	(kPa^{-1})	(-)	(-)	Log_{10}(m/s)
Standard deviation (σ)	0.064	0.154	0.041	0.776
Skewness (v)	0.824	0.016	0.026	-0.632

Table 7.1 Standard deviation and skewness of hydraulic and retention properties of river embankment soil.

	$1/\alpha$	n	θ_{sat}	$Log_{10}k$ (m/s)
	(kPa^{-1})	(-)	(m^3/m^3)	Log_{10}(m/s)
$1/\alpha$	1	-.17	.28	.40
n	-	1	.68	.24

θ_{sat}	-	-	1	.76
$Log_{10}k$ (m/s)	-	-	-	1

Table 7.2 Correlation matrix of hydraulic and retention properties of river embankment soil.

7.2.1 Probabilistic seepage analysis: result and discussion

A series of 16 hydro-thermal seepage analysis have been performed for the two considered application of the PEM. In processing data, skewness of the distribution of soil retention and hydraulic parameters have been considered; for each random variable (θ_{sat}, *n*, α and k_{sat}) two point estimate locations, X+ and X-, with the associated weights, P+ and P-, have been evaluated, as shown in Table 7.3.

	1/α	n	θ_{sat}	$Log_{10}k$ (m/s)	ϕ_R'	ϕ'_F
	(kPa^{-1})	(-)	(m^3/m^3)	Log_{10}(m/s)	(°)	(°)
Mean	0.163	1.328	0.395	-5.804	32.00	28.80
X+	0.204	1.483	0.437	-5.237	33.94	32.00
X-	0.071	1.175	0.355	-6.866	30.06	25.60
P+	0.69	0.50	0.49	0.65	0.50	0.50
P-	0.31	0.50	0.51	0.35	0.50	0.50

Table 7.3. Point estimate locations and relative weights of random variables

7.2.1.1 Point estimations with normal distribution

In Figure 7.1 values of h_d in the control nodes (which definition has been introduced in Chapter 5), both for deterministic and probabilistic analysis, are plotted; results refer to the procedure described as PE-I. As shown, the use of probabilistic seepage allows to individuate a range of variation for all types of solution; in particular, the values for $\mu \pm \sigma$ are displayed in Figure 7.1, representing some possible boundaries for the most probable outcomes. Being the solution fully characterized, as hypothesis, by a normal distribution, the range boundaries are symmetric respect the mean values. By comparing probabilistic and deterministic outcomes, it can be noticed that results obtained using the average values for hydraulic and retention parameters are generally included in the range of main variation identified by the use of PEM. Discrepancies between

deterministic and average values for h_d could, however, be expected, being the seepage problem in relation to soil hydraulic and retention parameter variability characterized by a highly nonlinear response.

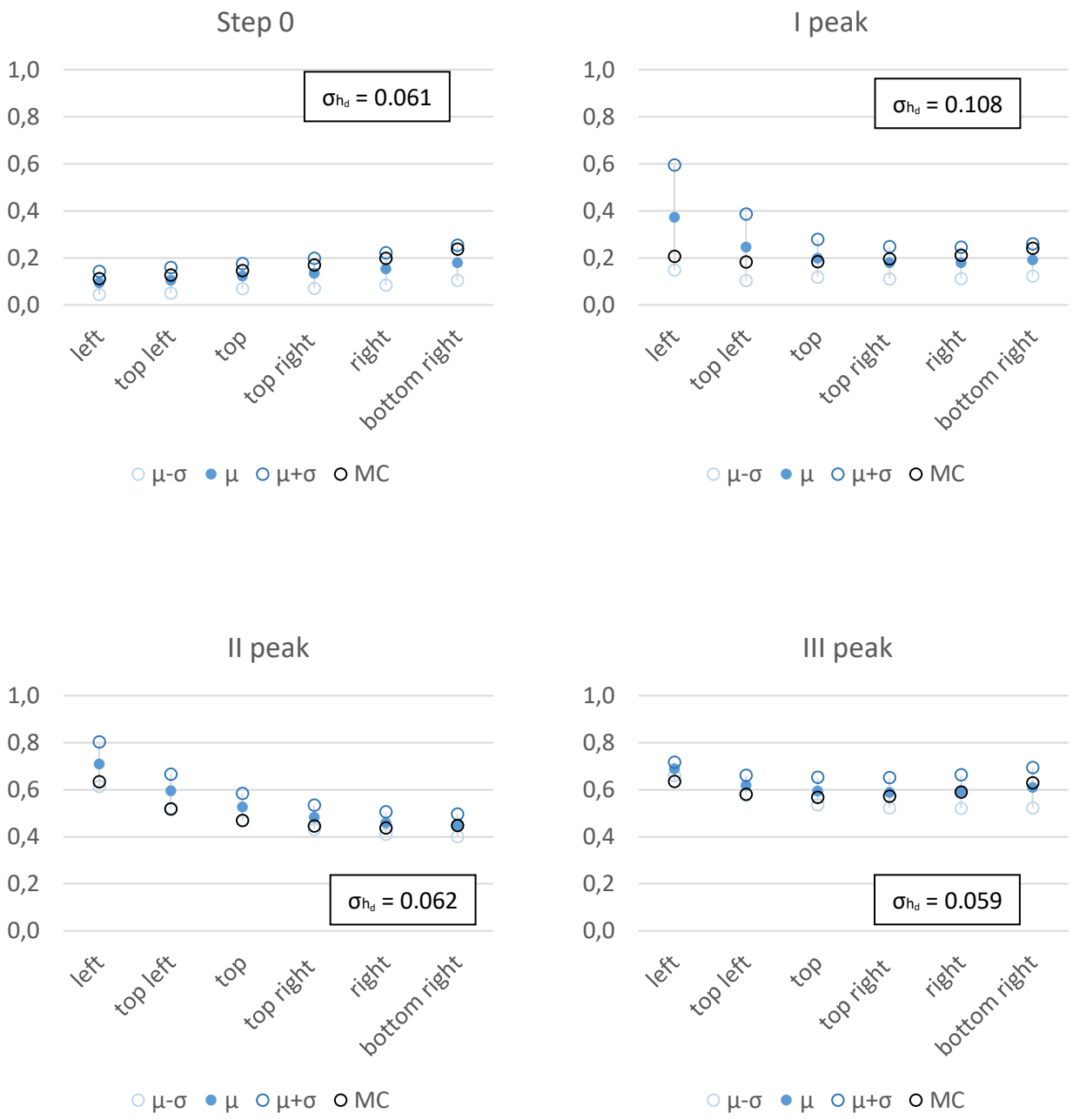

Figure 7.1. Dimensionless head of the control nodes computed both for deterministic and probabilistic (PE-I) seepage analysis.

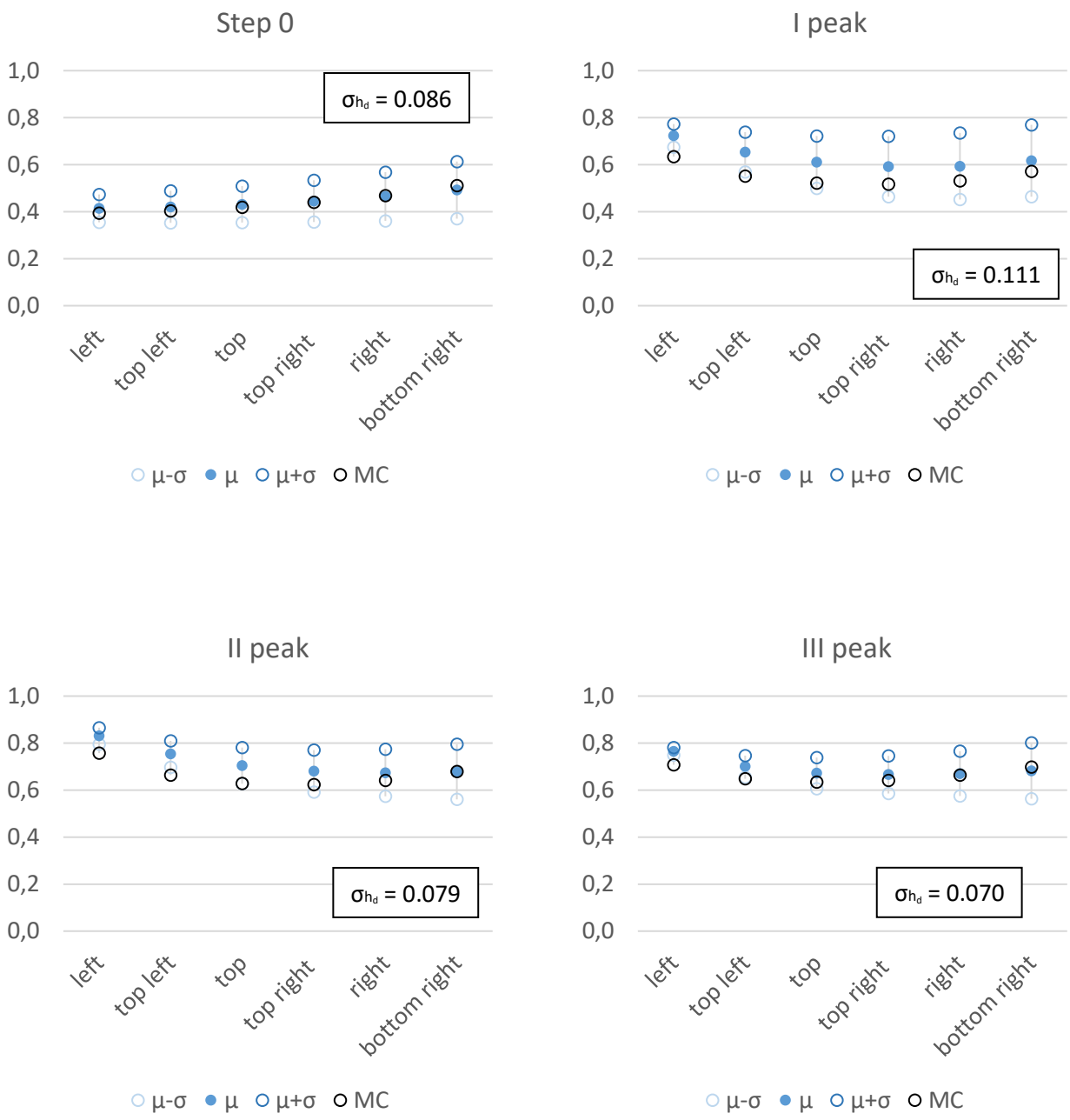

Figure 7.2. Dimensionless head of the control nodes computed both for deterministic and probabilistic (PE-II) seepage analysis.

Figure 7.2 shows of deterministic and probabilistic seepage analysis in terms of h_d for the control nodes, considering the procedure named as PE-II. The use of a rather simplified procedure for the definition of initial conditions lead, as should be expected, to higher values in terms of pressure head in the control nodes; however, this effect is less evident with the progression of the elapsed time and with the progression of the high-water event, e.g. for the third hydrometric peak. In this perspective, the use of PE-II for riverbank safety assessment could lead to less reliable results for the actual seepage conditions, but however be comparable

to more sophisticated a procedure (PE-I) which take into account a model spin-up for a proper definition of the initial conditions in terms of unsaturated soil state variables. In Figure 7.3 are plotted the pore water pressure, suction and soil water content vertical profiles (progressive = 26.3m) estimated both from probabilistic (PE-I) and deterministic seepage analysis. Variability range for probabilistic estimation are determined assuming normal distribution both for pore water pressure/suction and soil water content. A first remark should be related to the effect of soil parameters variability on seepage assessment; considering a probabilistic approach, in fact, is possible to obtain a possible range of variation for numerical output, with the possibility to quantify the uncertainties of results. In particular, it could be stated that suction values in the riverbank are affected by a standard variation, on average, between 6.7kPa to 5.7kPa from the initial to the last elapsed time-step; soil water content values, then, suffer an estimated variation, on average varying from 0.027m^3/m^3 to 0.033 m^3/m^3. Minimum and maximum values for σ_u along the profile range for each considered time step are listed in Table 7.4 and 7.5.

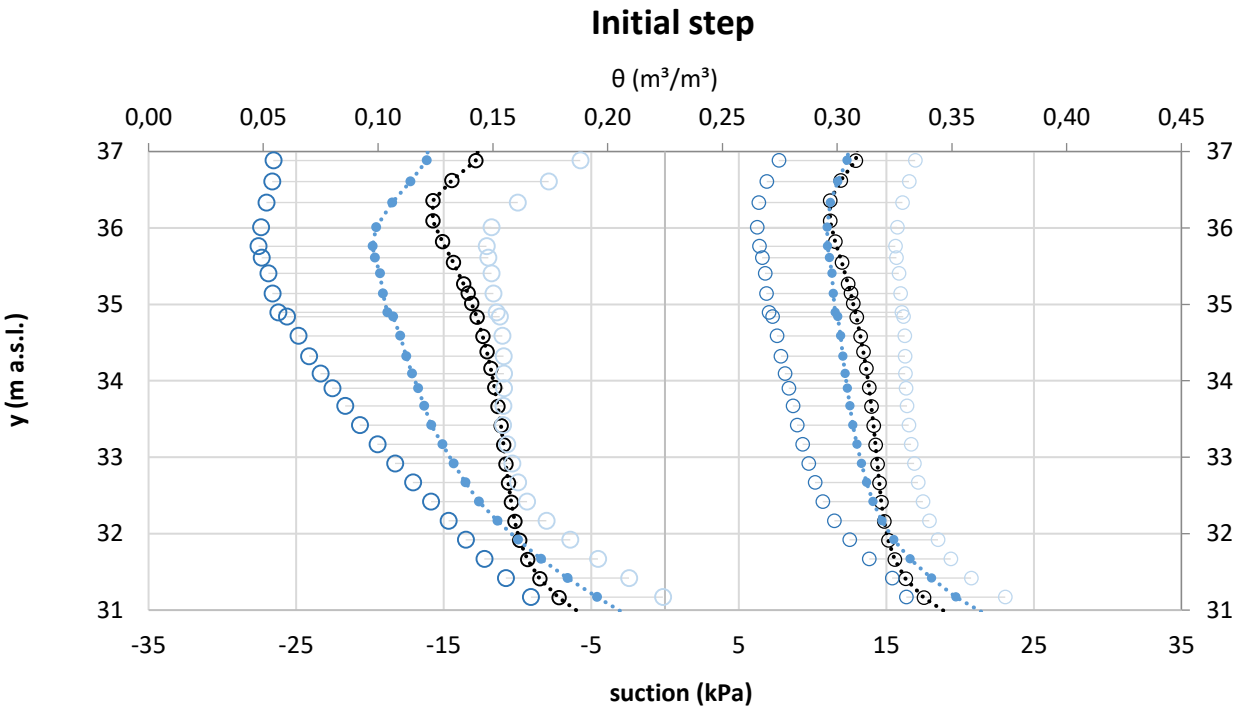

I peak

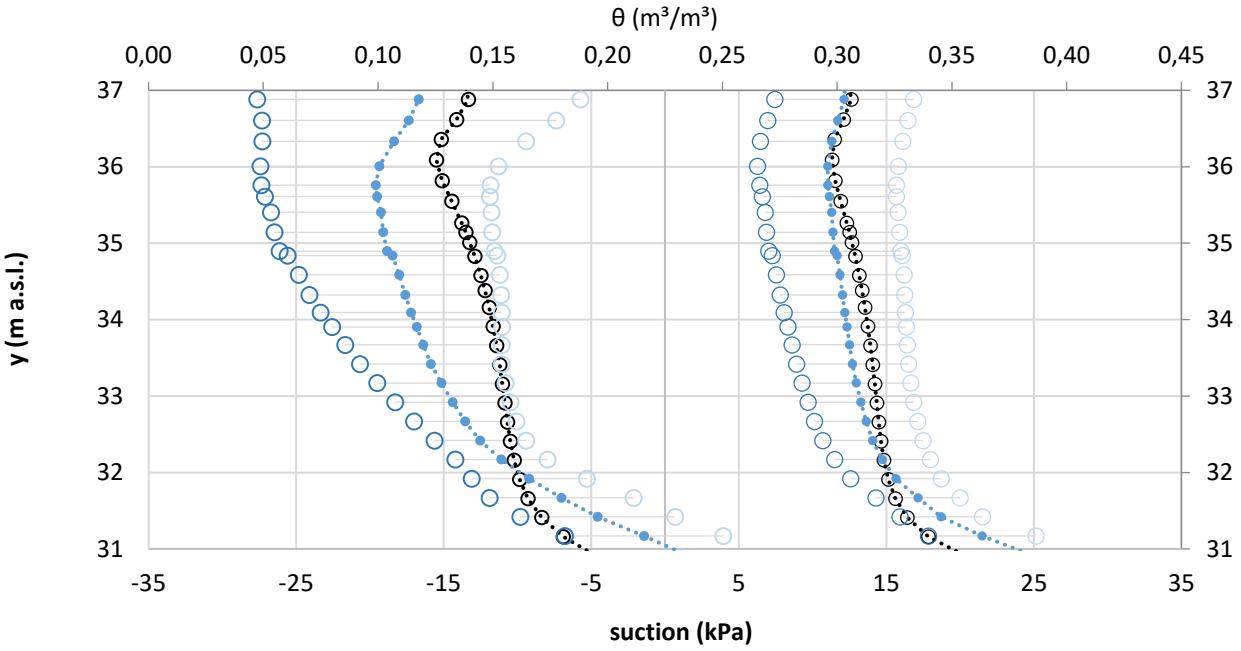

II peak

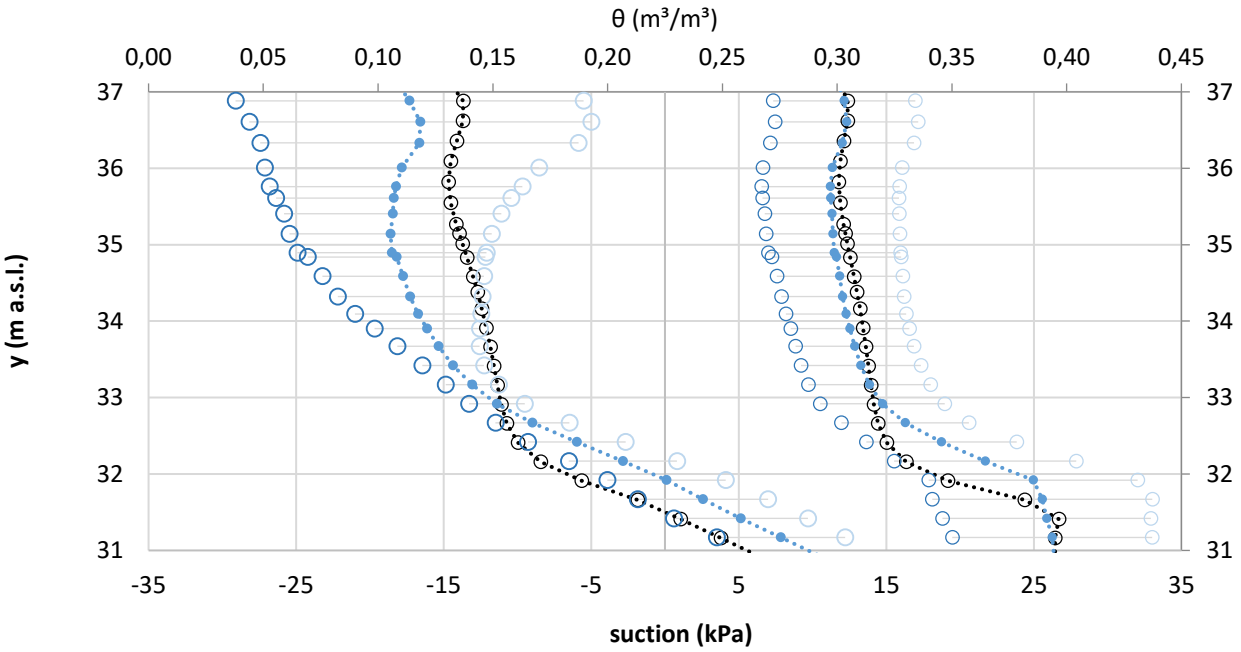

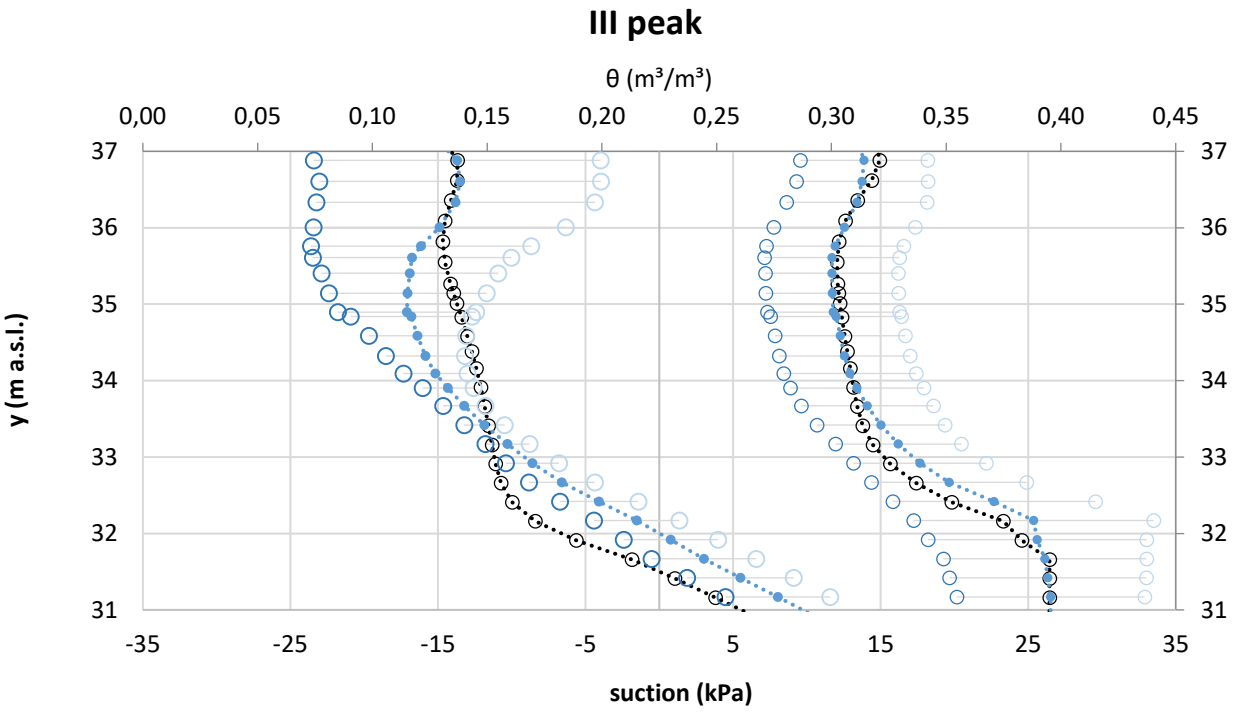

Figure 7.3. Pore water pressure, suction vertical profiles and volumetric water content computed in correspondence of the centre of the river embankment, for various hydrometric peaks, considering normal distribution for PEM results interpretation.

It can be noticed that a comparable trend is evidenced among mean values and deterministic values for soil water content, for the selected vertical profile. However, not giving the PEM a unique correspondence between soil water content to suction values, this remark cannot be extended to soil suction estimations, which evidence significant difference both in shapes and values. However, it should also be stated that was not expected faultless agreement for soil suction and pore water pressure distribution in the riverbank, which determination is strongly nonlinear, whose distribution is generally far to be considerable normal, even since skewness, correlation and asymmetry have been taken into account for the definition of hydraulic and retention parameters to be used in probabilistic seepage analysis.

	Probabilistic approach (PE-I) - Norm. Dist.				Deterministic approach	
	suction (kPa)		θ (m³/m³)		suction (kPa)	θ (m³/m³)
	μ	|σ|	μ	σ	-	-
Initial step	-14.56	6.77	0.313	0.027	-11.78	0.314
I peak	-14.10	6.83	0.309	0.027	-11.69	0.311
II peak	-11.38	6.08	0.308	0.030	-12.07	0.309
III peak	-10.54	5.62	0.315	0.031	-11.72	0.315

Table 7.4. Results of soil suction and volumetric water content computed in correspondence of the centre of the river embankment, for various hydrometric peaks, for probabilistic (PE-I, normal distribution) and deterministic analysis.

Probabilistic approach (PE-I) – Norm Dist.

	suction (kPa)		θ (m³/m³)	
	$\lvert\sigma_{min}\rvert$	$\lvert\sigma_{max}\rvert$	σ_{min}	σ_{max}
Initial step	3.25	12.74	0.017	0.033
I peak	3.11	11.73	0.018	0.042
II peak	1.80	11.79	0.020	0.048
III peak	1.37	10.03	0.020	0.052

Table 7.5. Minimum and maximum variation for soil suction and volumetric water content computed in correspondence of the centre of the river embankment, for various hydrometric peaks, for probabilistic analysis (PE-I, normal distribution).

7.2.1.2 Point estimations with combination of lognormal and normal distribution

Lognormal distribution for soil suction have been, in alternative, considered for the seepage results processing; in this case, the profiles have been obtained by processing soil suction (absolute) values using lognormal function hypothesis for the shape of the PDF; this has been made for all nodes and step for which all PE analyses give in turns negative values for PWP. However, for nodes with elevation up to 32.6m a.s.l., fluctuation around zero are computed for at least one point estimation; for these cases, normal distribution function has been assumed for data processing. This assumption has found to be necessaire in consideration that data series characterized by fluctuation around zero cannot be directly interpreted by using typical lognormal distribution; different solution, as the use of missing values, excluding some estimation from the analysis, or transformation methods, which consists in adding arbitrary constant value to data prior to applying the log transformation, are not taken into consideration considering that their use could lead to criticism for data interpretation. In Figure 7.4 are plotted pore water pressure and suction vertical profiles, for various hydrometric peaks, obtained assuming lognormal distribution for suction (absolute) values and normal distribution for values oscillating around zero; the range of variation is expressed as EXP(lnμ±lnσ) and μ±σ, for lognormal and normal distribution respectively. Results shown in Figure 7.4 evidence a better fitting with deterministic results compared to Figure 7.3; this remark could be stated as consideration that normal distribution is usually not considered for describe the variability of pore water pressure values in probabilistic seepage analysis, generally in advantage of lognormal or Gumble distributions (Alén, 1998; Phoon et al. 2010).

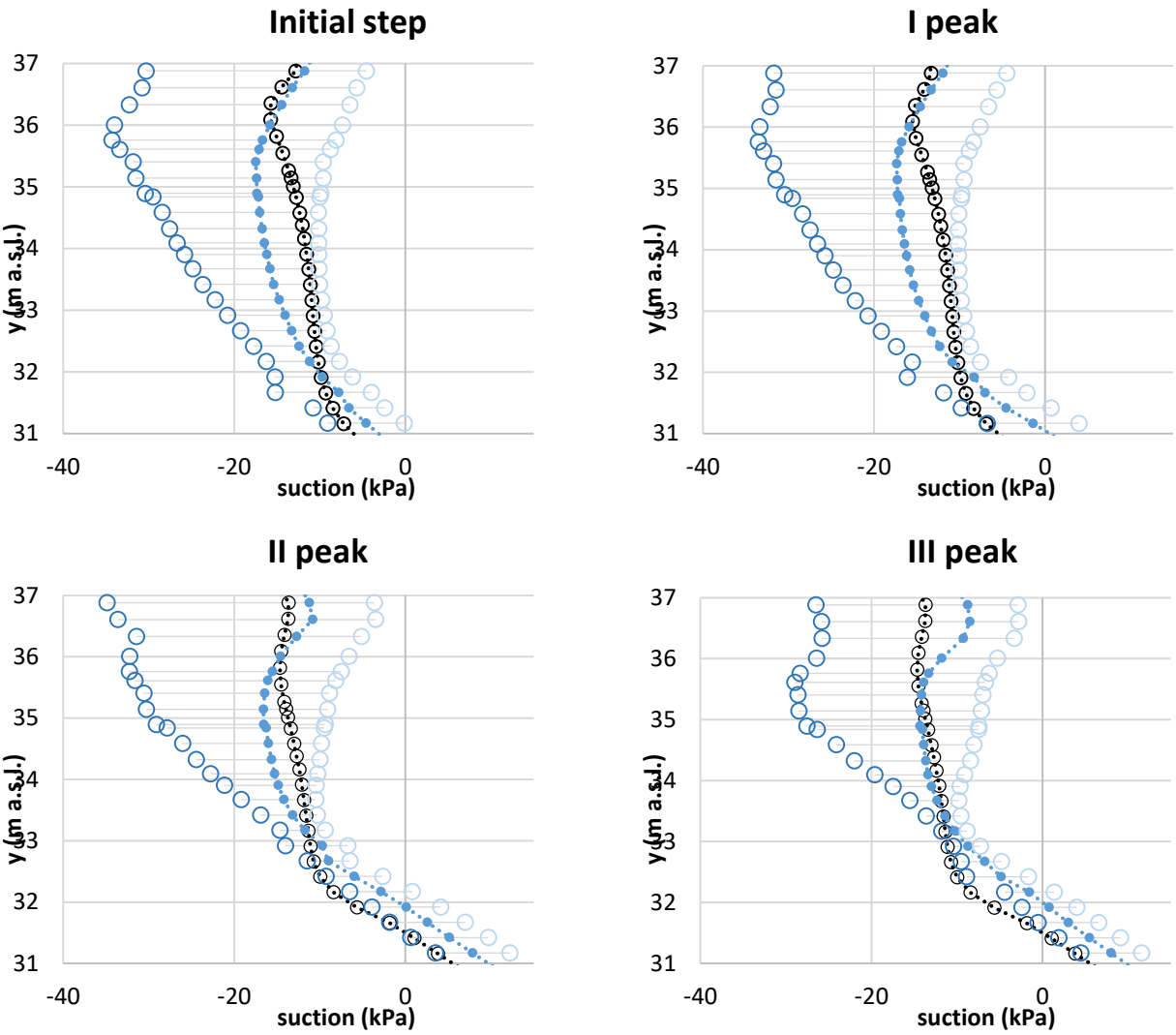

Figure 7.4. Pore water pressure and suction vertical profiles computed in correspondence of the centre of the river embankment, for various hydrometric peaks, considering lognormal distribution for PEM results interpretation.

	Probabilistic approach (PE-I) - LogNorm. Dist.						
	Suction profile (kPa)						
	|mean|	|negative offset|			|positive offset|		
	-	min	average	max	min	average	max
Initial step	12.93	6.73	13.41	21.19	4.55	6.95	8.57
I peak	12.74	6.66	13.44	22.17	4.52	6.95	8.39
II peak	12.8	2.94	12.56	23.63	2.35	6.14	8.06
III peak	11.65	1.59	10.92	18.90	1.37	5.18	7.23

Table 7.4. Results of soil suction computed in correspondence of the centre of the river embankment, for various hydrometric peaks, for probabilistic (PE-I, lognormal distribution) analysis, in terms of mean value and negative and positive offsets.

In Table 7.6 are, then, listed the mean values for soil suction along the various showed profile and minimum, average and maximum values for positive and negative offset, which are here intended as the minimum, average and maximum values obtained for soil suction distribution showed in Figure 7.4 for each profile.

7.2.2 Application of PE and MC methods for the probabilistic stability assessment of riverbank

Both Point Estimate and Monte Carlo Methods have been tested for riverbank safety assessment. For each procedure, in addition to references provided in previous Chapters, some specifications need to be here debated. Among the most important features for PEM applied to LEM, as implemented in Slope/W in the framework of this Thesis, could be found that the critical slip surface is found, for each analysis, among those considered admissible and compatible with the geometric boundaries (details are given in Chapter 3), selected to individuate an overall collapse mechanism for the outer slope. As consequence, the use of different set of parameters for the determination of pore water pressure and suction to be used for limit equilibrium analysis allows to store a critical slip surface specific for the solution of the parent seepage analysis. This procedure guarantee to effectively study the stability conditions for the riverbank towards a pre-determined, but general, collapse mechanism for which a maximum value for probability of failure is generally determined. The PEM, so, allows the slip surface to be changed, searching randomly for the most critical slip surface in terms of safety factor for each point estimate combination. Differently, the application of Monte Carlo procedure as implemented by the software code performs the user-prescribed number of trials on each slip surfaces among those considered; this means that the use of certain sampled set of parameters for LE analysis won't provide the minimum safety factors among those theoretically obtainable for the considered slip surfaces, which is preliminary fixed. The mean values for the safety factor distribution computed by numerical calculation is, so, certainly minor than those obtainable if for each sampled set of parameters the slip surface would be free to be located; nonetheless, the computed standard deviation for safety factor is major than cases of variable slip surfaces (being part of the SF distribution even the higher values), partially balancing the effect of using a fixed slip surface for the determination of critical values for probability of failure related to a specific collapse mechanism. However, it should be also stated that PEM allows to provide global insight to the safety assessment, even considering that the restricted amount of analysis and the necessaire hypothesis on the shape of the safety factor distribution could constitute a limit for its application; the strength of MC simulation, indeed, consists on the rigours determination on the shape of the cumulative distribution functions for SF, even if relative to a specific slip surface which could not eventually represent the most critical situation for a fully comprehensive probabilistic approach. Uncertainties in retention and hydraulic soil parameters are directly accounted when using PEM for stability assessment both in terms of variability of seepage results and unsaturated soil strength.

For MCM, as implemented in the numerical code, these features are not directly accounted, but an indirect possibility is represented by the use of pore water pressure and suction distribution obtained from deterministic seepage analysis as random variable for the problem. Through this procedure, the offset probability distribution and sampling functions need to be assigned to the model, posing a novel problem for the description of the input data. The definition of pore water pressure variability could be, in general, estimated on the base of direct measurement for specifically instrumented embankment sectors, or by means of detailed analysis focusing on the effect of the soil hydraulic and retention properties variability of the riverbank on results.

In absence of direct measurements, different hypothesis on the shape and variance of pore water pressure have been estimated on the base obtained for PE-I. In addition, on the base of the variability of the typical river water level variance among a year, simplified assumptions have been also made on the offset distribution functions for pore water pressure and suction values computed from deterministic seepage analysis, and then used for probabilistic stability analysis still performed Monte Carlo method. In next sections, details are provided on all procedures above introduced, and results compared. Remarks, features, general observation and comments involving the analysis performed in the previous Chapters are, then, provided.

7.2.2.1 Probabilistic stability analysis: results and discussion

The estimation of probability of failure for overall instability mechanism due to the action of external water level time-variability have been performed by means of Point Estimate and Monte Carlo Method. With regard to PEM, a series of 64 limit equilibrium analysis have been performed for all discretized time step of the seepage analysis. The number of analysis is related to the random variables selected for the probabilistic study (θ_{sat}, n, α k_{sat}, ϕ'_A, ϕ'_B), resulting in $2^6 = 64$ combinations for hydraulic, retention and strength set of parameters. Following the procedure defined in Chapter 2, and consistently with probabilistic seepage analysis discussed in the previous section, the PEM has been so applied to obtain from a series of (64) deterministic limit equilibrium analysis, the mean value and standard deviation of the safety factor distribution, once assumed the shape of the output distribution function (normal for SF). Pore water pressure and suction distribution for the limit equilibrium analysis have been obtained from the application of PEM-I and PEM-II as described in the previous section. The contribution of each variables on the safety margins towards the considered collapse mechanism has been estimated on the base of the relative weight of each combination and to the skewness for each random variable, which define the point estimate locations. In detail, according to the notation given in Chapter 2, the contribution for each random variable is expressed as:

$$\left(\frac{\sum_i^+ w_i SF_i}{\sum_i^+ w_i} - \frac{\sum_i^- w_i SF_i}{\sum_i^- w_i}\right) \Big/ \left(2\sqrt{1+\left(\frac{\nu}{2}\right)^2}\right)^2 \quad (7.1)$$

expressed as percentage of the complete probability of failure for each time step. Furthermore, the effect of asymmetry and correlations among hydraulic and retention parameters on results is debated.

Benefiting from the low computational efforts required from this phase of analysis, it was possible to compute the limit equilibrium calculation for all the time-step considered in the seepage analysis, obtaining time-variable distribution for reliability index and probability of failure towards instability mechanisms, instead of their punctual estimation. By this approach, it is so possible to rapidly individuate the most critical scenario for safety assessment during an even extended high-water event.

With regards to the use of MCM for stability assessment, respect to previous applications, it will for some cases also additionally considered the pore water pressure computed by means of deterministic seepage analysis as probabilistic parameter for the problem, included in the sampling procedure. Through this simplified procedure, it could be so possible to indirectly but effectively account for the hydraulic and retention soil parameters when safety assessment is required. In the present work, both normal and lognormal distributions both considered for the PDF of pore water pressure and suction in the embankments. For the first application Point Estimate Method (PE-I) series of limit equilibrium analysis have been performed in order to study the effect of high-water sequences accounting for mechanical, hydraulic and retention parameters of soil in safety assessment, considering an initial condition consistent with the specific set of assumed parameters. In Figure 7.5 are plotted results obtained in terms of mean value and standard deviation for Safety Factor distribution (μ_{SF} and σ_{SF}, respectively) computed at each time step considered for the seepage analysis (time interval between each time step = 21600 sec = ¼ day); the time is expressed in days from the beginning of the high-water event (February, 16th 2015). For the results elaboration, normal shape for SF distribution have been considered at each time step. In the same graph, are plotted the deterministic value of safety factor obtained using average values for hydraulic and retention parameter for seepage analysis; at specific time step are reported results from probabilistic analysis performed by means of MC-I, both in terms of μ_{SF} and σ_{SF}.

A preliminary analysis of result suggests a clear similarity between trend and values for deterministic and mean Safety Factors. However, it has also to be stated that, mainly for most critical time step, deterministic analysis tends to overestimate the margins of safety; in these correspondences, generally with some delay with the maximum water height, the hydraulic characteristics for the riverbank assume a crucial importance for the stability condition of the riverbank; then, accounting for probabilistic seepage analysis became central for a reliable safety analysis. Furthermore, the use of MCM with only soil strength parameters provide a

narrow range of variation for the SF distribution, indicating a consequent higher, and so overrated, margin of safety. It has to be, furthermore, noticed that when PEM is used, the envelope of minimum safety factor computed among the 76 individuated by proper geometric boundaries slip surface is considered for the determination of statistical moment for critical SF distribution.

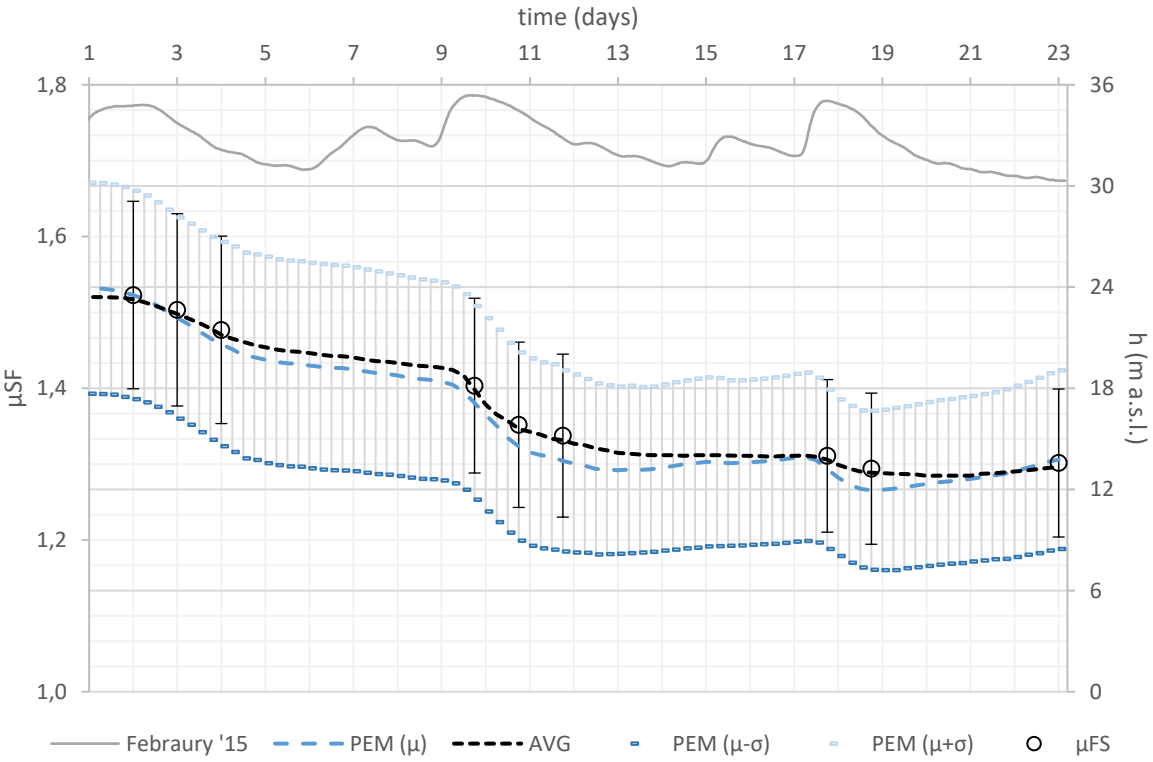

Figure 7.5. Safety Factor distribution variability expressed as deterministic values (black square dot line) and means and standard deviations for probabilistic limit equilibrium analysis performed with PE-I (blue lines) and MC-I (in correspondence of specific time step).

The use of PEM presents the remarkable advantage to provide the complete distribution of SF distribution for all the considered time step, with limited computational efforts if compared with MCM using the implementation procedure described in the previous section. In specific, accounting for a total number of 50 iterations for the Safety Factor convergence (on average required for each Limit Equilibrium analysis by means of Morgenstern and Price Method) for each slip surface determined by the assumed geometric conditions, and considering 76 possible mechanism of failure, a total number of 100x76x92(time step) = 699200 calculations are performed for each set of parameter, becoming 22374400 for the total implementation of PEM to probabilistic seepage analysis. Considering the same amount of iteration and geometric boundaries for slip surfaces, the implementation of MCM using 100000 trials and 9 time step

require a number of 3420000000 calculations, revealing about two order of magnitude in difference with PEM respect to stability analysis; this difference is, nevertheless, partially compensated with seepage analysis, for which the ration between the number of analysis required for MC and PE methods is 1:16. However, this last aspect also lead to the considerable advantage of a more consistent determination of initial conditions and inclusion of hydraulic and retention parameters in PE probabilistic approach.

Both PE and MC methods have been tested also considering a simplified and unique hypothesis for initial conditions in correspondence of the beginning of the considered high water sequences, where each seepage analysis have been performed considering pore water pressure and suction distribution defined for $S.A.1_b$ as initial conditions (Figure 5.17), leading to PE-II and MC-II. In this case (Figure 7.6) lower values for Safety Factor (both from deterministic and probabilistic limit equilibrium analysis) are determined. Furthermore, also for this case, it is evident the effect of neglected source of uncertainty related to hydraulic and retention parameter estimations, when using MCM respect to PEM, which always provide a wider range of variation, particularly for the Then, it can be worth to notice a lower influence for the progression of the high-water event on the riverbank stability conditions, which seems to be strongly affected on the assumption on the initial conditions in terms of pore water pressure and suction distribution still at the end of the considered event. This feature, however, can be also interpreted as the possibility to thoughtfully represent unsaturated soil state of the riverbank in reference to a specific period, limiting the eventually neglected effect of various source of uncertainties (as hydraulic and retention parameters variability) in the framework of a simplified approach; the reliability of this procedure, however, being strongly dependent on the initial assumption, require confident knowledge on the possible variation of soil suction distribution, which could be achieved e.g. by means of direct measurement in combination with extended preliminary numerical studies.

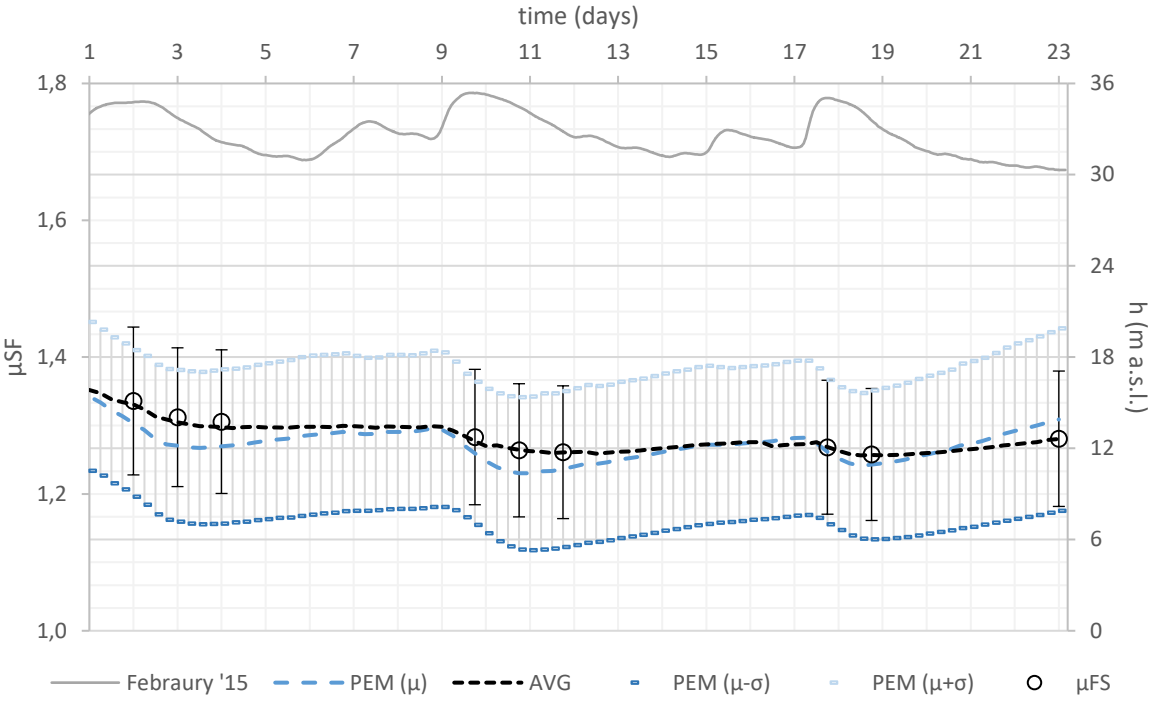

Figure 7.6. Safety Factor distribution variability expressed as deterministic values (black square dot line) and means and standard deviations for probabilistic limit equilibrium analysis performed with PE-II (blue lines) and MC-II (in correspondence of specific time step).

7.2.2.2 Contribution of retention parameters to riverbank stability assessment

In Figure 7.7 are plotted the values of critical probability of failure estimated for all considered time step, together with the contribution of each parameter considered in the probabilistic seepage and stability analysis for PE-I. The trend of Pf is conceptually similar to the one estimated for μ_{SF}; with a general reduction in safety conditions (increment in Pf) with time, and critical incidence in correspondence of the days immediately subsequent to the hydrometric peak. With the progression of the high-water event, α and n parameters of the soil water retention curve seems to evidence a lower incidence in stability assessment; this could be mainly due to their minor effect on the seepage characteristic then saturation degree increase in soil riverbank. In combination, it can be parallelly revealed an increment in k_0 contribution complementary to a reduction for mechanical strength parameters. Even if, singularly, the single effect of retention parameters variability could be considered negligible if compared to the equivalent in terms of friction angles, two aspects have to be considered to proper evaluate their influence on results. Firstly, the predominant effect of soil mechanical parameters variability in stability assessment when considering an overall mechanism of failure involving both riverbank and foundation could be certainly assumed as the most important source of uncertainty, for whose proper characterization main efforts have to be devoted (as prescribed for standard geotechnical applications).

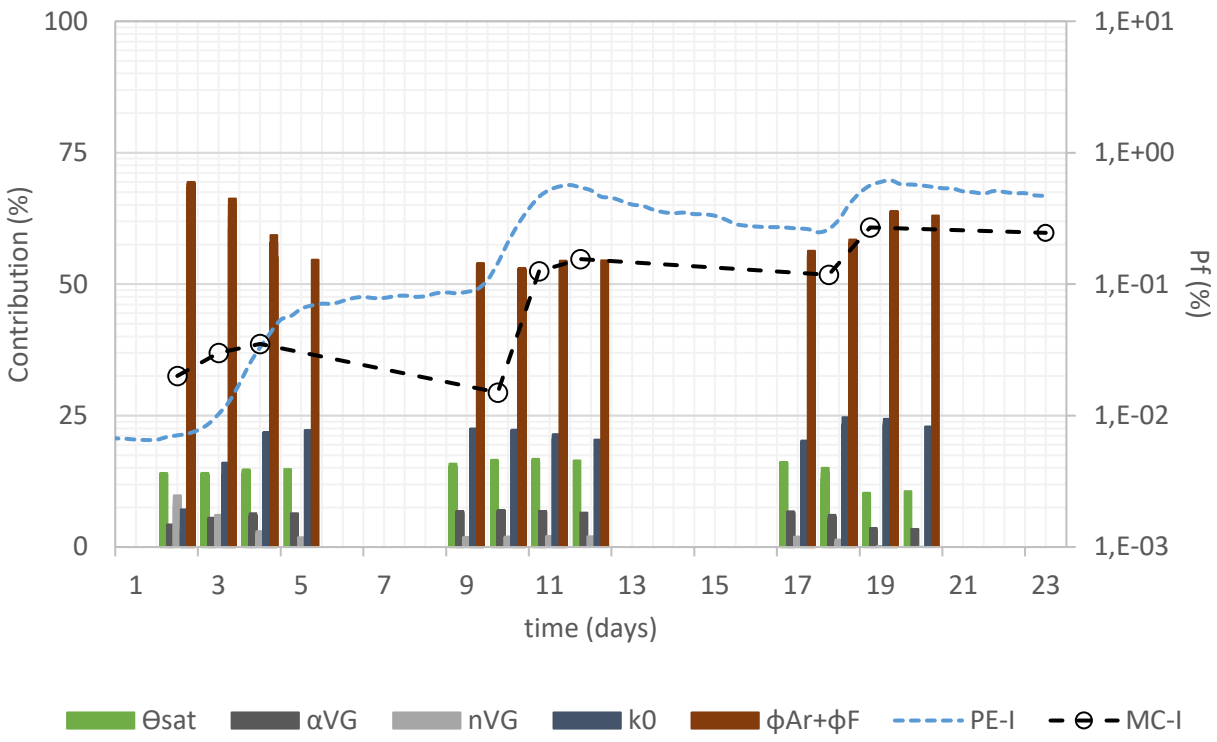

Figure 7.7. Time variability for critical probability of failure estimated by means of MC-I and PE-I considering correlation among parameters, together with contribution of mechanical, hydraulic and retention parameters on Safety Factor distribution variance for PE-I.

Nevertheless, the global influence of hydraulic and retention parameters varies from around 30% (for the first hydrometric peak) and 47% (for the third hydrometric peak), representing indubitably a significant issue for a reliable estimation of riverbank safety assessment. Consistency of these outcomes could be found considering the correspondence between increases in the contribution of hydraulic and retention parameter together with variance between Pf obtained by means of PE-I and MC-I, plotted in Figure 7.7, and vice versa.

The use of MC-I provides, for the main part of the high-water event, significantly lower values in terms of safety assessment. Maximum differences are evidenced in correspondence of the second hydrometric peak, for which the Pf obtained from MC-I is underestimated of about one order of magnitude compared to PE-II estimations. However, at the beginning of the high water event, MC-I seems to provide higher values for Pf, meaning that when the effect of hydrometric variation is limited, the use of MCM seems a more rigorous numerical methods for safety assessment.

Results in terms of Pf obtained by means of MC-II and PE-II, considering correlation among parameters, are plotted in Figure 7.8.

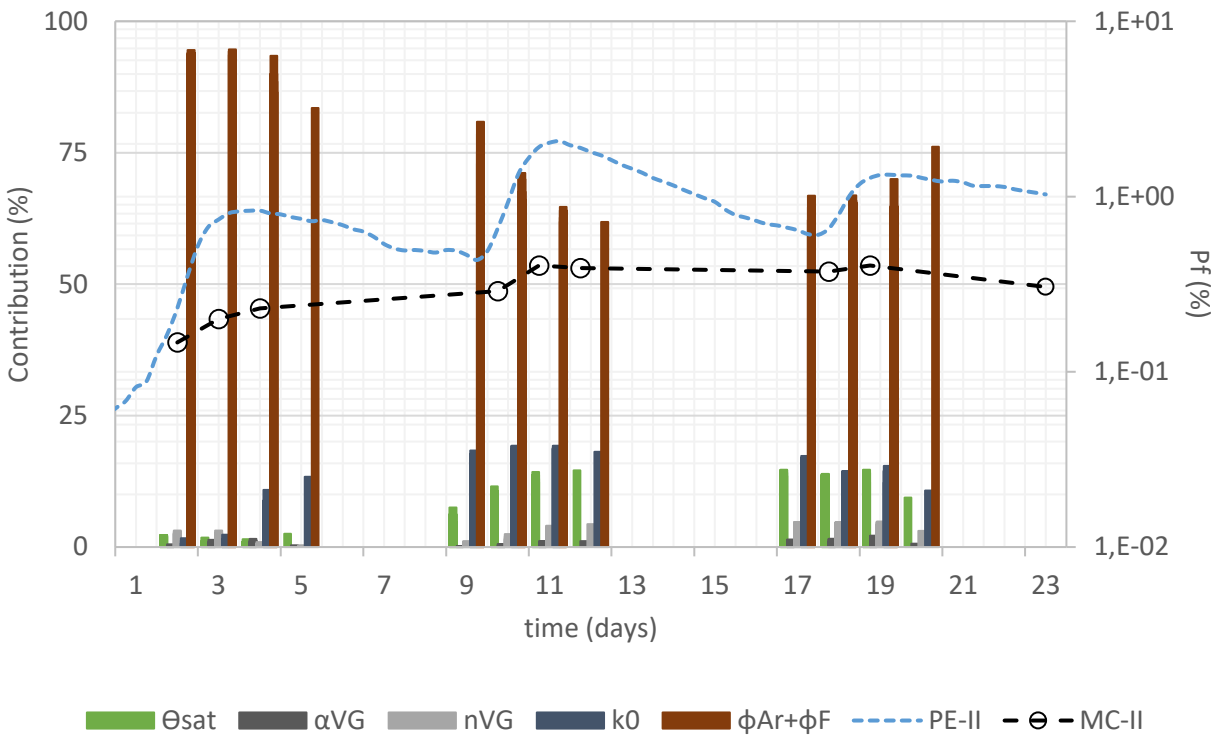

Figure 7.8. Time variability for critical probability of failure estimated by means of MC-II and PE-II considering correlation among parameters, together with contribution of mechanical, hydraulic and retention parameters on Safety Factor distribution variance for PE-II.

For the showed case, it is worth to observe the generally higher values for Pf computed at all elapsed time-step and the limited effect of retention parameters on results; this evidence the conservative choice for the initial conditions, which produces lower influence of unsaturated soil parameters on stability assessment (considering that maximum absolute values of 15kPa has been considered for the initial suction distribution above the phreatic line, considered at approximately 32m (a.s.l.). Only slight variation are evidenced during the event for MC-II analysis; this means that the influence of the initial conditions strongly affect the results, and could be considered, once more, as one of the most impacting factors for safety stability assessment when seepage analysis are performed on the base of simplified assumptions and in absence of direct measurements.

In order to estimate the effect of the use of correlation matrix, in Figure 7.9 are plotted the critical Pf and the contributions of the considered parameters to SF variance with time, estimated for PE-I application. A series of remarks can be immediately deducted from showed results; firstly, the critical probability of failure evidence an increment of about 40% respect to the case in which correlation is accounted for probabilistic analysis.

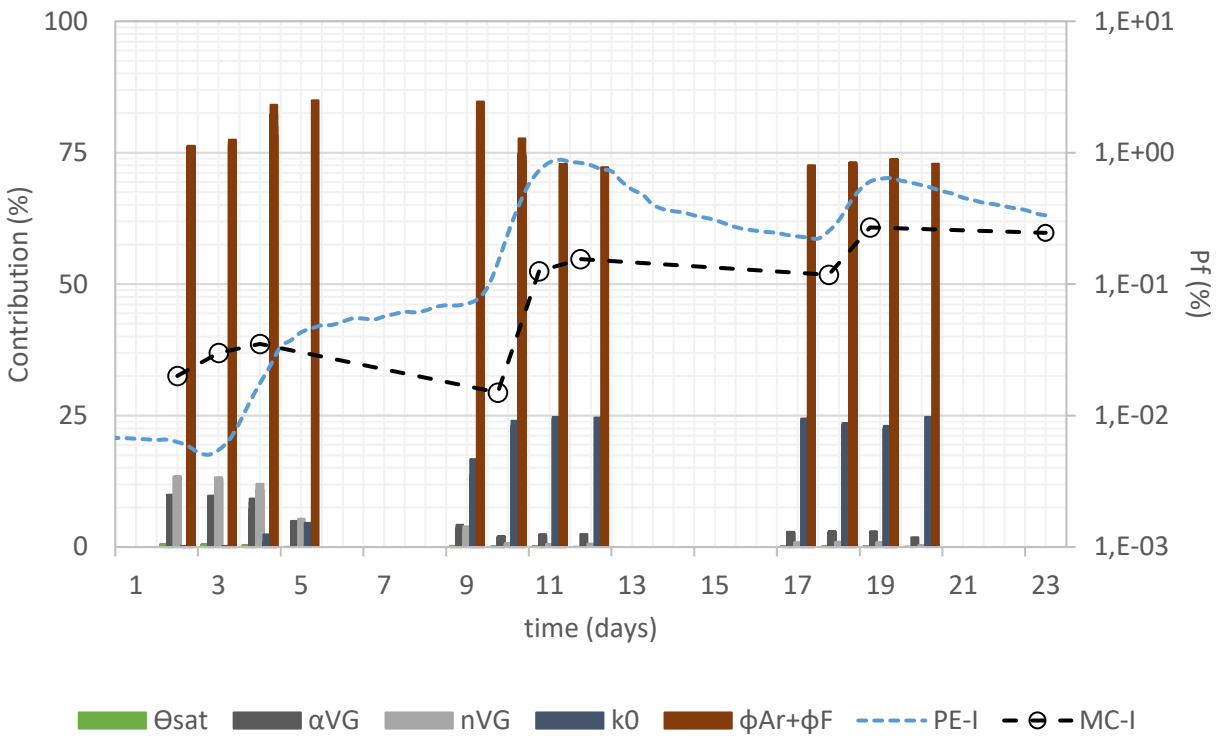

Figure 7.9. Time variability for critical probability of failure and contribution of mechanical, hydraulic and retention parameters on Safety Factor distribution variance, estimated by means of PE-I without considering correlation among parameters.

These results are in line with the for the role that correlation structure generally assumes; in fact, the use of additional information for parameters characterization should reduce the uncertainty of results if the lack, or limited source, of knowledge is intended to be generally accomplished by higher margin of safety. However, similar results have been obtained for slope stability assessment in literature (Zhang et al., 2003; Zhang et al., 2010). For the present case, it should be stated that the use of correlation matrix, in combination with statistical moments assumed for parameters distribution, both presented in Chapter 3, have the effect to provide higher values in weight for the combinations which have been found to be critical for the stability assessment, e.g. when combination of n-, α-, θ+ are considered for point estimate locations. Even for this reason, an additional effect of the use of correlation matrix in probabilistic analysis here provides higher contribution for the retention parameters to the SF variance, being more impactive for the riverbank stability assessment. Furthermore, even the time occurrence changes from the 19th day to the 11th day, revealing a more incisive effect of the second river level peak, when highest hydrometric values are reached, respect to the third, when the progression of the phreatic line in the riverbank is generally higher and soil turns to be more saturated.

7.3 Safety Factor distributions: MCM vs PEM

For a specific examination of the showed results it could be useful here to discuss the effect of various hypothesis and estimation of Safety Factor distribution defined for various methods. With reference to values of Pf time-variability obtained using MC-I (Figure 7.7), this method seems to be more conservative compared to those obtained using PE-I, if considering the first high water event; however, this evidence is not found when comparison among methods is made in terms of μ_{SF} and σ_{SF} (Figure 7.5). This feature can be clarified on the base of the various assumption for the Pf estimation at the base of the various methods. In fact, considering PE and MC methods, while β values are similarly estimated on the base of μ_{SF} and σ_{SF}, the critical Pf is numerically estimated for MCM as the ratio between the number of failure and the total number of trials, and for PEM on the base of the hypothesis on the SF distribution (see Chapter 2). By this, differences could be evidenced when terms of safety for MCM are expressed using μ_{SF} and σ_{SF} or Pf, particularly when margin of safety are considerable (low-order Pf). In Figure 7.10 and 7.11 are plotted the outcomes for each LE trial analysis computed on each MC simulation in terms of SF probability distribution; elapsed the time steps are corresponding to the first and the last hydrometric peak for the considered event; low frequencies outcomes around SF = 1 are also showed. Safety factor distribution computed with PEM and fitted normal distribution for MCM (characterized by terms of μ_{SF} and σ_{SF}) are, also, compared.

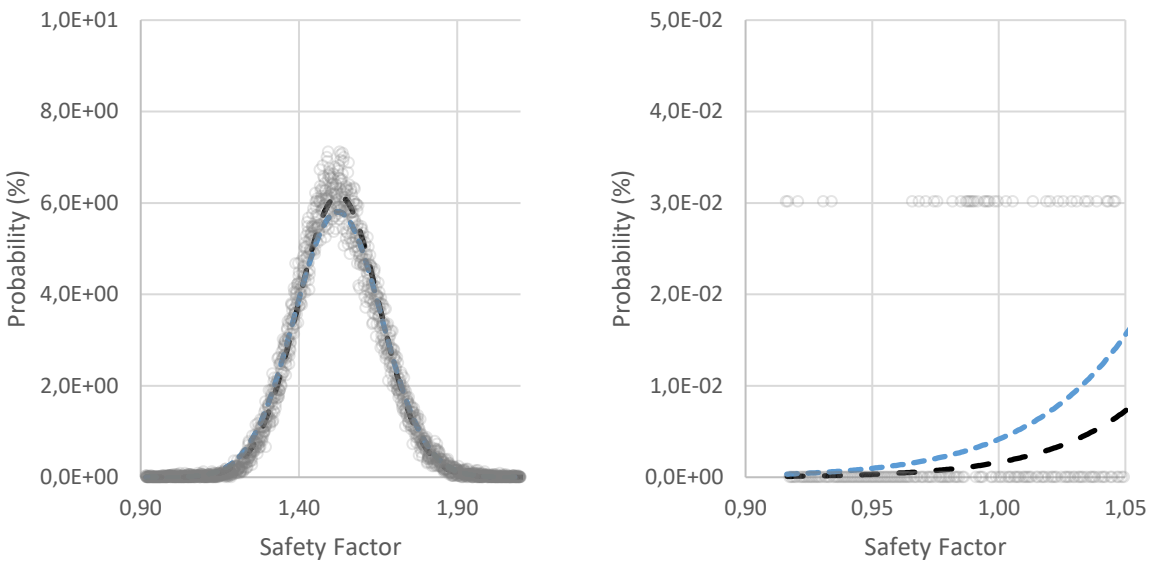

Figure 7.10. Safety Factor distributions computed by means of MC-I (100.000 trials) and PE-I in correspondence of the first hydrometric peak, in terms of number of trials and normal distribution.

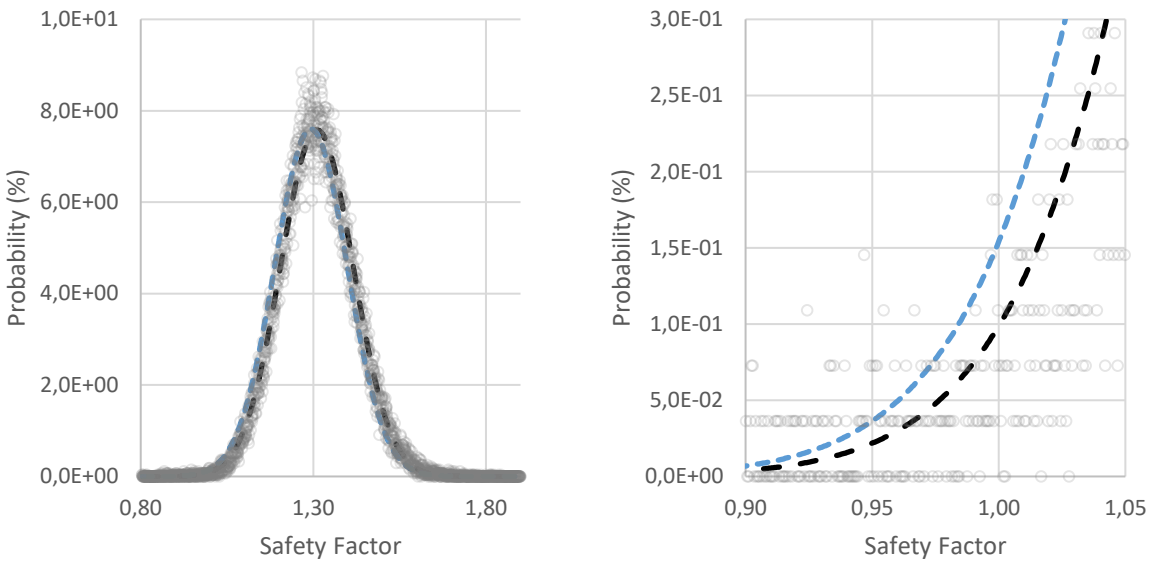

Figure 7.11. Safety Factor distributions computed by means of MC-I (100.000 trials) and PE-I in correspondence of the third hydrometric peak, in terms of number of trials and normal distribution.

As can be seen, the overall shape of the SF distribution, determined by the complete set of MC trials, could be certainly approximate using normal function (left); however, differences may be evident for safety factor around 1.0 (right). In fact, the Pf estimated on the base of the total amount of failure trials is certainly higher than the Pf estimated through the definite integral of the SF distribution function among the interval 0 – 1. The first method of estimation provides the critical value for Pf when using MCM, while the second is relative to the Pf associated to the μ_{SF} and σ_{SF}; by this, the estimation of the β (properly based on μ_{SF} and σ_{SF}) could indicates a different safety conditions respect to those estimated on the base of Pf. However, these types of differences are strongly reduced when considering higher values for Pf; an example is provided in Figure 7.12, where Safety Factor distribution, and its specific around unitary value, is plotted when using MC-I. Numerical results in terms of Pf, obtained using both equations 2.18 and 2.28 can are listed in Table 7.5, evidencing how the assumption on SF distribution affects results in terms of Pf in relation to its magnitude.

Time	PE-I	MC-I	
days	Pf (SF normally distributed) (%)	Pf ($N_{trials,f}/N_{tot}$) (%)	Pf (SF normally distributed) (%)
2	0.007	0.025	0.002
3	0.010	0.030	0.004
17.7	0.262	0.158	0.107
18.7	0.563	0.270	0.158

Table 7.4. Parameters for the pore water pressure and suction sampling functions.

Discussion of results in terms of β for safety assessment comparison towards different analysis, however, have been widely used in this work; as also described in Chapter 3, this has been mainly motivated by the possibility to consistently, and concretely, relate probabilistic outcomes to β even for safe conditions. In fact, the estimation of Pf obtained by MCM, and its trustworthiness, is strongly dependent on the number of trials performed and the possible related errors is, in turn, strongly affected by the magnitude of Pf. Variations in Pf among various peaks of a high water event could be of different order of magnitude, particularly for low-order values of Pf, which could lead to erroneous remarks in the safety assessment interpretation. Differently, the estimation on β is mainly dependent on μ_{SF} and σ_{SF}, once defined the shape of the SF distribution function. Even if the assumption on the shape of the PDF defined for SF distribution could be a limitation, this procedure lead to more appropriate comparison among various cases, which could be so based on a similar assumption (the hypothesis on the SF distribution).

The knowledge on the real shape of SF distribution constitutes a significant benefit for MCM, represent one of the main advantages of the method when correctly adopted, and is here also useful in comparison with PEM results. Firstly, the hypothesis on the SF distribution (necessaire in PEM) can be verified; then, the value of Pf obtained by means of MCM could be referenced as reliable terms of safety in cases rigorous method is applied, even if with some limitation. The direct influence of soil hydraulic and retention parameter variability in PEM, in combination uncertainties related to mechanical properties, lead to critical values for Pf however higher than those estimated with MCM.

7.4 Accounting for PWP variability in MC procedure

Finally, stability analyses have been performed in order to simulate the effect of hydraulic and retention soil parameters using MC procedure. In particular, pore water pressure and suction distributions are here considered as random variable for the problems, so that their deterministic estimation is formerly corrected by on the base of values sampled at each MC trial, once defined proper probability density and offset functions for the selected random variables. The idea of using pore water pressure and suction distribution as random variable has been discussed and adopted in quite a few literature studies. Alén (1998) discussed a study on probability in Geotechnics applied to slope stability analysis, for which pore water pressure has been modelled in statistical analysis (performed by means of MC method) using Gumbel distribution; various applications (Hassan and Wolff, 1999; Bhattacharya et al., 2003; Cheng, 2015) consider the pore water pressure ration, r_u (which is defined as the ratio of pore water pressure to the soil unit weight), as random variable varying with normal distribution. In the framework of this thesis, pore water pressure and suction distribution computed from deterministic seepage analysis are now considered as random variable, with this aiming to account indirectly for more detailed seepage probabilistic analysis (e.g. PE-I). For this purpose, four

hypotheses have been defined on the base of simplified assumptions and results obtained from previous analysis, detailed in Table 7.6, for the MC procedure.

	Normal PDF		LogNormal PDF		
ID	N1	N2	L1	L2	L3
μ (kPa)	0	0	12.5	6.25	-6.25
σ (kPa)	6.25	3	12.5	6.25	6.25
Min sampled (kPa)	-25	-12	-12.5	-6.25	-18.75
Max sampled (kPa)	25	12	37.5	18.75	6.25
Offset	0	0	-12.5	-6.25	6.25

Table 7.6. Parameters for the pore water pressure and suction sampling functions.

For the definition of the first hypothesis (N1) it has been simply considered the range of variation for the hydrometric baseline during the period ’14-’15, which is 27.5m – 30.0m. The standard deviation of this population is 1.25m, which has been intended in terms of equivalent range for the most likelihood offset values for pressure head in the riverbank. Considering that this range is about ±2σ when normal distribution is assumed, it turns to be σ = ¼·1.25m, which in terms of pressure is about 6.25kPa. The L1 hypothesis have been derived from the frequency of the TMA 241-width estimated for the period ’13-’16, on the base of the best fitting obtained using a LogNormal distribution. Both distribution are plotted in Figure 7.12. Frequency for hydrometric water level, TMA 241-w, and N1 and L1 schematization in terms of frequency of occurrence.in terms of total head.

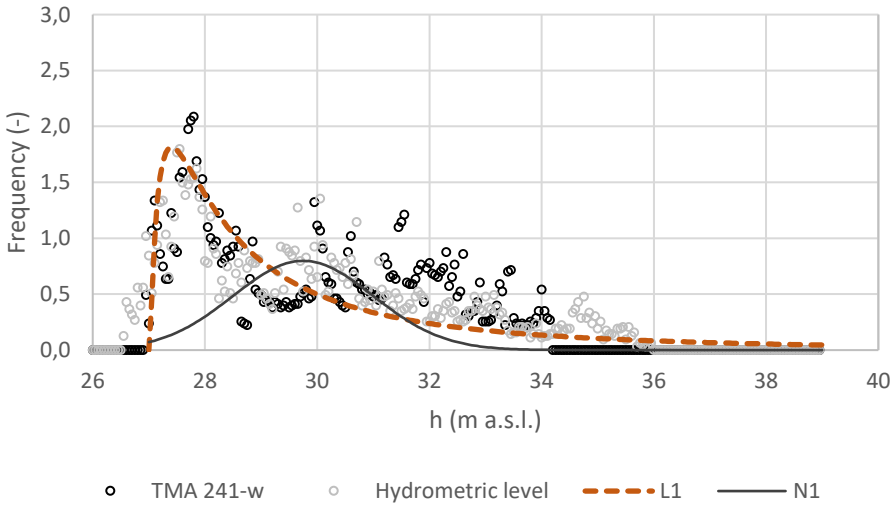

Figure 7.12. Frequency for hydrometric water level, TMA 241-w, and N1 and L1 schematization in terms of frequency of occurrence.

The sense to include measured water level and baseline estimations in the definition of pore water pressure and suction distributions is to account, in a rather simplistic procedure, for the terms of initial and boundary conditions on the variability of seepage characteristic. Then, N2, L2 and L3 have been defined on the base of the results of probabilistic seepage analysis obtained by means of PE-I. Probability density function and cumulative distribution function of the offset considered for riverbank and foundation soils in Monte Carlo simulations are plotted in Figure 7.9; referring to parameters listed in table 7.6, the standard deviation for N2 is derived from the average variation of the progression of the phreatic line in the riverbank, which has found to be equal to 0.3m in terms of pressure head when considering normal distribution in processing h_d data. The standard deviation for L2 is derived from the lognormal distribution of suction above the phreatic lines, for which an overall average absolute value of 6.25m is obtained for standard deviation, mean value and offset. L3 represents, instead, a variation of the L2, for which opposite values for offset estimation are considered. The use of this last function has been considered appropriate to properly represent the results from probabilistic seepage analysis (Figure 7.4), for which the estimated PWP profiles in the riverbank from probabilistic seepage analysis are characterized by significantly high variability in negative offset values, which are, however, mainly associated to the hypothesis on the distribution (lognormal).

Proper limitation to the sampling function, suitable for the geometric and soil properties of the riverbank, have been selected (Table 7.6). In Figure 7.13 are reported the probability density function and cumulative distribution function of the offset considered for PWP in N2, L2 and L3 cases for Monte Carlo sampling procedure. Results obtained for the various approach (PE-I considering correlation among parameters, MC-I, MCM using N1-2 and L1-2-3 specifics for PWP distribution) are, finally, plotted in Figure 7.14.

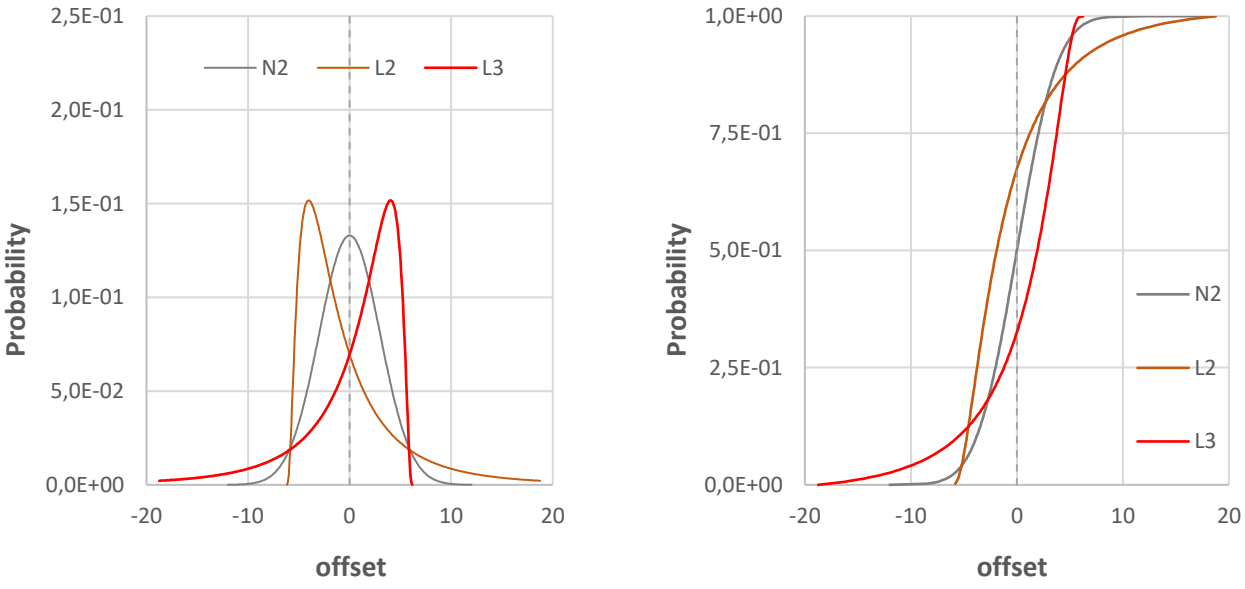

Figure 7.13. Probability density function and cumulative distribution function of the offset considered for riverbank and foundation soils in Monte Carlo simulations.

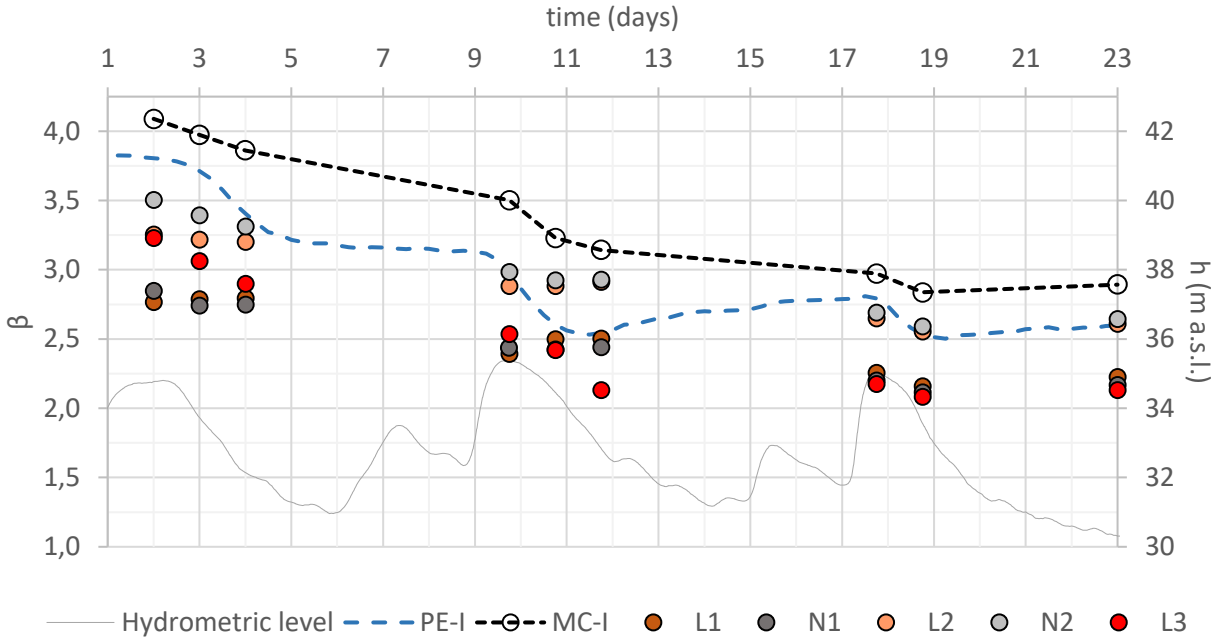

Figure 7.14. Time variability for critical probability of failure estimated by means of MC-II and PE-II considering correlation among parameters, together with contribution of mechanical, hydraulic and retention parameters on Safety Factor distribution variance for PE-II.

8 Experimental investigations on soil retention properties for partially saturated soils

In the framework of the present thesis, focused on the determination of soil hydraulic and retention properties with specific reference to earthen water retaining structure, an important part has been represented by a field study of ground movements due to water changes in partially saturated silty clays. In order to study of the efficiency of the hydration process carried out by the application of an electro-osmotic flow, an experimental site has been specifically selected and thoroughly instrumented to study in detail the problem. Aiming to collect water content variations in the active zone to the deep and ground soil deformations, a varied and accurate geotechnical monitoring system - including soil moisture and suction measurements at different depths – has been installed in the field, and is now operating for longer than a full seasonal cycle. Various types of probes are used for soil moisture and suction measurement. Purpose of this research has been to extend knowledges and improve practises on the actual application of electro-osmosis technology as stabilization method for expansive soils; several topographic surveys have been so performed in order to relate changes in unsaturated soil state parameters to ground and deep movements. In the present section, discussion on electro-osmotic treatments for soil stabilization has been disregarded, being out of the purpose of the present thesis; additional details on the scopes, observations and developments on the project can be found in Preda et al. (2017). However, the field study has represented a concrete and significant source of experience unsaturated soil related issues, with special regards to measurements of water content in the vadose zone and its effect on hydraulic and mechanical soil behaviour.

8.1 Field study, materials and methods

The experimental field, site at Ozzano dell'Emilia (east of Bologna, Italy), has been specifically selected and thoroughly instrumented, in order to verify and improve the methodology of electro-osmotic soil improvement for expansive clays in partially saturated conditions. The main target for the part experimental study here involved has been the estimation of ground movements due to volumetric changes in partially saturated soils. To this purpose, it was fundamental to monitoring in continuous the principal unsaturated soil state variables, individuated in soil suction and water content in the volume of interest among the active zone, at depths ranging from 1.0m to 3.5m. Preliminary, an accurate geotechnical characterization of the site has been performed by means of site and laboratory tests. Once defined the boundaries of the experimental field, the site investigation campaign, based on 28 piezocone tests (CPTU) and 4 boreholes (BH) with undisturbed sample extraction, was carried out along two representative alignments, as in Figure 8.1.

Figure 8.1. Location of the monitoring site (Ozzano dell'Emilia, Bologna, Italy): 44°26'06.67''N; 11°28'56.19''E. Alignments are referred to the geotechnical model reported in Figure 8.2.

Figure 8.2 shows profiles of the corrected cone resistance, q_t, obtained from a series of 13 representative piezocone test CPTUs, located on two orthogonal sections, together with the positions of boreholes. The CPTUs data have been interpreted by the revised classification framework proposed by Robertson (2009), aimed at identifying the in-situ Soil Behaviour Type (SBT) from values assumed by the piezocone-based material index I_c. The principal, well-defined, unit characterizing the monitored zone has been classified as fat, expansive, silty clay. This layer has found to be rather homogeneous for the most of the studied verticals, and thickness up to 10m from the soil surface. Local discontinues layers, composed by a complex assortment of silty sand and sandy silt, with decimetric to metric thickness, have been detected at various depths. These lenses of the subsoil, even if being less predominant respect to clay and silty clay, has however a tangible incidence on results obtained from monitoring data on unsaturated soil state variables. At depths ranging from 8m to 12m, sandy layer has been also evidenced from data obtained from in situ test, which receive less attention from laboratory geotechnical characterization being significantly far from the zone of interest for the purpose of the project and monitoring system. The water table has been located at a depth of approximately 5-6 m from the ground level, as suggested by field data provided by the Casagrande-type piezometer installed into borehole BH2 and BH3 as well as by interpretation of CPTU pore pressure profiles.

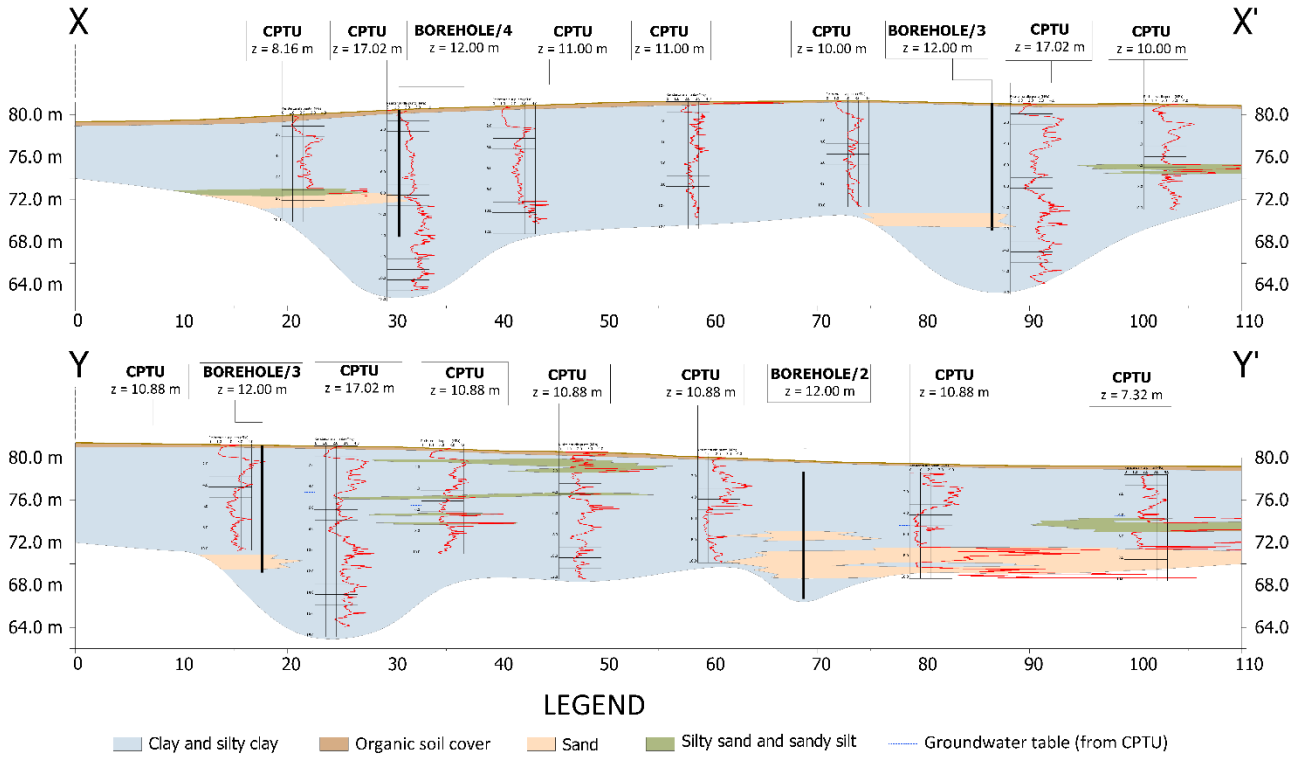

Figure 8.2. CPTUs profiles and CPTU-based soil classification for two main characterized section.

Remodelled samples were then used to derive textural and physical soil properties; particle size distribution is based on the fractions of sand, silt and clay of the samples following USCS classification. The laboratory experimental programme included a significant number of tests for the determination of basic physical properties of soils, Atterberg limits, particle size distribution, oedometer tests, in conjunction with conductivity tests for the estimate of electrical resistivity and conductivity parameters of sediments. Classification test conducted on undisturbed samples, deriving from the principal lithotype, evidenced for the main unit a fine-grained soil percentage around 95% (35% silt and 60% clay), characterized by a PI ≅ 55%. Estimated basic physical properties for the main subsoil layer are listed in table 8.1.

γ_d	PL	LL	IP	G_S	G	S	M	C	e_0
kN/m³	(%)	(%)	(%)	(-)	(%)	(%)	(%)	(%)	(-)
15,76	24	79,4	55,4	2,76	1,7	2,8	35,5	60,0	0,681

Table 8.1 – Estimated soil basic physical properties.

Classification test conducted on disturbed sample, deriving on BH4 at depth 1.8m – 2.0m evidenced a less pronounced presence of clayey fraction, but still typical for fine-grained soil (57% silt, 33% clay), characterized by a a PI ≅ 27%. The PL is 18% and the LL is about 45%; G_S and unit dry weight average measured values are 2.75 and 16.5 kN/m³, respectively. Of interest for the topic of this thesis, soil's retention and hydraulic properties have been carefully studied in laboratory, performing two set of measurement using Evaporation Test (EVT) in conjunction with Dew Point Method (DPM). Soils samples have all been collected at depths between 1.90 m and 3.30 m, deriving from the same lithotype. The set of retention measurements were obtained combining result from two different tests conducted in a complementary suction range. Firstly, evaporation test has been conducted: a saturated sample, enclosed in cylindrical steel ring, has been placed on a high-precision balance monitoring the evaporative water loss; simultaneously, pressure head has been constantly measured using mini-tensiometers at 12.5 mm and 37.5 mm height from the sample bottom. Before test execution, Mini-tensiometers and equipment base were refilled with degassed water and then putted under vacuum for 24 h, as suggested by the manufacturer (HYPROP, UMS). Three test repetitions have been conducted on each soil sample, preliminarily saturated at the end of the test; for each repetition, the measuring suction range was approximately 0 – 85 kPa. The mini-tensiometers ceramic tips have a 0.3 µm pore size and therefore cannot block ions; thus, an influence of osmosis on the measurements is negligible because ion concentration differences are equalized quickly. Subsequently, an aliquot of the sample was used to determine the water potential as measured through dew point method ranging from 3 to 75 MPa. According to the manufacturer, the used equipment (WP-4, Decagon Devices) can measure water potential to an accuracy of ± 0.1 MPa from 0 to 10 MPa and 1% from 10 to 300 MPa. The soil samples were equilibrated in the closed chamber at constant temperature in a plastic sample holder (1.4 cm height and 4 cm diameter) at various potentials by wetting the soil with deionized water and letting the water evaporate for different amounts of time. For each soil water potential, three replicates were used. As the dew point method measures the sum of the matric and osmotic potentials, the contribution of the osmotic component has been estimated independently by measuring the water potential of a saturated paste extract; then, the osmotic component of the water potential obtained from the paste extract was assumed to be representative of the conditions of the undisturbed soil samples, following the procedure described in Bittelli and Flurry (2009). The experimental soil water retention data were analysed by fitting to a modified van Genuchten-Mualem model (Ippisch et al., 2006). Equations and parameters adopted in this part of the work to describe soil water retention curves are presented in Chapter 2. The described model was fitted to the various sets of measured retention data, gathered using Evaporation experiments in conjunction with Dew Point methods, in order to evaluate soil water retention curve and its related parameters for each tested sample (Table 8.2). The nonlinear fitting algorithm used has been written in Python language (Bittelli et al., 2015), basing on the minimization of the sum of least squares, as described by Marquardt (1964) and as implemented by Press et al. (1993) translated from the Fortran language. The used code is free source and available on request by the

relative authors (Bittelli et al., 2015). For EVT results, the standard deviations between the three repetition were always <0.05 m^3/m^3, indicating a small variability among replicates for this measuring technique and a good precision. The saturated paste extracts showed no measurable potentials, i.e., the water potential was too close to 0 m H2O, and could not be measured with the WP4-T. Based on these results, it was assumed that the osmotic potential did not significantly affect the total water potential for the studied samples.

Sampling depth	θ_r	θ_s	α_{VG}	n_{VG}
(m)	(m^3/m^3)	(m^3/m^3)	(kPa^{-1})	(-)
3.0 – 3.3	0.00	0.696	0.141	1.136
1.8 – 2.0	0.00	0.53	0.049	1.85

Table 8.2 – Estimated soil main retention properties and sampling depths.

8.1.1 Monitoring system: methodologies and application

A various and diffused monitoring system has been implemented in field for the continuous measurement of unsaturated soil state variables, aiming to study the soil response to electro-osmotic hydration; then, the system has been used for monitoring the seasonal fluctuation of soil suction and water content and to compare the effectiveness of the various probes used. In particular, the typology of instruments adopted have found large application in several agricultural field, for which the thickness of the monitored zone is often limited to the first meter of depth from the ground surface, so characterized by limited difficulties for the installation and efficiency of the probes. With the main purpose to underline the possibility to extend the use of this kind of monitoring system to depths beyond the classical agronomic applications, in this part of the thesis will be provided some outlines of the monitoring system placed in-situ; furthermore, partials data measured subsequently, and so independently, to the original study project will be presented and discussed. Suction and water content measurements have been, then, integrated and compared to laboratory data. It will be so possible to concretely present the possibility for the implementation of a fully comprehensive monitoring system for various geotechnical applications. A typical case is represented by riverbank seepage and stability assessment, which is strongly affected by unsaturated soil state, as largely discussed in the previous sections. However, the complete set of monitoring data and accurate comparison between measurement collected from different types of probes will be overlooked, being out of the framework of this thesis and still matter of debate. In Figure 8.3 is showed a sketched figure for the monitoring system placed in-situ. FDR (Sentek EnviroSCAN multisensory probes) and TDR (TDR100, Campbell Scientific) probes, installed for measuring soil water content at depth ranging from 1.0 m to 3.5 m; tensiometer (Jet Fill) and Heat Dissipation (HD229, Campbell Scientific) probes, installed for measuring soil suction at depths ranging

from 1.0m to 3.0m. Various instruments have been placed at same measuring points, in order to obtain a punctual estimation for soil suction and water content, to be used for the definition of retention properties, and then to effectively assess the reliability of the used probes comparing results obtained on the same monitored variables.

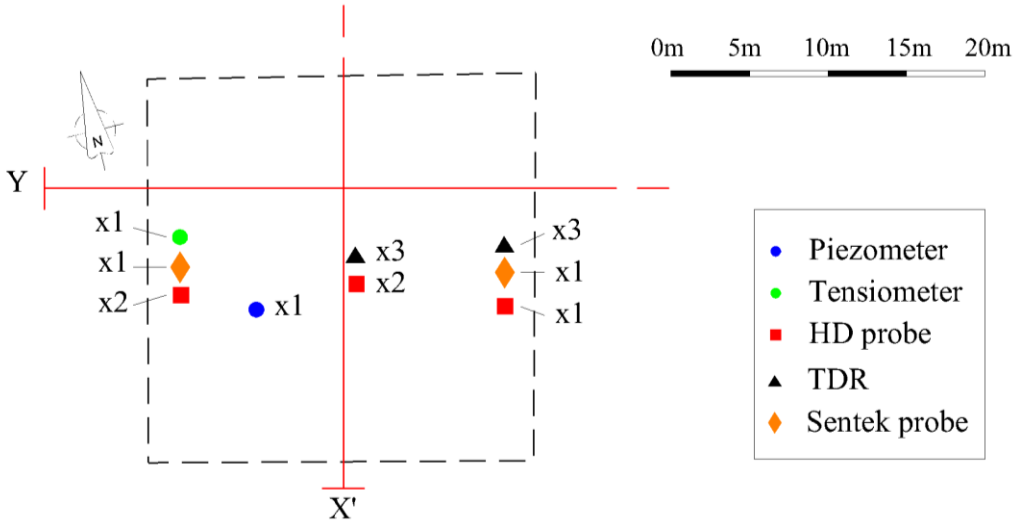

Figure 8.3 Scheme of the monitoring system placed in situ for saturated and unsaturated soil state variables.

Details on soil water content measurement instruments implemented in the monitoring system (TDR, FDR) can be found in Chapter 2 and referenced literature studies. Heat Dissipation Sensor provide an indirect measurement for soil suction using a heat dissipation technique, based on the estimation of the conductivity properties of the medium in which the measurement system is buried. The basic principle for this kind of measurement is the consideration that heat dissipation rate for porous media is highly sensitive to the thermal properties of the various components. In case of soil, it turns to be that heat dissipation process is strongly influenced by the presence, and variability, of water content. For this application, a series of early studies have been conducted on the use of electrothermal method for the estimation of moisture change in soil (Shaw and Baver, 1939; Bloodworth ad Page, 1957; DeJager and Charles-Edward, 1969); however, an exhaustive description of the method has been firstly provided by Phene et al. (1971). The types of sensor used in field is constituted by a cylindrically-shaped porous ceramic body; a thermocouple is located in the middle of the ceramic and heating cylinder, which has diameter of 1.5cmq and length of 3.2cm. The range of measurement of this kind of probe is about -10kPa to -2500kpa (Campbell Scientific, 2009), so it could accurately fit the expected values in soils investigated for large part of the season cycle. Relative flow between the ceramic cup and the surrounding media can exist in correspondence of hydraulic gradients; so, changes in water potential of the soil produces a water flux through the porous ceramic element. The consequent change in water potential and water content of the ceramic matrix causes variations in the

thermal conductivity of the global system. For operative elements, a constant power is supplied, and then dissipated, from the thermocouple located in the middle of the ceramic cup. The dissipation from the resistor probe will be, so, dependent on the thermal properties of the ceramic and water system surrounding the heather. For drier conditions, the dissipation measured in terms of temperature variation in the thermocouple will be reduced due to lower thermal conductivity; opposite behaviour is registered for wetter conditions. The direct output provided by the probes is expressed in terms of differential temperature (ΔT) estimated in a defined time interval from the beginning of the power supply (30s for the study case). For this kind of indirect measurement is, so, required a calibration, which should also be specific for each instrument installed, and is define by (Shiozawa and Campbell, 1990):

$$\Delta T = T_f - T_0 = \frac{q}{4\pi k} ln\left(t_f - t_0\right) \quad (8.1)$$

Where T_f (°C) and T_0 (°C) are temperature values measured in the thermocouple at the end and at the beginning of the measuring interval, k is the soil heat conductivity (W/m/s), q is the rate of heat input (W/m) and t_f (s) and t_0 (s) are the boundaries of the measuring interval. The temperature rises are quick when heat is firstly applied, and then with lower rate for longer heating times.

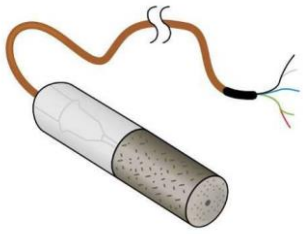

Figure 8.4. Sketch of a Heat Dissipation Matric Water Potential Sensor.

However, the rise in temperature will be affected by T_0; in order to reduce the influence of T_0 on the final data, and even to reduce the effect of probe-to-probe variability, a temperature correction can be accounted for; as suggested by Flint et al. (2002), in the present applications it has been used the normalized temperature, T_{norm}, defined as:

$$T_{norm} = \frac{\Delta T_{dry} - \Delta T}{\Delta T_{dry} - \Delta T_{wet}} \quad (8.2)$$

Where ΔT_{dry} is the change in temperature during measurement for dry sensor, ΔT_{wet} is the change in temperature during measurement for saturated sensor, and ΔT is the measured change in temperature.

8.1.2 Monitoring data for the period 01/2013 – 12/2015

The monitoring system has been operative in field from 01/2013 to 12/2015; in Figure 8.5 are plotted rainfall events intensity, minimum and maximum daily temperature registered in the neighbourhood of the study field. Furthermore, among the available data for this study, three specific time period has been considered and will be referenced for discussion on the site measurement, corresponding to:

- July, 15th to August, 15th 2013, typical for a drying period;
- September, 10th 2014 to December, 30th 2014, typical for a wetting period;
- September, 10th 2015 to October, 20th 2015, typical for a transition period.

These specific time periods are evidenced in Figure 8.5.

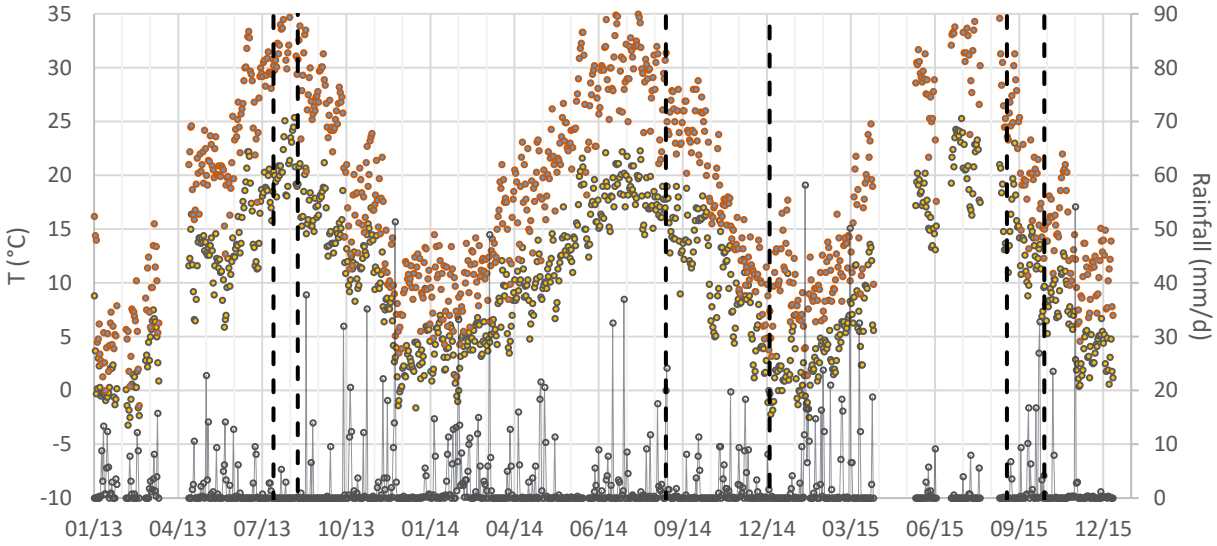

Figure 8.5. Meteorological data collected in the neighbourhood of the monitoring site; in black bold dot lines are marked the time period considered for the output of this thesis.

Firstly, from July, 15th to August, 15th 2013 are expected reduction in soil water content near the soil surface and in the active zone, in general combined with increase in (absolute) values for soil suction. Consistent data are provided from various probes placed in situ, e.g. the TDR probes installed at depth 2.5m and 3.5m in

correspondence of the centre of the monitored area (hereafter referred as TDR1). In combination to these values, it could be useful to report the high suction values registered from Heat Dissipation Probes installed at limited distance from the TDR1. None significant rainfall event was registered for the previous 20 days, so wetting process are to be considered not part of the hydrological process in the subsoil for the considered period (Figure 8.6 to 8.8). In Figure 8.8 are showed, then, values obtained from TDR2 installed at 1.5m and 2.5m depth from ground surface; it is here evident the strong effect of climatic boundaries on the soil hydrological balance for depth at least equal to 1.5m, leading the water content to heavy variations in limited amount of time, due to evaporation and infiltration process. It is worth to notice that the absence of significant vegetation lead to disregard the effect of evo-transpiration on the interpretation of the showed monitoring data.

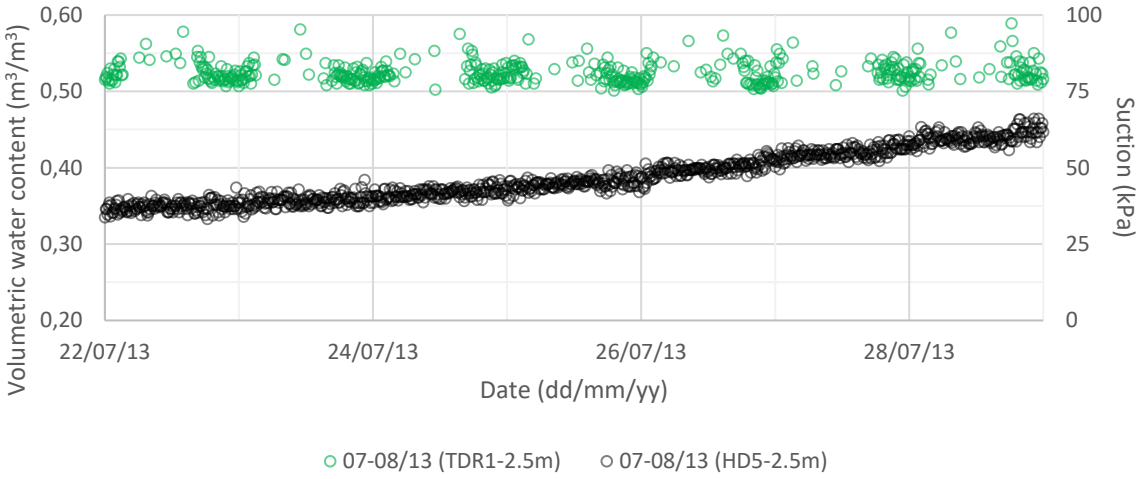

Figure 8.6. Soil water content and suction measured from TDR1 and HD5 installed at 2.5m depth, for the period 17/07/2013 – 29/07/2013.

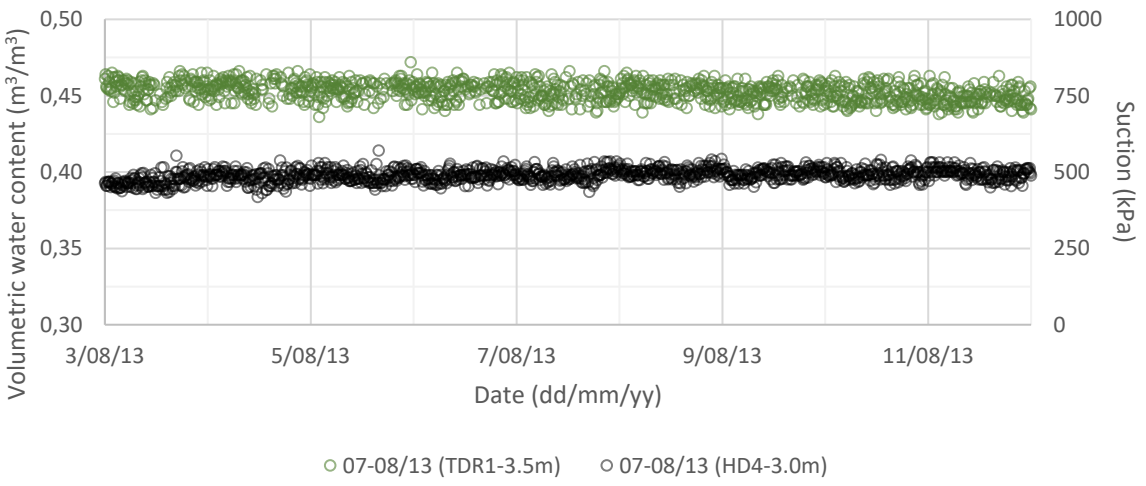

Figure 8.7. Soil water content and suction measured from TDR1 and HD5 installed at 3.0m and 3.5m depth, for the period 03/08/2013 – 12/08/2013.

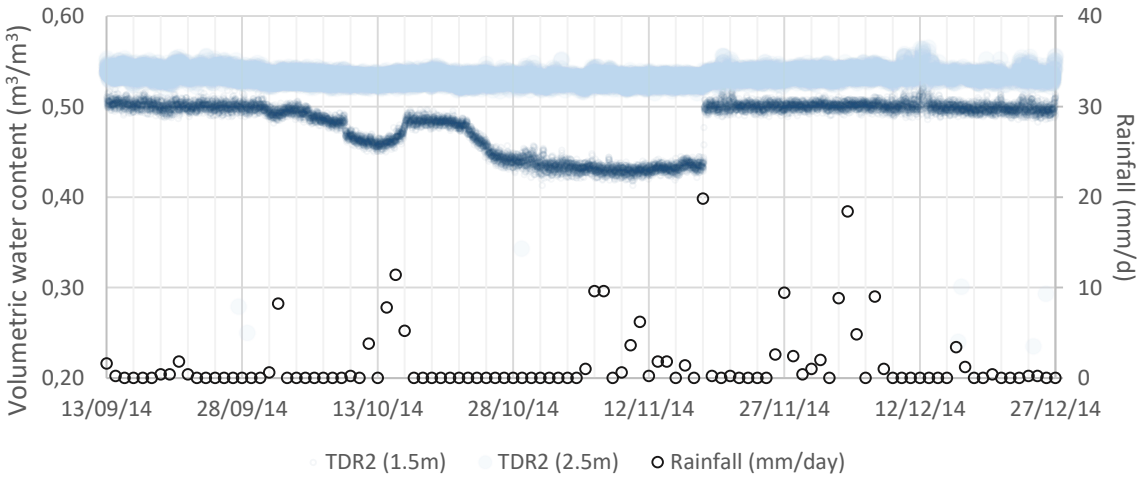

Figure 8.8. Soil water content measured from TDR2 installed at 1.5m and 2.5m depth, and from for the period 13/09/2014 – 27/12/2014.

For the third elapsed time period, soil suction and water content data collected from TDR2 and HD2, both installed at 2.5m depth from the ground surface, are plotted in Figure 8.10. For the considered time period, the reduction of soil water content is rather correspondent to the increase in (absolute) suction values; this, however, seems not to be led by the atmospheric conditions.

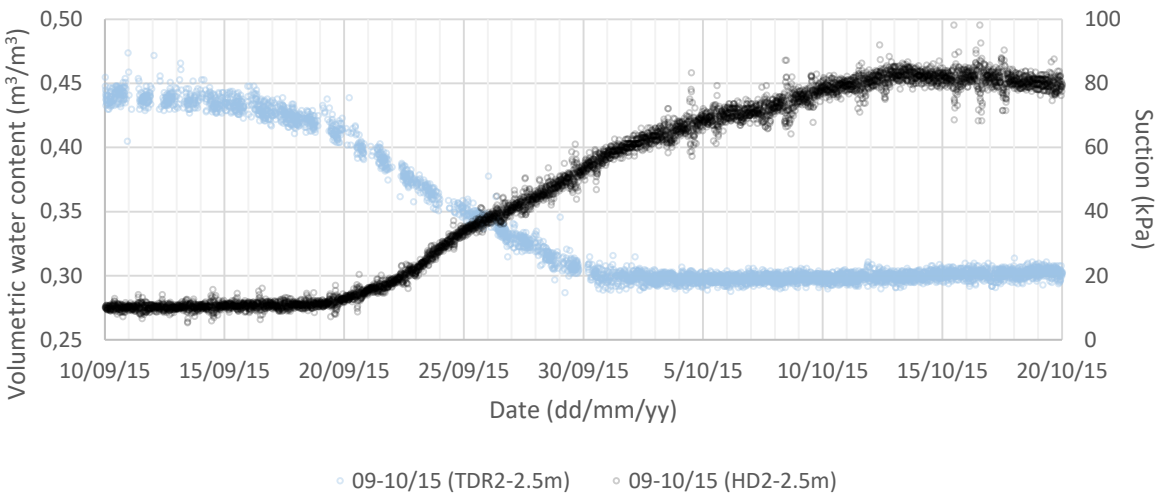

Figure 8.9. Soil water content and suction measured from TDR1 and HD5 installed at 2.5m depth, for the period 10/09/2015 – 20/10/2015.

Furthermore, the equilibration values of soil suction and water content, that seems to be reached at the end of the considered period, seems to underestimate the retention properties of the studied silty clay soil. This last consideration could be clarified considering that in correspondence of the monitoring volumes of TDR2-HD2, have been identified a weighty silty sand and sandy silt layer. Pairs of water content and matric suction measured in situ at the same depth are compared to retention curve obtained in the laboratory. In particular, both main drying retention curves obtained from soil sampled at depth from 1.8m – 2.0m and 3.0m – 3.3m are plotted. A significant remark is the soil heterogeneity evidenced both from laboratory and field data.

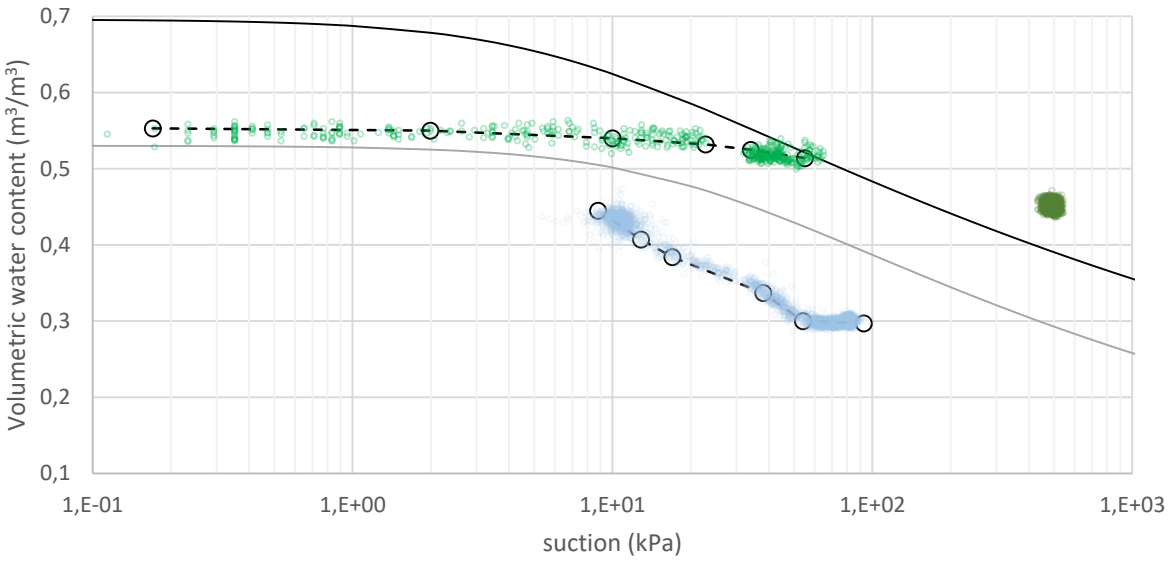

Figure 8.10. Soil water retention curve in drying paths obtained for different soil lithotypes.

8.2 Experimental study on the hydraulic and retention behaviour for an instrumented earthen water retaining structure

For the determination of hydraulic behaviour for an earthen water retaining structure, as river embankment, and the consequential safety assessment towards local or global collapse mechanism, principal attention and efforts are generally devoted to the soil characterization, the hydrometric level forecasts and the estimation of the rainfall intensity, while in situ measurements usually receive less attention both for standard and advanced practice. However, up-to-dated estimation of suction and soil water content distributions in embankment have a strong influence on the reliability of seepage and stability properties, as also evidenced by the large number of numerical analysis presented in the previous section, and their direct or indirect measurement could strongly improve the trustworthiness of numerical and analytical predictions; in fact, when time variable is considered in the analysis of seepage process, further uncertainties related to initial and boundary conditions and external loads, in addition to the definition of soil parameters (Jommi, 2014). Even considering progress and enhancement achieved in the last decades, demonstrated and verified by the realization of various study cases (Anderson and Kneale, 1980; Ridley et al, 2004; Hughes et al, 2009; Mendes, 2011; Calabresi et al., 2013; Papa et a., 2013; Toll et al., 2016) site monitoring on hydraulic and retention soil behaviour on structure and natural slopes could actually represents a noteworthy tool in safety assessment; however, their implementation in early-warning systems and risk management procedures is actually limited to restricted cases, heavily underused in comparison to their possible applications, so that research projects in this field are topical for advanced geotechnical engineering. Basing on these considerations, a monitoring system for the measurement of actual soil moisture and suction in the unsaturated silty soils of a river

embankment has been designed and is going to be fully implemented, with the purpose of linking the collected data to the boundary conditions and hence obtaining a more reliable estimate of the failure probability for the riverbank section under investigation. In this section, the main features regarding monitoring apparatus are discussed, focusing on installation and serviceability issues.

8.2.1 Experimental site and monitoring system

The embankment section selected for the implementation of the monitoring is part of the river Secchia earthen water retaining structure, placed approximately 15 km downstream to the section collapsed on January, 19th 2014, in direction of the Po River. Various factor guided the selection; firstly, the accessibility of the crest and bank of the sector, which is not always completely guaranteed in terms of service and facilities. Then, the zone afferent to the selected section has been interested by an earlier monitoring system, which aim to estimate soil water content and water pressure by means of ADR and piezometric measurements, respectively. In addition, the neighbourhood of the selected sector has been previously involved in various operations aiming to improve the safety towards under seepage mechanisms. Even if these operations do not interested directly the section designated for the present studies, they all contribute to provide a sufficient level of knowledge and confidence with riverbank and foundation soils properties, hydrological features for the embankment sector, which could be used as preliminary information for the first hypothesis on the monitoring design. In regard to the specific embankment geometry, revealed by means of DTM processing and direct measurements (Figure 8.11) it was clear that, in correspondence of high-water event, the riverbank soil would be interested by remarkable flow seepage induced by river hydrometric level variation, due to the relatively limited shoulder width, if compared to other part of the same embankment system. With this, it should be so expected for the considered section the eventuality to efficiently monitor the unsaturated soil state variable both in drying and wetting paths, gaining useful information on the hysteretic riverbank soil behaviour from site measurements. In Figure 8.11 is, then, pointed out the embankment area (in shaded) interested by the designed monitoring system, mainly located above a reasonable phreatic line (evidenced in blue bold line) that could be determined during a high-water event; part of the instruments is, instead, installed in the embankment shoulder, which hydraulic and retention properties influence both the seepage characteristic of the riverbank for rapid event and the stability performance of riverside slope. In blue dotted line is showed a 1:4 tilted line, representing a saturation line that is frequently assumed in preliminary design situation.

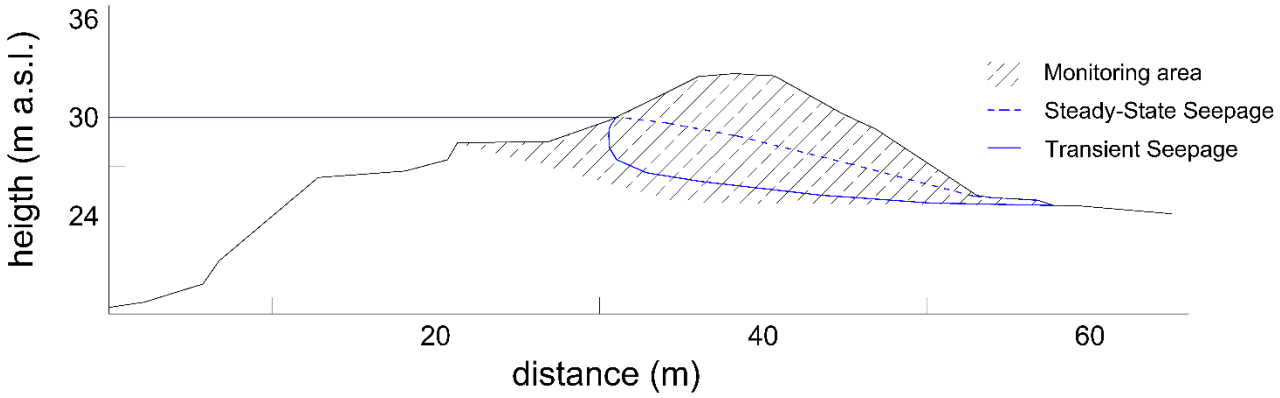

Figure 8.11. Schematic geometry of the riverbank selected for monitoring; in hatch (shaded), is evidenced the designed monitoring area; in blue dotted and straight lines are showed the phreatic lines for preliminary design situation (steady-state seepage) and a realistic transient seepage condition, respectively.

Aiming to improve the knowledge on soil stratigraphy and geotechnical properties for the area of interest, a series of four CPTU test have been performed. In specific, two CPTU test have been conducted from the riverbank top and two from the embankment shoulder, up to depths ranging from 25m to 15m from the surface level. Three main soil unit have been, so, identified for the section, namely: Unit A, composing the embankment, consisting of a complex alternation of silt and sandy silt, with different thin sandy layers, with thickness of about 8m from the crest level; Unit B, composing the embankment foundation, consisting of interbedded silt and silty clay with thickness ranging from 10m to 6m, lower in correspondence of the flood channel; Unit C, composing the subsoil, consisting of a primarily clayey layer, present up to the maximum investigated depth. For the CPTUs results interpretation, semi-empirical correlation proposed by Robertson (2009) was used. Remodelled and undisturbed samples were taken from each section to assess geotechnical soil properties. The main physical, mechanical and laboratory properties determined from site and preliminary laboratory investigation are listed in Table 1, for different depths and soil units. Classification test conducted on disturbed samples evidenced a fine-grained soil percentage in Unit A, composing the riverbank soil, between 10% to 20%, characterized by a PI generally around 10% and by a natural water content lower than w_L up to 5m depth from top surface. Soil riverbank retention and hydraulic properties have been preliminary studied in laboratory through a series of evaporation tests conducted on remodelled samples for various depths using different initial void ratio values ranging from 0.90 to 0.65.

Depth (m)	sand/silt (%)	silt/clay (%)	w_P (%)	w_L (%)	G_S (-)
1.8 – 2	70.6	20.1	16.70	29.43	2.65

2.8 – 3	62.2	16.2	19.31	29.90
3.8 – 4	61.7	15.4	18.11	30.03
4.5 – 5	57.2	7.0	18.71	34.70

Table 8.3. Physical, mechanical and hydraulic properties from site and laboratory investigations.

8.2.2 Soil water content and suction probes used for monitoring system

The possible and combined knowledge for soil suction and water content in various points of the riverbank would provide a series of significant benefits for the study of stability, hydraulic and retention characteristics for the instrumented riverbank, which is useful to briefly report in this section. As discussed in different part of this work, suction is widely intended as principal unsaturated soil stress variable (Fredlund and Rahardjo, 1992), while water content is usually accounted in various failure mechanism (Vanapalli et al., 1996; Fredlund and Vanapalli, 2002). Then, soil hydraulic conductivity is directly affected on both these variables, influencing local and global flow paths and properties. Pairs of soil water content and suction, would so directly used for the estimation of riverbank stability and seepage assessment. In particular, a possible estimation of these variables, by means of direct and indirect site measurements, would so be either implemented in numerical analysis as initial conditions for seepage analysis as well as for stability analysis, and for data calibration. Monitoring data, furthermore, would be suitable for soil hydraulic and retention properties evaluation, in combination and comparison with laboratory test results. These concepts and purposes have found finds a direct application in the design and installation of a monitoring system on river Secchia embankment. On the basis of the soil characterization, preliminary and specific for the selected section, the monitoring system has been designed and, partially, installed, reaching depths up to 7m using both soil suction and moisture probes. Hydrometric levels are derived using data from river stream gauges. For the determination of soil water content at significant depths for the riverbank, the GS3 probes (Decagon Devices Inc.) have been selected and installed in situ. These sensor uses the measure of the dielectric permittivity of the media in which are placed through the generation of electromagnetic field, by supplying a 70MHz oscillating wave to the sensor prongs that charges according to the water content of the surrounding soil.

The use of calibration equation depending on the type of charge, soil lithology and prongs length is needed for the interpretation of output data (Decagon Devices, 2016a); in order to improve default accuracy, and to adapt the readings to the applications of the present study, user calibrations have been performed in laboratory for a typical installed probe. A total of five GS3 have been placed in situ, in the neighbourhood of the suction measuring points defined by the positions of MPS-6; in specific, three probes have been installed

from the top of the riverbank at depths ranging from 2.3m to 7.1m, while two probes have been installed in the embankment shoulder at depths ranging from 0.7m to 2.2m.

Two different installation procedures have been used for these instruments; in details, the probes to be installed at the bottom of the borehole have been thrust in soil using metallic beams, obtaining a vertical direction for the metallic prongs. Differently, the intermediary probes have been placed soil from the vertical side of the boreholes by means of an experimental equipment able to push the prongs through a lever system connected to extension shafts, obtaining a horizontal direction for the metallic prongs up to depth of 5m from surface level. The installation phases have been inspected by means of a pipeline video inspection, which confirm the achievement of the designed target and the correct execution of the site operations.

Soil suction at different point has been determined using MPS-6 probes (Decagon Devices Inc., 2016b). These instruments perform an indirect estimation of the water potential of soil through a direct measure of the dielectric permittivity of a solid matrix which constitutes the monitoring point. This quantity is strongly dependent on the amount of water present in the ceramic disc pore space of the probe, which knowledge allow to determine the water potential of the surrounding soil, when hydraulic equilibrium is reached. So, MPS-6 measures the water content of porous ceramic discs and convert the measurement to water potential using the known characteristic curve of the ceramic porous media. The instrument accuracy in of about 10% of reading + 2kPa over a range -9kPa to -100kPa, and measured can be extended for the complete path to air-dry conditions up to -100MPa (Decagon Devices, 2016a). A total of five MPS-6 sensors have been installed in situ; in specific, three probes have been installed from the riverbank top at depths ranging from 3.0m to 7.0m, while two probes have been installed in the embankment shoulder at depths ranging from 0.9m to 2.7m. In order to properly reach the designed depths, to protect the instruments and still ensuring reliable measures, the MPS-6 were preliminary placed in separate cylindrical soil volumes, made by material extracted from the riverbank, which dimensions could fit the borehole drilled for the instrumented vertical. As for what concerned the instruments used for the Ozzano field test, although the proposed tools are widely used in agronomy as well as in geotechnical engineering, they have not been typically used for monitoring riverbank silty soils at multiple depths and in association with relevant stability analyses. Furthermore, in situ measurements of soil suction and water content at different depths of geotechnical interest (from 1m to 10m) still represents one of the main tasks for practical applications, and promote to investigate different installation methodologies in the framework of this project. Parallelly to site measurement and laboratory test, numerical simulations have been performed for the interpretation of registered data, using geometrical and geotechnical information collected for the specific site.

8.2.3 Laboratory test: methodology and applications

Laboratory test represent the major direct source of knowledge on unsaturated soil behaviour, allowing to monitor different state variables operating in controlled conditions; nevertheless, standard laboratory test are often not exhaustive and novel applications are required and, partially, performed in this study (hysteresis). Aiming to perform a preliminary study for the determination of hydraulic and retention properties for riverbank soil, a series of Evaporation test have been performed; details on the used laboratory equipment are provided in section 8.1. At this stage, test have been conducted on disturbed and reconstituted samples from the river embankment. Specific procedures for the determination of soil properties both in drying and wetting paths has been settled has follows; for each considered sample, Evaporation test have been performed keeping a slow flux rate in the soil sample and with the external boundary. The method consists in the use of two tensiometers to measure matric suction of the soil column at two depths, while any change of soil mass due to the loss of moisture was monitored by an electronic balance (Figure 8.12). Through this operation, achieved limiting the evaporation rate from the soil surface, it was possible to obtain a rather uniform suction profile among the measuring point (¼ and ¾ from the soil base). Past researches (Romano and Santini, 1999; Tarantino et al., 2008), in fact, has shown that during evaporation, a very dry layer of low hydraulic conductivity would develop quickly near the soil surface, making the further increase in suction below this surface much harder. This would hence create a highly nonlinear suction profile along the soil column, leading to a questionable soil mass measurement (which represents the overall specimen) to be related to the water potential measurement (which represents only two points of the specimen). The use of slow evaporation is, so, needed to justify the uniformity of suction within the soil sample, so that the two independent measurements can be linked to construct a SWRC. However, the disadvantage of this procedure is the significant amount of time required to reach cavitation of the mini-tensiometers ceramic cup, of about 100kPa in terms of soil suction.

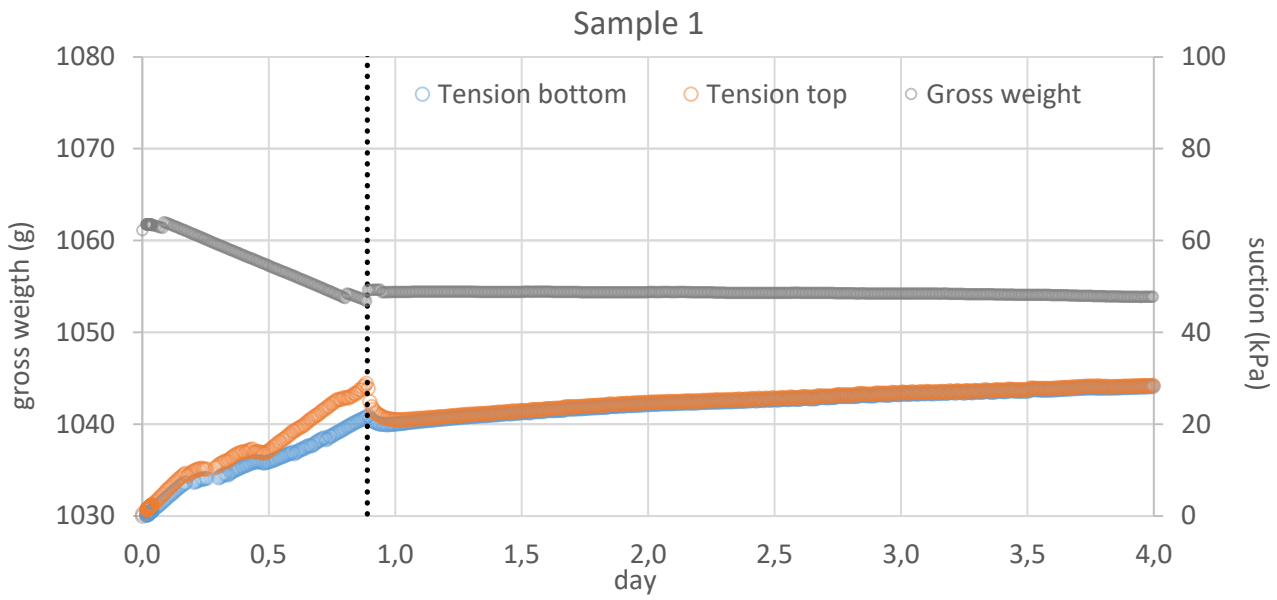

Figure 8.12. Evaporation test in free (up to 0.89d) and constricted slow conditions (further than 0.89d).

Aiming to study the effect of hysteresis on retention properties, a series of wetting-drying paths flow have been defined for the soil sample, focusing on suction varying from -9kPa to -90kPa (Figure 8.13). In approximating the curves between the main and drying curves, various modelling of hysteresis has been considered in water retention behaviour (Jaynes, 1984); assuming linear trend (in semi-log scale) for the considered soil suction range, the wetting-drying paths are located on scanning curves, and characterized by values for Lk ranging from -1.01 to -0.58. Furthermore, due to simplicity, linear scanning curves are often used in numerical analyses (Liu et a., 2016). In Figure 8.13 is plotted, furthermore, the main drying curve (in black dot line) obtained from slow evaporation test on soil sample with initial void ratio $e_{0,I}$ = 0.646,, basing on the minimization of the sum of least squares (Marquardt, 1964) of experimental data. Then, the second repetition of the evaporation test performed on the same textural soil sample characterized by higher initial void ratio ($e_{0,II}$ = 0.755). Results for the retention parameters of the van Genuchten model, obtained for both tested samples, are listed in table 8.3. In particular, the main drying curve for the soil characterized with higher initial void ratio is provide lower values of water content being equal the measured suction, as expected.

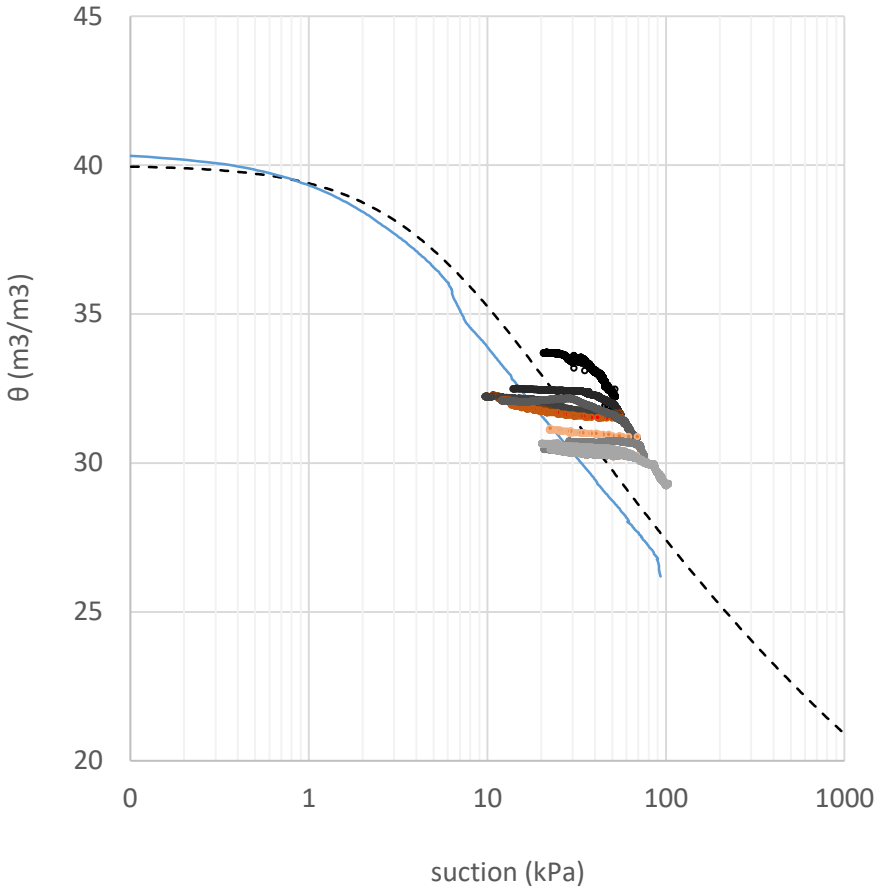

Figure 8.13. Soil water retention data obtained from laboratory test on wetting (in red to orange dots) and drying (from black to grey dots) for slow flux of rate in the soil sample; main drying curve is plotted in black dashed line; second repetition in blue continuous line.

Sampling depth	Repetition	e_0	θ_r	θ_s	α_{VG}	n_{VG}
(m)	(-)	(-)	(m^3/m^3)	(m^3/m^3)	(kPa^{-1})	(-)
4.7 – 4.9m	I	0.646	0.05	0.385	0.036	1.231
4.7 – 4.9m	II	0.755	0.05	0.405	0.018	1.151

Table 8.3 – Estimated soil main retention properties, initial void ration and sampling depths.

However, it should be also stated that the use of this laboratory equipment for hydraulic and retention hysteresis characterization could lead to frequent erroneous considerations; in fact, due to transient process established during the wetting phase, the use of punctual suction measurement in combination with a unique and, hypothetically, homogeneous value for soil water content could be inappropriate, not properly taking into account the effective distribution of water content in soil sample, which could be rather irregular; to

overcome these types of errors, for each wetting branch, an appropriate equilibration time should be considered for, then, consistently coupling the punctual suction measures with a unique value for soil water content (Figure 8.14).

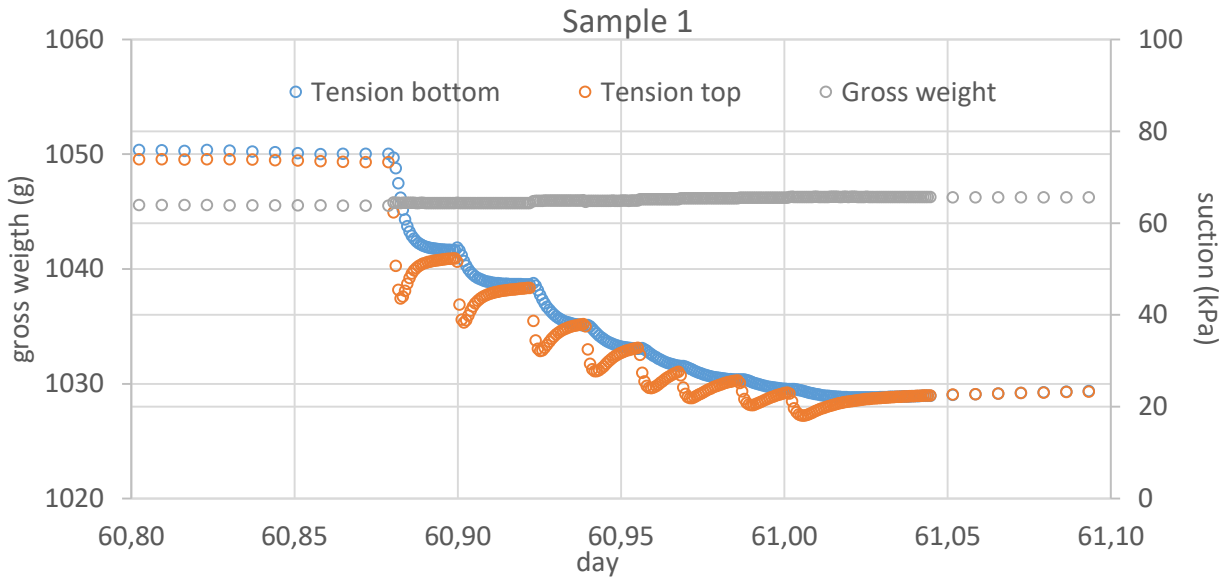

Figure 8.14. Results from laboratory test for soil hydraulic and retention hysteresis; detail on wetting process.

An alternative methodology is the use parameter estimation analysis of the evaporation method for determining soil hydraulic properties by means of inverse solution (Kool et al., 1987; Šimunek et al., 1998; Ritter et al., 2003).

8.2.4 Preliminary numerical analysis for riverbank seepage and stability assessment

For a better insight on the riverbank instability mechanism induced by soil water content and suction variations due to high water events, a series of bi-dimensional transient seepage and slopes stability analyses has been performed, using a combination of VADOSE/W and SLOPE/W softwares (GeoSlope International Ltd, 2007). The hydrometric data used in this study were collected on the Secchia river from the stream gauge at Ponte Motta (Lat. 44.747546, Lon. 10.98734) north of the city of Modena, with an hourly sampling frequency; while the relative humidity, temperature and precipitation data were recorded by a meteorological station at Cortile di Carpi (Lat. 44.778387, Lon. 10.971285), about 4.5km away. Significant results of the numerical analysis are showed in Figure 8.15. In details, a series of 2D seepage analysis have been performed using the commercial code Vadose/W (Geo-Slope International Ltd, 2008), which use hydraulic and climatic boundary conditions to perform hydro-thermal unsaturated flow analysis. Different hypothesis on initial conditions have been tested, aiming to get a suitable comparison with the experimental

data. Pore water pressure and suction distribution computed at specific time-step of the seepage analysis have been, then used to perform deterministic Limit Equilibrium Analysis using the numerical code Slope/W (Geo-Slope International Ltd, 2008). In specific, in Figure 8.15 are plotted the isolines determined for seepage analysis, using as initial conditions a water table 1.5m below the ground level and hydrostatic suction increment (in absolute value) above the phreatic line up to a value of -5m for pressure head, and boundary conditions measured from September, 09th 2015; differences in pore pressure between two adjacent is 10kPa. The safety map, representing the area of the most critical slip surfaces identified through geometric boundaries, is then showed. Results are referred to the November, 23th 2016, and, even being preliminary and strongly dependent on the soil hydraulic and retention parameters, seems to give an acceptable agreement with the site measurement for the considered period in this phase of the study.

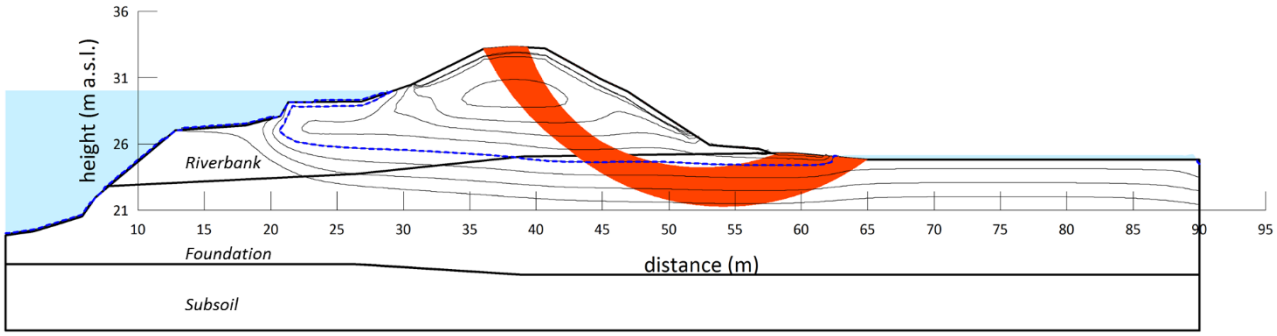

Figure 8.15. Results of seepage, in terms of isolines, and stability analysis, in terms of safety map.

Further developments

In the present section, observations, remarks and partial outcomes for the monitoring activities of a full-scale river embankment have been presented and discussed. Site investigation and preliminary geotechnical characterization guided the installation of various probes for the indirect measurement of soil water content and suction at different significant depths for the earthen structure both in riverbank and embankment shoulder. Standard installation procedures have been improved using novel and experimental techniques, for which details are provided. The data collected, even being prelaminar, are however able to provide useful indication on the unsaturated soil state for the river embankments, representing an important source of knowledge to define seepage and stability characteristic for the considered structure. Further studies will be devoted to the validation and verification of collected data, using site and laboratory direct measurement for soil suction and water content, to a more accurate soil hydraulic and retention characterization and to the interpretation of site measurements under significant high-water events. The combined and complementary use of laboratory test, numerical analysis and field measurements represent a key point for this research project, and seems the best method to account all unsaturated soil related issues.

9 Concluding remarks and further research activities

The geomechanical analysis of river embankments is a key aspect in geohazard assessment and represents a topical issue for applied geotechnical researchers; these structures are usually characterized by unsaturated soil conditions for all their operative lifetime. Changes in soil water content and suction are induced by time-variable hydraulic and climatic boundary conditions with generally seasonal occurrence, and can produce significant loss of strength and former modifications to soil hydraulic and retention properties; a critical combination of these factors, can induce, or trigger instability, loss of serviceability or, at least, important modification to the safety margins towards failure mechanism which was originally estimated. In addition, river embankments are characterized by significant variability in soil hydraulic and mechanical properties; in general, this aspect is emphasized by the general use of soil availability on-site for the filling material due to their large extension, while for other typical earthen structures the optimal characteristics of the building material could be properly selected and frequently accessible and argues significant limitations to the soil properties requirements.

Nonetheless, due to the large amount of geotechnical issues involved, both stability assessment and design for river embankment sectors are usually performed in rather to extreme simplified conditions, e.g. neglecting the soil parameters uncertainties and heterogeneities, disregarding unsaturated soil related issues and generally assuming steady state seepage conditions.

Aiming so to overcoming the large use of simplistic hypotheses typical for actual standard and recommendations, an experimental and numerical study have been performed for the reliable assessment of river embankments. In this framework, special attention has been given to the effect of variable water content in riverbank safety evaluation; the investigations have been carried out through three complementary parts: numerical analysis, laboratory test and in situ activities. Seepage and stability numerical analysis have been performed using data collected on different riverbank sectors in Italian basins, by means of finite element and limit equilibrium methods; heterogeneity and uncertainty on soil properties and initial and boundary conditions have been taken into account using both simplified and more rigorous approach. Laboratory test for saturated and unsaturated hydraulic soil characterization have been performed and interpreted, comparing standard procedures and advanced practices.

A methodology for assessing the stability conditions of existing water retaining structure was presented and discussed. The proposed approach is based on a mathematical study of riverside water level measurements, which aims to individuate a hydrometric spectrum for a specific site. Through this operation, the frequency range included in the data, and its principal characteristics, can be identified in order to obtain a characteristic range of variation of the input data with respect to typical seasonal trends. Using this synthetic description, a wide series of transient seepage numerical analysis have been performed, to investigate the effect of the

time history of the hydrometric water level on the hydraulic response and on the stability evaluation of the slopes of the banks.

The definition of initial conditions represents a crucial point for transient seepage analyses and is a fundamental issue in safety assessment; this influence has been deeply studied by means of numerical analysis. Various methodological procedures for their definition has been tested and compared and the effectiveness of using sophisticated vs simplistic hypothesis has been discussed.

A realistic riverbank stability evaluation has been performed accounting for all source of uncertainty related to soil properties in probabilistic analysis, for a reliable definition of Probability of Failure. The probabilistic analyses have been performed using the Point Estimate Method, in comparison with the more accurate Monte Carlo method. The combined effect of soil hydraulic, retention and strength properties have been accounted for stability assessment. Quantification of the contribution of the various source of uncertainties evidence the significant effect of the variability related to hydraulic and retention parameters on safety factor variance. The two adopted probabilistic methodologies have been compared in relation to their implementation procedures, evidencing the benefit of using the uncertainty propagation PEM for directly accounting various source of variability, the possibility to use MCM for indirectly but effectively accounting the effect of hydraulic and retention properties variability, but even the criticism on the basic assumption and implementations of the two methods.

The various adopted methodologies can be a useful tool to forecast and assess the vulnerability conditions for existing riverbanks, with the possibility to achieve good predictive models. The combined and complementary use of laboratory test, numerical analysis and field measurements, in general conceived to study the effect and contribution of retention properties into the stability evaluation of earthen water retaining structures, represent a key point for this research project.

The present Thesis study constitutes a remarkable guide to the design of a monitoring system focused on the soil suction and water content measurements, recently implemented on river Secchia embankment. This research activity, still ongoing, is conceived to the estimation of soil hydraulic and retention behaviour for the instrumented riverbank, providing fundamental data for reliability of numerical analyses.

The final aim is to combine monitoring and forecasted hydro-meteorological data with numerical probabilistic analysis to provide a flood early-warning system, to be implemented in the present risk assessment strategy, able to define in continuous progressive alert level for potential riverbank failures.

References

Abramson L.W., Lee T.S., Sharma S., Boyce G.M. 2001. Slope Stability and Stabilization Methods. 2nd edition, John Wiley & Sons.

Adger W.N. 2006. Vulnerability. Global Environmental Change. 16: 268–281.

Ahmadabadi M., Poisel R. 2015. Assessment of the application of point estimate methods in the probabilistic analysis of slopes. Computers and Geotechnics, 69: 540-550.

Alén C. 1998. On probability in geotechnics – Random calculation methods exemplified on slope stability analysis and ground-superstructure interaction. Doctoral thesis. Chalmers University of Technology, Gothenburg, Sweden.

Anderson M., Kneale P.E. 1980. Pore water pressure and stability conditions on a motorway embankment. Earth Surface Process, 5: 37-46.

Aysan, Y.F., 1993. Vulnerability assessment. In: Natural Disasters: Protecting Vulnerable Communities. Thomas Telford, London, pp. 1 – 14.

Baecher G.B., Christian J.T., 2003. Reliability and Statisctics in Geotechnical Engineering. John Wiley & Sons.

Baldassarre G., Viglione A., Carr G., Kuil L., Salinas J.L., Bloeschl G. 2013. Socio-hydrology: conceptualising human-flood interactions. Hydrology and Earth System Sciences. 17: 3295–3303.

Baroni, G., Facchi, A., Gandolfi, C., Ortuani, B., Horeschi, D., and van Dam, J. C. 2010. Uncertainty in the determination of soil hydraulic parameters and its influence on the performance of two hydrological models of different complexity. Hydrology and Earth System Sciences, European Geosciences Union, 14(2): 251-270.

Becker R., Huebner, C. and Stacheder, M. 2006. Electromagnetic simulation of time domain reflectometry probes: simplified approaches to assess calibration curves, sensitivity, field extent and transient response. Proceedings TDR 2006, Purdue University, IN, US.

Bell J.P., T.J. Dean and M.G. Hodnett, 1987. Soil moisture measurement by an improved capacitance technique: Part II. Field techniques, evaluation and calibration. Journal of Hydrology. 93: 79-90.

Benjamin J.R., Cornell C.A. 2014. Probability, Statistics and Decision for Civil Engineers. Doover Publications, NY.

Benson, C.H. Modeling Unsaturated Flow and Atmospheric Interactions. Theoretical and Numerical Unsaturated Soil Mechanics. Springer Proceedings in Physics, 113: 187-201.

Bergland, GD. A guided tour of the fast Fourier transform. IEEE Spectrum, 1969, 6: 41-52.

Bhattacharya, G., Jana, D., Ojha, S. & Chakraborty, S. (2003). Direct search for minimum reliability index of earth slopes. Computers and Geotechnics, 30(6): 455–462.

Birkmann, J., 2006: Measuring vulnerability to promote disaster-resilient societies: conceptual frameworks and definitions. In: Measuring Vulnerability to Natural Hazards: Towards Disaster Resilient Societies [Birkmann, J. (ed.)]. United Nations University Press, Tokyo, Japan, pp. 9-54.

Bittelli M., Campbell G.S., Tomei F. 2015. Soil Physics with Python. Oxford University Press.

Bittelli M., F. Salvatorelli, and P. Rossi Pisa., 2008. Correction of TDR-based soil water content measurements in conductive soils. Geoderma 143:133–142.

Bittelli M., Flury M. 2009. Errors in water retention curves determined with pressure plates. Soil Science Society of America Journal, 73(5): 1453–1460.

Bittelli M., Ventura F., Cambell G.S., Snyder R.L., Gallegati F., Rossi Pisa P. 2008 Coupling of heat, water vapor and liquid fluxes to compute evaporation in bare soils. Journal of Hydrology, 362: 191-205.

Bittelli, M., 2011. Measuring Soil Water Content: A Review. Horttecnology, 21, 293-300.

Bloodworth M.E., Page J.B. 1957. Use of thermistors for the measurement of soil-moisture determinations. Soil Scientific Society of America, 21:11-15.

Bond A and Harris A. Decoding Eurocode 7. CRC Press, 2008; London, UK.

Calabresi G., Coleselli F., Danese D., Giani G.P., Mancuso C., Montrasio L., Nocilla A., Pagano L., Reali E., Sciotti, A. 2013. A research study of the hydraulic behaviour of the Po river embankments. Canadian Geotechnical Journal, 50(9): 947-960.

Campbell Scientific. 2009. 229 Heat Dissipation Matric Water Potential Sensor. Instruction Manual. Revision 5/09.

Casagli N., Rinaldi M., Gargini A., Curini A. 1999. Pore water pressure and streambank stability: results from a monitoring site on the Sieve River, Italy. Earth Surface Process and Landforms, 24: 253-277.

Celia M.A., Bouloutas E.T., Zarba R.L., 1990. A general mass − conservative numerical solution for the unsaturated flow equation. Water Resources Research. 26(7): 1483-1496.

Cheng Y.M., Li L., Liu L.L. 2015. Simplified approach for locating the critical probabilistic slip surface in limit equilibrium analysis. Natural Hazards and Earth System Sciences, 15:2241-2256.

CIRIA, Ministry of Ecology, USACE. The International Levee Handbook (C731). CIRIA, 2013; London, UK.

Congdon P. 2007. Bayesian Statistical Modelling. John Wiley & Sons Ltd, 2nd edition.

Construction Industry Research and Information Association (CIRIA). 2013. The International Levee Handbook. British Library Cataloguing, London, UK.

Cooley, JW and Tukey OW. An algorithm for the machine calculation of complex Fourier series. Mathematics of Computation, 1965. 19: 297-301.

Davis E.H., Booker J.R., 1973. Some applications of classical plasticity theory for soil stability problems. In Proceeding of Role Plasticity in Soil Mechanics, Cambridge , England, 24-43.

Dawson E.M., Roth W.H., Drescher A. 1999. A slope stability analysis by strength reduction. Géotechnique, 49(6): 835-840.

Dean T.J., J.P. Bell and A.J.B. Baty, 1987. Soil moisture measurement by an improved capacitance technique: Part I. Sensor design and performance. Journal of Hydrology. 93:67.

Decagon Devices. 2016a. GS3. Water Content, EC and Temperature Sensors. Decagon Devices, Inc. Pullman, WA, United States.

Decagon Devices. 2016b. MPS-2 & MPS-6. Dielectric Water Potential Sensors. Decagon Devices, Inc. Pullman, WA, United States.

Delager J.M., Charles-Edward J. 1969. Thermal conductivity probe for soil-moisture determinations. Journal of Experimental Botany, 20(62): 46-51.

Delage P., Tarantino A., Romero E. 2008. Recent developments in the techniques of controlling and measuring suction in unsaturated soils. In Proceedings of the 1st European Conference, E-UNSAT 2008, Durham, United Kingdom, 33–52.

Doocy S., Daniels A., Murray S., Kirsch T.D. 2013. The human impact of floods: a historical review of events 1980–2009 and systematic literature review. doi: 10.1371/currents.dis.f4deb457904936b07c09daa98ee817.

Duncan J.M. 1996. State of Art: limit equilibrium and finite-element analysis of slopes. Journal of Geotechnical Engineering, ASCE, 122(7): 577-596.

Duncan J.M. 1999. Factors of Safety and Reliability in Geotechnical Engineering. The 7th Spencer J. Buchanan Lecture, University Drive East, TE.

Duncan, J.M. 2000. Factors of safety and reliability in geotechnical engineering. Journal of Geotechnical and Geoenvironmental Engineering, ASCE, 126(4): 307-316.

Emergency Events Database – EMDAT. 2016. The OFDA/CRED international disaster database, University Catholic Louvain-Brussels, Belgium. http:// www.emdat.be.

EN 1997-1. Eurocode 7: Geotechnical Design. Part 1: General rules. CEN. 2004.

European Parliament. 2007. Directive 2007/60/EC of the European Parliament and of the Council of 23 October 2007 on the assessment and management of flood risk. Official Journal of the European Union. L.288/27.

Evett S.R. and G.W. Parkin., 2005. Advances in soil water content sensing: the continuing maturation of technology and theory. Vadose Zone Journal 4: 986–991.

Evett S.R., Tolk J.A., and Howell T.A., 2006. Soil profile water content determination: Sensor accuracy, axial response, calibration, temperature dependence, and precision. Vadose Zone Journal, 5, 897-907.

Fellenius W. 1936. Calculation of the Stability of Earh Dams. Proceedings of the Second Congress on Large Dams, 4: 445-463.

Fenton G.A. 2014. Simulations. Stochastic Analysis and Inverse Modelling. ALERT Doctoral School, Aussois.
Ferré P.A., Kachanoski R.G., 1996. Spatial averaging of water content by time domain reflectometry: implications for twin rod probes with and without dielectric coatings. Water Resources Research, 32(2) :271-279.

Feyen L., Watkiss P., 2011. River Floods: The Impacts and Economic Costs of River Floods in the European Union, and the Costs and Benefits of Adaptation. Technical Policy Briefing Note 03.

Flint A.L., Campbell G.S., Ellet K.M., Calissendorff C. 2002. Calibration and Temperature Correction of Heat Dissipation Matric Potential Sensors. Soil Scientific Society of America Journal, 66: 1439-1445.

Frank E., Eakin H., Lopez-Carr D. 2011. Social identity, perception and motivation in adaptation to climate risk in the coffee sector of Chiapas, Mexico. Global Environmental Change. 21: 66-76

Fredlund D.G. 1974. Slope Stability Analysis. User's Manual CD-4,, Department of Civil Engineering, University of Saskatchewan, Canada.

Fredlund D.G., Krahn J. 1976. Comparison of Slope Stability Methods of Analysis. 29th Canadian Geotechnical Conference, Vancouver, British Columbia, 8: 56-74.

Fredlund D.G., Rahardjo H., Fredlund M.D. 2012. Unsaturated Soil Mechanics in Engineering Practice. John Wiley & Sons, Inc.

Fredlund, D.G. and Vanapalli, S.K. 2002. Shear strength of unsaturated soils. Agronomy Soil Testing Manual, Agronomy Society of America, 329-361.

Gabriel J.L., Lizaso J.I., and Quemada M., 2010. Laboratory versus field calibration of capacitance probes. Soil Science Society of America Journal, 74: 593-601.

Gee, G.W., Or, D., 2002. Particle-size Analysis. Methods of Soil Analysis. Part 4. Physical Methods. SSSA Book Ser. 5. SSSA, Madison, WI, 255–293.

Gee, G.W., Ward, A.L., Zhang, Z.F., Campbell, G.S., Mathison, J., 2002. The influence of hydraulic nonequilibrium on pressure plate data. Vadose Zone Journal, 1: 172–178.

Geo-Slope International Ltd. 2008. Seepage Modelling with SEEP/W 2007. Geo-Slope International Ltd., Calgary, Canada.

Geo-Slope International Ltd. 2008. Stability modeling with SLOPE/W 2007. Geo-Slope International Ltd., Calgary, Canada.

Geo-Slope International Ltd. 2008. Vadose Zone Modelling with VADOSE/W 2007. Geo-Slope International Ltd., Calgary, Canada.

Gottardi G., Gragnano C.G. 2016. On the role of partially saturated soil strength in the stability analysis of a river embankment under steady-state and transient seepage conditions. 3rd European Conference on Unsaturated Soils – E-UNSAT 2016, Paris. doi: 10.1051/e3sconf/20160919002.

Gottardi G., Gragnano C.G., Rocchi I., Bittelli M. Assessing River Embankmet Stability Under Transient Seepage Conditions. VI Italian Conference of Researchers in Geotechnical Engineering – CNRIG2016, 158: 350-355.

Gottardi G., Gragnano C.G., Ranalli M., Tonni L. Accounting for the intrinsic variability of unsaturated soil hydraulic parameters in assessing the probability of river bank failure. *Submitted to* Canadian Geotechnical Journal, November, 04th 2016.

Golub G.H., Welsch J.H., 1969. Calculation of Gauss Quadrature Rules. Mathematics of computation, 23(106): 221-230.

Gragnano C.G., Gottardi G., Jommi C. 2016. On the effect of Hydrometric Water Level Time-Variability on Riverbank Stability Evaluation. 1st International Conference on Natural Hazards and Structures, Chania Greece (in press).

Greco, V.R. 1996. Efficient Monte Carlo Technique for Locating Critical Slip Surface. Journal of Geotechincal Engineering. 122(7): 517-525.

Griffiths D.V., Fenton G.A. 2007. Probabilistic methods in Geotechnical Engineering. Springer-Verlag Wien.

Griffiths D.V., Lane P.A. 1999. Slope stability analysis by finite elements. Géotechnique 49(3): 387-403.

Guber A.K., Pachepsky Y.A., Rowland R., and Gish T.J., 2010. Field correction of the multisensor capacitance probe calibration. International Agrophysics, 24: 43-49.

Gui S., Zhang R., Turner J.O., Xue X., 2000. Probabilistic slope stability analysis with stochastic soil hydraulic conductivity. Journal of Geotechnical and Geonvironmental Engineering. 126(1): 1-9.

Harr M.E. 1989. Probabilistic estimates for multivariate analyses. Applied Mathematical Modelling, Elsevier, 13(5): 313-318.

Hassan AM. Wolff TF. Search algorithm for minimum reliability index of earth slopes Journal of geotechnical and geoenvironmental engineering, ASCE, 125(4): 301–308.

Harlan R.L., Nixon J.F. 1978. Ground Thermal regime. *In* Andersland O.B., Anderson D.M. (Eds). Geotechnical engineering for cold regions. McGraw-Hill, NY.

He J., Sällfors G. 1994. An optimal point estimate method for uncertainty studies. Applied Mathematical Modelling, 18: 494-499.

Heimovaara T.J., Bouten W., Verstraten J.M. 1994. Frequency domain analysis of time domain reflectometry waveform. A four-component complex dielectric mixing model for soils. Water Resources Research. 30(2): 201-209.

Hirabayashi Y., Mahendran R., Koirala S.,Konoshima S., Yamazaki D., Yamazaki D., Watanabe S., H., Kanae. 2013. Global flood risk under climate change. Nature Climate Change letters 3: 816–821.

Hong H. P. 1998. An efficient point estimate method for probabilistic analysis. Reliability Engineering and System Safety 59(3): 261–267.

Hughes P.N., Glendinning S., Mendes J., Parkin G., Toll D.G., Gallipoli D., Miller P.E. 2009. Full-scale testing to assess climate effects on embankments. Special Issue of Engineering Sustainability: Proc. Institution of Civil Engineers, 162(2): 67-79.

Hurtado J.E., Barbat A.H. 1998. Monte Carlo Techniques in Computational Stochastic Mechanics. Archives of Computational Methods in Engineering, 5(1): 3-30.

Intergovernmental Panel on Climate Change – IPCC. 2007. Climate Change 2007. Impacts, Adaptation and Vulnerability. Cambridge University Press, Cambridge, UK, pp. 7-22.

Intergovernmental Panel on Climate Change – IPCC. 2012. Managing the Risks of Extreme Events and Disasters to Advance Climate Change Adaptation. Cambridge University Press, Cambridge, UK.

Ippisch O., Vogel H.J., Bastian P., 2006. Validity limits fort the van Genuchten-Mualem model and implications for parameter estimation and numerical simulation. Advances in Water Resources, 29: 1780-1789.

Ippisch O., Vogel H.J., Bastian P., 2006. Validity limits fort the van Genuchten-Mualem model and implications for parameter estimation and numerical simulation. Advances in Water Resources, 29: 1780-1789.

Istituto Superiore per la Protezione e la Ricerca Ambientale – ISPRA. 2015. Hydro-geological instability in Italy: vulnerability and risk index.

Jaynes D.B., 1984. Comparison of soil–water hysteresis models. Journal of Hydrology, 75(1): 287–299.

Jommi C. 2014. Analysing time dependent problems. Stochastic Analysis and Inverse Modelling. ALERT Doctoral School, Aussois.

Kelleners T.J., Soppe R.W.O., Ayars J.E., Skaggs T.H., 2004. Calibration of capacitance probe sensors in a saline silty slay. Soil Science Society of America Journal, 68: 770-778.

Knight J.H., Ferré P.A., Rudolph P.A., Kachanoski R.G., 1997. A numerical analysis of the effects of coatings and gaps upon relative dielectric permittivity measurement with time domain reflectometry. Water Resources Research, 33(6): 1455-1460.

Kool J.B., Parker J.C., van Genuchten M.Th. 1987. Parameter estimation for unsaturated flow and transport models – A review. Journal of Hydrology, 91: 255-293.

Kraus J.D., Fleisch D.A. 1999. Electromagnetics with applications. McGraw-Hill.

Kundzewicz, Z.W., Kanae, S., Seneviratne, S.I., Handmer, J., Nicholls, N., Peduzzi, P., Mechler, R., Bouwer, L.M., Arnell, N., Mach, K., Muir-Wood, R., Brakenridge, G.R., Kron, W., Benito, G., Honda, Y., Takahashi, K., and Sherstyukov, B.: Flood risk and climate change: global and regional perspectives, Hydrological Sciences Journal; 59, 1–28, doi:10.1080/02626667.2013.857411, 2013.

Laloui L. 2010. Mechanics of Unsaturated Geomaterials. John Wiley & Sons, Inc.

Lambe T.W., Silva F. 1995. The ordinary method of slice revisited. Geotechnical News, 13(3): 49-53.

Lavell, A., 1999: Environmental degradation, risks and urban disasters. Issues and concepts: Towards the definition of a research agenda. In: Cities at Risk: Environmental Degradation, Urban Risk and Disasters in Latin America [Fernandez, M.A. (ed)]. A/H Editorial, La RED, US AID, Quito, Ecuador, 19-58.

Le T.M.H., Gallipoli D., Sanchez M.,Wheeler S.J. 2012. Stochastic analysis of unsaturated seepage through randomly heterogeneous earth embankments. International Journal for Numerical and Analytical Methods in Geomechanics, 36 (8):1056–1076.

Liao, K., Xu, S., Wu, J. and Zhu, Q. 2014. Uncertainty analysis for large scale predictions of the van Genuchten soil-water retention parameters with pedotransfer functions. Soil Research, 52(5): 431-442.

Lichtenecker K. 1926. Die dielektrizitatskonstante naturlicher und kunstlicher mischkorper. Physikalische Zeitschrift, 27: 115-158.

Likos, W.J., Lu, N. and Godt, J.W. 2014. Hysteresis and uncertainty in soil water retention curve parameters. Journal of Geotechnical and Geoenvironmental Engineering, 140(4): 1090-0241.

Liu K., Vardon P.J., Arnold P., Hicks M.A. Effect of hysteresis on the stability of an embankment under transient seepage. Proceeding of International Symposium on Geohazards and Geomechanics – ISGG2015. 2015.

Liu K., Vardon P.J., M.A. Hicks, Arnold P. Combined effect of hysteresis and heterogeneity on the stability of an embankment under transient seepage. Engineering Geology (in press). 2016.

Liu S.Y., Shao L.T., Li H.J., 2015. Slope stability analysis using the limit equilibrium method and two finite element methods.

Lourenço S.D.N., Gallipoli D., Toll D., Evans F., Medero G. 2007. Determination of the Soil Water Retention Curve with Tensiometers. In Experimental Unsaturated Soil Mechanics, (ed.T. Schanz), Springer, pp. 95 - 102.

Lourenço S.D.N., Gallipoli D., Toll D.G., Augarde C.E., Evans F. 2011. A new procedure for the determination of the Soil Water Retention Curves by continuous drying using high suction tensiometers. Canadian Geotechnical Journal, 48(2): 327-335.

Marquardt D.W. 1963. An Algorithm for Least-Squares Estimation of Nonlinear Parameters. Journal of the Society for Industrial and Applied Mathematics, 11(2): 431-441.

Mayne P.W., Campanella R.G. 2005. 16th International Conference on Soil Mechanics and Geotechnical Engineering, Osaka, Japan, 12-16 September, 2005, 721-724.

McGranahan G., Balk D., Mcgranahan G., Bartlett S. 2007. The rising tide: assessing the risks of climate change and human settlements in low elevation coastal zones. Environmental and Urbanization 19: 17–37.

Mendes J. 2011. Assessment of the impact of climate change on an instrumented embankment: an unsaturated soil mechanics approach. PhD Thesis, Durham University. Available online: http://etheses.dur.ac.uk/612/

Milington R.J., and Quirk J.P. 1961. Permeability of porous media. Nature, 183: 387-388.

Mills, E. 2005. Insurance in a climate of change. Science. 309: 1040–1044.

Milly, P.C.D, 1982. Moisture and heat transport in hysteretic, inhomogeneous porous media: A matric head based formulation and a numerical model. Water Resources Research, 18(3): 489-498.

Ministry of the Environment and Land Protection. 2008. The hydro-geological risk in Italy.

Morgenstern N.R., Price V.E. 1965. The analysis of the stability of general slip surfaces. Géotechnique 15(1): 79-93.

Mualem Y. 1976. A new model for predicting the hydraulic conductivity of unsaturated porous media. Water Resources Research, 12(3): 513-522.

Müller R. 2013. Probabilistic stability analysis of embankments founded on clay. Doctoral Thesis, Division of Soil and Rock Mechanics, Department of Civil and Architectural Engineering, Royal Institute of Technology, Stockholm.

Munich Re, 2011: Topics GEO, Natural Catastrophes 2010, Analyses, Assessment, Positions. Munich Re, Munich, Germany.

Munoz-Carpena R., Shukla S., Morgan K. 2004. Field Devices for Monitoring Soil Water Content. University of Florida IFAS Extension. Publication #BUL343.

Napa-García G.F., Beck A.T., Celestino T.B. 2017. Reliability analyses of underground openings with the point estimate method. Tunnelling and Underground Space Technology, 64: 154-163.

Nemes A., Schaap M.G., Leij F.J., Wösten J.H.M. 2001. Description of the unsaturated soil hydraulic database UNSODA version 2.0. Journal of Hydrology, 251: 151-162.

Olivella S., Gens A. 2000. Vapour transport in low permeability unsaturated soils with capillary effects. Transport in porous media, 40: 219-241.

Paltineanu I.C., Starr J.L., 1997. Real-time soil water dynamics using multisensor capacitance probes: Laboratory calibration. Soil Science Society of America Journal, 61: 1576-1585.

Papa R., Piron M., Nicotera M.V., Urciuoli G. 2013. Seasonal groundwater regime in an unsaturated pyroclastic slope. Géotechnique 63(5): 420-426.

Paraskevas C., Georgiou, P., Ilias, A., Panoras, A., and Babajimopoulos, C., 2012. Calibration equations for two capacitance water content probes. International Agrophysics, 26: 285-293.

Park D., Kim H.M., Ryu D.W., Song W.K., Sunwoo C., 2012. Application of a point estimate method to the probabilistic limit-state design of underground structures. International Journal of Rock Mechanics and Mining Sciences, 51: 97–104.

Parlange J.Y., 1976. Capillary hysteresis and the relationship between drying and wetting curves. Water Resources Research, 12(2): 224-228.

Patterson K.E. 1955. The Early History of Circular Sliding Surfaces. Géotechnique, 5: 275-296.

Peters A., Durner W. 2008. Simplified evaporation method for determining soil hydraulic properties. Journal of Hydrology, 356: 147-162.

Pham H.T.V., Fredlund D.G. 2003. The application of dynamic programming to slope stability analysis. Canadian Geotechnical Journal, 40(4): 830-847.

Pham H.Q., Fredlund D.G., Barbour S.L. 2005. A study of hysteresis models for soil-water characteristic curves. Canadian Geotechnical Journal, 42(6): 1548-1568.

Phene C.J., Rawlins S.L., Hoffman G.J. Measuring soil matric potential in situ by sensing heat dissipation within a porous body. Theory and sensor construction. Soil Scientific Society of America, 35: 27-33.

Phoon K. 2008. Reliability-Based Design in Geotechnical Engineering: Computations and Applications. CRC Press.

Phoon K.K., Santoso A., Quek S.T. 2010. Probabilistic analysis of soil-water characteristic curves. Journal of Geotechnical and Geoenvironmental Engineering, ASCE, 136(3): 445-455.

Pickles A. and Sandham R. Application of Eurocode 7 to the design of flood embankments (C749). CIRIA Repot C749.

Press H.W., Teokolsky S.A., Vetterling W.T., Flannery B.P. 1993. Numerical Recipes in Fortran 77. Cambridge University Press.

Rahardjo H., Zhai, Q., 2013. Quantification of uncertainties in soil–water characteristic curve associated with fitting parameters. Engineering Geology, 163: 144–152.

Ridley A., McGinnity B., Vauhan P. 2004. Role of pore water pressures in embankment stability. Special Issue of Geotechnical Engineering: Proc. Institution of Civil Engineers, 157(4): 193-198.

Rinaldi M., Casagli N., Dapporto S., Gargini A. 2004. Monitoring and modelling of pore water pressure changes and riverbank stability during flow events. Earth Surface Process and Landforms, 29: 237-254.

Ritter A., Hupert F., Munoz-Carpena R., Lambot S., Vanclooster M. Using inverse methods for estimating soil hydraulic properties from field data as ana alternative to direct methods. Agricultural Water Management, 59: 77-96

Robertson, P. K. 2009. Interpretation of cone penetration tests - a unified approach. Canadian Geotechnical Journal, 46(11): 1337-1355.

Robinson D.A., S.B. Jones, J.A. Wraith, D. Or, and S.P. Friedman., 2003. A review of advances in dielectric and electrical conductivity measurement in soils using time domain reflectometry. Vadose Zone Journal 2:444–475.

Romano N., Santini A. 1999. Determining soil hydraulic functions from evaporation experiments by a parameter estimation approach: experimental verifications and numerical studies. Water Resources Research, 35(11): 3343-3359.

Rosenblueth, E. 1975. Point estimates for probability moments. Proceedings of the National Academy of Sciences of the United States of America, 72(10): 3812-3814.

Roth K., R. Schulin, H. Fluhler, and W. Attinger., 1990. Calibration of time domain reflectometry for water content measurement using a composite dielectric approach.Water Resources Research, 26: 2267–2273.

Scanlon B., Christman M., Reedy R., Porro I., Šimunek J., Flerchinger G. Intercode comparisons for simulating water balance of superficial sediments in semiarid regions. Water Resource Research Journal, 38(12): 1-16.

Schaap, M.G., Leij, F.J. and Van Genuchten, M.T. 1998. Neural network analysis for hierarchical prediction of soil hydraulic properties. Soil Science of America Journal, 62(4): 847-855.

Schelle H., Heise L., Jaenicke K., Durner W. 2013. Water retention characteristics of soils over the whole moisture range: a comparison of laboratory methods. European Journal of Soil Science, December 2013, 64: 814–821. doi: 10.1111/ejss.12108.

Schelle H., Iden S.C., Peters A. Durner W. 2010. Analysis of the Agreement of Soil Hydraulic Properties Obtained from Multistep-Outflow and Evaporation Methods. Vadose Zone Journal. doi:10.2136/vzj2010.0050.

Schindler U, von Unold G, Müller L. 2015. Laboratory Measurement of Soil Hydraulic Functions in A Cycle of Drying and Rewetting. International Journal of Emerging Technology and Advanced Engineering, 5(4): 281-286.

Schindler U., Durner W. von Unold G., Mueller L. 2010a. Evaporation Method for Measuring Unsaturated Hydraulic Properties of Soils: Extending the Range. Soil Science Society of America Journal, 74 (4): 1071–1083.

Schindler U., Durner W., von Unold G., Mueller L., Wieland R. 2010b. The evaporation method – Extending the measurement range of soil hydraulic properties using the air-entry pressure of the ceramic cup. Journal of Plant Nutrition and Soil Science, 173 (4): 563–572.

Schindler U., Müller L., da Veiga M., Zhang Y., Schlindwein S. L., Hu C. 2012. Comparison of water-retention functions obtained from the extended evaporation method and the standard methods sand/kaolin boxes and pressure plate extractor. Journal of Plant Nutrition and Soil Science 174(4): 527-534.

Schweiger H.F., Turner F., Pottler R. 2001. Reliability analysis in geotechnics with deterministic finite elements. International Journal of Geomechanics, 1(4): 389-413.

Shaw B., Baver L.D. 1939. An electrothermal method for following moisture changes of the soil in situ. Soil Scientific Society of America, 4: 78-83.

Shiozawa S., Campbell G.S. 1990. Soil thermal conductivity. Remote Sensors Reviews, 1990, 5: 301-310.

Simpson B., Vogt N. and van Seters AJ. Geotechnical safety in relation to water pressure. 3rd International Symposium on Geotechnical Safety and Risk, 2011; Munich.

Šimunek J., Šejna M., Saito, H., Sakai, M. & Van Genuchten, M., Th. 2009. The HYDRUS-1D software package for simulating the one-dimensional movement of water, heat, and multiple solutes in variably-saturated media. 4.08 Ed.

Šimunek J., Wendroth O., van Genuchten M.Th. 1998. Parameter Estimation Analysis of the Evaporation Method for Determining Soil Hydraulic Properties. Soil Science Society of America Journal. 62: 894-905.

Sleep M. and Duncan J. 2013. Effects of initial conditions on the results of transient seepage analyses. In Proceedings of the Geo-Congress 2013: Stability and Performance of Slopes and Embankments III, San Diego, Calif., 3-7 March 2013. ASCE, 1081-1090.

Solone R., Bittelli M., Tomei F., Morari F. 2012. Errors in water retention curves determined with pressure plates: Effect on the soil water balance. Journal of Hydrology, 470-401: 65-74.

Spencer E. 1967. A Method of Analysis of the Stability of Embankments Assuming Parallel Inter-Slices Forces. Géotechnique, 17: 11-26.

Stoica P and Moses RL. 2005. Spectral Analysis of Signals. Pearson Prentice Hall, NJ.

Strang G. 1993. Wavelet transforms versus Fourier transforms. Bulletin of the American Mathematical Society, 28: 288-305.

Tamari S., Bruckler L., Halbertsma J., Chadoeuf J. 1993. A simple method for determining soil hydraulic properties in the laboratory. Soil Science of America Journal, 57(3): 642-651.

Tanoue M., Hirabayashi Y., Ikeuchi H. 2016. Global-scale river flood vulnerability in the last 50 years. Scientific Reports. 6: 1-9.

Tarantino A., Romero E:, Cui Y.J. (Eds.) 2008. Laboratory and field testing of unsaturated soils. Springer, London.

Toker N, Germaine J, Sjoblom K, Culligan P (2004) A new technique for rapid measurement of continuous soil moisture characteristic curves, Géotechnique, 54(3):179–186.

Toll D.G., Asquith J.D., Fraser A., Hassan A.A., Liu G., Lourenço S.D.N., Mendes J., Noguchi T., Osinski P., Stirling R.A. 2015. Tensiometer techniques for determining soil water retention curves. Proc. 6th Asia-Pacific Conference on Unsaturated Soil. Guilin, China.

Toll D.G., Lourenço S.D.N., Mendes J. 2013. Advances in suction measurements using high suction tensiometers, Engineering Geology, 165: 29-37.

Topp G.C., Davis J.L., and Annan A.P., 1980. Electromagnetic determination of soil water content: Measurements in coaxial transmission lines. Water Resour. Res., 16, 574-582.

Tsaparas I., Rahardjo H., Toll D.G., Leong E.C., 2002. Controlling parameters for rainfall induced landslides. Computers and Geotechnics, 29 (1): 1–27.

Twarakavi N.K.C., Šimůnek J., Schaap M., 2009. Development of pedotransfer functions for estimation of soil hydraulic parameters using support vector machines, Soil Science Society of America Journal, 73(5): 1443-1452

U.S. Army Corps of Engineers. 1999. Risk Based Analysis in Geotechnical Engineering for Support of Planning Studies. Engineering Circular 1110-2-554, Department of the Army U.S. Army Corps of Engineers. Available online at http://usace.army.mil/usace-docs.

U.S. Army Corps of Engineering. 2006. Reliability Analysis and Risk Assessment for Seepage and Slope Stability Failure Modes for Embankment Dams. US Corps of Engineers Publication No. ETL 1110-2-561.

U.S. Army Corps of Engineers. 2015. Best Practices in Dam and Levee Safety Risk Analysis. Department of the Army U.S. Army Corps of Engineers, v. 4.0. Available online at http://usace.army.mil/usace-docs.

UNDHA, 1992: Internationally agreed glossary of basic terms relating to disaster management. UNDHA, Geneva, Switzerland.

UNDRO, 1980: Natural Disasters and Vulnerability Analysis. Report of Experts Group Meeting of 09-12 July 1979, UNDRO, Geneva, Switzerland.

van Genuchten, M. Th. 1980. A closed-form equation for predicting the hydraulic conductivity of unsaturated soils. Soil Science of America Journal, 4(5): 892–898.

Vanapalli S.K., Fredlund D.G., Pufahl D.E., Clifton A.W. 1996. Model for the prediction of shear strength with respect to soil suction. Canadian Geotechnical Journal, 33(3): 379-392.

Vereecken H., Weynants M., Javaux M., Pachepsky Y., van Genucthen M.Th., 2010 Vadose Zone Journal 9: 795–820.

Vogel T., van Genuchten M.Th., Cislerova M., 2001 Effect of the shape of the soil hydraulic functions near saturation on variability-saturated flow predictions. Advances in Water Resources, 24: 133-144.

Von Hippel A.R. 1954. Dielectrics materials and applications. MIT Press. Cambridge, MA.

Wendroth O., Ehlers W., Hopmans J.W., Kage H., Halbertsma J., Wosten J.H.M. 1993. Reevaluation of the evaporation method for determining hydraulic functions in unsaturated soils. Soil Science of America Journal, 57(6):1436-1443.

White G.F. 1945. Human Adjustment to Floods. University of Chicago, Department of Geography Research, Paper no. 29.

White, G.F., 1973: Natural Hazards Research. In: Directions in Geography [Chorley, R.J. (ed)]. Methuen and Co., London, UK, 193-216.

Wilson, G.W. 1990. Soil evaporative fluxes for geotechnical engineering problems. Ph.D. dissertation, University of Saskatchewan, Saskatoon, Canada.

Wind G.P. 1968. Capillary conductivity data estimated by a simple method. In Proceedings of the Symposium: Water in Unsaturated Zone, Wageningen, Netherlands, June 1966. International Association of Scientific Hydrology, Paris, pp. 181-191.

Wolff T.F. 1996. Probabilistic slope stability in theory and practice. In Uncertainty in the Geologic Environment. Edited by C.D. Shackelford, P.P. Nelson and M.J.S. Roth. ASCE, University of Wisconsin–Madison Press, Madison, WI, 419-433.

Wösten J.H.M., Lilly A., Nemes A., Le Bas C. 1999. Development and use of a database of hydraulic properties of Europead soils. Geoderma, 90: 169-185.

Wraith J.M., D. Or, 1999. Temperatures effects on soil bulk dielectric permittivity measured by time domain reflectometry: Experimental evidence and hypothesis development. Water Resources Research, 35 (2), 361-369.

Zanchettin, D., Traverso, P., and Tomasino, M., 2008. Po River discharges: a preliminary analysis of a 200-year time series, Climatic Changes. 89: 411-433.

Zhang L.L., Deng H.Z., Zhang L.M. 2010. Reliability analysis of slope stability considering correlations among soil hydraulic parameters. Journal of Shenzhen University Science and Engineering, 27(1): 114-119.

Zhang L.L., Zhang L.M., Tang W.H. 2003. Importance of considering correlations among parameters of soil-water characteristic curve. 9th International Conference on Applications of Statistics and Probability in Civil Engineering, San Francisco, 06-09 July, 2003, 1423-1429.

Zheng H., Sun G., Liu D. 2009. A practical procedure for searching slip surfaces of slopes based on the strength reduction technique. Computers and Geotechnics, 36(1-2): 1-5.

Zienkiewicz O.C., Humpheson C., Lewis R.W. 1975. Associated and non-associated visco-plasticity and plasticity in soil mechanics. Géotechnique, 25(4): 671-689.